Large Scale Renewable Power Integration with Electric Vehicles

Long term analysis for Germany with a renewable based power supply

Von der Fakultät für Energie-, Verfahrens- und Biotechnik der Universität Stuttgart
zur Erlangung der Würde eines Doktor-Ingenieurs (Dr.-Ing.)
genehmigte Abhandlung

vorgelegt von
Diego Luca de Tena Costales

aus Madrid

Vorsitzender: Prof. Dr.-Ing. Alfred Voß
Hauptberichter: Prof. Dr. Dr.-Ing. habil. Hans Müller-Steinhagen
Mitberichter: Prof. Dr.-Ing. Ulrich Wagner
Mitberichter: Prof. Dr. rer. nat. K. Andreas Friedrich

Tag der mündlichen Prüfung: 10.04.2014

Institut für Thermodynamik und Wärmetechnik
der Universität Stuttgart

2014

Declaration of academic integrity

I hereby declare that this doctoral thesis has been written by the undersigned without the unauthorised assistance from third parties.

Furthermore, I confirm that no sources have been used in its preparation than those indicated in the thesis itself.

Madrid, 21/06/2013

Table of contents

Index of tables

Index of figures

Acronyms

BEV	Battery Electric Vehicle
CAES	Compressed Air Energy Storage
CCGT	Combined Cycle Gas Turbine
CD	Charge Depleting
CCS	Carbon Capture and Sequestration
CHP	Combined Heat and Power
CNG	Compressed Natural Gas (vehicle)
CNG_{Hyb}	Compressed natural gas-electric hybrid vehicle
CS	Charge Sustaining
CSP	Concentrated Solar Power
D	Diesel (vehicle)
D_{Hyb}	Diesel-electric hybrid vehicle
DLR	German Aerospace Centre
DNI	Direct Normal Irradiance
DoD	Depth of Discharge
DSM	Demand Side Management
EREV	Extended Range Electric Vehicle
EU	European Union
EV	Electric Vehicle (comprises BEV, EREV and FCV)
FCV	Fuel Cell Vehicle
G	Gasoline (vehicle)
G_{Hyb}	Gasoline-electric hybrid vehicle
GHG	Greenhouse Gas
GSM	Global System for Mobile Communications
GT	Gas Turbine
HDV	Heavy Duty Vehicles
HEV	Hybrid Electric Vehicle
HVDC	High Voltage Direct Current
ICE	Internal Combustion Engine
ICT	Information and Communications Technology
IEC	International Electrotechnical Commission
IT	Information Technology
MiD	Mobilität in Deutschland (Germany wide mobility survey)
NEDC	New European Driving Cycle
NTC	Net Transfer Capacity
OPEC	Organization of Petroleum Exporting Countries
PEV	Plug-in Electric Vehicle
PHEV	Plug-in Hybrid Electric Vehicle

PS	Pumped Storage
PTDF	Power Transmission Distribution Factor
PV	Photovoltaic
RE	Renewable Energy
RES	Renewable Energy Sources
SM	Solar Multiple
SoC	State-of-Charge (as energy stored in the car batteries)
SR	Steam Reforming
ST	Steam Turbine
TCO	Total Cost of Ownership
TSO	Transmission System Operator

Acknowledgements

The present thesis was mostly written during the three years I had the opportunity to work at the Institute of Technical Thermodynamics of the German Aerospace Center. I want to thank Prof. Dr.-Ing. Hans Müller-Steinhagen and Prof. Dr.-Ing. Ulrich Wagner for supervising this thesis, Dr.-Ing. Wolfram Krewitt (†) for the confidence granted, Dr.-Ing. Thomas Pregger for providing very valuable comments to this dissertation as well as Dr.-Ing. Yvonne Scholz and all former colleagues at the DLR for their support, encouragement and for the positive working environment.

Summary

The use of electricity from renewable energy sources (RES) in the transport sector has many advantages compared to the internal combustion engine (ICE). A transition from a fossil fuel based mobility to one based on electricity from renewable sources can allow for significant greenhouse gas reductions (GHG) as well as of air pollutants and noise in urban areas. In addition, greater independence from imported oil in the transport sector can be achieved.

The aim of this work is to study the feasibility and system impact of electric mobility in the German power system with a high share of fluctuating renewable energy. One major advantage of electric vehicles (EV) is the high flexibility in charging times, which can be used to integrate renewable power generation and to make the operation of the system more efficient. This work will focus on the period comprised between 2030 and 2050, since at that time it can be assumed that electric vehicles under favourable conditions can reach a significant magnitude for the power system.

The REMix model developed at the DLR couples the in the energy economics well established approach of linear optimisation with a geographic information system (GIS) that provides spatial and temporal information of the renewable energy potentials. The GIS-based dataset is a key element of the model and is calculated based on satellite measurements, weather service and land cover data for the whole of Europe with a high spatial (10 x 10 km) and temporal (hourly) resolution. In contrast to other planning models, in which only typical load situations are represented, REMix considers real weather conditions and thus allows representing the particularities of fluctuating renewable energy sources in an optimization model.

The results prove the feasibility of a power system with a RES share of over 85% assuming an ambitious network expansion based on underground HVDC lines. The analysis points out that controlling the charging times of plug-in electric vehicles (PEV) and with a flexible hydrogen production for fuel cell vehicles (FCV) not only the additional demand of EVs but also the renewable power generation required to power these vehicles can be integrated in the system. These actions allow completely avoiding increases of the residual peak demand, of surpluses from RES, as well as of the required transmission network expansion.

Summary (German)

Die Nutzung von Strom aus erneuerbaren Energiequellen hat im Verkehrssektor viele Vorteile gegenüber dem Verbrennungsmotor. Ein Übergang in eine auf erneuerbarem Strom basierende Mobilität, kann erhebliche Treibhausgas- sowie Luftschadstoff- und Lärmminderungen vor allem in städtischen Gebieten ermöglichen. Darüber hinaus kann die Abhängigkeit von importiertem Öl im Verkehrssektor stark vermindert werden.

Das Ziel dieser Arbeit ist es, die Wechselwirkungen zwischen der Elektromobilität und einer Stromversorgung mit einem hohen Anteil fluktuierender erneuerbarer Erzeugung in Deutschland zu untersuchen. Ein großer Vorteil von Elektrofahrzeugen ist die hohe Flexibilität bei den Ladezeiten, die zur Integration erneuerbarer Erzeugungskapazitäten und zur Effizienzerhöhung des Systems beitragen kann. Die Arbeit fokussiert auf Deutschland in den Jahren zwischen 2030 und 2050, da zu diesem Zeitpunkt davon ausgegangen werden kann, dass Elektrofahrzeuge unter günstigen Bedingungen eine signifikante energiewirtschaftliche Größenordnung erreichen können.

Das am DLR entwickelte Modell REMix verknüpft den in der energiewirtschaftlichen Systemanalyse etablierten Ansatz der linearen Optimierung mit einem Geografischen Informationssystem, das räumlich und zeitlich aufgelöste Daten über die Potenziale der erneuerbaren Energien bereitstellt. Die GIS-gestützte Datenbank stellt die zum Teil aus Satellitendaten, Wetterdienst- und Landnutzungsdaten ermittelten Potenziale für ganz Europa in hoher räumlicher (10 x 10 km) und zeitlicher (stündlicher) Auflösung zur Verfügung. Im Gegensatz zu anderen Planungsmodellen, in denen nur typische Lastsituationen berücksichtigt werden, finden in REMix reale Wetterbedingungen Verwendung. Dies ermöglicht, die im Laufe eines Jahres auftretenden Besonderheiten der fluktuierenden erneuerbaren Energien in einem Optimierungsmodell adäquat abzubilden.

Die Ergebnisse belegen die Machbarkeit eines Systems mit einem EE-Anteil von über 85% unter Annahme eines ehrgeizigen Netzausbaus auf Basis erdverlegter HGÜ-Leitungen. Die Analyse weist darauf hin, dass bei Verwendung gesteuerter Ladestrategien für aufladbare Elektrofahrzeuge und einer flexiblen Wasserstoffproduktion für Brennstoffzellen-Fahrzeuge nicht nur der zusätzlicher Bedarf für EVs aber auch die erneuerbare Stromerzeugung, die für emissionsfreies Fahren benötigt wird, integriert werden kann. Durch diese Maßnahmen eine Zunahme der Spitzennachfrage, der Überschüsse aus regenerativer Stromerzeugung und des erforderlichen Netzausbaus kann vollständig vermieden werden.

Large Scale Renewable Power Integration with Electric Vehicles

1 Actual context of electric vehicles

Since the 19th century several electrical[1] and hybrid vehicles[2] have been developed. For the time being the electric vehicle technology has not become a competitive alternative for the mass-market. The purpose of this chapter is to analyse the technology's long term perspectives, starting from its historical context and analysing the present situation.

1.1 Historical background

Figure 1: Historical development of motor vehicle registration in Germany (from 1970), and market-share of different traction systems in the USA (1900 and 1905) and Germany (from 1970)

Source: Mock and Schmid, 2008.
Pictures: La jaimais contente, the Detroit Electric car, the Golf CitySTROMer (VW), the EV1 (GM) and the Smart Fortwo ED (Daimler).

---
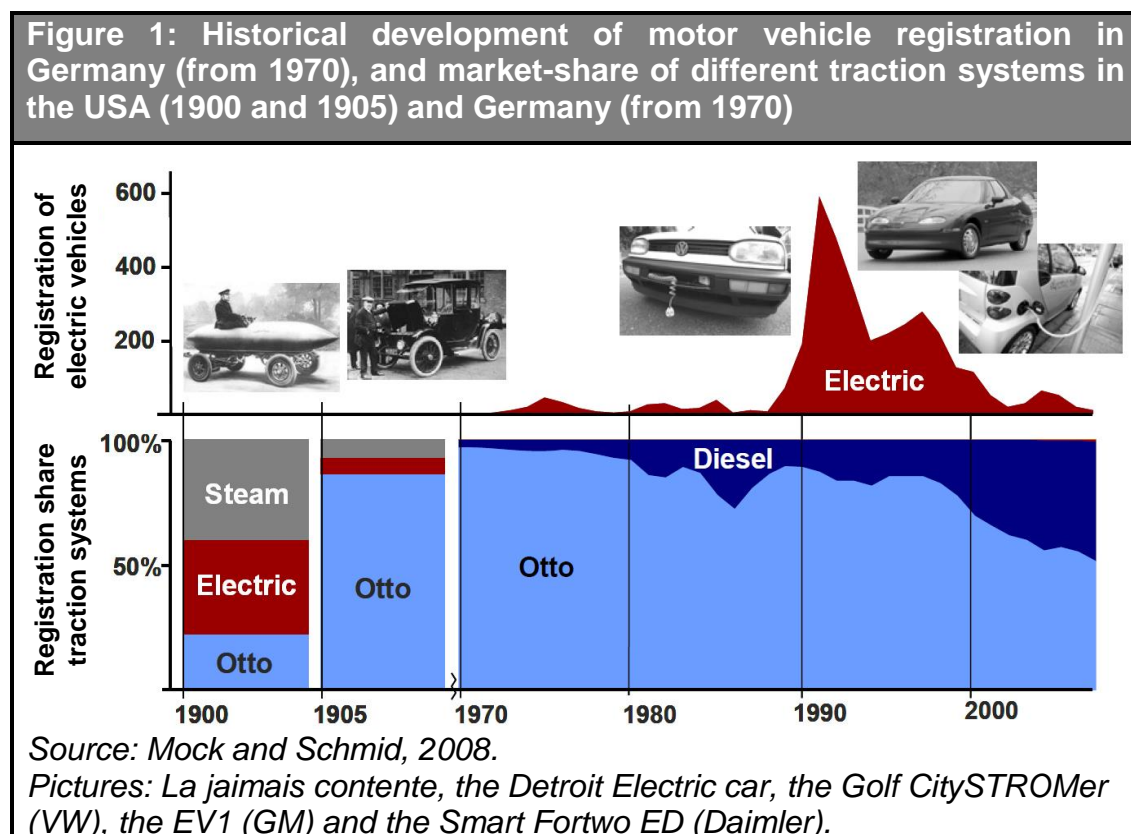
[1] La jamais contente from Camille Jenatzy became in 1899 the first road vehicle to go over 100 km/h.

[2] In 1899 Ferdinand Porsche built the Lohner-Porsche one of the first gasoline-electric series-hybrid automobile in the world.

In the beginning of the twentieth century around 38% of all registered cars in the USA were electric powered, whereas five years later Otto motors powered more than 85% (see Figure 1). Inventions, like the starter motor, that made Otto motors more comfortable to use as well as the limited range of battery electric powered cars (Möser, 2002) contributed to the clear dominance of the internal combustion engine (ICE), mainly Otto motors, during the next one hundred years though since 1970 a growing share of diesel can be observed in Germany as in other parts of the world. During the 1970's and 1980's oil crisis the interest in electric vehicles grew, and during the research programs at the beginning of the 1990s the registration on electric vehicles (EVs) in Germany peaked with 600 units. During this decade several electric vehicles were developed by industry. The General Motors EV1 was a compact car built in series as a reaction to a Californian law from 1990 for emissions reductions. The vehicle was first brought to market in 1996; however, the program was cancelled by GM in 2003 alleging it was not profitable due to the low demand. In Germany Volkswagen produced between 1992 and 1996 in very small series an electric version of the VW-Golf, the Golf CitySTROMer. The electric Golf was not designated to be sold to private customers but to be used by utility companies.

The efforts made by industry and researchers in those years did not trigger a transformation in the transport sector and many initiatives from industry were discontinued. In that time the energy densities of lead-acid and Ni-MH batteries employed in the EV1 or in the CitySTROMer were significantly lower than those achievable with today's lithium batteries, the electric drive train was not as mature as it is nowadays, furthermore oil prices remained on very low levels during the decade at around 20 $/bl and renewable energy technologies were not developed enough to supply EVs with clean energy at affordable prices.

In the next section the main drivers that could have an impact on EVs' penetration will be discussed, with the purpose of analysing the changes that have taken place in the last years which could this time lead to a long term development of EVs.

1.2   Present situation

In the last years, climate change indicators, such as glaciers' melting in Greenland, are increasing public and political awareness of the potential irreversible changes in the earth's climate which are taking place at the moment. The increasing scarcity of fossil fuels, the very significant technical improvements in key technologies such as battery and information technology, as well as the on-going expansion of power generation from RES have modified the prospects of EVs significantly. Especially, since it is evident that the potentials of bio fuels from sustainable production are limited.

Climate change

New scientific findings support that the global temperature increase due to greenhouse effect is man-made and that, in order to avoid irreversible changes on the world's climate, the average global temperature should not exceed 2°C compared to pre-industrial levels (IPCC, 2007).

Figure 2: Development of the total Green-House-Gas emissions in EU-27 until 2050 for different emitting sectors

Source: EC, 2007
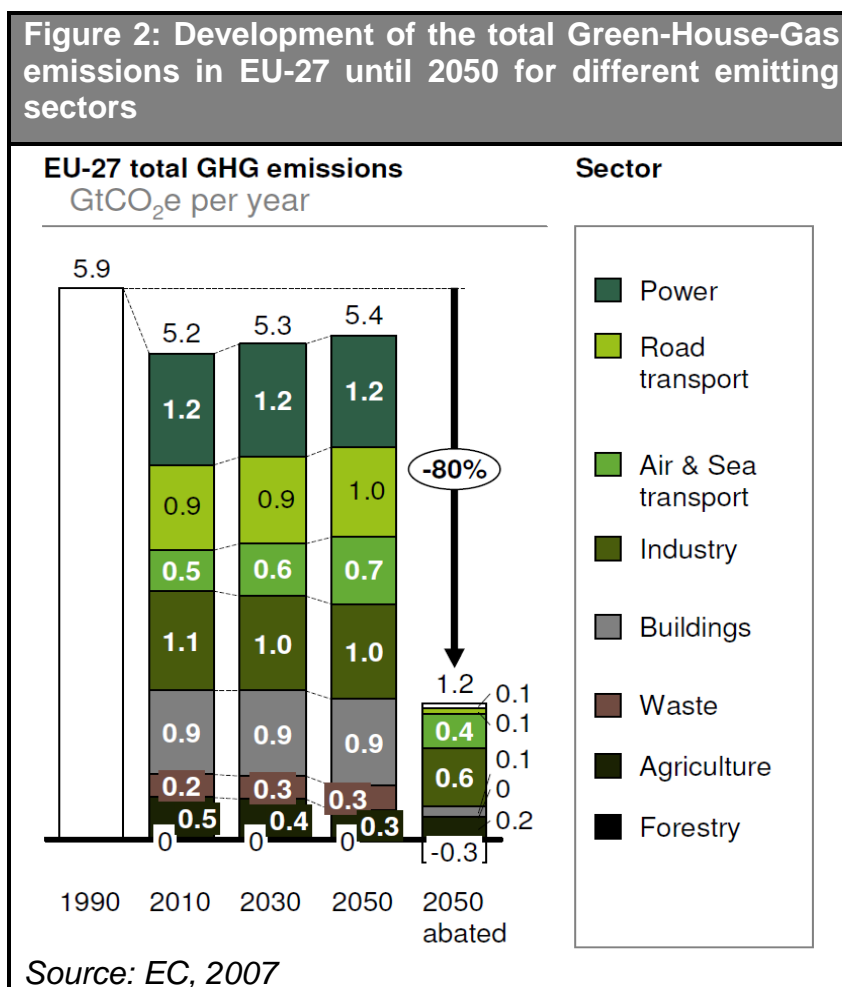
The EU committed to a reduction of 20% until 2020 of GHG emissions compared to 1990, for year 2050 recognises that at least a reduction between 60% and 80% is needed in developed countries to "*limit the impacts of climate change and the likelihood of massive and irreversible disruptions of the global ecosystem*" (EC, 2007). These GHG reductions are not expected to be uniform for all sectors, namely the power and road transport sector (see Figure 2) could present reductions of 95% attending to a recently published scenario (ECF, 2010). So as to make the future emission reduction targets possible, emissions from the road transport sector, which in the EU accounts for approximately 17% of the total GHG emissions, as well as from the power sector (23%), will have to be substantially reduced. The European Parliament has set emission performance standards to enforce a progressive reduction on CO_2 emissions of passenger cars; the goal is to achieve fleet emissions of 120 gCO_2 per km by 2015 and of 95 gCO_2 per km by 2020. For deviations from these goals car makers would incur in penalty payments, of 5 € per registered vehicle for the first gram, of 15 € for the second, 25 € for the third, and of 95 € for every additional gram (EUR, 2009).

Figure 3: Specific GHG emissions of medium size vehicles in 2030 with different traction systems

Source: Pehnt et al., 2011.
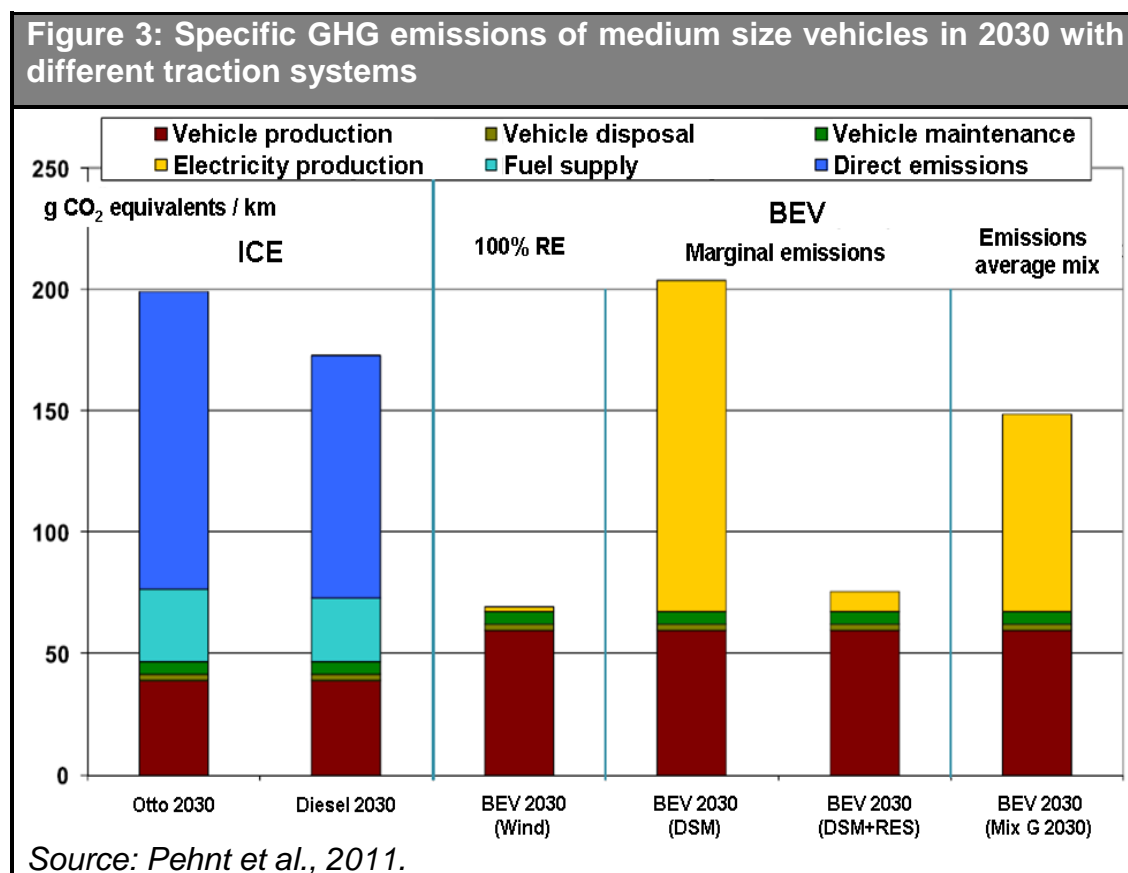
Figure 3 shows for the year 2030 the life-cycle GHG emissions of a car with ICE for both Diesel and Otto fuels, and those of a medium size BEV depending on the source of the electric power (see Pehnt et al., 2011).

The assumed vehicle is a medium size passenger car, as the Golf VI[3], driving 15.000 km per year; the fuel consumption is based on the driving profiles assumed in "*Handbuch Emissionsfaktoren 3.1*" (HBEFA, 2010) with a 30% urban, 40% extra urban and 30% on motorways and including the auxiliary electricity consumption. The calculation method is described in (Helms, 2010).

It can be seen that the GHG emissions of EVs powered with the 2030 electricity mix in Germany are only slightly lower than those achievable in 2030 with Otto or Diesel vehicles. The reason is that, in spite of the higher efficiency of the electric drivetrain, due to the high emissions of the electricity production step and of vehicle manufacturing, the total emissions are higher. Restricting the electricity consumed to wind power results in significantly lower GHG emissions. The global impact of EVs on GHG emissions can be assessed with the marginal emissions caused by the additional power demand of the EVs. The marginal emissions in the scenarios with demand-side management (DSM) and with an additional installation of renewable generation capacities (DSM+RES) show that EVs can offer significantly lower GHG emissions only in the latter case. The construction of additional renewable power generation capacity must be causally attributable to electric cars to achieve reductions of GHG emissions in line with the long term target of the EU; simply relabeling existing renewable power plants would not help reduce the GHG emissions (Pehnt, 2010) as less renewable electricity would be available for other consumers. The reason is that the additional electricity demanded by the EVs would be otherwise produced by thermal power plants using coal or natural gas, as typically renewable power plants do not increase their electricity production with electricity demand but depending on wind speed, solar irradiation or precipitation[4].

Cap and trade emissions trading schemes, such as the EU Emissions Trading System (EU ETS) establish a limit on the amount of certain GHG that can be

---

[3] Volkswagen AG, 2008.

[4] With the exceptions of renewable power generation surpluses, which are reduced, and of power plants using biomass, though this depends on the retribution structure.

emitted by large combustion plants such as certain factories and power plants, and at the moment covers 40% of GHG emissions in the EU[5]. The GHG emissions of passenger cars are at present excluded in the ETS schemes, but as those of the power sector are, the increments that EVs would cause would be compensated by the participating actors in the ETS scheme through price increases in carbon dioxide emission certificates.

Whatever mechanism is used to offset the GHG emissions in the power system attributable to electric mobility, it has to be ensured that the use of EVs leads to significant reductions in GHG emissions. Otherwise the additional costs of electrical mobility if compared to conventional or hybrid vehicles would not be justified.

Oil scarcity and dependence

Since the 1973 oil crisis there have been important efforts in most economies to reduce the oil dependence. Oil price shocks, as that of 1973 "have been held responsible for recessions, periods of excessive inflation, reduced productivity, and lower economic growth" (Barsky and Kilian, 2004). The latest conflict between Russia and Ukraine about natural gas supply reminds how vulnerable many countries are to hydrocarbon imports. The European transport sector is very dependent on oil imports, as it relies to 95% on oil (OECD/IEA, 2006) of which nowadays around 80% is imported. This share is growing and is expected to reach 88% in 2030 (VGB, 2009/2010).

In accordance to the reference scenario of the World Energy Outlook 2009 (OECD/IEA, 2009) oil prices will rise again after dropping during the 2008 financial crisis. In 2020 prices will present 100$/bl and in 2030 115$/bl[6]. By June 2013 the Brent Crude traded at around 106 $/bl or inflation adjusted at 94.6 $2007/bl[7]. The world oil consumption in year 2030 will be around 25% higher than it was in 2008, where Asia and Middle East account for most of the increase. Unconventional oil, as extra heavy oil or from oil sands, as well as from liquids

---

[5] For more information: http://ec.europa.eu/clima/policies/ets/index_en.htm

[6] In real year-2007 prices.

[7] Adjusted using the Consumer Price Index for All Urban Consumers (CPI-U) published by the U.S. Department of Labor, Bureau of Labor Statistics.

originated from natural gas will account for most of the production increase. The production of unconventional oil is more energy-intensive than that of conventional oil, and the oil-production related emissions for oil sands are around 3-4 times higher (IPCC, 2007). The production costs of unconventional oil are also higher, ranging from $6.6 to $19.7/GJ, compared to those of conventional oil, typically between $1.6 and $6.6/GJ (ETSAP, 2010).

Development of key technologies

One of the main reasons why electric vehicles have not become a competitive alternative for personal and commercial transportation was the limited energy density of batteries (Möser, 2002). Lithium-Ion batteries, as seen in Figure 4, can provide higher energy and higher power densities than other commercial battery technologies (Kalhammer et al., 2007). This battery technology can also provide a larger cycle life, better storage performance, higher charging and discharging currents, as well as a lower self-discharge rate (Nishi, 2001). Depending on the electrode materials significant differences in battery properties can be observed, these concern energy and power density, safety, ageing, as well as production costs. High energy batteries are better suited for BEVs, as the driving range is the most important factor, whereas high power batteries are more indicated for hybrids, as they have to provide a similar amount of power with a significantly smaller battery.

One of the main drawbacks of Lithium-Ion batteries are the higher costs. According to a recent study (BCG, 2010) the total cost of a 15 kWh battery pack, which in a small BEV allows for a driving range of around 100 km between charges, would be in 2009 16.000 $ (11.200 €) and in 2020 due to experience and scale effects 6.000 $ (4.200 €) respectively.

Technical improvements are also expected. Through the further development of existing concepts conventional Lithium-Ion batteries could reach an energy density of 250 Wh/kg (Wohlfahrt-Mehrens, 2010). Other technologies as Li-sulphur or Li-air, as well as the adoption of silicon as anode material may lead to much higher energy densities, (see DLR/IFHT/ISE, 2012).

Figure 4: Energy and power density of battery technologies

Source: Kalhammer et al., 2007
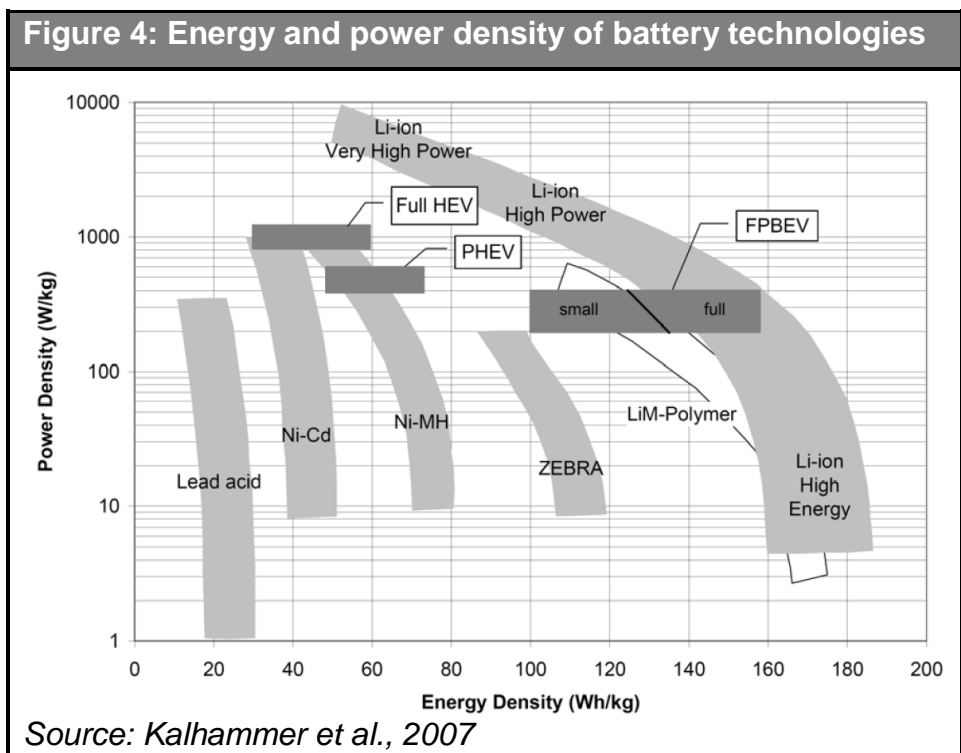
Renewable energy availability

As seen above, a significant reduction of GHG emissions in EVs can only be achieved if EVs are charged to a large extent with electricity generated from non-carbon emitting power sources, other options for climate change mitigation such as the use of bio fuels in conventional vehicles or hybrids have to be discussed as well.

It is proved that the use of bio fuels in the transport sector can contribute to a reduction in carbon emissions, nevertheless, this solution has significantly higher abatement costs than other options as renewable power generation, and present associated problems as the high land use or those concerning food and water supply (JRC, 2008; Pimentel et al., 2008). The world bio crops potentials are uncertain and could be comprised between 97 EJ and 6 EJ (Seidenberger et al., 2008), where the maximum corresponds to the business as usual scenario (BAU) and the latter to the ecological and sustainable scenario, in which "…ecological goals in land cultivation and landscape utilisation are pursued more strongly throughout the world". Other analysis considering surplus agricultural land, marginal or degraded land for farming, as well as biomass residues and waste point out that 33 EJ per year as biomass for energy would be available worldwide in 2050 (Hoogwijk et al., 2003). The IEA assumed for their 450 Scenario a bio

fuel penetration of 9% (11.7 EJ) in 2030 of the total transport fuel demand of 126 EJ (OECD/IEA, 2009), and for their Blue Map Scenario a penetration of 26% (29 EJ) of total transportation fuel demand 112 EJ in 2050 (OECD/IEA, 2008). Assuming that the potential of sustainable biomass is comprised between 6 and 33 EJ it would cover a maximum of 30% of the transportation fuel demand scenarios of the IEA by 2050.

In the last years, power generation from RES has become significantly more important in many regions of the world. In the EU power generation from RES accounted in 2007 for 15.6% of the total electricity demand and in 2010 for 21% (EUROSTAT, 2010). This positive trend is expected to continue thanks to effective promotion schemes, but also driven by further cost reductions and by fossil fuel price increase. The Energy Concept of 2010 (BMWi, 2010) sets a long term target in Germany of 80% of power generation from RES by 2050. The feasibility of these high renewable penetrations has been demonstrated in several publications of the DLR Institute of Technical Thermodynamics, e.g. (Scholz, 2012) and (Nitsch et al., 2012).

Other factors

There are other important factors, such as the expected significant required reductions of urban air pollution, governmental support programs of key industries, increasing urbanization that could favour vehicle electrification.

In contrast to conventional vehicles, EVs do not cause "tank-to-wheel" emissions, either carbon, other air pollutants; even engine noise is much lower. These pollutants can pose high risk for human health especially in big cities where their concentration is higher causing asthma, bronchitis and even cancer (Seifert, 2005). With the purpose of reducing pollution and streets congestion some cities, as Stockholm, London, Singapore or Shanghai, have introduced congestion charge for cars entering the city centre. A different approach has been followed in certain German areas with high population density[8], where circulation for vehicles with higher emissions is prohibited. The emissions of soot particles and of nitrogen oxides of the new car market is regulated in Europe by the Euro-norms, the new Euro-6 coming in September 2014 is expected to present stricter

---

[8] In German defined as Umweltzonen.

emission standards for diesel vehicles (Euractiv, 2007). Large Asian cities are also facing problems concerning air pollution and are undertaking similar measures as those in Europe (PDO, 2008, Xinhuanet, 2011).

Besides, other government measures as reducing registration and circulation taxes or introducing a rebate at the purchase price of green cars, as in Belgium, Spain and in China may impact EVs' introduction. A review of these measures can be found in (Hacker et al., 2009).

In 2050 there will be around 9.2 billion people on earth, the urban population will increase in an over proportional way, from around 50% in 2010 of the total world population to almost 70% in 2050 (UNPD, 2007). This increased urbanisation may contribute to pave the way to mobility electrification, as in urban mobility the limited driving range of EVs is less critical, however this could also increase the use of public transportation.

The latest improvements in route guidance systems and in IT could as well favour the introduction of electric cars; in contrast to the beginning of the 1990s these systems could now provide information of the closest available loading stations or of the remaining electrical range for a relatively low price, and significantly reduce range anxiety.

The expected development of distribution networks to smart grids, could simplify the billing as the required IT infrastructure would in part be already available. Besides, the smart grid would allow incentives for EVs to provide system services. These revenues from system services added to the significantly lower costs of electricity if compared to gasoline or diesel fuels would contribute to increase the cost effectiveness of EVs. Research in this area applied to the German market can be found in (Biere et al., 2009).

1.3   Future perspectives

As seen above, there are many factors that could contribute to the introduction of EVs. One of the main factors is climate change. As the EU's recognises, reductions between 60 and 80% of GHG emissions will be needed in the long term. Through a more efficient energy use of the electric drive train and through a shift from fossil fuels to low carbon fuels significant reductions can be achieved. The transport sector relies principally on oil imports. In this context of higher oil

prices, growing demand, progressive depletion of conventional oil resources, and an increasing dependence on foreign oil, it becomes clear that a diversification of energy carriers and the introduction of new technologies will be needed in the transport sector to avert the consequences of future price shocks and supply restrictions, which may occur more often in the future than in the past.

At the time when this thesis was written most car makers have already started or are planning to produce EVs in small series, a detailed list of EVs already present in the market or expected to be commercialised in the near-term can be found in (Perujo and Ciuffo, 2010). However, in order to make EVs a competitive alternative compared to conventional cars further technical development is needed along with cost reduction. Hybrid cars use a relatively small battery and an electric motor to support the internal combustion engine, and can achieve higher fuel efficiencies than conventional automobiles. The development of the hybrid technology might contribute to the introduction of EVs by providing experience in production and integration of electrical traction systems in automotive applications and by driving down production costs through experience and scale.

In the first decade of the 21st century power generation from RES has experienced a sustained growth in many parts of the world. This growth is expected to continue in order to achieve the long term carbon emission reductions, of which power generation is expected to cover an over-proportional share. The higher this share is, the higher the reduction of carbon emissions that can be achieved with EVs.

Due to the reasons presented above, a deep change will be needed to achieve a sustainable transportation; a shift from conventional vehicles with an internal combustion engine to vehicles powered with renewable generated electricity can contribute to reduce global carbon emissions, and to increase security of energy supply.

2 Scope of the present thesis

According to the targets set in the *Energiekonzept* 2010 of the German Government 50% of the electrical demand in 2030 shall be covered by RES (BMWi, 2010). A research project of the German Federal Ministry for the Environment, Nature Conservation and Nuclear Safety goes beyond and shows that in 2030 the share of RES in the German power generation sector could exceed 60% when extrapolating the current market dynamics (Nitsch et al., 2012).

Most RES, such as wind, solar and hydropower[9], depend on weather conditions and power generation based on these energies is therefore not controllable. To represent the impact of these fluctuating power sources on both the requirements of power generation capacity as well as on the utilisation of power generation the load duration curve can be used. The curve can be calculated by sorting in descending order the load values of each time step.

Figure 5 shows the 2010 load duration curve as well as the residual load duration curve in Germany in the same year and the expected for 2030. In the two latter curves, the power generated from fluctuating renewable energy sources has been subtracted from the power demand to show the impact of these power sources on the power system. The power demand profile was obtained from the Consumption Data published by the ENTSO-E and scaled up in order to include the demand of rail transportation according to the power consumption scenario from the study *Lead Scenario 2010*[10] (Nitsch et al., 2011). The power generation from photovoltaic, hydropower and wind power was calculated with the model *REMix*[11] as described in (SRU, 2010). These generation profiles are based on the method described in (Hammer et al., 2003) and (Schillings et al., 2004) for photovoltaic, on wind data from the German weather service (DWD, 2007) and on measured river discharge data (GRDC, 2008).

---

[9] Only run-off-river plants, due to lack of reservoir capacity.

[10] Nitsch et al., 2011

[11] DLR Institute of Technical Thermodynamics.

Due to the expansion of weather dependant RES, the volatility of the residual power demand will increase as it is shown in Figure 5. First, it can be seen that a higher penetration from RES causes higher variations of the residual load, as the difference between maximum and minimum becomes larger; second with the assumptions taken in the *Lead Scenario 2010*, the generation from water, solar and wind power could exceed the power demand by far in some episodes of the year.

Figure 5: Load duration curve of power demand and of the residual power demand

Own analysis based on: ENTSO-E*, Nitsch et al. 2011, DLR, DWD, GRDC.*
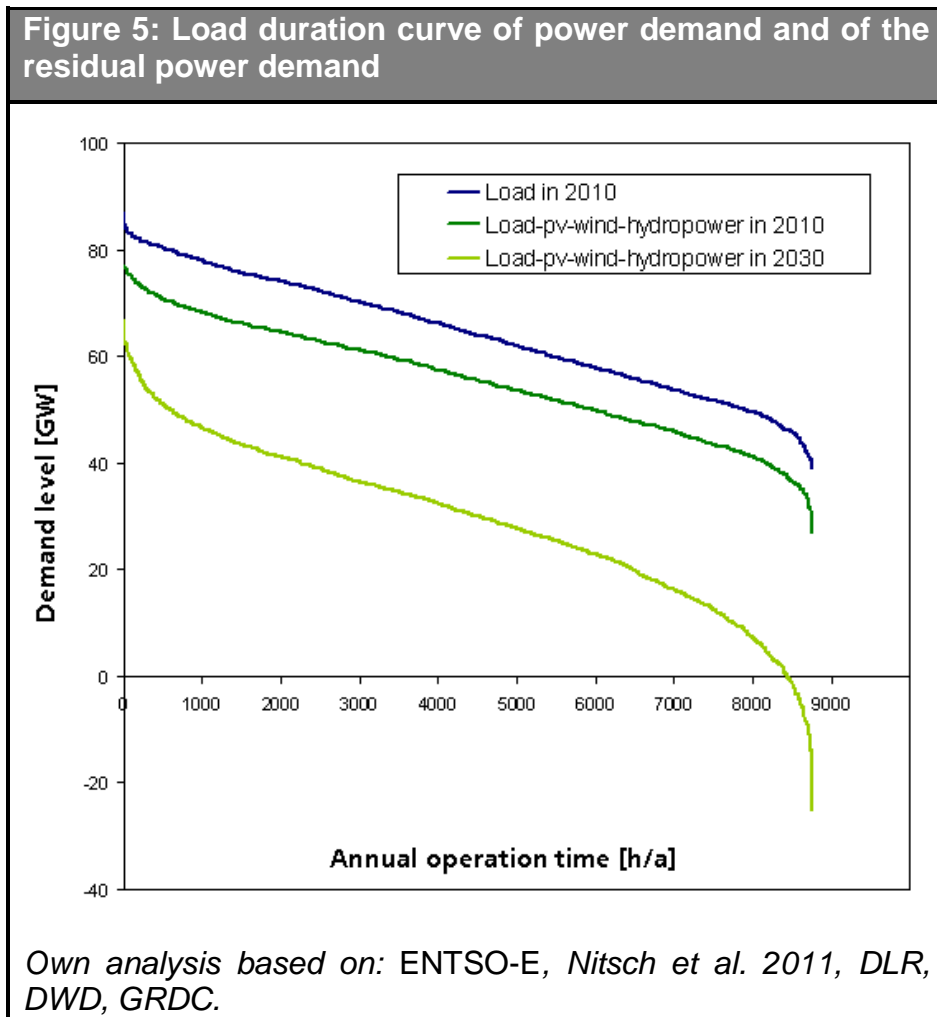
The residual load can be covered by controllable generators, like fossil power plants but also from controllable renewable plants like biomass or solar thermal plants with heat storage. Pumped storage power plants have been used for over 100 years to adapt power generation to demand variations. Other technologies like compressed air energy storage (CAES), hydrogen storage, industrial batteries, or even methane synthesis using RES are at the moment subject of research. Nevertheless, storage generally requires high investments and always

presents substantial energetic losses during the energy conversion processes. An additional option is to increase the transmission capacities of the electricity network, so that in periods of low generation from RES power can be imported from abroad. This can be achieved by building new power lines, which can present long and costly approval processes as well as by upgrading the existing ones. Another possibility is Demand Side Management (DSM), which entails actions to adapt electricity demand to the availability of RES.

Electric vehicles are well suited for DSM as cars remain idle most of the time, it can be decided whether and when the charging takes place. This load management does not affect customers as long as the battery level does not compromise following trips. Furthermore, it can contribute to renewable power integration by charging during wind surpluses and by avoiding it when wind power is low. A promising technology is called vehicle-to-grid (see section 3.2.3). This technology allows for bidirectional power transmission between EVs and the electric power grid, and can thus be used to deliver electricity back to the grid when the residual demand is highest and most expensive.

Using EVs for load management purposes can present important advantages for power system operation. First, by charging EVs in periods of high renewable energy generation or low power demand a higher fuel-efficiency and capacity utilization of conventional power plants can be achieved. Second, the flexibility in the charging of EVs can help to reduce start-up procedures of thermal units as well as the operating reserves' requirements of conventional power plants and storage capacities, which are expected to increase with power generation from RES.

It becomes clear that electrical vehicles and renewable energies present a high degree of interdependence: on the one hand a higher penetration of RES makes EVs more attractive compared to conventional automobiles due to the lower carbon emissions. On the other hand EVs can contribute to the integration of RES through load management and by providing system services.

2.1 Other works analysing the integration of electric vehicles

The broad topic of electric vehicle integration in the power system has been analysed in several studies. Many publications focus on medium-sized areas such as on the state of Colorado (Parks et al., 2007) or on the province of Milan (Perujo and Ciuffo, 2010). Other works concentrate on distribution grids (Probst and Tenbohlen, 2010) (Pieltain et al., 2011) or on the contribution of electric vehicles to control power reserve (Dallinger et al., 2010) (Kempton and Tomic, 2004).

In a research project funded by the Federal Ministry of Economics and Technology in Germany named Net-Elan[12] grid integration issues of vehicles with electrical power train were analysed. This work focuses on the period from 2010 to 2030. The power system scenario considered in this work is based on the *Energieprognose 2009*[13], which in its reference scenario assumes a moderate expansion of renewable power generation, with a renewable energy penetration in electricity of 36% in 2030. The analysis was conducted for typical days, with which the very different situations that can occur during a year were reduced to a small number of days. This methodology is adequate for regional power systems based on conventional power generation; in large interconnected power systems with a high share of renewable and fluctuating power generation this simplification can be misleading, as the large possible combinations of power generation from wind and solar in the same or in different regions, e.g. in Great Britain and in Germany, would remain unconsidered.

Other works from the U.S. focus on the impact of plug-in electric vehicles on the power grid (Kintner-Meyer et al., 2010), the power system used in the analysis is based on a projection of power generation capacities published by the department of energy (DOE, 2009), the projection assumes in the three scenarios for 2030 less than 15% renewable generation as well as a fossil generation accounting for more than 65% of the power generation, coal for over 45%. In this study it was assumed that 11% of the light duty vehicle stock is electric powered,

---

[12] http://www.net-elan.de/

[13] Die Entwicklung der Energiemärkte bis 2030, Energieprognose 2009, Essen, Mannheim, Stuttgart.

and PHEVs achieve a maximum market share of 30% on the new vehicle market by 2050.

The impact on the power system of EVs in California has been analysed in a dissertation for different scenarios of the power system (McCarthy, 2009). Different charging strategies have been considered, such as daytime charging, off-peak charging and also a valley filling. In this work the integration of fluctuating renewable power does not take central stage and future developments in the power system such as the use of an overlay transmission network or storage capacities to integrate large amounts of intermittent renewable power were not considered. The work concludes with "*future analysis should consider renewable-heavy scenarios in greater detail*".

2.2   Existing methods

In the last decades various energy system models have been developed for providing answers to questions of different nature, see (Baños et al., 2011) and (Foley et al., 2010). Some focus on the long term and are more oriented to capacity expansion planning, while others are more oriented to power plant operation. Some models comprise the whole energy sector, and others consider only electricity. Among the different models, the size of the considered area also varies to a great extent. Models of stand-alone applications coexist with others comprising the energy supply of a country or of a group of countries. The mathematical formulation of the models and the algorithms used also varies to a large extent, many models make use of linear programming (LP), others also including integer variables (MILP), some use genetic algorithms (GA) and other exotic algorithms. The purpose of this section is to provide a review of different existing models used in large scale energy and electricity models and introduce some of their limitations.

The *MARKAL* family of models has contributed to energy, environmental and economic planning since the early 1980s. The model *TIMES*, an evolved version of *MARKAL*, has become broadly used in research and other institutions such as International Energy Agency (IEA) for the *Energy Technology Perspectives*

(ETP) studies[14]. These established models with more than 100 licensed users were designed to develop long-term scenarios of energy systems from a global to a local point of view using a least cost optimisation approach. The model considers both daily and seasonal variations using typical days for each season.

The *PRIMES*[15] energy system model has been developed in the framework of research programmes of the European Commission in the E3MLab of the National Technology University in Athens (NTUA) and has been successfully peer reviewed by the European Commission in 1997. The model is designed for medium to long term forecasting, for scenario development and as an energy policy analysis tool. *PRIMES* is constructed in modules and allows analysing the interactions between one of them, like the electricity market, with the transport, residential or the industrial sectors via the power demand and its price. So as to analyse load coverage in each model region *PRIMES*, as well as the *MARKAL/TIMES* family of models defines a set of time slices to represent the different load situations that can occur during a year, considering day and night variations as well as those between the summer and the winter season.

The models *E2M2s* and *JMM* have been developed at the Institute of Energy Economics and the Rational Use of Energy of the University of Stuttgart to analyse long and short term issues of the power system, a detailed description of both models can be found in (EWIS, 2008) and in (Hundt et al., 2009). The first model *E2M2s* focuses on the long term planning of power systems, the model calculates capacity expansion based on the annualised investment costs, seasonal hydro planning as well as international interchanges on a minimal cost basis. Each optimisation is conducted considering perfect foresight for a simplified year consisting of 12 days with 12 time slices per day. The second model *JMM* focuses on the short term and is able to define the optimal operation of power plants including unit commitment on a least cost basis. For this purpose the model of each power plant considers different restrictions to operation such as start-up time, minimum operation time, or the minimum generation. The model

---

[14] Energy Technology Systems Analysis Program (ETSAP). http://www.etsap.org
[15] E3M Lab National Technical University of Athens. http://www.e3mlab.ntua.gr/

is able to take into account the uncertainty of wind power generation using rolling planning defining wind power generation as a stochastic variable.

A further energy model is *ifeon* developed at the Institute of Energy Economics of the Technical University of Munich. The aim of the model is to optimize capacity expansion of thermal power plants. The optimization criterion is the minimization of the discounted costs for the entire power supply in the period. The model ifeon is based on an evolutionary algorithm to optimize the investment and operating costs of electricity generation throughout the period under review. The model was used in the framework of the research initiative Kraftwerk 21[16] to develop a capacity expansion scenario until 2040. In this analysis Germany was considered as an electrical island without import or export. Another model from the same institute, named KEP, was developed to analyse power plant operation issues, such as unit commitment with a higher detail and can be used for validation of the results of ifeon and is also based on an evolutionary algorithm. Further information of the mentioned models can be found in (BET, 2009) and in (Roth and Kuhn, 2008).

The described models are very sophisticated. Some models, such as PRIMES or TIMES, allow modelling not only the electricity sector but also its interactions with related sectors. Other can represent thermal units with a higher level of detail, considering start-up costs and technical limitations to its operation, and take these properties, as well as other factors like the stochastic nature of wind power, into account when calculating power generation capacity expansion. The progressive substitution of fossil power plants by power generation based on RES poses not only additional requirements to power systems but also to power system models. Wind in different regions does not blow with the same intensity at the same time; solar irradiation presents not only very important variations between day and night or between seasons but also from one day to the next. The increasing impact of weather conditions on the power system requires a correct representation of the interdependence of weather related phenomena

---

[16] Kraftwerke des 21. Jahrhunderts. Financed by the German Federal Governments of Baden-Württemberg and Bavaria. http://www.kw21.de/

with the power system and invalidates the use of typical days, which are broadly used in energy models including those presented above.

In the last years some models have been developed, which try to solve this problem by combining a conventional model, e.g. based on optimisation, with geo-referenced weather related data, such as wind speed, solar irradiation or temperature. In the next lines a short overview of the different investigations in the field will be given, for a more detailed description see (Scholz, 2012). One of the first works in the field, developed in the framework of a doctoral thesis (Biberacher, 2004), demonstrates the feasibility of combining geo-referenced potentials of RES with an energy system model based on linear programming; with this modelling approach it is possible to represent the temporal and geographical dependency of power systems with a high penetration of renewable energy. Another important contribution to the field (Czisch, 2005) demonstrated the feasibility of a large scale power system based on renewable power sources covering Europe, North Africa and West Asia. Power generation in the base scenario is based on wind power using hydro power and biomass plants for load balancing; this scenario relies on a strong overlay power grid for the transport of electricity from RES over long distances.

A further model called REMix[17], developed at the DLR Institute of Technical Thermodynamics in the framework of a doctoral thesis (Scholz, 2012), is a further development of the two previously described works. The model is able to calculate the least cost power supply system in Europe and North Africa on a least cost basis using a green field approach. For this purpose the model uses geo-referenced power generation potentials from RES with a high temporal and spatial resolution, other model parameters, such as the electric power demand, technical properties and other cost parameters are taken externally as input.

2.3   Objectives of the present work

The studies mentioned in section 2.1 focus basically on the potential impact of a moderate amount of electric vehicles on power systems, which do present a limited amount of renewable generation but are mostly based on power

---

[17] Sustainable Renewable Energy Mix for Europe.

generation from conventional sources. The present work, written in the framework of a doctoral thesis, aims to study the perspectives of electric mobility in the long term - 2030 to 2050 - when both a high share of RES as well as a widespread use of electric vehicles can be expected. For this situation the use of typical load and renewable power generation situations should be avoided and thus real weather conditions are used.

In this work general aspects will take priority over more specific issues, which are difficult to forecast, and the focus will lie on the fundamental aspects to provide understanding of the main implications of a mobility based on electric vehicles in a power system with a high penetration of power generation from renewable sources. The focus will be Germany, due to its ambitious long term goal for renewable power generation. This dissertation runs parallel to the research project named *Perspectives of Electric and Hybrid Vehicles in a Power System with High Penetration of Distributed and Renewable Power Sources* funded by the Federal Ministry of Economics and Technology of Germany (DLR/IFHT/ISE, 2012). For the next decades a significant increase in long range power transport is expected, this is mainly driven by the expansion of renewable power generation, such as wind power generation in northern Europe or solar electricity from southern Europe and northern Africa. Hence the present work must take this long range electricity transport into account as RES as well as the transmission grid required can greatly impact the German power system. Besides, the model used should represent renewable power generation considering its temporal and spatial interdependence of the different sources and thus avoid the use of typical days or load duration curves which have major drawbacks regarding the representation of renewables in large scale models.

For this analysis, the optimisation model *REMix* will be further developed and used. In contrast to purely stochastic methods for modelling fluctuating renewable power generation, *REMix* provides a representation of real weather conditions and hence allows taking into account the complex interactions between wind and solar power as well as heating. The model will be further developed to include the electric vehicle fleet as a controllable load and a potential storage, for this purpose the charging requirements for driving will be derived from real driving patterns. Besides, the future electric vehicle sales were quantified with the scenario based simulation model *Vector21* (see Mock, 2010)

which was developed in the framework of (DLR/IFHT/ISE, 2012). This model, developed in the DLR Institute of Vehicle Concepts, is capable of simulating the competition between conventional and alternative propulsion concepts on the German new vehicle market. The conventional power plants will be included with a higher level of detail than in the first version of *REMix*, due to the impact of them on very important aspects of this work, such as on the electricity price and on the CO_2 emissions from the power system. Additionally a new model of the CHP plants will be developed. This new model will allow considering the CHP plants as flexible power generators and its impact on the load balancing requirements for electric vehicles by reducing the volatility of the residual load. The model of the power grid is based on the present European transport network consisting of both the AC network and individual HVDC lines, and will be used in order to estimate in cooperation with the FGH[18] the power transmission capacity requirements for different penetrations of renewable power generation and of electric vehicles. The model will allow a differentiation between different regions in Germany, such as coastal areas with typically low population densities and high wind energy penetration and areas with higher population densities like southern and western Germany.

---

[18] The Forschungsgemeinschaft für Elektrische Anlagen und Stromwirtschaft e.V. (FGH) together with its member companies has developed the network planning system INTEGRAL. INTEGRAL is used among others by all German transmission network operators.

3   Low carbon vehicle concepts

At the moment intensive efforts are been made by industry and research for the development of new alternative vehicle concepts, such as hybrids or electric vehicles. However, the internal combustion engine has still significant potential for improvement. New combustion processes, downsizing and turbo-charging, a variable valve actuation or even cylinder deactivation can lead to lower specific consumptions. Some of these methods also reduce air pollutant emissions. Further reductions can be achieved with particulate filters, catalytic converters, or through exhaust gas recirculation. Though with these solutions stricter emissions standards can be achieved, the vehicle costs are higher and the potential improvements of fuel consumption are limited (Wallentowitz and Freialdenhoven, 2011).

Due to oil scarcity, to climate change and as the potentials for emissions reductions of ICEs are limited, either by technology or by costs, the introduction of alternative vehicle concepts seems from today's point of view unavoidable. The purpose of the present chapter is to present the main concepts surrounding alternative vehicle concepts as well as the assumptions made in this work.

3.1   Hybrid electric vehicles

The propulsion system of Hybrid electric vehicles (HEV) combines an internal combustion engine (ICE) with an electrical drive with the purpose of achieving both lower energy consumption and a better driving behaviour. Figure 6 shows the torque curve of electric and combustion engines, its specific fuel consumption and the driving resistance (see Wallentowitz and Freialdenhoven, 2011). It can be appreciated that at low engine and driving speeds, when the required driving torque is reduced, combustion engines present bad fuel efficiency while electric motors can provide not only a higher efficiency but also a superior torque. The combustion engine, in contrast to the electric drive, can still provide at higher speeds a high torque with a relatively good efficiency. Through a combination of both driving trains the combustion engine can be operated closer to its point of maximum efficiency and the driving dynamics can be improved, besides, regenerative braking allows an additional efficiency increase.

Figure 6: Torque characteristic of electric and combustion engines

Source: Wallentowitz and Freialdenhoven, 2011
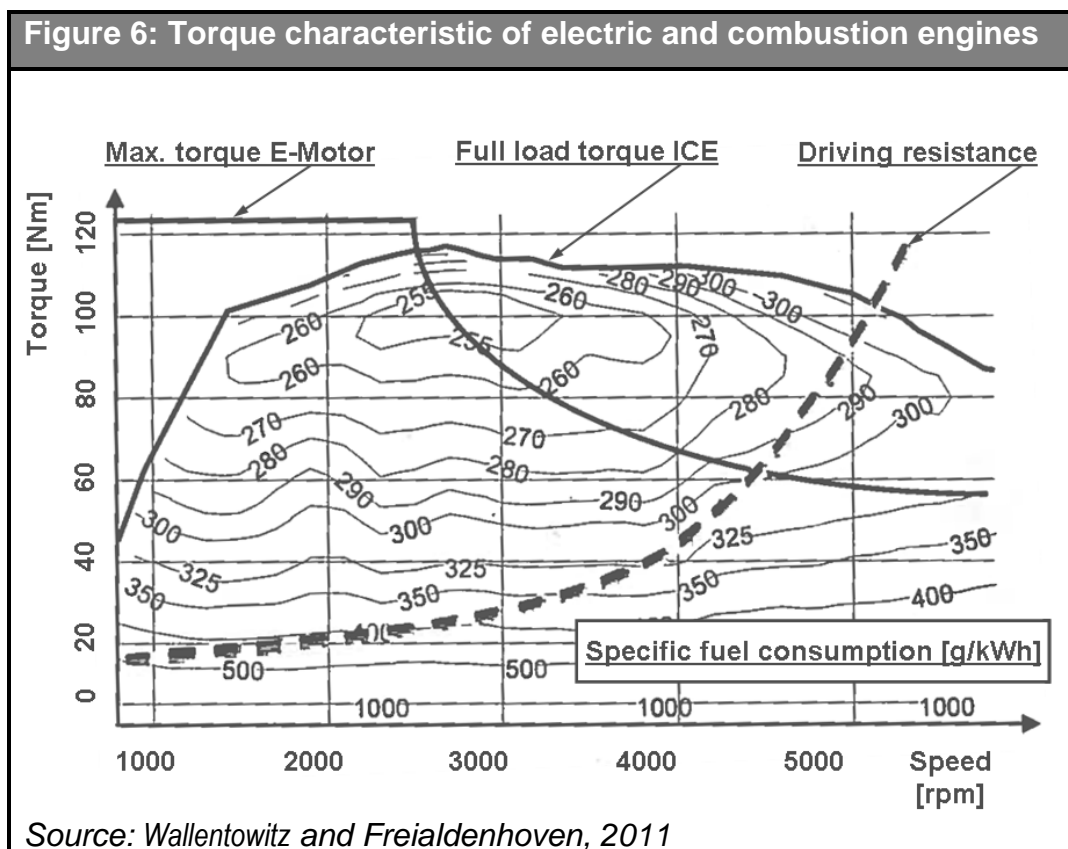
Hybrid vehicles can be classified depending on their degree of electrification. Thus, micro hybrids with a relatively small battery can provide start-stop functionality reducing fuel consumption between 7 and 11% (Naunin, 2007). Including a larger battery and electric drive mild hybrids are able to support the conventional generator during acceleration; the required electricity is produced through regenerative braking. Full hybrids allow additionally a pure electrical operation. A further classification can be made based on the powertrain configuration. In parallel hybrids there is a direct mechanic linkage between the combustion engine and the wheels while in series hybrids the link is electrical and the combustion engine is used to provide additional electrical energy and range. An example of hybrid vehicle is the Toyota Prius, the car in its ZVW30 version has consumption of 3.9l/100 km and tank-to-wheel CO_2 emissions of 89 g/km under the combined New European Driving Cycle (NEDC)[19].

The difference between an extended range electric vehicle (EREV) and a hybrid vehicle lies in the size of the energy storage (VDE, 2010). In this work the EREVs have been considered as electric vehicles as they are designed to be mainly operated with

---

[19] See http://www.toyota.de/cars/new_cars/prius/specs.aspx

electricity from the grid. Due to the reduced battery capacity of hybrid vehicles in comparison to EVs, and often to the lack of plugging capability to the electrical grid, their impact on the power system can be assumed as very reduced and will not be further considered in this work.

3.2   Electric vehicles

The term electric vehicle summarizes various vehicle concepts, as Battery Electric Vehicle (BEV), Extended Range Electric Vehicle (EREV), and Fuel Cell Electric Vehicle (FCV), the first and the second will be presented in the following paragraphs and the latter in section 3.3. In these vehicles, the driving torque is exclusively provided by an electric motor with an inverter drive and the driving energy requirements are taken from an accumulator with electrical output (VDE, 2010). BEVs, as the Nissan Leaf, typically include a high energy battery with an electric range of around 150 km. which is enough for most daily trips, as in countries like Germany 80% of them are shorter than 50 km (infas, 2003). The limited electric range of EVs is solved in EREVs, with a compact gasoline engine able to extend the range to more than 300 miles, or 480 km (BET, 2009). It is assumed that these alternative powertrains will require offering at least similar performance than conventional ones in order to achieve relevant market shares, in this work the cars are dimensioned accordingly.

3.2.1   Specifications of the vehicle types

The vehicles parameters used in this work have been defined in the framework of the cited research project (DLR/IFHT/ISE, 2012), by the DLR Institute of Vehicle Concepts in cooperation with two major German OEMs and a Tier 1 supplier members of the project's advisory board [20]. Table 1 and Table 2 show the assumed technical specifications of BEVs and EREVs considered in this work for three vehicle sizes. Small BEVs are assumed to be city cars with an electric range starting in 2010 at 120 km, medium and large BEVs are suited for longer trips without having to charge the battery. The batteries of EREVs have been dimensioned for an electric range of around 70 km under the NEDC in 2010 and for 100 km in 2050. It is assumed that EREVs are

---

[20] Daimler AG, Robert Bosch GmbH, Volkswagen AG.

driven in a charge-depleting (CD) mode, and once the minimum SoC is reached the range extender starts and the vehicle runs in the charge-sustaining (CS) mode.

The lifetime of the battery chemistry chosen in this work for the car batteries (Lithium-Ion) depends on several factors, e.g. on temperature, on the SoC (Broussely et al., 2005), as well as on the depth of discharge (Kalhammer and Kopf, 2007). By restricting the usable battery capacity, and thus by avoiding deep discharges or high voltages inside the cell, longer life times can be achieved. The usable battery capacity assumed is oriented on the SoC windows the first EVs to be commercialised (see Tuttle and Baldick, 2010). For BEVs it ranges from 10% to 95% of the maximum battery capacity, whether for EREVs it is limited to a usable capacity ranging from 35% to 90%.

Table 1: Assumed technical specifications for BEVs							
		Small		**Medium**		**Large**	
Parameter	**Unit**	**2010**	**2050**	**2010**	**2050**	**2010**	**2050**
Max. speed	e	120		140		160	
Acceleration (0-100 km/h)	s	18		14		12	
Vehicle weight	kg	1155	806	1521	1028	1964	1303
Battery capacity (10-95% usable)	kWh	14	14	22.5	22	33	31
Consumption NEDC / Artemis	kWh/100km	10/14.8	7/10.5	12/19	8/12.9	14/25.3	9/16.8
Consumption aux. cons.[21]	kW	1.0	0.75	1.5	1.1	2.0	1.5
Electric range NEDC / Artemis	km	120/80	180/113	160/101	240/145	200/111	300/157
Source: based on DLR/IFHT/ISE, 2012							

The specific energy consumption for each vehicle type was calculated by the DLR Institute of Vehicle Concepts using dynamic simulations. The driving cycles used are those of the NEDC, which represents a technically feasible consumption though it typically underestimates the real consumption of the vehicle, as well as more realistic cycles based on the Artemis cycles[22]. The consumption data includes the electricity consumption from auxiliary systems, e.g. air conditioning and heating. The efficiency

---

[21] Heating, air conditioning, others.

[22] Highways - 26%, extra urban - 45% and urban - 29% (of driven kilometres).

improvement under the in this way modified Artemis cycles is in line with that under the NEDC.

Table 2: Assumed technical specifications of EREVs		Small		Medium		Large	
Parameter	Unit	2010	2050	2010	2050	2010	2050
Max. speed (cd)	km/h	120		140		160	
Max. speed (cs)	km/h	110		130		150	
Acceleration (0-100 km/h)	S	18		14		12	
Vehicle weight	Kg	1241	878	1574	1121	1966	1406
Battery capacity (35-90% usable)	kWh	13	13	16	16	18	17
Consumption (cd) NEDC / Artemis	kWh/100km	10/14.8	7/10.5	12/17.9	8/12.2	14/23.7	9/15.8
Consumption (cs) NEDC / Artemis	l/100km	4/5.9	2/3.0	4.5/6.7	2.5/3.8	5/8.5	3/5.3
Consumption aux. consumers	kW	1.0	0.75	1.5	1.1	2.0	1.5
Electric range NEDC / Artemis	Km	70/48	100/68	70/49	100/72	70/42	100/59
Source: based on DLR/IFHT/ISE, 2012							

Electric vehicles can extend its achievable range by including an electric generator, which – if connected in series – can provide the electric energy required for those trips which are too long to be carried out just with batteries. One example is the Chevrolet Volt, which includes a 16 kWh Li-Ion battery[23] providing around 50 km electric range as well as a 1.4 litre combustion engine as range extender. Several concepts such as Stirling generators or gas turbines are also conceivable as range extender (VDE, 2010), but also conventional ICEs, Wankel motors or fuel cells. Though still in prototype phase free piston linear generators (Pohl, 2008) present an enormous potential, allowing a higher power density, higher efficiency in partial operation points as well as multi-fuel use. However, Otto motors were considered in this work for future range extenders as the technology is already well known and present low costs. An efficiency comprised between 30 and 34% and a specific power density of 0.5 kW/kg were assumed.

---

[23] To increase battery life only 8.8 kWh can be used.

3.2.2   Loading technologies

Different loading systems regarding the place, speed and nature of the charging are possible. Though most electric cars are expected to be charged at home or at the workplace, public charging stations as back-up infrastructure could be also necessary as many drivers normally park on the street, to reduce range anxiety, or for recharging during longer trips. Whereas, in private domain only standard loading stations are expected, for the public domain fast charge and battery swapping stations are also conceivable. Table 3 provides a classification depending on the power connection (EURELECTRIC, 2011).

Table 3: Definition of different charging methods for EVs				
Power nomination	**Mains connection**	**Power in kW**	**Power in Amps**	**Recharge range/hour**
Normal power	1-Phase AC connection	≤ 3.7kW	10-16 amps	<20 km
Medium power	1- or 3-phase AC connection	3.7 -22 kW	16-32 amps	20 – 110 km
High power	3-phase AC connection	> 22 kW	> 32 amps	>110 km
High power	DC connection	> 22 kW	> 32 amps	>110 km

Source: EURELECTRIC, 2011

Standard station

It is expected that EVs will be predominantly charged during long parking times, i.e. during working hours or at home, therefore electrical sockets for electric cars are first to be expected there. The widespread normal single phase sockets with 3.7 kW connection are enough for most customers (Rehtanz, 2009), with this sockets a full charge of a 20 kWh battery would take around 6 hours, and additional sockets can be easily installed, e.g. in the 50% of German households with a garage (SBA, 2009). Three-phase sockets, presenting a typical power connection of 11 kW, are available in most households and would reduce charging time to around 2 hours.

Public loading stations are more costly than private stations. First, as they are exposed to bad weather conditions and vandalism, they need to be more robust. Secondly, for billing purposes they require both an electricity meter and a device for customer

identification. Commercial public loading stations are already offered by several companies[24]. Electric utilities, like RWE, offer their own charging stations for both public and private use, with a charging power up to 22 kW, including a smart meter and send the billing information via GSM[25]. The G-Station developed by Toyota has a power rating of 3 kW, provides user identification via contact-less smart-card, the economic version, Type A, costs 280.000 yen, or 2500 €, before taxes, installation and service fees[26].

The power outlet of a standard German household with 3.7 kW (single-phase 230 V, 16 A) was taken as reference for 2010. As the EV technology matures a higher share of three phase sockets with 11 kW can be expected. In this work a continuous increase in the average power connection is assumed with 5.5 kW in 2030 and 8.5 kW in 2050.

At the moment commercially available EV chargers present efficiencies of 90%. Higher values up to 97% have been achieved with transformerless chargers using silicon carbide transistors[27]. Here, for this long term analysis, it has been assumed that charging and discharging efficiencies of conventional stations present an efficiency of 95% for both directions.

3.2.3 Loading strategies for plug in electric vehicles

Uncontrolled loading

Is the simplest loading strategy, charging starts after plugging in and ends when completed. It is expected that in the introduction phase most EVs will use uncontrolled loading. EVs will be mainly charged at home after the last trip of the day, this time coincides with the present peak load time of the electricity network which occurs in the late afternoon, and therefore the electric vehicles could increase both the loading in distribution networks and the need for power generation capacities to cover the electricity demand peak. Figure 7 shows the electricity consumption with 100% EV penetration in the Freiburg region (southern Germany), considering the electricity consumption of 2008 based on (Wittwer, 2010). It can be seen that the contribution of

---

[24] ClipperCreek, 365 Energy Group, Toyota Motor Corporation, RWE.

[25] http://www.rwe-mobility.com/web/cms/de/236726/rwemobility/

[26] "*TMC Develops Charger for EVs and PHVs*". Press release, June 2011.

[27] Fraunhofer Institute for Solar Energy Systems. Press Release 20/07/2011.

EVs to the peak power demand can be considerable, and for the 100% penetration assumed the increase will be around 50%. This implies that both, power generation and the electricity grid, would have to be able to transport 50% more power, causing a lower utilisation factor as the consumption increase will be substantially lower.

Figure 7: Load demand in the Badenova grid with 100% EVs

Source: Wittwer, 2010
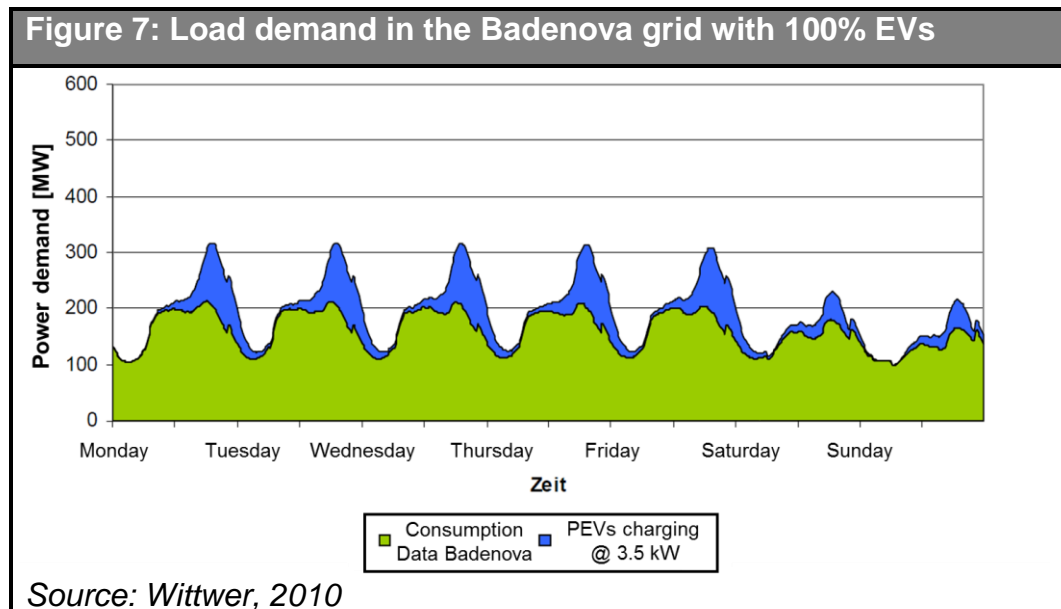
Though in the introduction phase no problems are expected, due to the high simultaneity of car use and power demand (see Figure 7), a certain expansion of distribution grids or a control of the loading times would be required at some point. In Germany for penetrations of fewer than 1 million EVs, objective of the German Federal Government for 2020, no grid reinforcements are expected to be required (VDE, 2010). For each distribution grid the impact of electric vehicles can vary to a large extent, i.e. in residential areas with a high EV density the impact will differ significantly from that in industrial or rural areas with low population density. An alternative to the expansion of the transmission network is controlling the charging process to reduce grid loading at peak.

Controlled loading

Due to the usually long parking times of personal vehicles, EVs present a high flexibility in the charging times, what could have positive effects for the integration of fluctuating energy sources as seen in Chapter 3. Both a direct control of the charging process from the Transmission System Operator (TSO) and an indirect control, e.g. using price signals, are conceivable. The first option, the direct control, could face problems concerning customer acceptance, as the TSO and not the customer decides when the

charging takes place. Nevertheless a pilot project in Berlin[28] showed that this does not seem to be a problem (Schuth, 2010). With the indirect control, electric vehicles would make use of price signals for controlling the charging process, what would present a higher customer acceptance than with the indirect control as the decision is taken on the driver's side. In the mentioned pilot project in Berlin the electricity company involved employed a charging station for each of the 50 vehicles participating in the project which was controlled by the utility via GSM with one phase 32 A connection which allows for a full charge in around 4 hours, the drivers had always the possibility to start charging immediately.

Vehicle to grid

Vehicle to grid (V2G) describes a system which allows electric vehicles for bidirectional electricity exchange with the power grid with the purpose of using the car batteries for power balancing or for providing ancillary services. Hence, in case of low wind power feed-in the EVs could contribute to cover electricity demand in peak times and in case of a sudden outage of a big power block to compensate for a limited time the missing power generation.

The possibility of V2G has been analysed in several papers[29]. In these it was calculated that assuming a power connection of 10 kW the potential net revenues by providing regulation services could account annually for 2554 $, other calculations (Dallinger et al., 2010) using German electricity market data and a power capacity of less than 2 kW arrived at net profits between 300 and 400 € annually. It has to be noted that these calculations assume actual market prices for ancillary services which on one hand may increase in the future as power generation from RES expands, on the other hand the more cars participating the less profitable it becomes.

Another important factor is that the cycle life achievable with batteries designed for EVs exceeds to a great extent the cycles required during a typical car's lifetime (VDE, 2010). During 10 years a typical car's battery will experience 1000 full cycles which is only one third of the typical battery's cycle life for automotive applications. Based on this, using the battery for V2G would not reduce in practice its lifetime. Therefore, the

---

[28] MINI E Berlin powered by Vattenfall, 2010

[29] Kempton and Tomic, 2004; Kempton and Tomic, 2004; Asplund, 2008; Dallinger et al., 2010.

additional costs due to battery wearing could be reduced. However, the battery capacity available and therefore the range could be affected.

3.2.4   Battery technology and wearing

The Lithium-Ion battery technology, due to its superior energy and power density, is the best suited for automotive applications at the moment (see Figure 4). Other technologies, such as NiMH, may present lower unitary costs today, nevertheless Li-Ion has higher potential for cost reduction (Axsen et al., 2008). Therefore Li-Ion batteries have been selected for this work.

Figure 8: Dependence of battery cycle life on SoC variations

Source: Rosenkranz, 2003
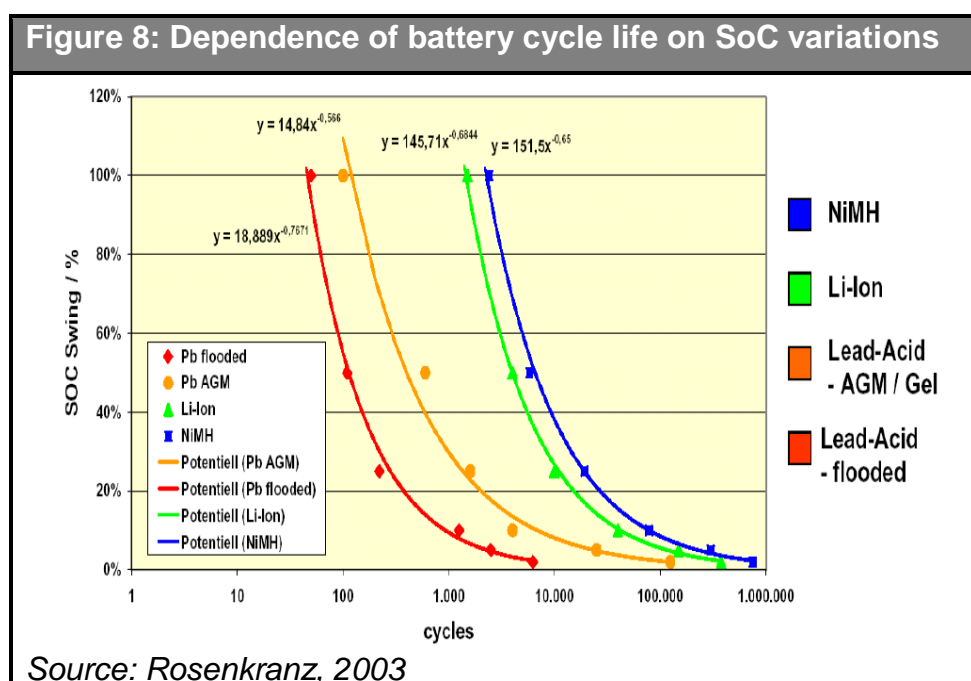
Figure 8 shows the impact of DoD on cycle life for NiMH, Li-ion as well as for lead-acid batteries. It can be observed that the behaviour is very similar, and that for low DoD[30] more cycles can be achieved for all chemistries.

Table 4 summarizes different cycle life data of EV batteries: first two battery goals from the U.S. Advanced Battery Consortium (USABC) as well as from the Sloan Automotive Laboratory at MIT are shown; additionally the cycle life from commercial cells (Li-Ion) is included for different DoDs. Again, as seen in Table 4, for today's commercial batteries as well as for the USABC and for the MIT goals presented, small cycles cause

---

[30] SoC Swing is assumed to be equivalent to DoD in this representation.

significantly lower degradation than deep discharges for the same energy processed[31] (Link et al., 2010) (Axsen et al., 2008).

Table 4: Li-Ion batteries cycle life depending on the charge mode for commercial batteries and the development goals				
Mode	DoD	USABC Goal	MIT Goal	Li-Ion
Shallow	3%	-	-	800,000
Charge Sustaining	est. 10%	300,000	175,000	-
Charge Depleting	70-80%	5,000	2,500	2,000
Source: Link et al., 2010, Axsen et al., 2008.				

To model battery degradation for different DoDs than those shown in Figure 8 a similar approach as in (Link et al., 2010) is used. The authors adopted the following equation to model battery wearing, and assuming for 70% DoD 5.000 cycles and for 3% 1,000,000 cycles obtained the parameters a and b[32].

$$N_{life}(DoD) = a \cdot DoD^b$$

Equation 3-1

In this work this approach was selected to model battery wearing assuming that the cycle life development goals from the USABC for Lithium batteries used in automotive applications are realised before 2030 and that they are valid until 2050.

The battery wearing model described in the previous equation is a very simplified model that does not take into consideration the highly complex reactions that take place in a battery during its lifetime, and both its calendar ageing as well as the degradation produced by high charging rates remain unconsidered. The purpose of this wearing model in the present work is to analyse to which extent and under which assumptions V2G makes economic sense. In the author's opinion V2G will take place mainly during long parking times, in which a normal power connection is assumed. In this situation the impact of the relatively low currents and of the low heat dissipated can be neglected. The impact of cell voltages remains also unconsidered, as it should be of little relevance due to the SoC limitations.

---

[31] As an example for Li-ion: with shallow cycles the equivalent of 800.000 x 3% = 24.000 full cycles are possible. With deeper cycles only 2.000 x 80% = 1.600 full cycles can be realised.

[32] For the given cycle life and DoDs the parameter "a" results in 2744.2 and "b" in -1.682

Other analyses have pointed out that for LiFePO$_4$ cells estimating battery degradation with the DoD might not be the best approach as degradation as it is more dependent on the energy processed regardless of the DoD experienced (Peterson et al., 2010). Nevertheless these results seem only to be suitable for LiFePO$_4$. In this work, which focuses on the long term perspectives of EVs, a more general approach has to be taken that suits most cell chemistries including those that may come in the future. Therefore, to model battery wearing, a DoD dependant approach was chosen. With the following equation the capacity fade per cycle can be calculated assuming a 20% capacity fade during the battery's lifetime.

$$\mathrm{Capacity\,Fade} = 20\% / N_{life}(DoD) \qquad \text{Equation 3-2}$$

The wearing cost per kWh can be calculated depending on the cost of the battery as follows:

$$\mathrm{Wearing\,Cost} = \mathrm{Battery\,Cost} / \mathrm{DoD} \cdot N_{life}(DoD) \qquad \text{Equation 3-3}$$

Figure 9 shows the capacity fade per cycle as well as the wearing costs per kWh obtained using Equation 3-2 and 3-3 assuming the cycle life goals from the USABC. Capacity fade has been approximated using five segments, which will be used to represent this relation in the linear optimisation model. It can be observed that this approximation is a conservative one as the estimation lies above the original curve (dotted) both for capacity fade and for the wearing costs. The error incurred through this approximation lies below 15% for DoDs larger than 10%, which is a small one if compared with other uncertainties involved.

Figure 9: Assumed impact of DoD on capacity fade and wearing costs including linear approximation

Analysis based on Link et al., 2010, assuming USABC goals
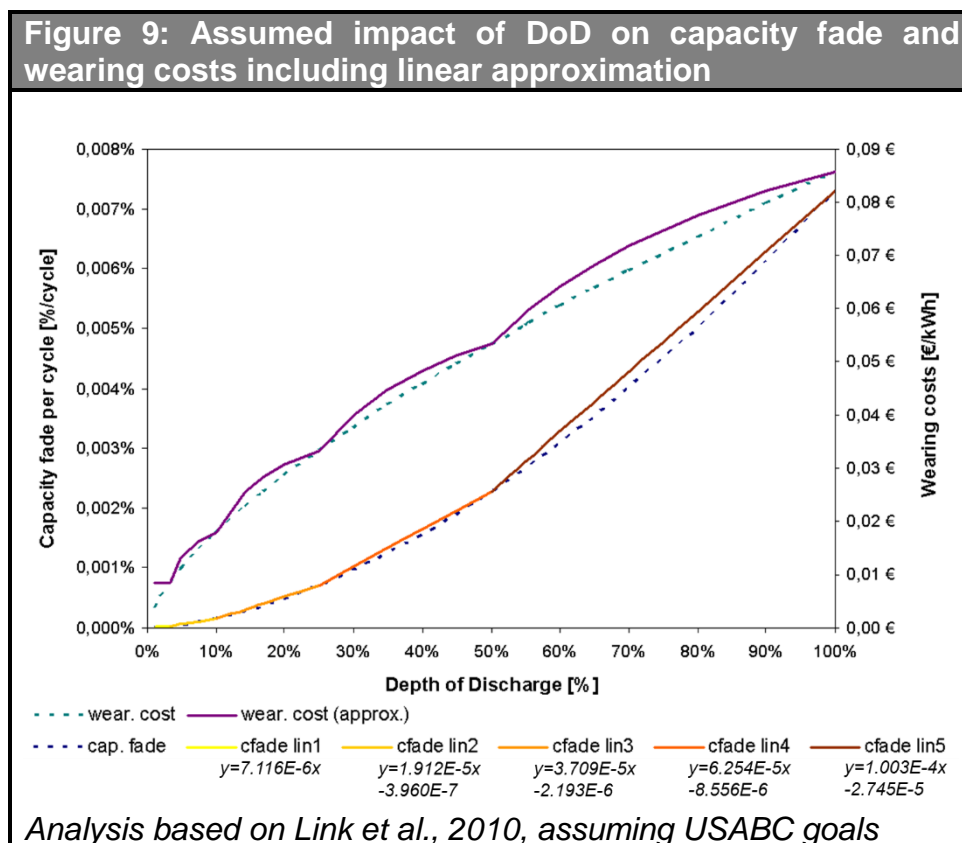
Table 5 shows the scenario of both technical and economical specifications used in this work based on (DLR/IFHT/ISE, 2012). Two different technology developments can be seen, the first scenario assumes a continuous development of existing lithium-ion batteries, whereas in the advanced batteries scenario the now in early development stage lithium-sulphur technology is assumed to be commercialised starting after 2030. In addition, new packaging concepts can provide further weight reductions on pack level. The cost scenario is based on today's values as well as on cost estimations for 2020. To estimate the costs until 2050 learning curves have been applied. In this scenario it has been assumed that the target of the German Federal Government of 1 million EVs in the fleet of 2020 are realised, and that in the long term the EV technology becomes the standard technology in passenger transportation. Important reductions in battery costs can be realised, due to scale effects, experience gained in production and also to further technological developments.

Table 5: Battery specifications assumed for automotive applications						
Business as usual		**2010**	**2020**	**2030**	**2040**	**2050**
Energy density (cell level)	Wh/kg	120	180	230	240	250
Surplus pack	%	50	45	40	35	30
Energy density (pack level)	Wh/kg	80	124	164	178	192
Advanced batteries		2010	2020	2030	2040	2050
Energy density (cell level)	Wh/kg	120	180	230	350	400
Surplus pack	%	50	45	40	20	15
Energy density (pack level)	Wh/kg	80	124	164	292	348
Costs (pack level)	€/kWh	1100	330	235	210	200
Calendar life	years	8	12	14	15	16
Source: DLR/IFHT/ISE, 2012						

3.2.5   Charging profiles

In order to assess the potential impact of the electrification of personal mobility on the power system, some considerations concerning the EVs, their energy demand as well as the availability of loading stations have been made. The assumed vehicles are described in section 3.2.1 and the driving behaviour is based on daily driving profiles published in the comprehensive survey Mobility in Germany (MiD)[33]. In the following the gasoline consumption from EREVs will be shown additionally and the different annual distances travelled of each vehicle type are taken into account.

In order to calculate the load balancing potential as well as the energy requirements of the EV fleet along the day the spreadsheet model *VEnCo*[34] was developed based on the methodology described in (Propfe and Luca de Tena, 2010). It simulates for each vehicle type 17,863 daily profiles of the MiD survey. For each of them, the electricity driving demand as well as the plug-in times are calculated based on the survey data and the plug-in probabilities shown in Table 8 with an hourly resolution. This large amount of profiles is filtered so that the driving distance obtained coincides with the vehicle scenario, besides in the case of BEVs only the daily profiles within the vehicle drivable range were considered.

---

[33] "Mobilität in Deutschland 2008", Federal Ministry of Transport, Building and Urban Development.
[34] Vehicle Energy Consumption.

Figure 10 shows how the maximum and minimum possible SoC are calculated, the maximum corresponds to an uncontrolled loading which starts just after the vehicle has been plugged in, the minimum corresponds to the maximum delay in the charging time, which allows that the last trip of the day still can be realised. For longer trips EREVs make use of a range extender to overcome the limited all-electric range, their fuel consumption is calculated assuming charging after the last trip, so that a potential delay in battery charging does not lead to an increased fuel consumption. It is assumed that PEVs will only provide load balancing in days in which the all-electric range is not expected to be a limiting factor, so that in days with a driving distance exceeding the all-electric range loading will start just after plugging-in.

Figure 10: Calculation of maximum and minimum State-of-Charge of individual driving profiles

Source: DLR/IFHT/ISE, 2012
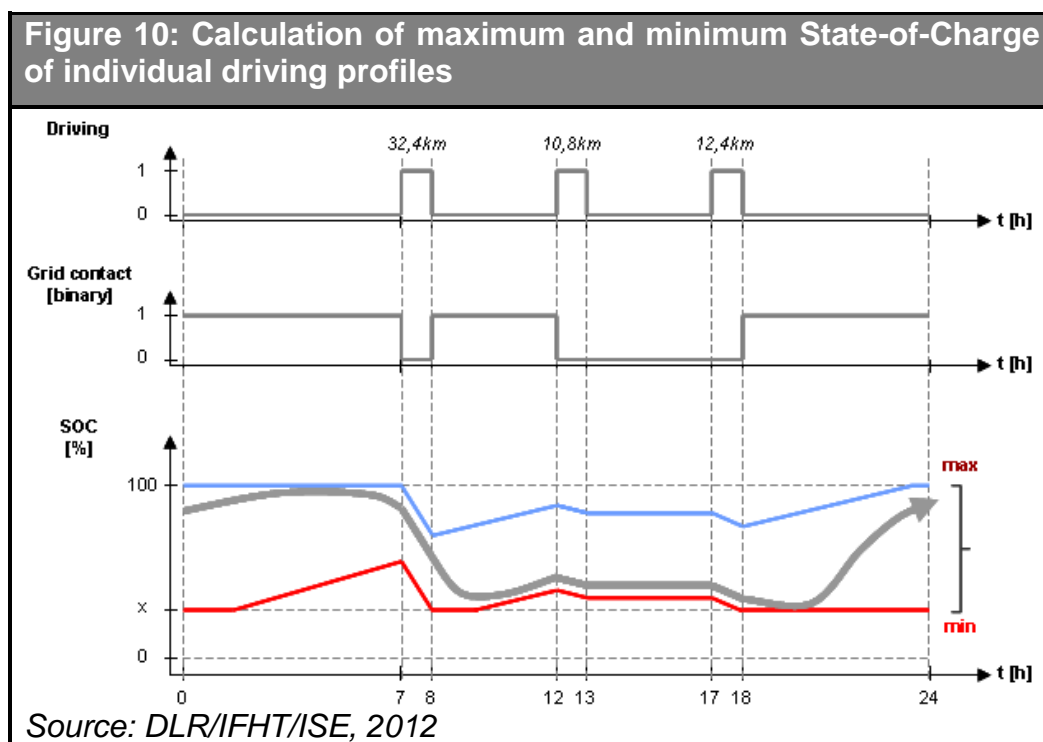
The potential of the EV fleet for load balancing can be assessed by applying confidence intervals to both the maximum and the minimum SoCs of the individual profiles. For a significance level of 95% only 5% of vehicles would require a higher SoC than the assumed minimum (orange line), and only 5% of them would not be able to have the maximum SoC (blue line). Figure 11 depicts the described approach. The blue lines represent the maximum SoC and the red/orange ones the minimum for different significance levels. The higher the significance level the more reduced the potential for load balancing. The calculation assumes perfect foresight and considers only technical

issues, such as the battery capacity, the power connection and the driving requirements. Though this might be taken as an optimistic estimate as there is uncertainty involved in electricity consumption, it can be said that the obtained results are robust if high significance levels are taken. As the maximum and minimum SoC limits of the vehicle fleet are calculated individually, it is possible that both curves intersect leaving no room for load balancing (as in can be seen in the example presented). For the present work a significance level of 95% was taken (darker blue and orange lines), more than high enough in the authors opinion to ensure the outcomes' feasibility, as the resulting SoC limits would be valid for the great majority of driving profiles.

Figure 11: Approach for calculating the load balancing potential of the electric vehicle fleet

Exemplary results of the VEnCo Model for 17.863 daily driving profiles of the MiD survey
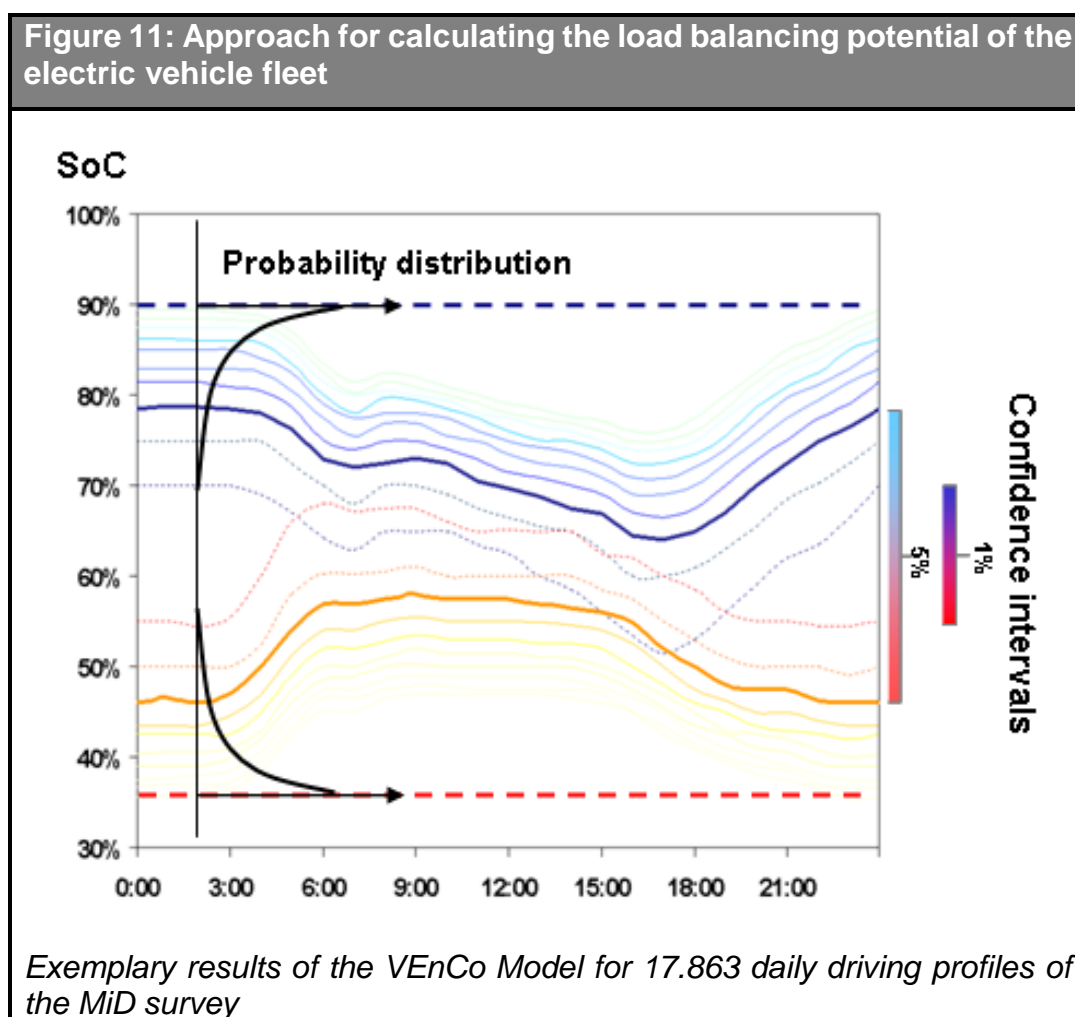
Figure 12 shows the results of the load balancing potential of the vehicle fleet assuming a significance level of 95% for all plug-in electric vehicles (PEV) considered. In all depicted figures it can be observed that the maximum charge requirements occur in the morning as many cars need a full battery to cover the energy requirements of the

trips of the starting day, in the afternoon it can be seen that the maximum SoC takes the lowest values as at the end of the day the vehicles' batteries will present a lower charge. EREVs have less capacity available due to the more limited all-electric range of these vehicles. When comparing the results for 2030 and for 2050 an appreciable increase in the DSM potential is observed for all vehicles as on the one side the all-electric range increases and on the other the annual distance travelled decreases (see Figure 17). Due to the bigger battery size larger PEVs present larger DSM potentials than smaller ones.

Figure 12: Calculated maximum and minimum State-of-Charge curves of the electric vehicle fleet

Results of the VEnCo Model for 17.863 daily driving profiles of the MiD survey, 95% significance assumed, vehicles based on DLR/IFHT/ISE, 2012
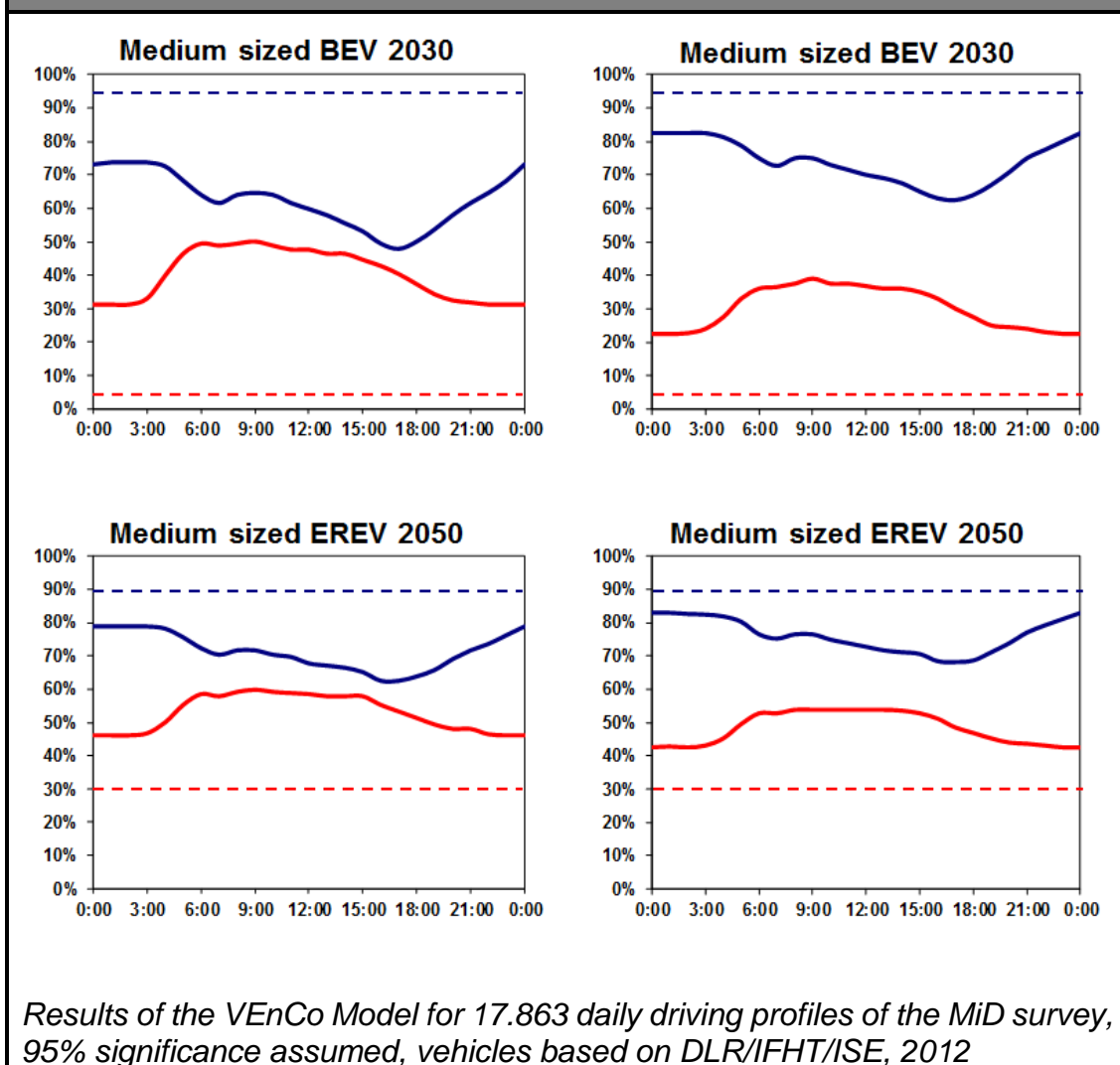
Figure 13: Daily profile of uncontrolled loading, of energy demand and of the share of vehicles plugged-in
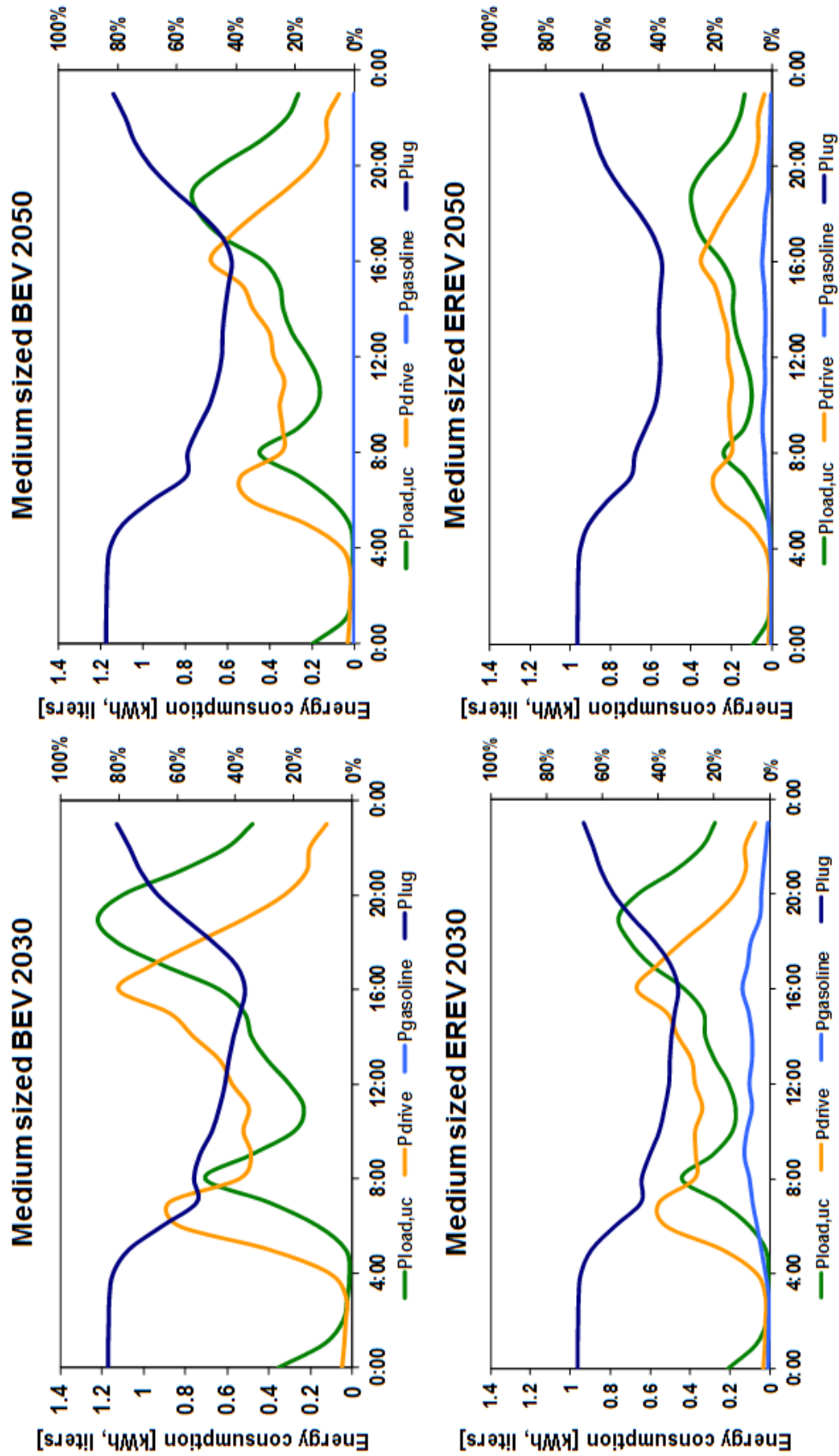
Results of the VEnCo Model for 17.863 daily driving profiles of the MiD survey, vehicles based on DLR/IFHT/ISE, 2012

The average values of the individual profiles can be used to estimate the energy requirements and the amount of grid-connected vehicles. The fleet's electricity and gasoline demand, the share of plugged-in vehicles as well as the power demand from the grid with uncontrolled loading are exemplarily shown in Figure 13 for medium sized BEVs and EREVs. It can be seen that the first present higher electricity consumption than the latter, as EREVs also use hydrocarbon fuels and consequently consume less electricity. The strong reduction in annual distance travelled on average between 2030 and 2050 (see Figure 17) as well as the efficiency increase assumed cause significant reductions in energy consumption per vehicle. For the made assumptions an average medium sized BEV would consume 38% less electricity in 2050 than in 2030 and an EREV over the same period 46% less electricity and 64% less gasoline. Additionally, the electricity requirements with uncontrolled loading are higher in the afternoon than in the morning, as there are vehicles without access to a loading station until the end of the day when they return home.

Table 6: Share of profiles considered and share of distance travelled in charge depleting and sustaining operation					
Vehicle	**Year**	**% MiD**	**% DSM**	**% CD**	**%CS**
BEV-S	2030	31%	97%	100%	-
BEV-M	2030	29%	99%	100%	-
BEV-L	2030	18%	99%	100%	-
BEV-S	2050	60%	99%	100%	-
BEV-M	2050	48%	100%	100%	-
BEV-L	2050	66%	100%	100%	-
EREV-S	2030	64%	67%	64%	36%
EREV-M	2030	47%	63%	62%	38%
EREV-L	2030	54%	63%	62%	38%
EREV-S	2050	98%	74%	78%	22%
EREV-M	2050	99%	74%	69%	31%
EREV-L	2050	77%	72%	68%	32%
Results of the VEnCo Model for 17.863 daily driving profiles of the MiD survey, vehicles based on DLR/IFHT/ISE, 2012					

Table 6 shows the share of daily driving profiles from *MiD* considered (%MiD), the share of the considered profiles which are suitable for DSM (%DSM) and the distance

traveled in charge depleting (CD) and charge sustaining (CS) mode. The considered MiD profiles result after filtering the data so that the BEVs can complete the daily trips and to have the same average annual distance travelled as in the scenario assumed. The results for BEVs in 2030 show a low share of suitable MiD profiles (18-31%), caused by the low range and the high annual distance travelled assumed for these vehicles. This low values indicate that these vehicles can be considered to only suit a small share of drivers, this is confirmed by the vehicle scenario as BEVs in 2030 represent less than 5% of all passenger vehicles. However, future EVs are not expected to be driven in the same way as passenger cars at present as driving patterns will change. The profiles considered suitable for DSM are those in which the daily driving distance lies below the all electric range, BEVs present a very high share of days which are suitable for DSM as they present a higher all-electric range, besides they will be driven most likely with frequent and short trips. EREVs are expected to be driven not only for frequent and short trips but also for longer ones in which battery capacity is depleted, this reduces the number of trips suitable for DSM. An increase in the all-electric range between 2030 and 2050 causes both, an increase in the daily profiles suitable for DSM and for EREVs an increase in CD operation.

3.3   Fuel cell vehicles

Fuel cell systems transform hydrogen directly into electrical power and produce no carbon emissions during conversion. Besides, hydrogen can be produced from RES, such as renewable electricity or biomass. Though its higher range indicates an important advantage if compared to PEVs the fuel cell technology has very high costs (Wallentowitz and Freialdenhoven, 2011), which additionally to the lack of a hydrogen supply infrastructure has hindered until today the series introduction of FCVs (DLR/IFHT/ISE, 2012). In this work, a very optimistic technical development of PEVs is assumed, and FCVs do not play a significant role in individual passenger transportation, see Figure 15. However, FCVs as Heavy Duty Vehicles (HDV) could become a long term solution for emission reductions as the ranges achievable with hydrogen are higher than those achievable with batteries.

3.3.1   Limited alternatives for sustainable hydrogen production

A wide range of options are possible for both hydrogen production and for the supply infrastructure. Its production can take place on-side, such as at fuelling stations, or in a few centralised facilities with distribution via pipeline or truck (see Ogden, 2004). The most common production method for hydrogen is steam reforming (SR) using fossil fuels like natural gas. When a high purity is necessary electrolysis can be employed; however, the costs are higher (Ball and Wietschel, 2009). There are other sustainable alternatives to electrolysis for hydrogen production; some of them are biomass gasification using solid wood, steam reforming or auto thermal reforming using ethanol. Due to the early development stage of hydrogen production from biomass, it is not possible to forecast at present the most adequate production technique. Nevertheless, due to its limited potential and to the concurrent use of biomass for electricity and heat production, as bio fuels in HDV or in air traffic the potential of biomass to fuel FCVs can be expected to be reduced at the moment. This dissertation will only consider hydrogen production from sustainably produced electricity.

3.3.2   Assumed hydrogen supply infrastructure

Defining and modelling the transport and distribution infrastructure for hydrogen supply from the actual point of view for the future is very complex, as "it is not possible to have infrastructure developments without demand and vice-versa" (ICCS-NTUA, 2007). If in the future the so called hydrogen economy is to be realised, it can be expected to be as infrastructure intensive as the electricity or natural gas supply (Hundt et al., 2009). Hence, for the comparatively low hydrogen consumption assumed here, mainly for HDVs and almost inexistent for personal passenger vehicles (Figure 15), an on-site production at the fuelling stations seems more adequate. This solution avoids the construction of a capital intensive ubiquitous distribution infrastructure, which would only be justified with higher demand.

The reference station used in this work for the electrolytic production is based on the HySTAT Hydrogen Fuelling Station [35]. This station comprises in its standard configuration an alkaline electrolyser producing hydrogen at 25 bar, a compressor to 450 bar, storage vessels, a booster, which compresses the hydrogen to 850 bar and

---

[35] Hydrogenics. http://www.hydrogenics.com/assets/pdfs/Fueling%20Station_English.pdf

finally a dispenser. The assumed configuration is based on the costs calculations in a Master Thesis (Fischer, 2011). Assuming variable electricity prices, stations with a larger storage tank and an over-dimensioned electrolyser allow consumption of electricity when electricity prices are low, i.e. with high renewable power generation and low demand. However, there are high investments required to over-dimension the electrolyser. Figure 14 shows the costs per unit of the produced hydrogen in a large H_2 fuelling station depending on the electrolyser's utilisation and on the storage size. The results point out that, in 2030, the hydrogen costs would be higher than the diesel price including taxes and that in 2050 these could lay well below assuming an annual increase of 2% in diesel price. Additionally, for the made assumptions, with 4000 hours of full operation an increasing utilisation has a very limited impact on the average production costs as here the variable costs, mainly electricity consumption, becomes the main cost driver.

Figure 14: Total on-site production costs for large hydrogen fuelling stations in 2050

Source: Fischer, 2011
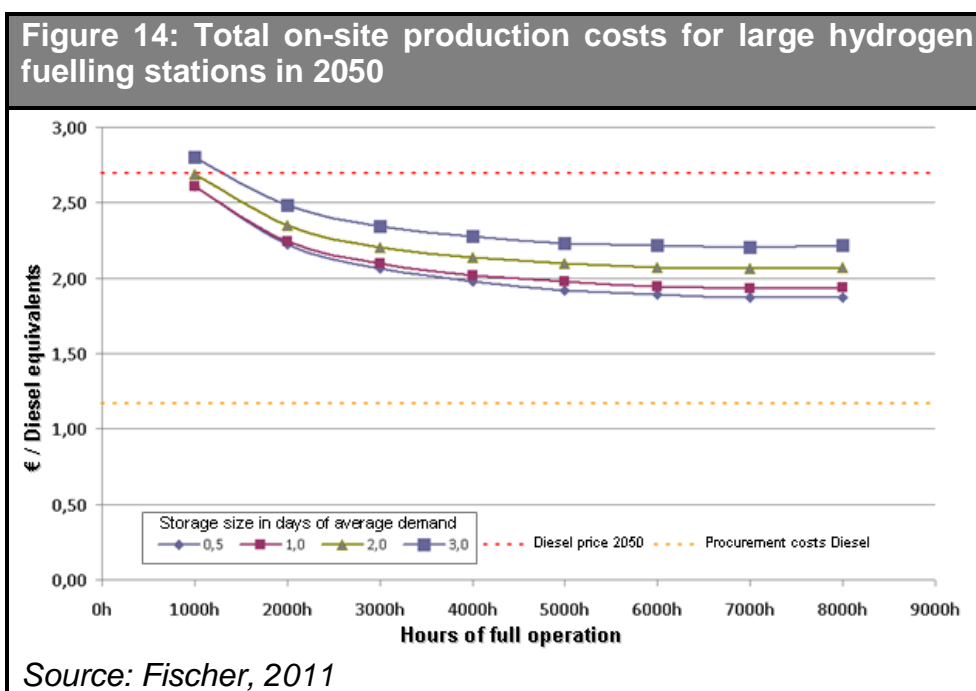
Table 7 summarises the main parameters assumed concerning the modelling of hydrogen stations. The present efficiency of the electrolysis process is obtained from the datasheet of present commercial stations[36], including the energy consumption associated to the 850 bar compression (Gardiner, 2009). An efficiency of 80% is

---

[36] Hydrogenics. http://www.hydrogenics.com/assets/pdfs/Fueling%20Station_English.pdf

technically feasible for electrolysers (FVS, 2004) though this high efficiency only considers the electrolyser and does not include the power consumption of the periphery. Additionally, an electrolyser utilisation of at least 4000 hours was chosen. Though with higher utilisations lower total generation costs can be achieved, a lower utilisation implies a higher production capability in days with lower electricity prices or higher demand. To guarantee an uninterrupted supply it was assumed that hydrogen can be stored at 350 bar, and that the storage size is 12 hours of the daily demand. This size allows compensating the load variations between day and night, and it was taken for future calculations as larger capacities do not seem economical (see Figure 14, from Fischer, 2011).

Table 7: Specifications of the considered reference fuelling station					
Parameter	2010	2020	2030	2040	2050
Efficiency electrolysis & periphery	57.6%	60.5%	63.7%	67.3%	71.3%
Efficiency electrolysis & compression 800 bar	54.8%	57.4%	60.3%	63.5%	67.0%
Utilisation electrolyser	> 4000 full load hours				
Storage capacity	12 hours				
Source: Fischer, 2011.					

If produced through electrolysis, hydrogen as fuel for FCVs causes an additional electricity demand that in the long term can be considerable. The hydrogen consumption scenario of freight and public transport used in this work is that in the scenario B of Nitsch et al., 2011, which assumes for Germany in 2030 a H_2 demand of 0.41 TWh, of 15.08 TWh in 2040 and 56.91 TWh in 2050. This consumption scenario will be scaled for the other European countries considered, depending on actual data of road freight transport[37].

---

[37] Eurostat 2009, Goods transport by road.

3.4 Electric vehicle development scenario

3.4.1 Market perspective

In this work the future scenario of the automobile fleet will be calculated with the simulation tool *Vector 21* (see Mock, 2010). *Vector 21* is able to model the competition between different vehicle technologies in the new car market on a least cost basis. In the simulation the modelled customers choose a certain vehicle depending first on its Total Cost of Ownership (TCO) and secondly on its well-to wheel emissions. The different customers are modelled considering their willingness to pay, their annual driving distance as well as the required vehicle size. On the supply side different vehicle types and variants are considered, the offered price of each vehicle variant varies dynamically depending on the market results of previous years, i.e. the cost reductions in the vehicle components are calculated using learning curves. The results have been validated with historical data of the diesel market share. The scenario assumed in this work has been calculated in the framework of a research project (DLR/IFHT/ISE, 2012). In this research project two scenarios were calculated, the first is a business as usual and the second scenario a sustainability scenario, Figure 15 shows market shares and vehicle stock of the different vehicle types considered.

Figure 15: Market share and vehicle stock scenarios in Germany

Vehicles: G: Gasoline, D: Diesel, CNG: Natural Gas, Hyb: Hybrid variants, EREV: Range-extender, BEV: Battery, FCV: Fuel Cell

Source: DLR/IFHT/ISE, 2012
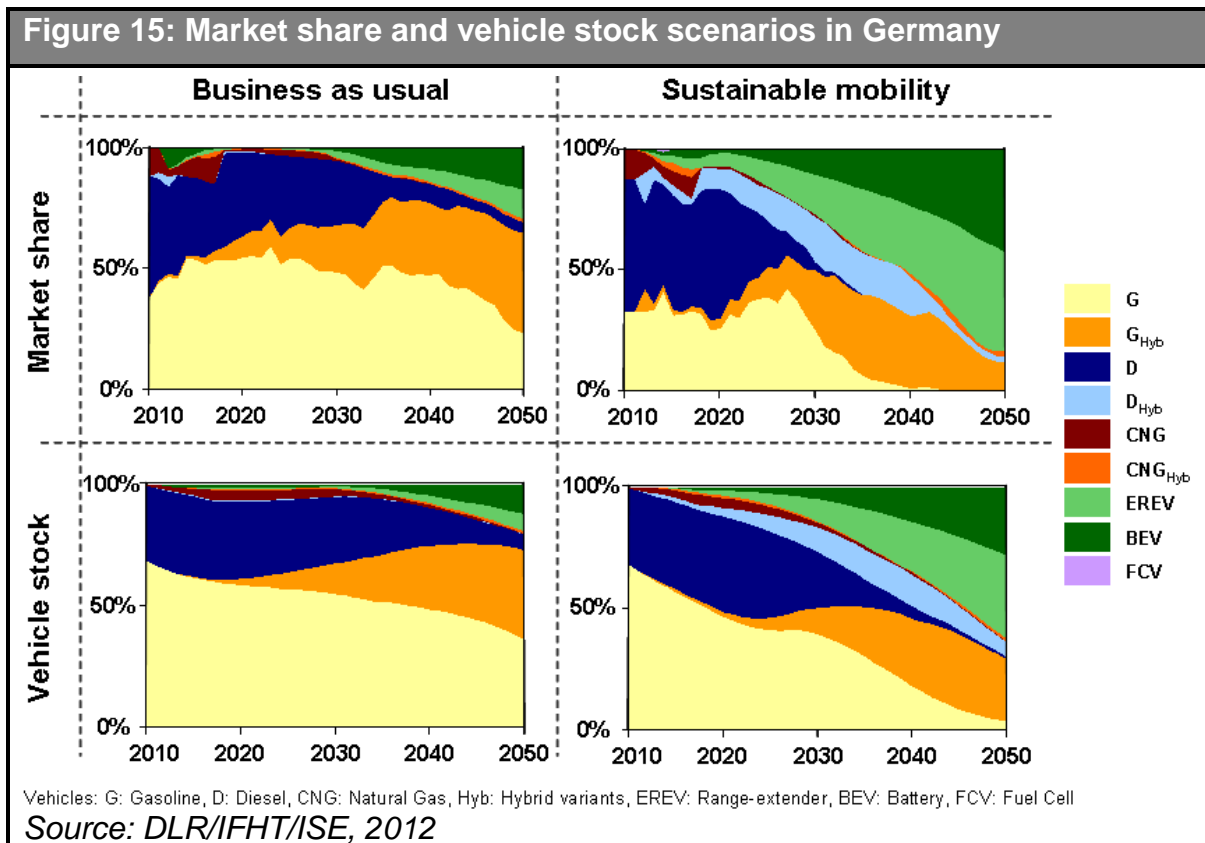
In the first scenario it can be detected that conventional vehicles as well as their hybrid variants still dominate the market in 2050, while in the sustainable mobility scenario BEVs and EREVs present the highest market share. In this second scenario an optimistic development of new lithium based batteries, such as lithium-sulphur, as well as stricter CO_2 emissions standards have been assumed. In both cases it can be seen that hybrid vehicles progressively substitute their conventional variants. Gasoline-HEVs achieve a higher share due to their lower costs if compared to diesel-HEV. It can be also seen that FCVs do not appear in significant amount in the considered period. This has also to do with the high costs of fuel cells and with the assumptions concerning the positive development of the battery technology. In the calculations, mostly due to the high costs of the fuel cell system, a price above 100 k€ was assumed for a medium sized FCV in year 2012. At the moment EREVs can be ordered for around 40k€[38] and BEVs without considering government subsidies or tax cuts for even less[39]. Nevertheless, the potentials for cost reductions are higher for FCV (NRC, 2010). The development of the fuel cell technology, especially a reduction in its costs, would lead to different results.

In the present work the Sustainable Mobility Scenario is chosen for further analysis. The scenario assumes for Germany around 1.4 million PEVs in 2020, 5 million in year 2030 and 27 million in 2050, implying a realisation of the ambitious political objectives set in Germany (NEP, 2009). For other European countries a similar development as in Germany is assumed, considering country specific social aspects, such as its population development or its vehicle ownership.

The model also provides both the energy consumption as well as the CO_2 emissions of the vehicle fleet, the results are shown for the Sustainable Mobility Scenario in Figure 16. A strong reduction of energy consumption can be observed; this has to do first with the higher efficiency of the electric drivetrain if compared to the combustion engine and second to future efficiency gains in all vehicle types. Even stronger reductions can be observed in the CO_2 emissions, this has also to do on the one side with the very important reduction in energy consumption and on the other with the shift from fossil fuels to renewable energy, such as wind power or biomass.

---

[38] "*Opel Ampera – revolutionäres Elektroauto ab 42.900 Euro*", press release 11/11/2010

[39] "*Nissan announces European prices of Nissan Leaf…*", press release 17.05.2010

Figure 16: Energy consumption and CO$_2$ emissions of the vehicle fleet in the Sustainable Mobility scenario

Source: DLR/IFHT/ISE, 2012
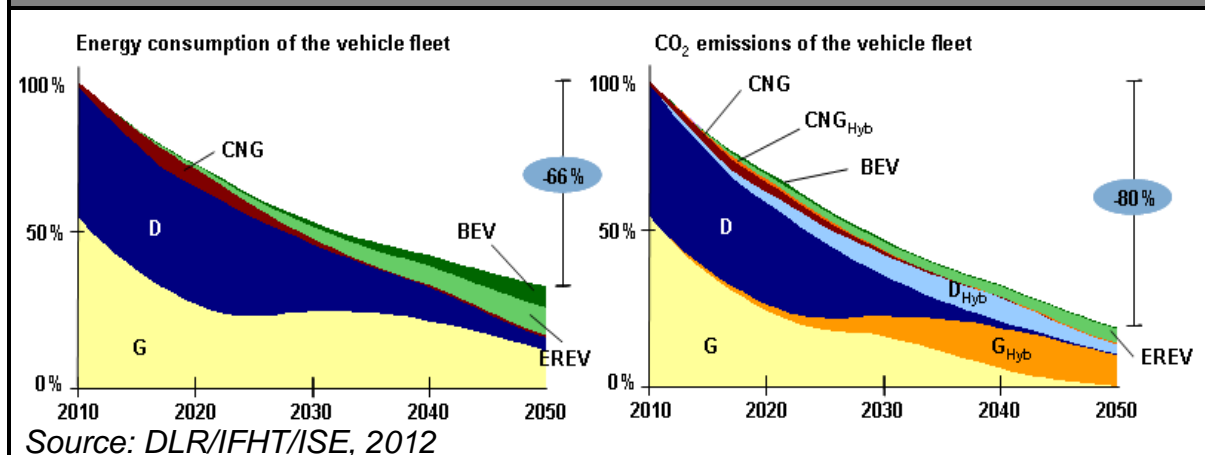
Alternative vehicle concepts have the advantage of lower operating cost, though they typically have higher purchasing costs. From a purely economic point of view, these vehicles can present an advantage if compared to ICEVs for customers with an annual distance travelled exceeding a certain breakeven point. Results of Vector 21 for the sustainability scenario (see Figure 17) show that customers of alternative vehicles drive on average more kilometres than those using conventional vehicles. This can be expected as the consumer choice model is TCO based. It can also be seen that diesel vehicles represent higher mileages than gasoline ones, HEVs would represent even higher annual mileages and EREVs and BEV would represent the highest. It can also be seen that apart from the years around 2015 this order is maintained with time. The average distance travelled of BEVs is lower than that of gasoline-HEVs due to regulatory support which is assumed to end between 2015 and 2020. As time passes and alternative vehicles experience cost reductions they become economical, not only for customers with a higher willingness to pay and higher distances travelled but also for customers with an average driving pattern.

Figure 17: Vehicle fleet average distance travelled for the considered vehicle concepts

Source: DLR/IFHT/ISE, 2012
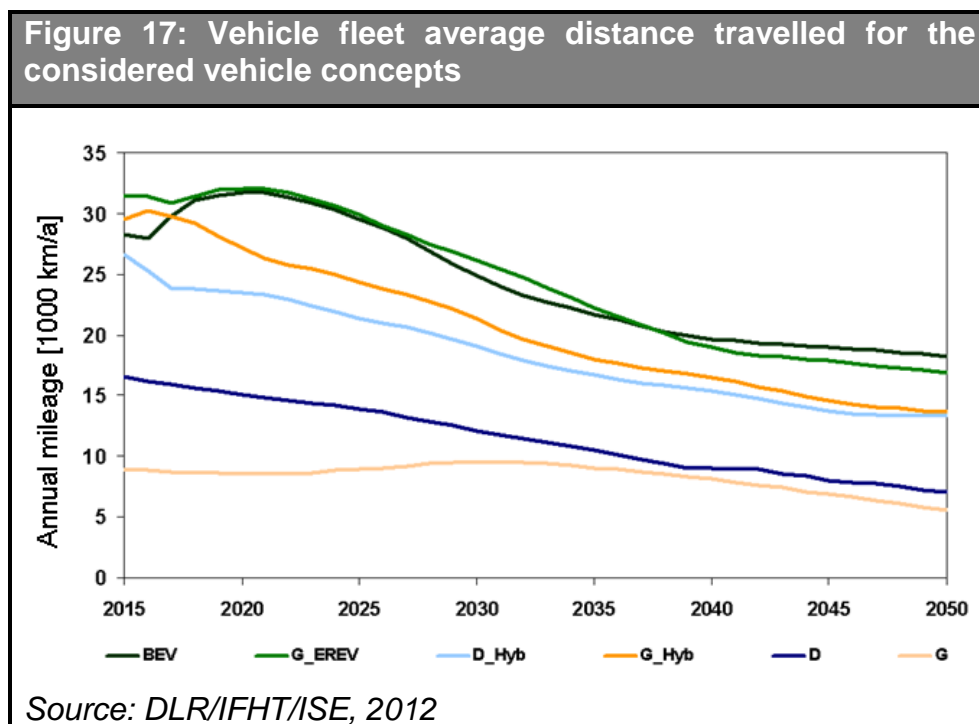
The model used to produce the passenger car scenarios used in this work, *Vector 21*, focuses on passenger vehicles. The electrification of motorcycles, of heavy duty vehicles or an increased use of rail transportation can contribute to further reductions in CO_2 emissions and in energy consumption. Consistently, the results point out that for the actual driving pattern EVs will only make a small share of the German passenger vehicle market until the time between 2020 and 2030 and for the whole fleet some years later. The results indicate a strong impact of utilisation on the cost effectivenes of PEVs, i.e. in the development phase they will only be cost effective with a very high annual distance traveled. Due to their limited range many argue that PEVs only make sense as a secondary car; however a recent consumer study of BEVs points out that most households prefered the BEV as their primary vehicle for reasons such as driving performance, operating costs and pollution (Turrentine et al., 2011). It is clear that driving behavior has a strong impact on the penetration of EVs.

3.4.2   Charging station deployment and use

An important matter concerning the charging of electric vehicles is the deployment and use of charging stations. In this thesis it is assumed that in the introduction phase the deployment will start in private areas, mostly at home and in the workplace (VDE, 2010), and will continue in public domains such as in parking lots, at train stations,

shopping malls and universities. After the introduction phase a quantitative deployment of loading stations is assumed as the EV fleet in Germany increases from 5 million in 2030 to 27 million in 2050.

Depending on the purpose of the trip specific probabilities for finding an available loading station and plugging-in have been considered. These probabilities are assumed to increase slowly during EV introduction as charging spots are installed in the public domain and then to remain constant. The following table shows the probabilities assumed for each of the driving purposes considered (Propfe and Luca de Tena, 2010).

Table 8: Probabilities of finding an unoccupied charging spot								
Work	Education	Business	Escort	Private	Shop.	Leisure	Other	Home
50%	40%	10%	10%	10%	30%	30%	10%	70%
Source: Propfe and Luca de Tena, 2010.								

In many of the actual pilot projects controlled loading is used to analyse with real car drivers the load balancing potential of EVs[40]. However, in this work it has been assumed that in the next decade due to the low EV penetration and to the higher costs involved the deployment will mainly consist of uncontrollable charging spots in the private domain. After 2020 as the EV technology becomes established and the load balancing requirements increase, mostly due to the higher share of intermittent power generation and to the problems associated with a higher demand from PEVs during peak time, controlled loading will progressively become more common. Finally saturation will be reached, as there will not always be a smart charging device available or due to customer related issues. A moderate share of bi-directional charging is assumed to start in 2030, and account for 35% of the vehicles in 2050. The assumed scenario (see Figure 18) during the development phase is in line with (Markel et al., 2010), as penetration of PEVs increases a growing share of managed loading is assumed.

---

[40] MINI E Berlin powered by Vattenfall, RegModHarz and Harz.EE-mobility projects.

Figure 18: Assumed share of the loading procedures depending on the loading strategy

Source: Own analysis based on Markel et al., 2010.
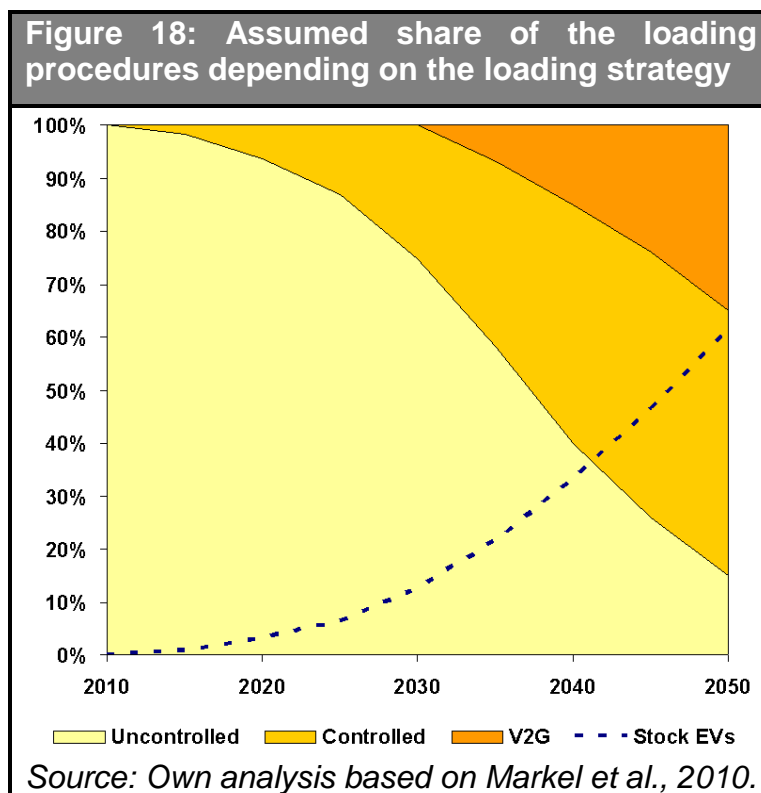
3.5   Other considerations

In this work it is assumed that charging at home or at work with connections up to 11 kW will cover most of the required electricity demand, that pure BEVs are not used so often for long trips, and that fast charging is not expected to represent an appreciable share of the total charging procedures for normal car use (Engel, 2010). Inductive loading stations can offer a more comfortable vehicle use; however, they are more expensive and less efficient than conventional charging stations with cables, and its impact on the total power consumption is assumed to be very low. A battery swapping system though it may be a good solution for fleets, such as taxis or delivery vehicles are not considered in this work for passenger cars, due to the higher system costs and problems related to battery standardisation.

4 Power system scenarios and modelling

As the transport sector, the power system is also expected to experience severe structural changes. In countries like Switzerland or Norway renewable energy sources like hydropower have played a major role in power generation throughout the 20th century. Other countries like Denmark, Germany and Spain have experienced in the last years a very significant increase in power generation from other renewable sources like solar or wind. The Desertec concept has recently gained support from government and industry with the creation of the non-commercial DESERTEC Foundation[41] and the DII[42]. In contrast to the transport sector, in power generation significant changes have taken place in the last years and power generation from renewable sources already produce an appreciable share of electricity consumption in many parts of the world. These changes imply a strong structural change. In most parts of the world power generation is based on large power plants using fossil or nuclear fuel, and make use of a hierarchical transmission network to transport electricity to consumers. The introduction of distributed power generation supposes a significant change in the way the power system has to be operated and planned.

4.1 Power system scenarios

Many different scenarios of power generation are conceivable. In most scenarios a continuous increase in power generation from renewable energy sources is assumed. Nevertheless their development rates as well as the role of other low carbon technologies such as nuclear power or CCS differ to a great extent from one scenario to another (see EC, 2008, GP/EREC, 2007, ECF, 2010). In the scenarios chosen for this work, a constant and sustained expansion of renewable power generation is assumed for Germany as well as for other European countries, which will progressively substitute conventional power generation and thus avoid the need of nuclear and CCS plants in order to fulfil the ambitious CO_2 reduction targets.

---

[41] DESERTEC Foundation, http://www.desertec.org/
[42] DII GmbH, http://www.dii-eumena.com/

4.1.1 Scenarios of electricity demand coverage

In the present work the power generation mix will be based on existing studies. The power generation mix in Germany will be based on a study developed for the Federal Ministry for the Environment in Germany, in which by 2050 electricity powered vehicles cover 66% of private passenger transportation, the additional electricity demand is covered in this scenario by RES accounting for over 87% of the electricity consumption (Nitsch et al., 2011). The scenario in other European regions modelled is based on the Trans-CSP study (Trieb et al., 2006), which also assumes a very high penetration of renewable sources in electricity of which around 15% would come from solar thermal plants in the solar rich regions of North Africa, these renewable imports will be considered in one scenario so as to assess the impact of EVs for different scenarios of the power system.

The purpose of this work is to analyse to which extent EVs can contribute to the integration of local RES. For this purpose, three different scenarios of power generation are used. The *Base Scenario* assumes that all renewable electricity consumed in Germany is also produced in Germany, i.e. local RES substitute renewable electricity imports. An additional scenario called *Trans* considers a Trans-European electricity supply with solar electricity imports from North Africa. In the *Base* scenario smart grids and DSM are more relevant and in *Trans* interchanges play a more important role. However, both scenarios represent a combination of smart grids and electricity highways, in which volatile renewable power generation is integrated both with storage and DSM but also through interchanges. The last scenario of power generation is based on the *Base* scenario but assumes that the electrification of the transport sector does not take off, so that neither PEVs nor FCVs become relevant when analysing the power system. In this scenario called *NEV* (no electric vehicles) power generation from renewable sources has been reduced to compensate the reduction in power demand.

Figure 19 shows the assumed total electricity demand, the demand excluding PEVs and H_2 stations, as well as the power generation from renewable sources[43] for Germany in the *Base* scenario. It can be seen that a very high share (over 85%) of RES electricity is assumed for 2050, in which the most important source is wind power.

---

[43] Renewable power produced in CHP plants has been excluded.

The *Trans* scenario assumes in 2050 130.65 TWh/a solar electricity imports from North Africa, whereas in the Base scenario this energy is produced using local RES. The scenario used in this work assumes that all deviations in EVs demand from Nitsch et al., 2011 and Trieb et al., 2006 are covered by RES. For demand important energy efficiency measures were assumed; hence the annual power demand presents a negative trend until 2030. Then, due to EVs it experiences a sustained increase until 2050, when it accounts for 625 TWh/a.

Figure 19: Development of renewable power generation and electricity demand in Germany - *Base* scenario

Source: Nitsch et al., 2011, Trieb et al., 2006
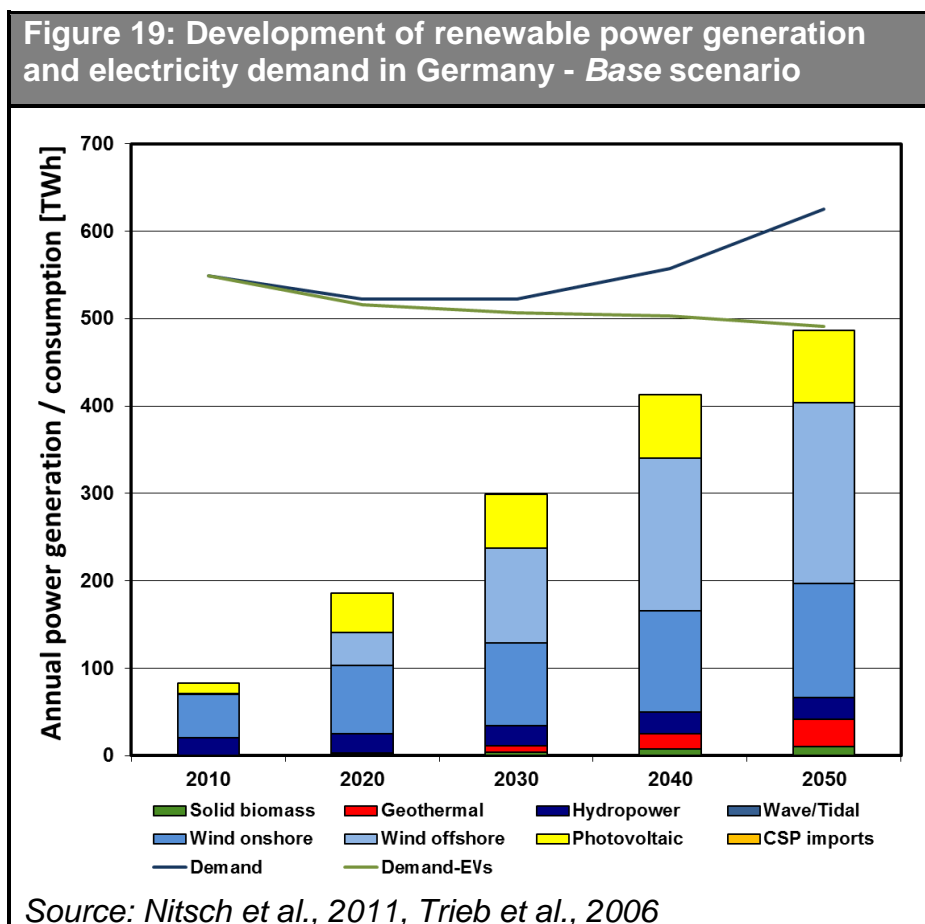
In the modelled European regions (see Figure 23) a similar RES-penetration as in Germany is assumed based on Trans-CSP (Trieb et al., 2006). Figure 20 shows, similarly to Figure 19, the total power demand and renewable power generation but now for all considered regions. Again, this scenario assumes a very strong increase in energy efficiency and eventually a decline in electricity consumption excluding EVs, which were not considered in the above mentioned study. The additional electricity demand for PEVs and H_2 stations in other European countries was based on the analysis made for Germany (see DLR/IFHT/ISE, 2012), and was obtained by extrapolating the scenario for Germany taking into account for passenger cars factors

like population development, vehicle ownership or freight transport statistics. Again, the additional electricity demand was covered by installing additional power generation capacity from RES. In the *Base* scenario the solar electricity imports assumed in Trans-CSP (Trieb et al., 2006) are substituted by local RES. The power generation capacity from RES was increased to take into consideration the additional demand for EVs so that the electric energy required by the EVs comes from renewable sources and in the *Base* scenario to compensate the lack of solar electricity imports. In order to allocate the additional renewable generation among the different technologies it was assumed that the total share of each renewable source in each region remains constant, unless by doing this the potentials calculated as described in (Scholz, 2012) are exceeded. In this case a cap is set and the remaining generation will be covered by other renewable sources.

Figure 20: Development of renewable power generation and electricity demand in all considered regions - Base scenario

Source: Nitsch et al., 2011, Trieb et al., 2006
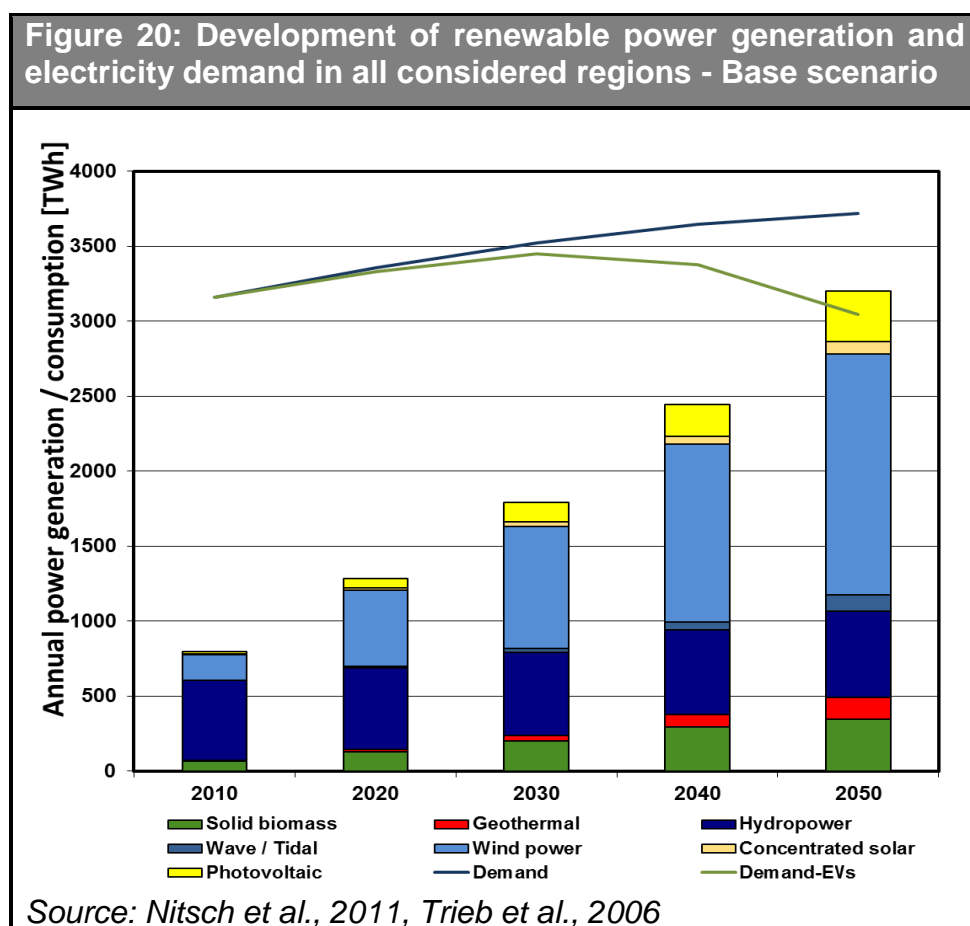
The annual power generation scenario from RES in the three considered scenarios is shown in Figure 21. The *Trans* scenario represents an optimistic development of EVs as well as of solar electricity imports, in the *Base* scenario it can be seen that the solar electricity imports are substituted by other RES mainly wind power. The NEV scenario

presents a lower power generation from RES, the difference corresponds to the annual demand of EVs as it is assumed that the total demand of EVs has to be covered by RES, as it is the only way to make EVs a sustainable option.

Figure 21: Renewable power generation scenario in the *Base*, *Trans* and *NEV* scenarios for all regions

Source: Nitsch et al., 2011, Trieb et al., 2006
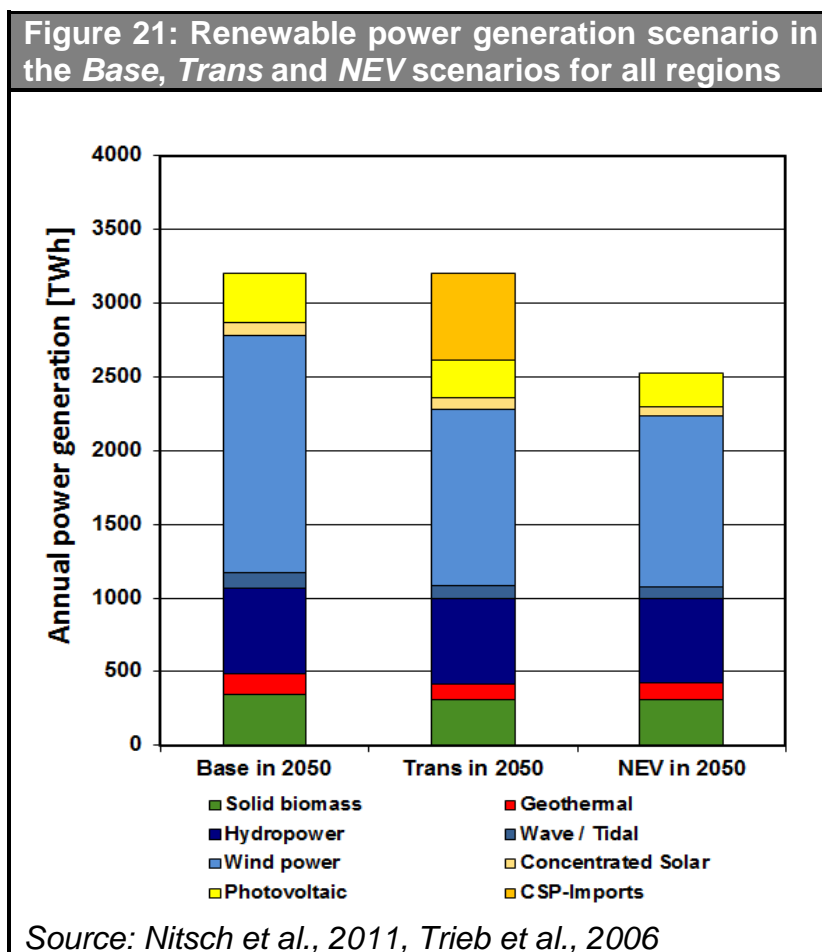
The scenario of conventional thermal power generation capacity is depicted in Figure 22 and is common to all scenarios. It shows the assumed installed capacities of steam, gas and combined cycle turbines depending on the fossil fuel used as well as those of distributed CHP plants in Germany. For thermal generation, installed capacity is shown instead of power generation, as the latter is not an input to the model but a result. First, it can be observed that an important reduction in installed capacity takes place as power generation from RES increases. However the scenario assumes that, though with a lower utilization, a certain generation capacity has to be maintained to warranty supply when wind and solar generation are low. A shift from base load plants fuelled with coal and nuclear fuel to peak and medium load using natural gas can also be seen. Nuclear power generation declines as older plants are decommissioned in line

with the nuclear phase-out of the German federal government[44]. Additionally, the installed capacity of distributed CHP plants using natural gas or biogas increases substantially resulting from energy efficiency support policies. In Europe a similar development of conventional thermal plants is assumed as in Germany with also a strong reduction of installed capacity as well as a strong reduction of nuclear and coal plants.

Figure 22: Installed capacity from conventional thermal units and CHP plants in Germany

Source: Nitsch et al., 2011, Trieb et al., 2006
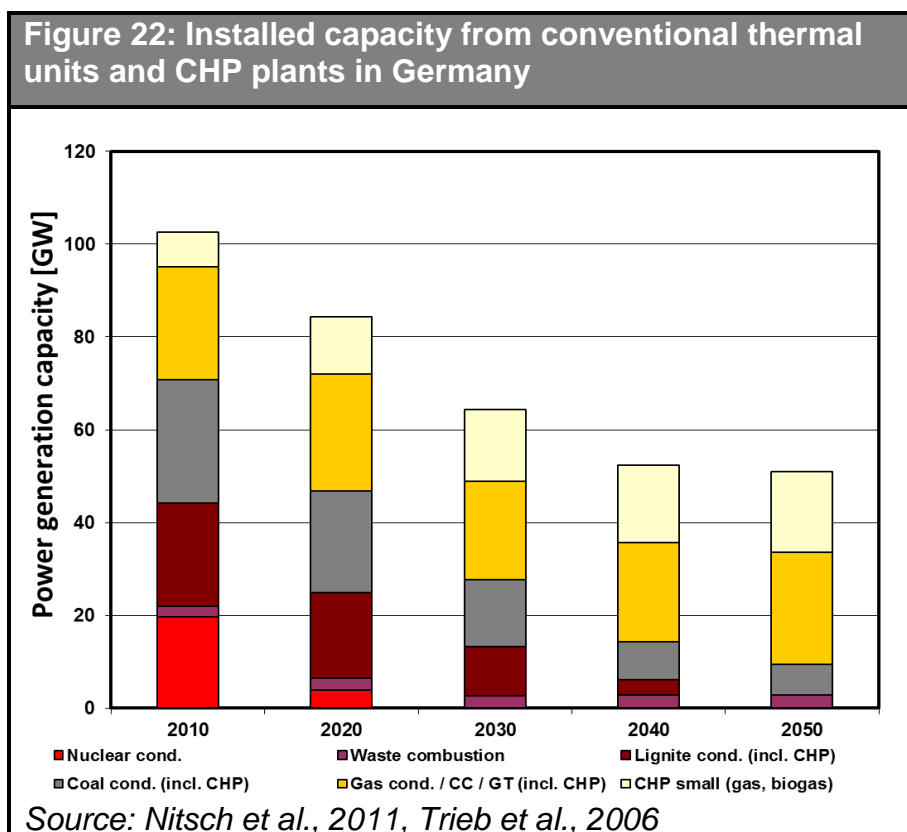
In order to optimize the operation of thermal power generation units more detailed information as that available in the mentioned studies is advantageous. For instance, the age of a thermal unit correlates strongly with its efficiency, costs and emissions, as typically older units are not as efficient as modern ones. In Trans-CSP no separate classification between non-CHP and CHP units or between coal and lignite plants was made, but lignite prices are much lower than those of coal and hence achieve longer operation times. An additional issue is that power generation was classified based on the type of fuel used and not on the power generation technology. GTs and CCGTs in Europe are aggregated in both studies into the categories gas and oil. Nevertheless

---

[44] According to "13. Gesetz zur Änderung des Atomgesetzes, 31st July 2011".

they have very different properties and dynamic behaviour so that they should be considered separately.

From a database of power plants in Germany (UBA, 2010) and in Europe (Platts, 2008) information about the construction year, fuel used and turbine type of the main units in operation and in the planning phase can be obtained. Based first on the mentioned scenarios and second on the information provided in the databases the scenario used in this work for the conventional power generation mix until 2050 was outlined. As a simplification it was assumed that the lifetime of thermal generation units reaches forty years and that the relative share of GTs and CCGTs in the group gas & oil and of lignite and coal in the group coal remains until 2050 as in 2010. In the annex the resulting scenarios used in this dissertation are shown for each considered region and power generation technology.

Figure 23: Delimitation of the modelled regions

Source: DENA, 2010, VDE, 2011.
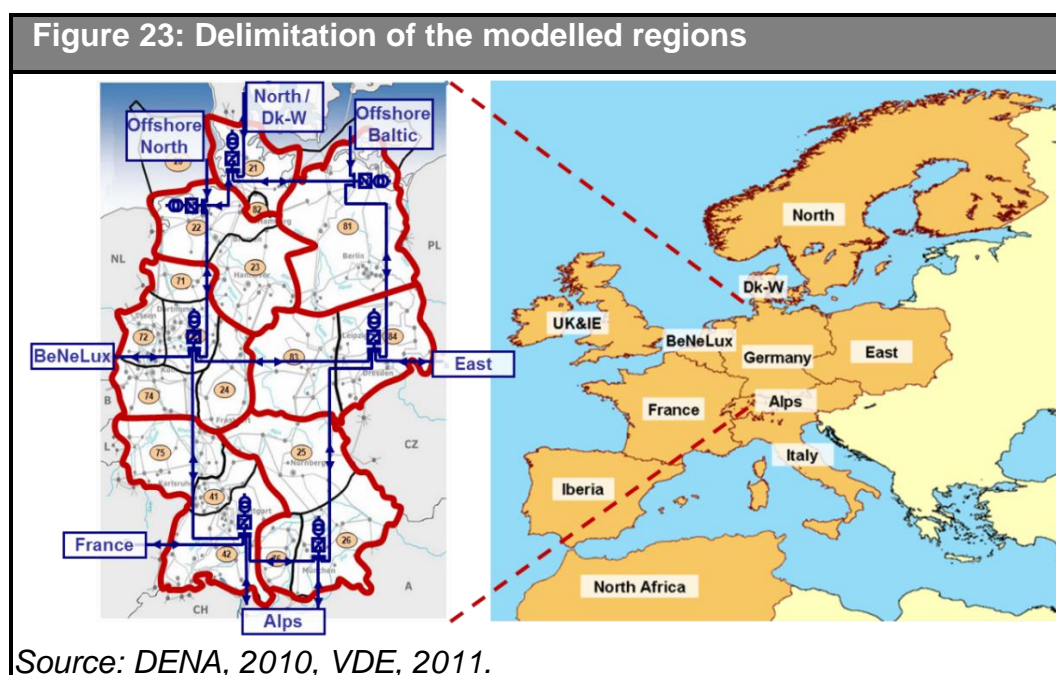
4.1.2   Regions considered

This work is focused on Germany, however in order to take the potential power flows from renewable resource rich regions to consumption centres the modelled region also includes other European countries as well as North Africa. The British Isles present very good conditions for wind power generation, while Southern European regions as well as North Africa are well suited for solar electricity production. Other regions such as North-Eastern Africa or the Middle East also have good conditions for solar electricity, however, due to the longer transport distances and the higher political

instability of these regions they are not considered in this study. Most wind parks in Germany are placed in northern regions where wind speeds are typically high; whereas photovoltaic generation has a higher relevance in the South, the power consumption centres are located in the West and in the South. Figure 23 shows on the left the zones into which the German transmission network used is divided, which results from the aggregation of the regions defined for a project of the German Energy Agency (DENA, 2010) based on the overlay transmission network structure depicted in (VDE, 2011), and on the right side the model regions defined to consider international interchanges. A definition of the modelled regions is shown in Table 9.

Table 9: Definition of the modelled regions		
Region	**Region ID**	**Regions comprised**
Germany North	D_N	21, 82
Germany Northeast	D_NE	81
Germany Northwest	D_NW	22, 23
Germany East	D_E	83, 84
Germany West	D_W	71, 72, 73, 74, 24
Germany Southeast	D_SE	25, 26, 76
Germany Southwest	D_SW	75, 41, 42
Alps	Alps	Austria, Switzerland
BeNeLux	BeNeLux	Belgium, Luxemburg, Netherlands
Dk-W	Dk-W	Denmark West (formerly UCTE member)
East	East	Czech Republic, Poland, Slovak Republic
France	France	France
Iberia	Iberia	Portugal, Spain
Italy	Italy	Italy
North	North	Dk (non UCTE), Finland, Norway, Sweden
UK&IE	UK&IE	Ireland, United Kingdom

4.1.3   Regional differentiation

In order to consider the spatial distribution of power generation, the different power generation profiles in each area were taken into account along with the distribution of the installed capacity of each technology. The latter was assumed as constant using a distribution factor, which for most power generation technologies was obtained from a

study published by the four German TSOs (see Figure 24, TSO, 2009). Additional assumptions were made for geothermal energy and for CHP plants, they are distributed among the defined regions depending on the geothermal potentials for power generation and on the heat demand, both calculated using the model developed in (Scholz, 2012). The electricity consumption of electric vehicles, both PEVs and FCVs, was distributed based on the population distribution data[45].

Figure 24: Distribution of power generation inside Germany in 2013

Source: TSO, 2009.

---
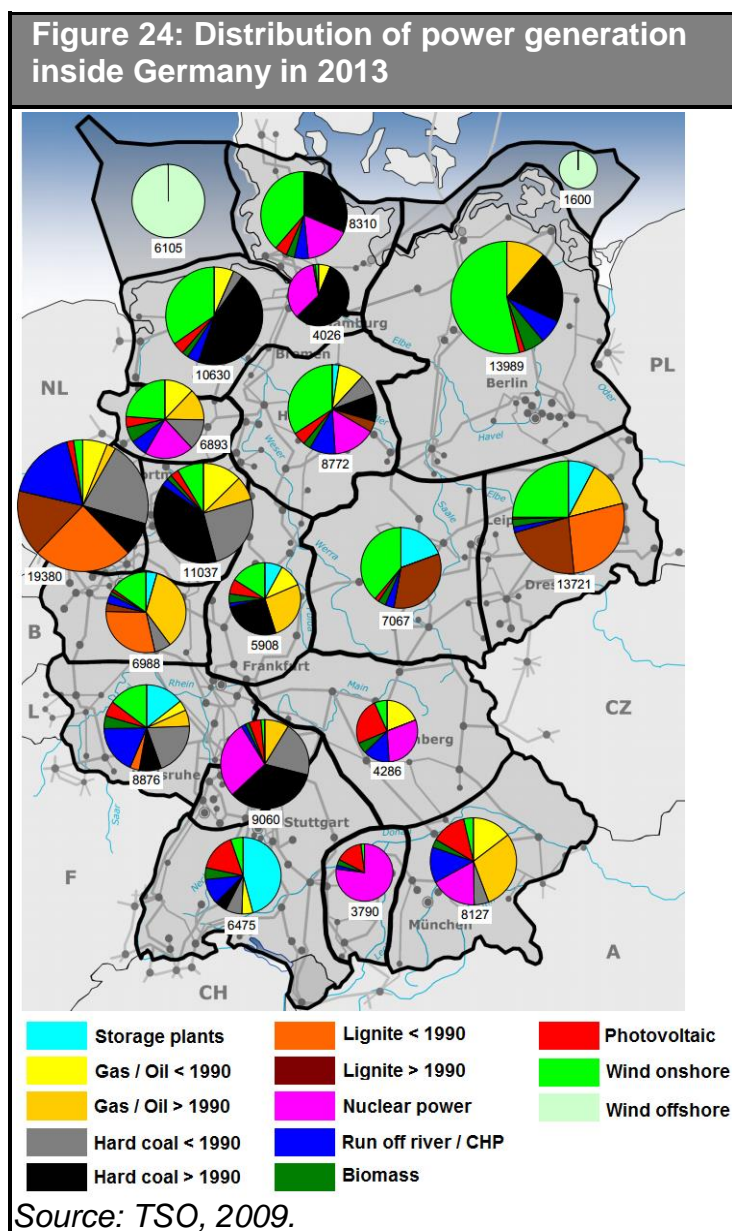
[45] Global Rural-Urban Mapping Project, 2000. Center for International Earth Science Information Network, Columbia University.

4.1.4   Economic framework

The price development of commodities related with the power sector can have a very strong impact on both power system planning and operation. Increases in fossil fuel prices increase the cost effectiveness of renewable power generation. Additionally, price variations in both fossil fuels and CO_2 certificates can make it uneconomical to operate certain power plants, i.e. increases in the price of CO_2 certificates make lignite less competitive for power generation. Figure 25 and Figure 26 show for large scale and for smaller scale CHP plants respectively high and medium fuel price development scenarios. They are based on (Nitsch et al., 2011 and Frontier/EWI, 2010) and reflect the possible range of rising fuel prices expected in the long term.

Figure 25: Fuel price development scenarios of large scale power plants

Source: Nitsch et al., 2011, Frontier/EWI, 2010.
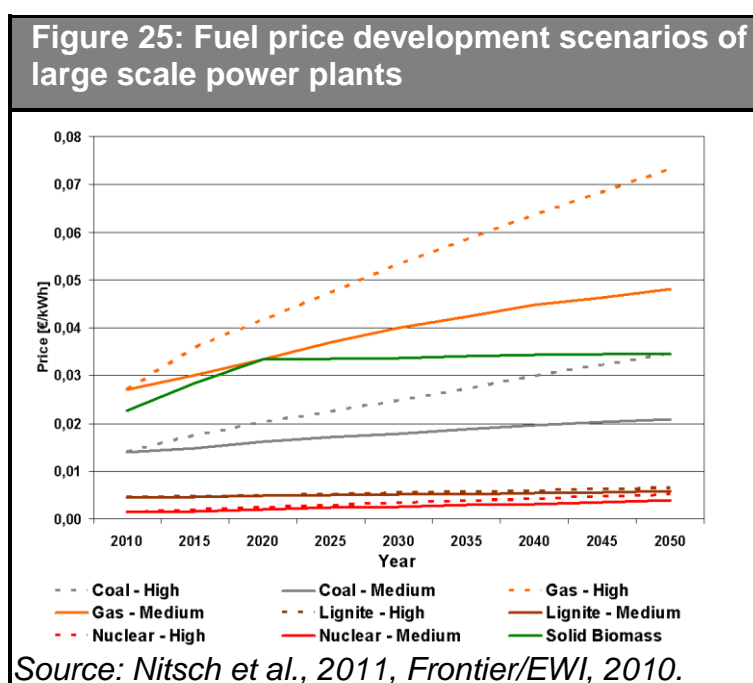
The European emissions trading scheme comprises currently around 40% of the total GHG emissions in the EU[46], considering among others those of the power sector from plants with more than 20 MW firing capacity. It has been assumed that by 2030 all electricity producers will have to internalize the cost of their carbon emissions. This could be implemented by expanding the group of power plants considered, or by

---

[46] Questions and Answers on the Commission's proposal to revise the EU Emissions Trading System, MEMO/08/35, Brussels, 23 January 2008.

introducing a tax on the fuel sold to non-registered emitters indexed to the CO_2 certificate's price.

Figure 26: Fuel price development scenarios of smaller scale CHP units

Source: Nitsch et al., 2011, Frontier/EWI, 2010.

Figure 27: Scenario assumptions of the CO_2 certificate price development

Source:Nitsch et al., 2011.
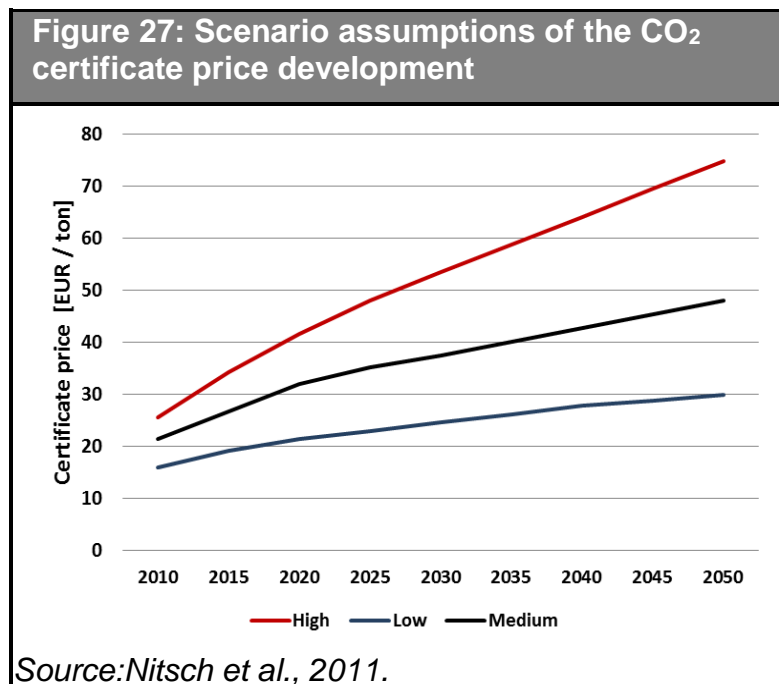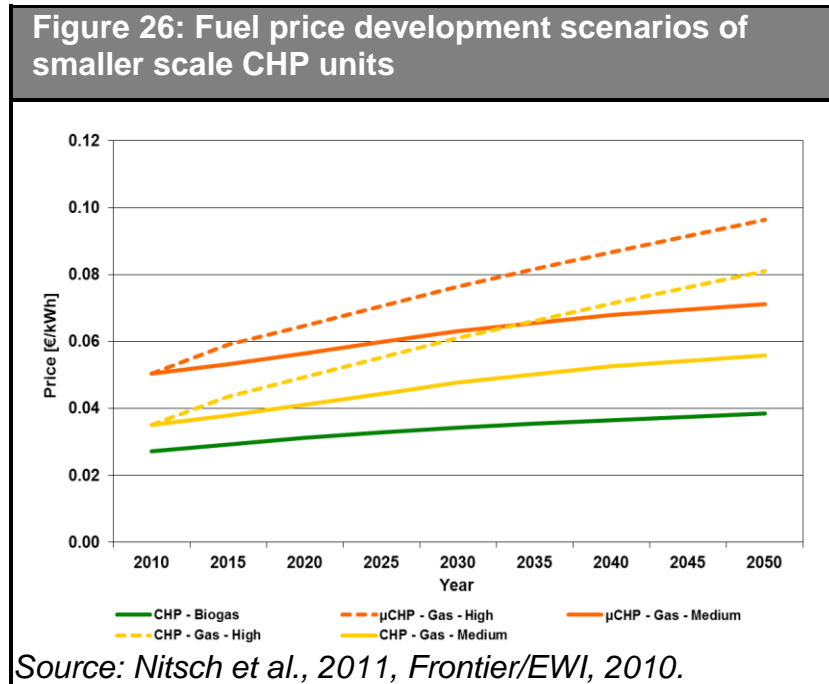
Figure 27 shows three possible developments of the cost of the CO_2 allowances, and Table 10 the specific CO_2 emissions used (Nitsch et al., 2011 and Johnke, 2011).

Table 10: Specific CO_2 emissions of fossil fuels	
Fuel	**Emissions [Kg./MWh]**
Natural gas	200
Hard coal	330
Lignite	400
Waste (non-biogenic)	220
Source:Nitsch et al., 2011, Johnke, 2001.	

4.2 Technology assumptions and modelling approach

Section 4.1 introduced the power generation and demand scenarios assumed in the present work. This section will present technology specific data concerning the assumed scenarios, costs and technical properties.

4.2.1 Concentrated solar power

The reference unit is a parabolic trough plant with a steam turbine and a capacity of about 200 MW. These plants require a direct normal irradiation (DNI) of about 2000 kWh / (m² a). In Europe the sites with such solar irradiation values are limited, particularly to southern Spain. In North Africa the potentials exceed the world's electricity demand by far. An additional advantage of solar thermal plants is that using a high-temperature thermal storage enables both a higher utilization of the steam turbine as well as a controllable and hence more valuable electricity production. A further advantage is that solar thermal energy can be combined with fossil fuels, such as natural gas. This could be employed to ensure that the temperature of the storage medium is kept above its solidification point or to adapt power generation to consumption (Espejo and García, 2010). In this work a net efficiency of 37% for the power generation block has been assumed, the storage operation causes an efficiency reduction of 5% due to temperature and pressure losses. The availability factor of these plants is assumed to be 95%.

The modelling of the solar radiation is based on the *HELIOSAT* method (see Hammer et al., 2003). This method uses satellite data, such as cloud cover, as well as aerosol datasets, to calculate both Global Horizontal Irradiance (GHI) and Direct Normal Irradiance (DNI). The first is used to estimate the power generation from photovoltaic, and the second from concentrated solar plants. The obtained hourly potentials were

obtained for each region and for a whole year, the profiles were scaled to the solar fields' installed capacity in the region to calculate the actual production from all solar fields.

The main data concerning the assumed scenario of power generation from solar thermal plants was presented in 4.1. To analyse how the plants are operated additional information concerning the dimensioning of the solar field compared to the turbine and that of the high temperature storage system is required. An additional issue is the share of the annual power generation coming from solar energy or from natural gas.

Table 11: Additional scenario parameters of solar thermal plants				
Region	**Av. DNI [kWh/m2/y]**	**Solar Multiple**	**Storage ratio [h]**	**Solar share 2030 (cofiring)**	**Solar share 2050 (cofiring)**
Africa	2835	3	6		
Iberia	2250	3	6	93% (7%)	99% (1%)
Italy	2000	4	6		
Source: Assumptions based on Trieb et al., 2006.				

The solar multiple (SM) is the ratio of the nominal solar field generation and the turbine's heat intake at its nominal operation point[47]. The storage ratio represents the hours of surplus heat generation at the solar field's nominal operation that can be stored. Thus with a solar multiple of 1 the solar field would deliver at the nominal point just the nominal heat intake of the steam turbine and no storage would be required. With a SM of 4 (see Figure 28) the solar field would deliver 4 times the nominal heat intake, in this case the heat storage would be able to store the surplus heat production during six hours of operation at nominal operation, that is the production of 75% of the solar field as 25% of it would be directed directly to the steam turbine.

---

[47] With a solar irradiance of 800 W/m2.

Figure 28: Definition of CSP plant configuration with different solar multiple

| SM1 | SM2 | SM3 | SM4 |

Solar Field 1 | Solar Field 2 | Solar Field 3 | Solar Field 4

Storage 1 | Storage 2 | Storage 3

Power Block → Electricity

Source: Trieb et al., 2009.
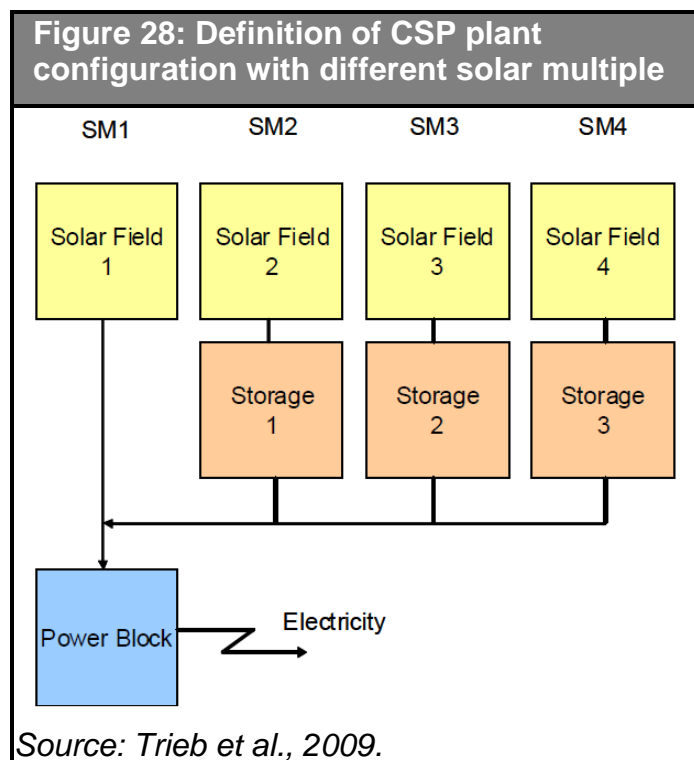
4.2.2   Photovoltaic and wind power

The power generation from photovoltaic panels was calculated for each considered region with the model REMix using the method described in 4.2.1. Figure 29 shows exemplarily the feed-in profiles during five days of summer in each of the modelled regions inside Germany. For each of them it can be seen that from one day to the next one power generation can change significantly as seen in the north-eastern region (*D_NE*, orange line).

The wind power generation profiles used in this work were calculated with the model described in (Scholz, 2012) using 2006 data from the German Weather Service such as wind speed and surface roughness to estimate wind speeds at different heights (DWD, 2007). The reference turbine is the E82 from ENERCON (ENERCON, 2010), assuming a sustained increase in the hub height for offshore turbines, rotor diameter and nominal capacity, with 3 MW in 2010, 6 MW in 2020 and 12 MW in 2050 and up to 5.5 MW for onshore turbines. Figure 30 shows exemplarily the power generation from onshore and offshore wind turbines in Germany and compares it with that in the region *UK-IE* during one week in the month of August. It can be observed that on the eight of August there is a high offshore generation in Germany, whereas in *UK-IE* it is below average. In the following days the opposite situation occurs.

Figure 29: Normalized feed-in profiles in each region of Germany

Source: Results of the REMix Model.

Figure 30: Normalized wind power generation profiles in German offshore and onshore regions as well as in UK-IE in a summer week

Source: Results of the REMix Model.
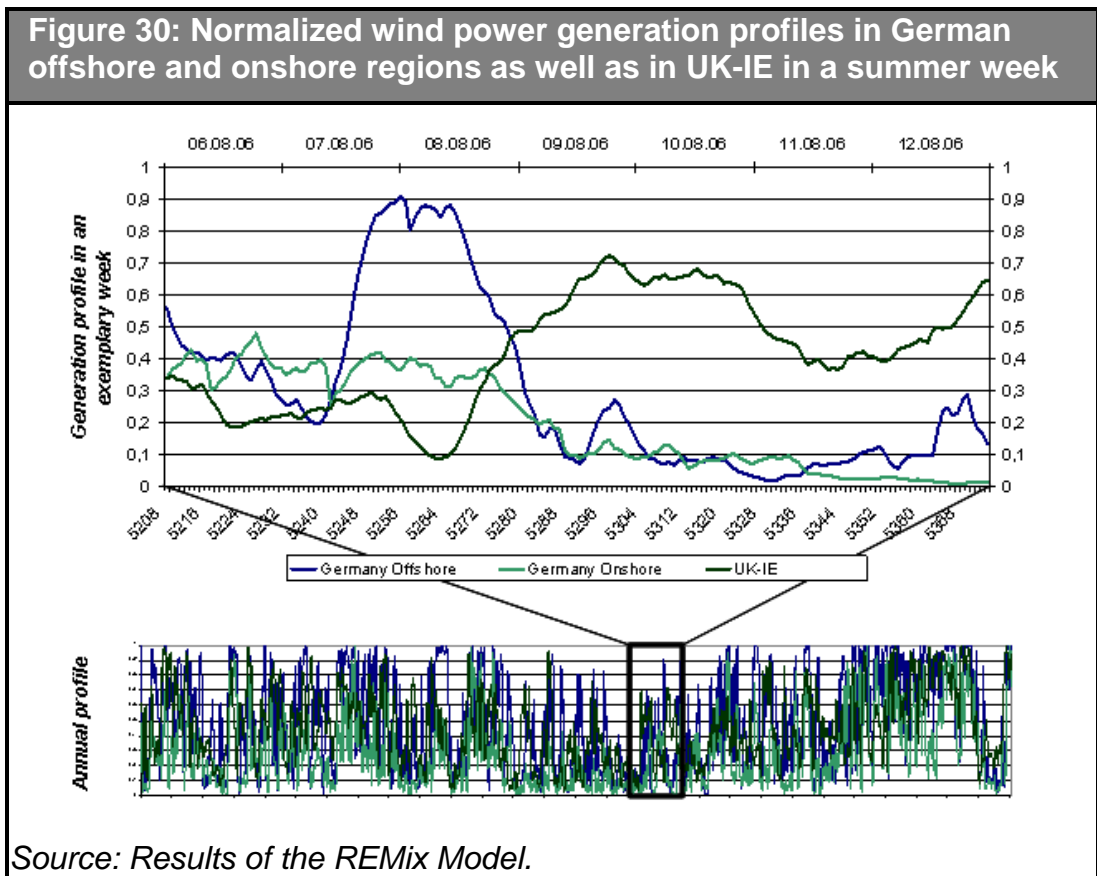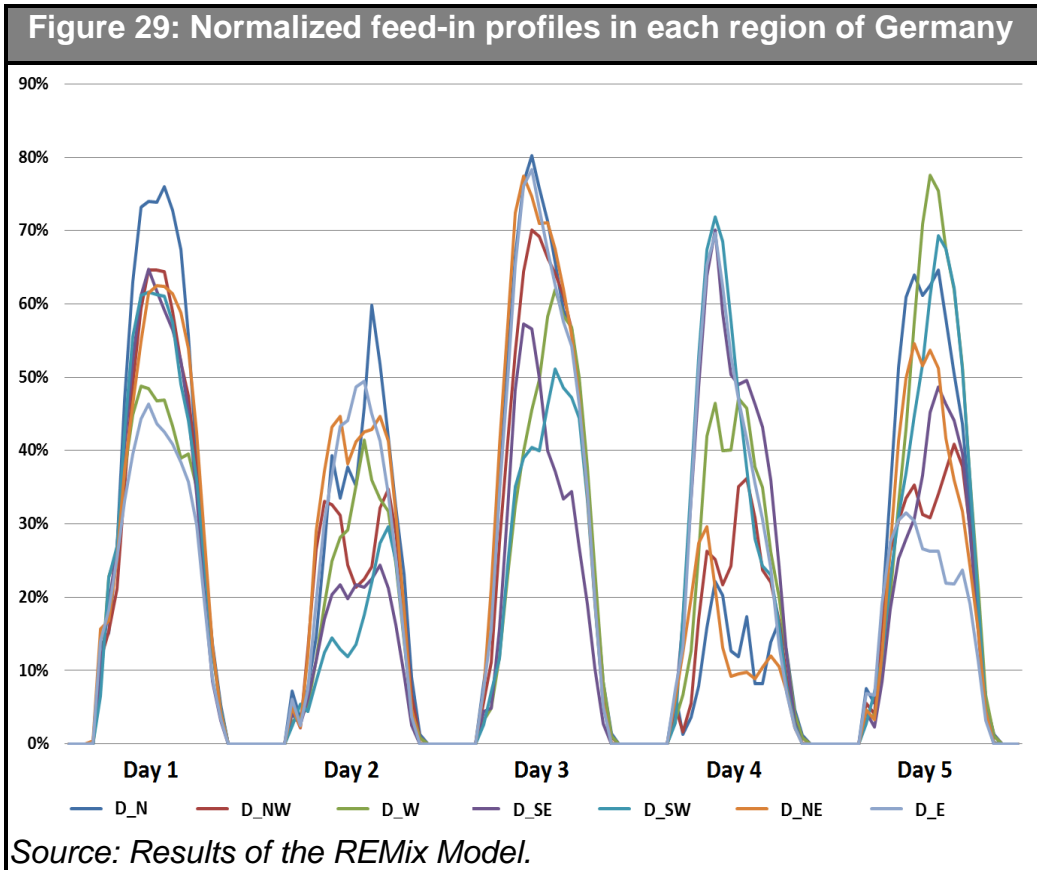
4.2.3 **Hydropower**

The developed model considers both storage and run-of-river power plants. Pure pumped-storage power plants with no natural inflows are included in the storage module (see 4.2.8). Figure 31 shows average daily water inflow of hydroelectric plants in terms of potential energy, which was calculated with the model REMix based on river discharge measurements (GRDC, 2008). The largest inflows correspond to *North*, especially in spring, due to the melting of the snow cover.

Hydroelectric power plants in some of the modelled regions, such as in Germany, consist of run-off-river plants with a very small storage capacity covering only a modest share of electricity demand. In other countries, like Norway or Switzerland, hydroelectricity covers a very high share of demand and present large reservoirs able to balance both daily and seasonal variations of demand and fluctuating power generation. In these regions hydropower generation has been classified as run-off-river or hydro storage based on a research report (Trieb et al., 2006), electricity statistics (Nordel, 2008) (BFE, 2009), on a database of hydroelectric plants in Norway[48], of power plants in Europe[49] as well as on expert estimations[50,51]. The modelling of run-off-river power plants is similar than for wind or photovoltaic generation and is calculated by scaling the profiles shown in Figure 31. The model of hydroelectric plants considers the size of the storage capacity, the minimum water flow required due to flow constraints as well as the installed capacity of pump turbines. For the conversion of potential energy into electrical energy an efficiency of 90% was assumed, for pumping operation 89%.

---

[48] Norwegian Water Ressources and Energy Directorate.

[49] UDI World Electric Power Plant Database. Platts 2008.

[50] Personal communication of Professor Olav Hohmeyer: As water reservoirs in Scandinavia are connected in cascade not the whole storage capacity is available, 85% was taken.

[51] Telephone interviews with Swedenergy, Generation division.

Figure 31: Annual water inflow in the considered regions

Source: Results of the REMix Model.
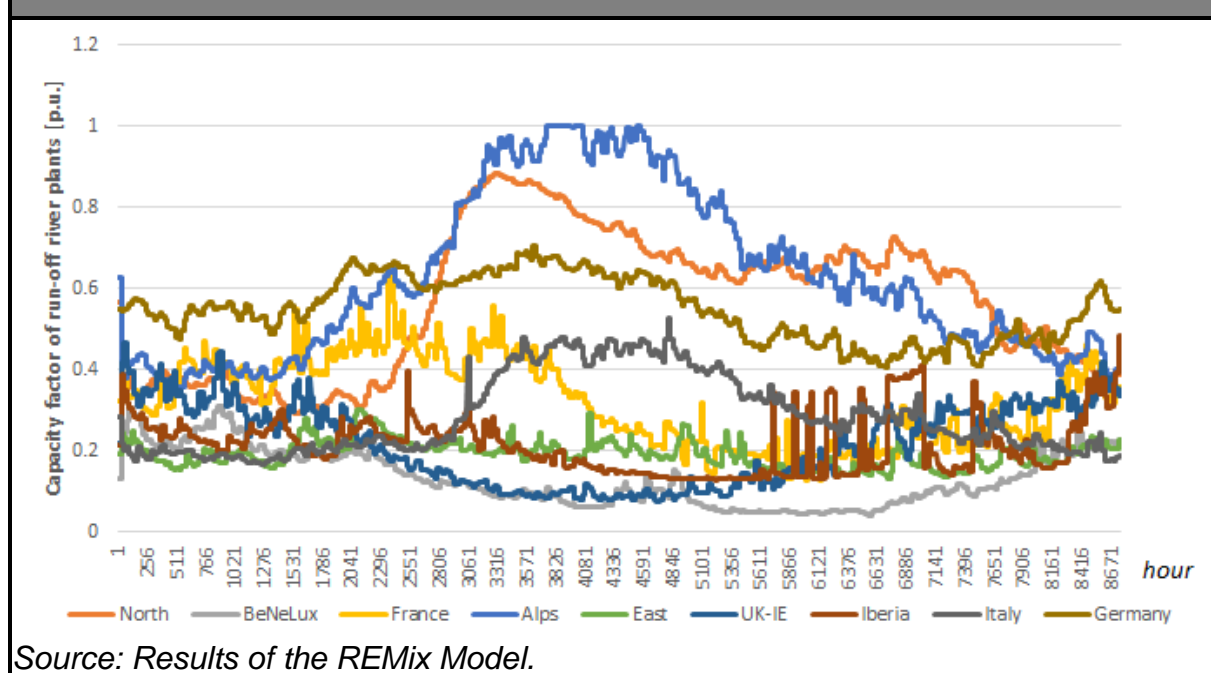
Table 12: Scenario of hydroelectricity in the regions *Alps* and *North*

Region	Technology	Unit	2010	2020	2030	2040	2050
Alps	Run-off-River	TWh	46.7	47.2	47.7	48.2	48.7
Alps	Reservoir	TWh	34.2	34.5	34.9	35.3	35.6
North	Run-off-River	TWh	32.7	33.7	34.8	35.8	36.8
North	Reservoir	TWh	206.8	209.9	213.0	216.1	219.2
Source: Scenario based on Trieb et al., 2006, Nordel, 2008, BFE, 2009.							

Table 13: Assumed parameters of hydroelectricity with storage

Region	Parameter	Unit	2010	2020	2030	2040	2050
Alps	Reservoir cap.	TWh			11.7		
Alps	Pump cap.	MW			>6012		
North	Reservoir cap.	TWh			103.7		
North	Pump cap.	MW			>846		
All	Minimum flow	%			25%		
Source: Nordel, 2008, BFE, 2009.							

4.2.4   Geothermal power generation

Due to the relatively low achievable temperatures power generation from geothermal sources often requires the use of a working fluid other than water, such as a mixture of water and ammonia which boils at around 50ºC or organic fluids, like isopenthane, and present low efficiencies for electricity production. Therefore, these systems are typically used primarily for heat production and use the geothermal heat for electricity production in times of low heat demand; this is the case of the plant in Neustadt-Glewe[52] and in Unterhaching[53]. Therefore, the generation of electricity during the winter months is significantly lower than in the summer months. Figure 32 shows the projected profile generation from geothermal power plants in Germany. Here an annual utilization of the steam turbine of around 6500 hours was assumed. The heat profile was calculated with the outdoor temperature assuming a certain share of temperature independent heat consumption (i.e. for industrial processes or as domestic hot water).

4.2.5   Other renewable power generation

Power generation from other sources, such as biomass or marine energy, can also contribute to further reductions in carbon emissions. The current version of the model allows an economic dispatch of biomass plants based on the cost of the bio fuel and on the price of electricity as well as a constant dispatch assuming a certain annual production. Electricity production from the energy of tides and waves accounts in the scenarios for a small share of power generation. In this work the marine energy generation has been approximated with a constant profile. For solid biomass plants it has been assumed that due to an advantageous regulatory framework or to low biomass prices it will be operated as a base load plant.

---

[52] "Geothermal Electricity Generation in Neustadt-Glewe". BINE Information Service, projekinfo 09/03.

[53] "Geothermal electricity generation combined with a heating network". BINE Information Service, projekinfo 10/09.

Figure 32: Scaled profile of geothermal power generation

Source: Results of the REMix Model.
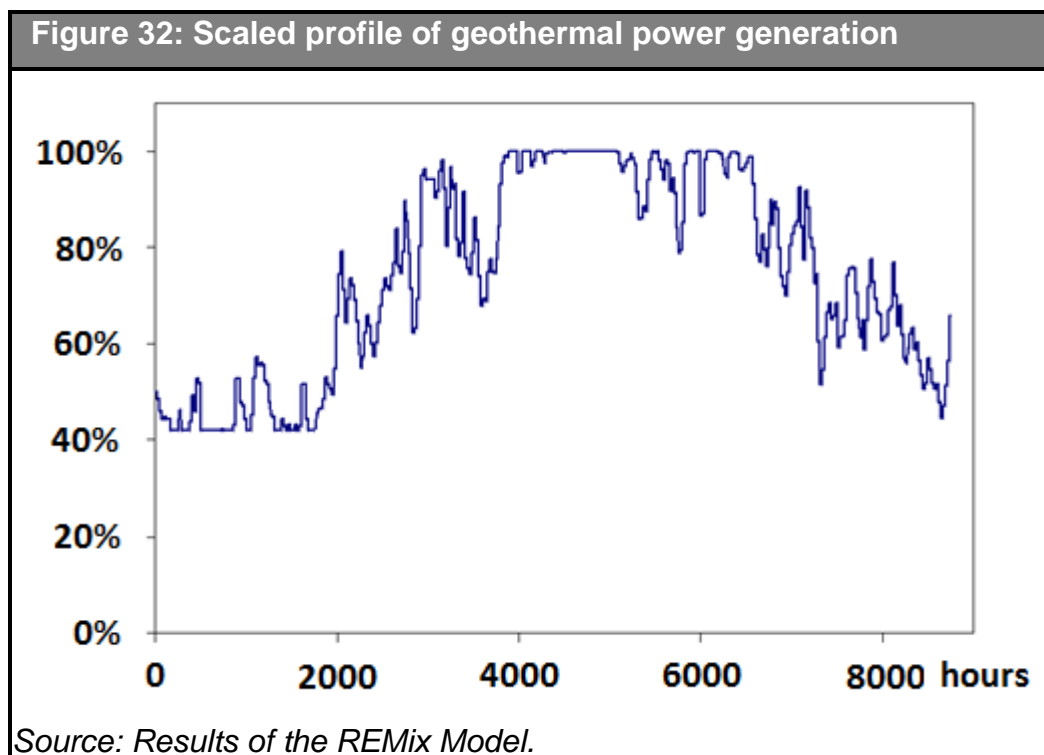
4.2.6   Conventional thermal power plants

Power generation units are dispatched depending on their variable costs following a merit order, with which the units with the lowest variable costs are used first, followed by those with the next higher variable costs until demand is met. The main variable costs of these plants consist on the costs of fuel supply, the costs of carbon emission allowances and those related to wear and tear.

The fuel consumption of the considered technologies is calculated according to its year of construction. Figure 33 shows the assumed development of the net efficiency of conventional power plant technologies for each age group, the data used until 2010 was obtained from publicly available sources[54]. The future development until 2050 was obtained from work produced by Nitsch et al., 2012.

---

[54] Such as project reports, utilities' publications and manufacturers' data.

Figure 33: Assumed development of net-efficiencies of thermal power plants

Source: Own analysis based on research reports, publication of utilities, manufactureres' data and on Nitsch et al., 2012.
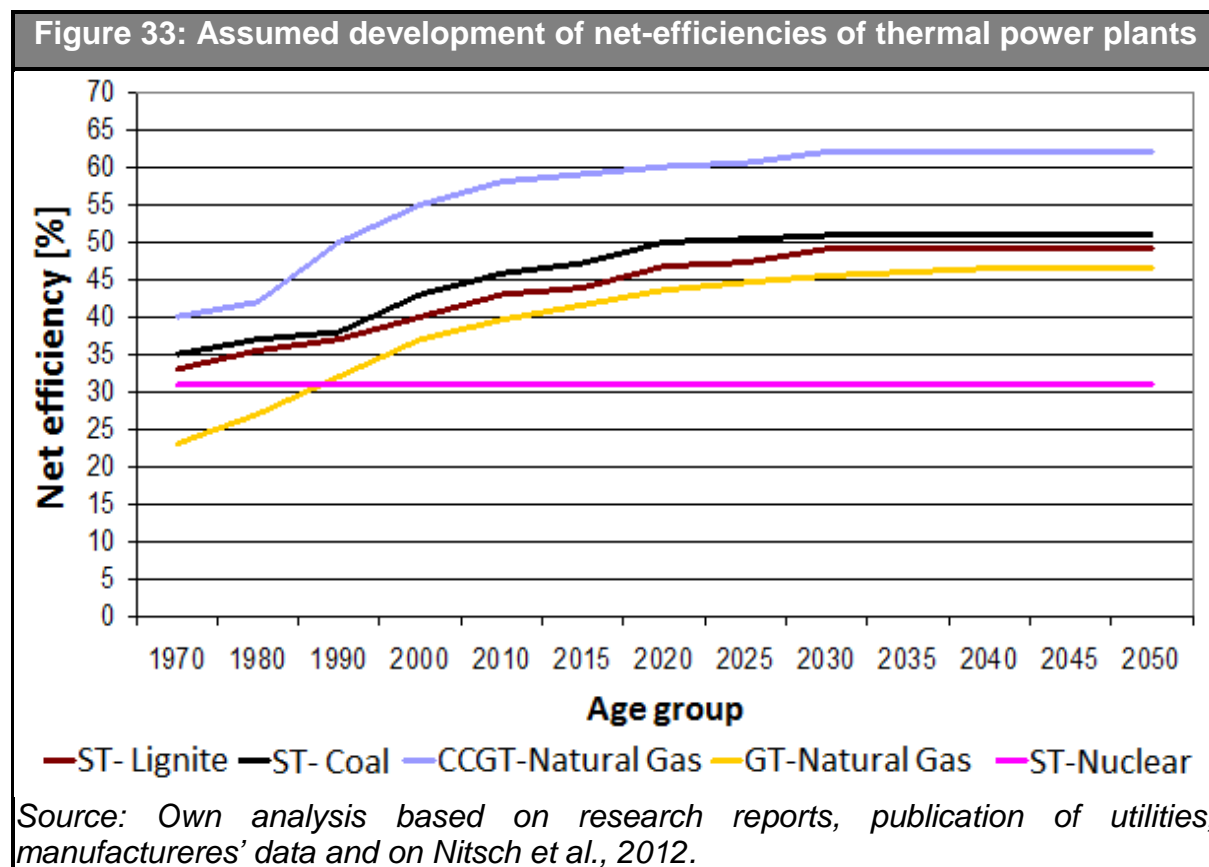
The merit order curve is obtained in the model by sorting the power plants by their variable costs and considering its installed capacity on the horizontal axis, Figure 34 shows exemplarily the resulting merit order curve of fossil power plants for Germany in 2030.

The merit order curve, though it is a very useful representation, does not model the costs related to the dynamic behaviour of thermal units, such as partial load losses or start-up costs. For short periods, the use of power plants situated in a higher point of the merit order can be economical if their start-up costs are lower. These costs are considered in REMix by adding costs related to changes in the output. These consist of the cost due to increased system wear and the fuel costs for a cold start. The assumption of a cold start overestimates the start-up costs, as the cost of a warm start is about 1 / 3 of that of cold start, however it also overestimates its flexibility (Genoese, 2010) and it does not consider partial load losses. The start-up cost components are shown in Table 14 and were obtained from (DENA, 2005), the availability related data was obtained in the framework of Nitsch et al., 2012.

Figure 34: Merit order curve of conventional thermal plants in Germany in 2030, assuming medium fuel and CO₂ certificate prices
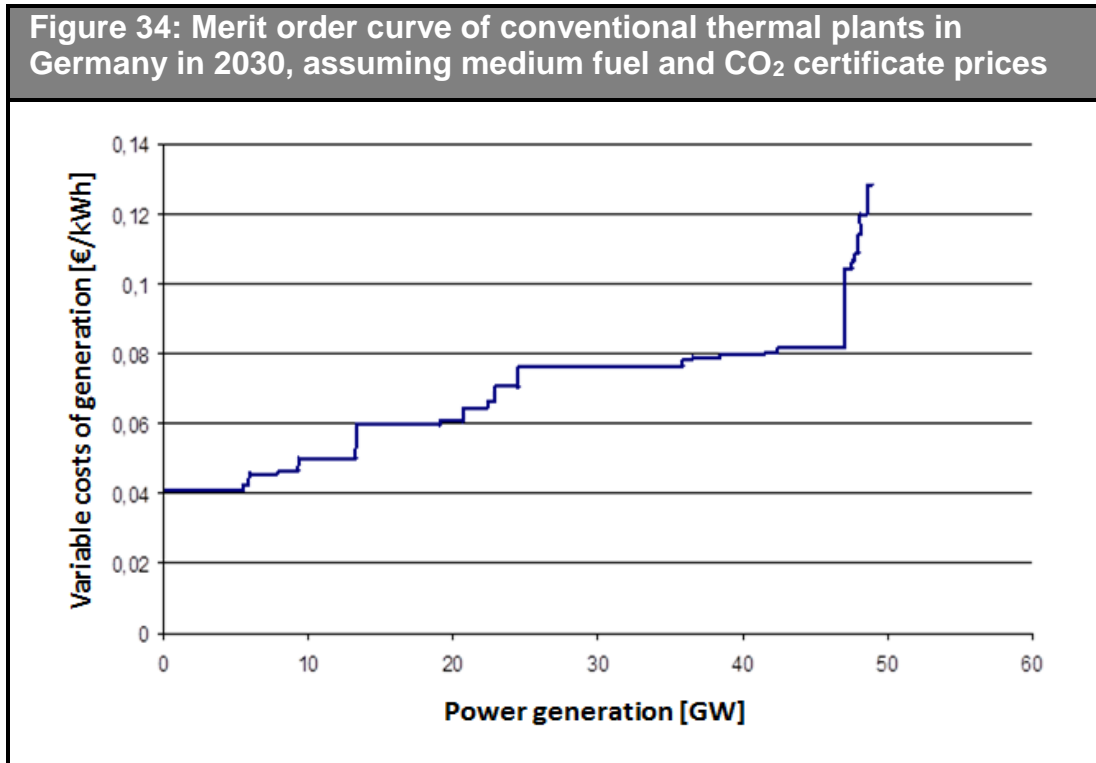
Table 14: Start-up cost components of fossil and nuclear power plant

Technology	Start-up fuel cons. [MWh$_{th}$/MW$_{el}$]	Start-up wear/tear costs [€2009/MWel]
ST-Lignite	6.2	3.2
ST-Coal	6.2	5.2
CCGT-Gas	3.5	10.7
GT-Gas	1.1	10.7
ST-Nuclear	16.7	1.8
Source: DENA, 2005.		

Due to maintenance reasons or to unexpected outages the total installed capacity is not always available. The model assumes for each power plant technology a certain availability factor to calculate the available power plant capacity throughout the year.

The presented model represents thermal generation aggregating the generating units based on their generation technology and decade of construction. Therefore, in contrast to other models focusing on the short term operation of the system with a block specific representation of thermal units, REMix simplifies issues related to

security of supply such as the provision of operating reserves for frequency regulation, must-run requirements for voltage support, as well as partial load losses.

Table 15: Total availability of thermal power plants	
Technology	**Total availability [%]**
ST-Lignite	90.2
ST-Coal	89.6
CCGT-Gas	96.0
GT-Gas	94.8
ST-Nuclear	90.0
Source: Nitsch et al., 2012.	

4.2.7 Combined heat and power

In the assumed scenario for Germany combined heat and power plants (CHP), both as small distributed combustion engines or as large steam turbines with heat extraction, is expected to play an important role in the next decades so as to increase the primary energy efficiency and to integrate solar and geothermal energy in the heating market. The model considers different technologies based on the type of heat customer, on the generation technology and on the fuel used. It has been assumed that district heating networks and large industrial plants consist of steam, gas or combined cycle turbines, whereas the remaining plants are mainly internal combustion engines of smaller size. For each plant type it is assumed, that a flexible operation will be possible in the future, i.e. that larger heat storages with an additional electric heater for using renewable excess power and facilities for generation management are installed. The following table describes the different technologies assumed. The modelling of CHP plants is based on (Nitsch et al., 2011) as well as on information provided by associations of the CHP plant operators in Germany[55,56].

---

[55] AGFW – Der Energieeffizienzverband für Wärme, Kälte und KWK e.V., Frankfurt am Main.
[56] VIK. Verband der Industriellen Energie- und Kraftswirtschaft, Essen.

Table 16: Classification of CHP plant			
Consumer type	**CHP type**	**Fuel**	**Typical installed capacity**
District heating	Steam & gas turbines	Lignite	>10 MWel
		Hard coal	
		Natural gas	
		Waste	
Local heating	Internal combustion engines	Natural gas	10 kWel – 10 MWel
		Biogas	
Distributed	Internal combustion engines	Natural gas	<10 kWel
		Biogas	
Large industrial	Steam & gas turbines	Hard coal	>10 MWel
		Natural gas	
Small industrial	Internal combustion engines	Natural gas	10 kWel – 10 MWel
		Biogas	
Source: Nitsch et al., 2012.			

The temperature dependent share of heat demand is estimated based on the outside temperature by the heating degree days method (EUROSTAT, 2008), which calculates the daily heat demand by multiplying the difference of the average daily temperature and a certain base temperature by a given factor. The used method assumes that buildings in the future due to better thermal insulation not only will require less heating, but also that it will be required in fewer days than today, i.e. the outside temperature heating limit is reduced. Depending on the type of consumers of the heat supplied by the CHP plant, the heat profile will change; this is modeled by specifying a different share of temperature independent heat demand for every CHP class. Typically the heat demand for sanitary hot water or for industrial processes is rather temperature independent, while the demand for room heating varies significantly. The following table shows the assumed proportion of temperature-independent heat demand on the total demand, developed in the framework of (Nitsch et al., 2012).

Table 17: Share of temperature independent heat demand					
Consumer type	**2010**	**2020**	**2030**	**2040**	**2050**
Industrial consumers	87%	88%	89%	89%	89%
Other consumers	23%	24%	24%	26%	28%
Source: Nitsch et al., 2012.					

Figure 35 shows exemplarily the coverage of the heat demand. It can be seen that most is covered by the CHP plant; the fossil fuelled boiler for peak demand coverage is used when the heat demand exceeds a certain level and the electric boiler in times of high wind power generation and low electricity prices. By operating distributed CHP units considering not only the heat demand but also the rest of the power system, i.e. using price signals, the curtailment of wind turbines can be reduced and the efficiency of the power system increased.

In this work only the heat demand to be covered by CHP will be considered. The heat demand profile can be calculated by the above described method for each consumer type and region. To scale the heat demand profile a maximum achievable utilization is used, which assumes that the CHP unit is operated in base load and thus only reduces its output for low values of heat demand. Figure 35 shows the data used to set the CHP layout.

Figure 35: Exemplary calculation and coverage of the heat demand
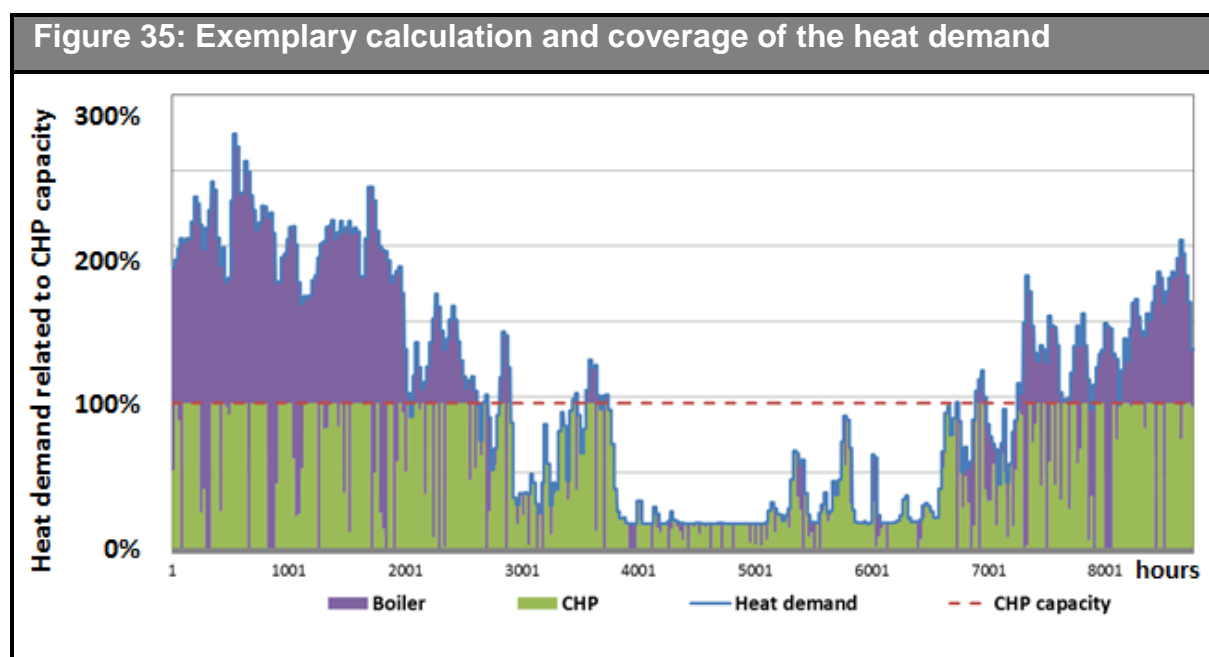
Table 18: Utilization and heat share of CHP plants						
CHP – Steam & gas turbines	**Unit**	**2010**	**2020**	**2030**	**2040**	**2050**
Maximum utilization	h/a	5807	5418	5057	4737	4649
Estimated utilization	h/a	5719	5120	4223	3624	3278
CHP - Internal Combustion Engines	**Unit**	**2010**	**2020**	**2030**	**2040**	**2050**
Maximum utilization	h/a	6134	5624	5355	5082	5075
Estimated utilization	h/a	6042	5315	4471	3888	3578
Source: Nitsch et al., 2012.						

While for back pressure turbines the power and heat production is coupled, steam turbines with heat can decouple them by modifying the extraction of condensed steam in the turbine (see Figure 36), the entire dotted area shows the possible operating points in the linear model.

Figure 36: Operational field of steam turbines with heat extraction
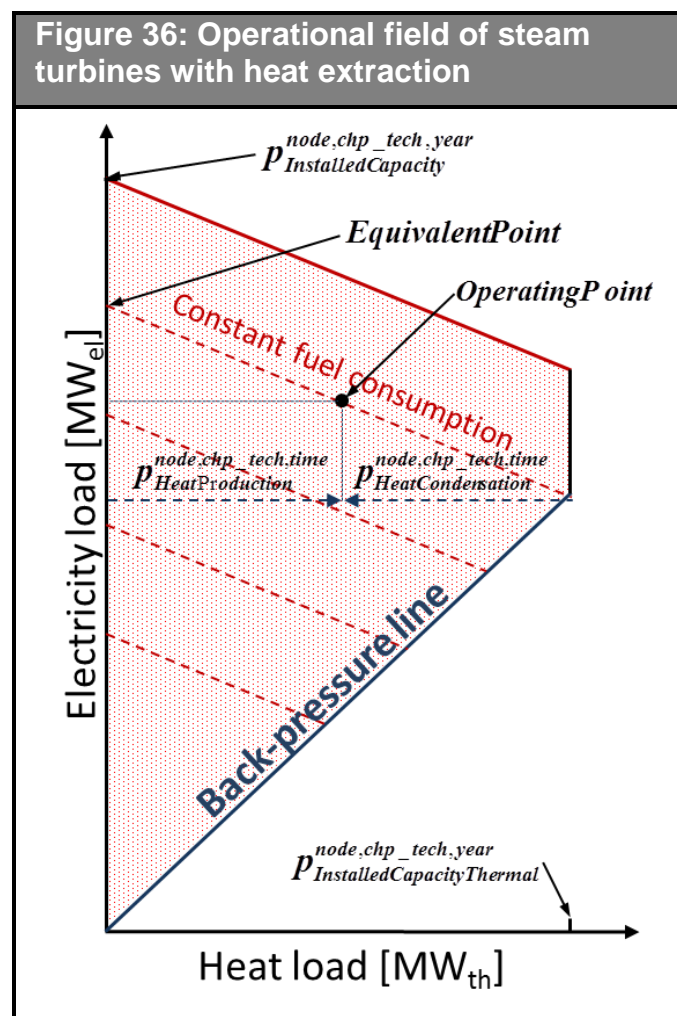
The operational field of a thermal unit with heat extraction is determined in the model with the CHP coefficient, the power loss coefficient and the maximum heat extraction. The CHP factor describes the ratio between the electrical and the thermal output. The power loss coefficient describes to which extent the electrical output of the unit is reduced due to heat extraction in the turbine. The equivalent point represents the operating point for the same fuel consumption that results in pure condensing mode, i.e. in case heat production is reduced to zero. The maximum heat output is given by the coefficient relating it with the installed power generation capacity. The model of ICEs and counter-pressure units is simpler than that of heat extraction units and both power and heat productions are strongly dependent. Table 19 shows the parameters used to model CHP (Nitsch et al., 2012).

Table 19: Assumed coefficients and efficiencies of CHP units						
	Unit	2010	2020	2030	2040	2050
District heating networks						
CHP coefficient	MW_{el}/MW_{th}	0.55	0.61	0.69	0.72	0.74
Power loss coefficient	MW_{el}/MW_{th}	0.20	0.20	0.20	0.20	0.20
CHP efficiency	%	85	87	89	90	90
Thermal capacity	MW_{th}/MW_{el}	1.6	1.6	1.6	1.6	1.6
Local heating networks						
CHP coefficient	MW_{el}/MW_{th}	0.72	0.74	0.76	0.78	0.80
CHP efficiency	%	85	87	89	90	90
Distributed						
CHP coefficient	MW_{el}/MW_{th}	0.44	0.47	0.52	0.55	0.60
CHP efficiency	%	85	87	89	90	90
Large industrial						
CHP coefficient	MW_{el}/MW_{th}	0.6	0.75	0.85	0.88	0.90
Power loss coefficient	MW_{el}/MW_{th}	0.20	0.20	0.20	0.20	0.20
CHP efficiency	%	85	87	89	90	90
Thermal capacity	MW_{th}/MW_{el}	1.45	1.45	1.45	1.45	1.45
Small industrial						
CHP coefficient	MW_{el}/MW_{th}	0.72	0.74	0.76	0.78	0.80
CHP efficiency	%	85	87	89	90	90
Source:Nitsch et al., 2012.						

Using a heat accumulator or a boiler, the electric output can be decoupled from the heat demand. The use of a heat storage device can increase the contribution of CHP to peak demand coverage as in times of high demand, i.e. during the day, more electricity and heat would be produced; in times of lower demand, i.e. at night, the

surplus heat production during the day would be utilized. For these storage systems losses of 0.1%/h were assumed.

Table 20: Storage ratio of CHP plants related to thermal output						
	Unit	**2010**	**2020**	**2030**	**2040**	**2050**
District heating	MWh /MW	2	5	8	10	12
Local heating		2	6	10	12	14
Distributed		2	2.4	2.8	4.6	6.4
Large industrial		0	0	1	1	1
Small industrial		2	6	10	12	14
Source: Nitsch et al., 2012.						

A boiler can provide redundancy in case of an outage of the CHP unit; its use also allows cogeneration units to achieve a higher utilization and flexibility, i.e. in times of low electricity prices it can be more economical to cover the heat demand using a boiler than using cogeneration. If electricity prices get even lower, i.e. in case of renewable electricity surpluses, an electric boiler can be used to substitute fossil fuel consumption by renewable electricity that would otherwise be wasted. Boiler efficiencies are located depending on the temperature of the heat required between 92% and 99%. Table 21 shows the assumed efficiencies and capacity of fossil fuel and electric boilers related to the nominal thermal output from CHP, it is assumed in this work that there is enough capacity of fossil fuelled boilers to cover demand in case of an outage of the cogeneration unit.

Table 21: Boiler capacity and efficiency scenario of CHP plants						
	Unit	**2010**	**2020**	**2030**	**2040**	**2050**
District heating						
Capacity electric boiler	%	0	4	8	11	15
Efficiency electric boiler	%	99	99	99	99	99
Efficiency fossil fuel boiler	%	95	95	95	95	95
Local heating						
Capacity electric boiler	%	0	8	15	23	30
Efficiency electric boiler	%	99	99	99	99	99
Efficiency fossil fuel boiler	%	95	95	95	95	95

Distributed						
Efficiency boiler	%	95	95	95	95	95
Large industrial						
Capacity electric boiler	%	0	4	8	11	15
Efficiency electric boiler	%	92	92	92	92	92
Efficiency fossil fuel boiler	%	92	92	92	92	92
Small industrial						
Capacity electric boiler	%	0	8	15	23	30
Efficiency electric boiler	%	99	99	99	99	99
Efficiency fossil fuel boiler	%	95	95	95	95	95
Source: Nitsch et al., 2012.						

4.2.8   Electricity storage

The model currently includes adiabatic compressed air energy storage, pumped storage and hydrogen storage via electrolysis and power generation process based on a combined cycle gas turbine.

Pumped storage is a mature technology with over a hundred years of existence. In the future no large increases in installed capacity are expected in Western Europe. Pumped storage plants are able to store electric energy by pumping water into a reservoir situated at higher level when electricity prices are low and use the stored energy for power generation when required. In Germany there are over 30 pumped-storage power plants with an installed capacity of around 6.7 GW. Additionally it has been assumed in this work that new plants will be in operation by 2030 providing an additional capacity of 1.400 MW.

Table 22: Parameter assumptions of pumped storage plants		
Technical specifications	**Unit**	**2010 - 2050**
Turbine efficiency	%	90
Pump efficiency	%	89
Losses per hour	1/h	0
Ratio storage capacity - installed capacity	kWh/kW	8
Availability factor	%	98

Economic specifications	Unit	2010 - 2050
Investment costs for reversible turbine	€/kW	640
Fix O&M[57] costs (% Invest.)	%/a	3
Amortization time rev. turbine	a	20
Investment costs storage	€/kWh	10
Amortization time storage	a	60
Variable O&M costs	€/kWh	0
Interest rate	%	6%
Source: DLR/IFHT/ISE, 2012.		

The Advanced Adiabatic Compressed Air Energy Storage technology (AA-CAES) is under development at the moment (see Project ADELE[58]) and is considered as an interesting long-term option for electricity storage. In conventional CAES compressed air is stored up to 70 bars in deep salt caverns a few hundred feet underground, during peak load periods the compressed air is driven through a gas turbine for electricity production. In adiabatic systems (AA-CAES), the heat produced when compressing the air is stored and used during decompression, so that no fossil fuels are used to heat up the cold air expanding in the turbine. The current research projects aim at a round trip efficiency of 70%. The geological potential for compressed air storage is limited to areas where suitable caverns can be built. Figure 6 shows the operation of an AA-CAES plant (Zunft, 2005).

Figure 37: Operation scheme of AA-CAES

Source:Zunft, 2005.

---
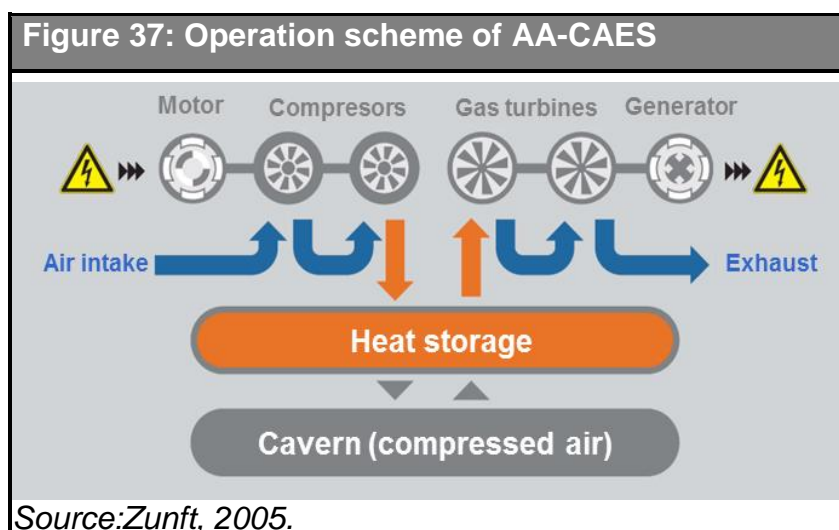
[57] Operation and Maintenance.

[58] The ADELE plant is being developed by RWE, General Electric, Züblin and the DLR. Installed capacity of 90 MWel, storage capacity of 360 MWh. Construction starting in 2013.

Table 23: Parameter assumptions of AA-CAES					
Technical specifications	**Unit**	**2010**	**2020**	**2030**	**2050**
Turbine efficiency	%	85	86	87	89
Loading efficiency	%	79	81	83	84
Losses per hour	1/h	0.002			
storage capacity ratio	kWh/kW	8			
Availability factor	%	95			
Economic specifications	**Unit**	**2010 - 2050**			
Investment costs power block	€/kW	650			
Fix O&M costs	%/a	3			
Amortisation time	a	20			
Investment costs cavern	€/kWh	30			
Amortization time cavern	a	40			
Variable O&M costs	€/kWh	0			
Interest rate	%	6%			
Source: DLR/IFHT/ISE, 2012.					

Table 24: Parameter assumptions of H$_2$ storage (electrolyser/CCGT)						
Technical specifications	**Unit**	**2010**	**2020**	**2030**	**2040**	**2050**
Turbine efficiency	%	57				
Loading efficiency	%	70				
Losses per hour	1/h	0				
Storage capacity ratio	kWh/kW	200				
Availability factor	%	95				
Economic specifications	**Unit**	**2010**	**2020**	**2030**	**2040**	**2050**
Investment costs power block	€/kW	1800	1650	1560	1520	1500
Fix O&M costs	%/a	3				
Amortization time power block	a	15				
Investment costs cavern	€/kWh	0.2				
Amortization time cavern	a	30				
Variable O&M costs	€/kWh	0				
Interest rate	%	6%				
Source: DLR/IFHT/ISE, 2012.						

An *alkaline* electrolyser can split water into oxygen and hydrogen at pressures up to 30 bar using electrical energy. The produced hydrogen can be further compressed and stored in an underground cavern at 50 to 80 bar achieving a much higher energy density than using compressed air or pumping water. In this work a combination of an *alkaline* electrolyser with a net efficiency of 70% and a combined cycle plant with 57% was assumed, however other uses for produced hydrogen are also conceivable. Table 24 shows the assumed parameters in this work. As with the compressed air storage, the technology is limited to certain areas.

4.2.9 AC power transmission

The power flows over the AC transmission network are calculated with the Power Transmission Distribution Factors (PTDF). This approach is based on the strong linear relation between power feed-in and demand and power flows and neglects reactive power flows between the defined model regions as well as transmission bottlenecks inside the defined region. The maximum exchange between two areas compatible with the applicable security constraints is given by the Net Transfer Capacities (NTC[59]). Both the PTDFs and the NTCs presented were calculated in the framework of (DLR/IFHT/ISE, 2012) based on publicly available information. The assumed parameters used to model the AC network can be found in the annex.

4.2.1 DC power transmission

Typically, the HVDC technology is used in situations in which an AC connection is not suitable because of the high transport distances, for sea cables or when linking networks with different frequencies. The main advantages of HVDC lines are that for long distances it presents lower losses and that it does not require reactive power compensation. Examples include the 6400 MW connection between the Xiangjiaba hydropower plant and Shanghai, with a total length of over 2,000 km, or the submarine cable linking the Netherlands with Norway over 700 km. In this work point-to-point links have been assumed. Data concerning the existing, planned and other potential new

---

[59] ETSO, 2001.

lines is included in the annex. The key assumptions to the losses and costs are shown below and were obtained in the framework of (Nitsch et al., 2012).

Table 25: Assumed specific costs and properties of the HVDC links				
Parameter	**Unit**	**2010**	**2030**	**2050**
Invest. overhead line 3.2 GW, 600 kV	€/MW·km	140	130	120
Invest. sea cable 3.2 GW, 600 kV	€/MW·km	975	900	825
Invest. underground cable 2.2 GW, 600 kV	€/MW·km	489	451	415
Invest. costs each conv. station	€/MW	120	102	90
Fix O&M costs	%/a	1		
Amortization time	a	40		
Interest rate	%	6%		
Losses overhead line	%/1000 km	4.5		
Losses sea cable	%/1000 km	2.7		
Losses underground cable	%/1000 km	2.7		
Losses station	%	0.7		
Source: Nitsch et al., 2012.				

4.2.2   Electricity consumption

The demand for electricity is relatively inelastic to price variations compared to that of other goods. However this could change with the introduction of PEVs and a further expansion of renewable power generation capacity. The price-inelastic power demand, named in this work conventional demand, in all considered regions is modelled using the "Consumption Data" of the UCTE[60] for the year 2006. This data has an hourly resolution and represents the complete load profile of the country including all consumers in transport, households, industry and commercial. The profiles are then scaled using the presented annual consumption scenarios to consider the future evolution of power demand.

Besides this price-inelastic demand for electricity the model also includes a price-elastic electricity demand consisting of the demand of controllable PEVs and of H_2 fuelling stations as well as of electric heating modules.

---

[60]https://www.entsoe.eu/resources/publications/former-associations/ucte/graphical-statistics/consumption-data/

5 The REMix model

In the previous sections the main assumptions concerning the future power system and electric vehicles were presented, the present section describes the model used and further developed for this work. The model uses geo-referenced data of weather-related phenomena to consider the spatial and temporal components of renewable power generation. In contrast to other models, i.e. stochastic models, this approach allows a representation of intermittent power generation without reducing the number of possible situations which may in the end lead to an inadequate representation; namely the model considers real weather conditions and thus takes into account the complex interactions between wind and solar power as well as the heat and electricity demand. Using a fundamental bottom-up approach based in linear optimisation the model is able to calculate the least cost operation and expansion of the power system for a given year. The model REMix[61] consists of two coupled modules namely the resources module that calculates the power generation potentials of renewable power sources and the optimisation module to analyse operation and planning issues.

The resources module is able of calculating the potentials of various renewable energy sources on the basis of geo-referenced data of land use and of weather-related phenomena, such as solar irradiation, wind speed, river discharge data or outdoor temperatures. The module is programmed in the C language and provides of intermittent sources both hourly feed-in profiles and the installable generation capacity for each defined region. Additionally it also delivers the biomass production potential, the inflows of hydroelectric plants as well as heat and electricity demand profiles. A detailed description of the resource module can be found in (Scholz, 2012).

The optimization module developed for this work is based on the first version developed by (Scholz, 2012). The model performs a calculation of the least cost operation and expansion that meets the heat and electricity load. The model has been formulated as a linear problem using the GAMS software[62] and uses the CPLEX[63] solver. Technical and economic properties of the considered technologies, the

---

[61] Renewable Energy Mix for sustainable electricity supply (Scholz, 2012).

[62] General Algebraic Modeling System. GAMS Development Corporation.

[63] IBM ILOG CPLEX Optimization Studio.

scenarios of the power system and of electric vehicles are included in a MS Access 2003 database[64] and are read by the optimization module using a built-in application of the optimisation package. The feed-in profiles as well as the electricity and demand profiles calculated with the Resources module are saved in text files which for this case presented a significantly higher read-in performance due to its larger size.

Figure 38: Structure of the REMix model
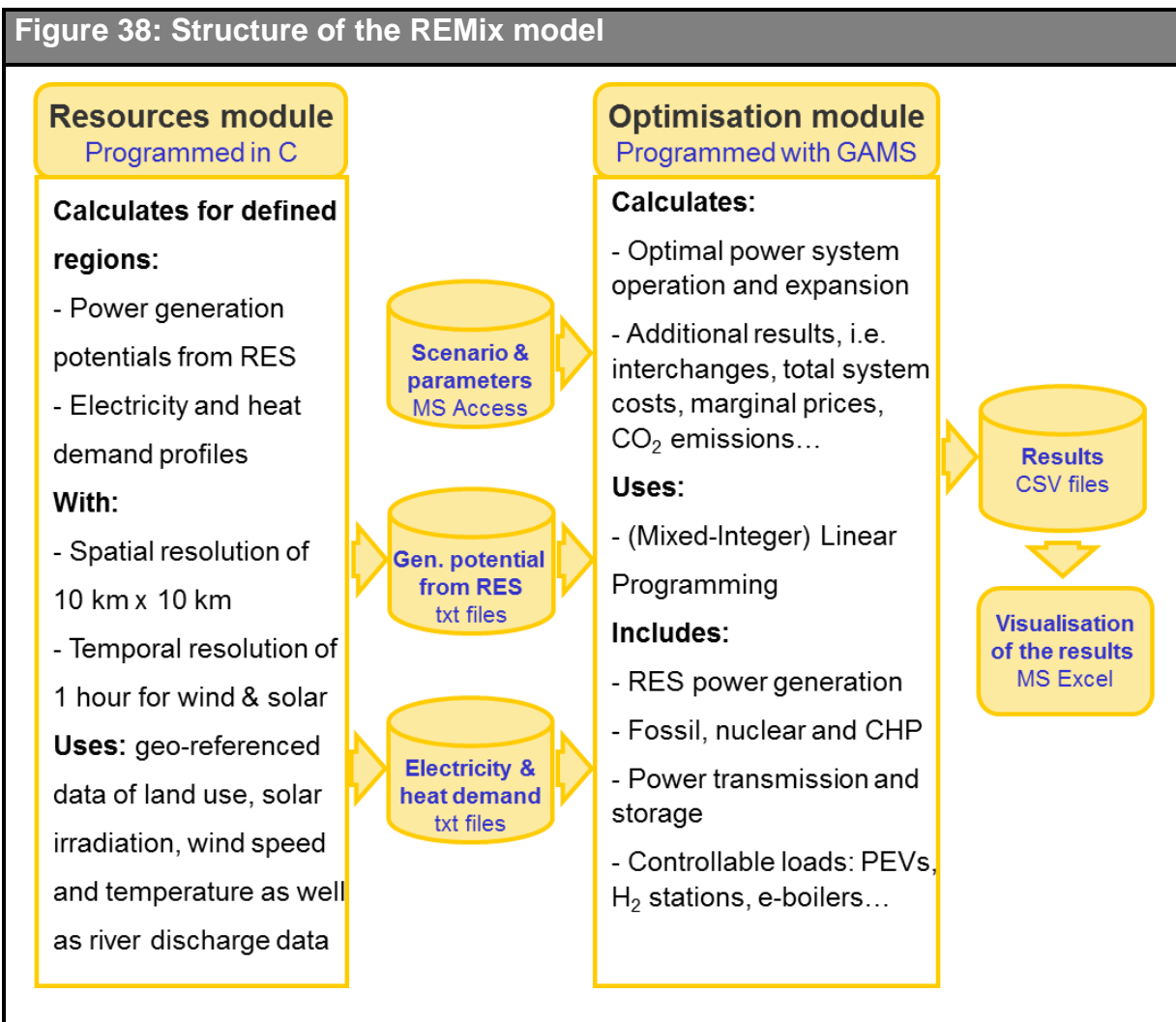
5.1   Formulation of the optimisation module

The mathematical formulation of this linear model consists of an objective function which models the different costs incurred as well as the constraints that characterize power generation, the demand side and the transmission network. The objective function and the constraints are formulated using parameters, which characterise the

---

[64] Microsoft Access 2003. Microsoft Corporation.

technical properties and the costs of the considered elements, and with variables, which are to be determined by the solver.

The model is able to calculate for a given year the optimal power plants mix and transmission expansion with both a green field approach and assuming a scenario of generation capacity expansion.

5.2 Main and common equations

Indices	Description
time	The time slices considered
node	The modelled nodes of the power grid
ffz	The free flow zones of the system containing one or many nodes
area	The defined areas of the power grid containing one or many ffz
tech	The power generation, storage and transmission technologies
conv_tech	The conventional thermal generation technologies
stor_tech	The electricity storage technologies
geo_tech	The geothermal power generation technologies
bio_tech	The biomass power generation technologies
chp_tech	The CHP power generation technologies
hydro_tech	The hydroelectric power generation technologies
csp_tech	The CSP generation technologies
pw_tech	The considered wind and PV technologies
dc_tech	The DC power transmission technologies
h2_tech	The hydrogen production technologies
fuel	The different fuels considered
pollutant	The different pollutants considered
year	The set of years that can be analysed
obs_year	The year to be analysed
year_class	The thermal units classification depending on construction year

Variable	Description	Unit
$P_{Generation}^{node,tech,(year\_class),time}$	Net power generation of each technology	[MW]
$P_{TotalPowerGeneration}^{node,time}$	Total power generation of all technologies	[MW]
$P_{Potential}^{node,tech,time}$	Generation potential from renewable sources	[MW]
$E_{FuelConsumption}^{node,tech(year\_class),time}$	Fuel consumption of generation units	[MWh]
$M_{TotalEmissions}^{node,tech,pollutant,time}$	Pollutant emissions	[t]
$P_{InstalledCapacity}^{node,tech,year}$	New installed capacity	[MW]

$P_{Surplus}^{node,tech,time}$	Power generation surplus	[MW]
$P_{StorageLoad}^{node,tech,time}$	Loading of the storage system	[MW]
$P_{StorageDischarge}^{node,tech,time}$	Discharge of the storage system	[MW]
$E_{StorageLevel}^{node,tech,time}$	Fill level of the storage system	[MWh]
$P_{LoadPEV}^{node,time}$	Demand of the plug-in electric vehicle fleet	[MW]
$P_{FeedInPEV}^{node,time}$	Feed-in power of the plug-in electric vehicle fleet	[MW]
$P_{ElectricityDemandH_2}^{node,h2\_tech,time}$	Electricity demand for hydrogen production	[MW]
$P_{ElectricHeating}^{node,chp\_tech,time}$	Electricity demand for heat production	[MW]
$P_{TransmissionDC}^{node,dc\_tech,time}$	Net electricity feed-in in HVDC nodes	[MW]
$P_{TransmissionAC}^{node,time}$	Net electricity feed-in in HVAC nodes	[MW]
$P_{NotSuppliedPower}^{node,time}$	Not supplied power	[MW]
$N_{StartUps}^{node,tech,(year\_class),time}$	Amount of generation units going online	[#]
$N_{InOperation}^{node,tech,(year\_class),time}$	Generation units in operation	[#]
$C_{StartUp}^{node,tech,(year\_class),time}$	Start-up costs of conventional thermal units	[k€]
$C_{Fuel\&Emissions}^{node,tech,(year\_class),time}$	Fuel and pollutant emission costs of thermal units	[k€]
C_{System}^{year}	The total considered system costs	[k€]
$C_{Operation}^{tech,year}$	The operation and maintenance costs	[k€]
$C_{Investment}^{tech,year}$	The considered investment costs	[k€]
$C_{BatteryWearPEV}^{year}$	The costs related to battery wearing of PEVs	[k€]
Parameter	**Description**	**Unit**
$p_{Demand}^{node,time}$	The inelastic electricity demand	[MW]
$f_{Profile}^{node,tech,time}$	Capacity factor profile of renewable generators (related to installed capacity)	[p.u.]
$p_{InstalledCapacity}^{node,tech,(year\_class)}$	Installed power generation capacity	[MW]
$p_{InstalledCapacityThermal}^{node,chp\_tech,(year\_class)}$	Installed thermal generation capacity	[MW]
$p_{AverageBlockSize}^{tech,(year\_class)}$	Average block size	[MW]
$p_{OtherGeneration}^{node,other\_tech,time}$	Power generation from other sources	[MW]
$e_{AnnualImports}^{area,year}$	Annual electricity imports	[MWh]

$f_{CCS}^{tech,(year\_class)}$	Emissions' sequestration share	[p.u.]
$f_{SpecificEmissions}^{fuel,pollutant}$	Specific pollutant emissions of each fuel	[t/MWh]
$f_{StartUpFuel}^{tech,(year\_class)}$	Specific start-up fuel consumption	[MWh/MW]
$f_{Availability}^{test,(year\_class)}$	Availability factor of generation units	[p.u.]
$m_{MaximumEmissions}^{area,pollutant,year}$	Maximum limit of pollutant emissions	[tons]
$h_{Utilisation}^{node,tech,year}$	Annual utilisation	[h]
$f_{StorageRatio}^{tech,year}$	Dimensioning ratio of the storage system	[h]
$f_{LossRate}^{tech,year}$	Self-discharge losses	[p.u./h]
$f_{Annuity}^{tech,year}$	Annuity factor for investment cost calculation	[p.u.]
$\eta_{Net}^{tech,(year\_class)}$	Net efficiency	[p.u.]
$\eta_{Gross}^{tech,(year\_class)}$	Gross efficiency	[p.u.]
$\eta_{Discharge}^{tech,year}$	Net efficiency of the storage discharge process	[p.u.]
$\eta_{Load}^{tech,year}$	Net efficiency of the storage loading process	[p.u.]
$\eta_{RoundTrip}^{tech,year}$	Net round trip efficiency (storage & discharge).	[p.u.]
$c_{CCS}^{year,pollutant}$	Specific pollutant sequestration cost	[k€/ton]
$c_{StartUp}^{tech,(year\_class)}$	Specific wear / tear costs per start-up	[k€/MW]
$c_{O\&M\,var}^{tech,year}$	Variable operation & maintenance expenditures	[k€/MW]
$f_{O\&Mfix}^{tech,year}$	Fix operation and maintenance expenditures	[p.u.]
$c_{AllowanceCost}^{year,pollutant}$	Cost of emission allowances	[k€/ton]
$c_{Fuel}^{year,fuel}$	Fuel procurement costs	[k€/MWh]
$c_{NotSuppliedEnergy}$	Costs of energy not supplied	[k€/MWh]
p_{Intlen}	Length of the time slice	[h]

Power balance

One of the main equations is the one relating power demand and generation in each node, which can be derived from Kirchhoff's first law. The electricity demand must be met in each node for each time step by either power generation units and/or storage plants. The demand for electricity in the model consists on the sum of the inelastic demand, the charging power of PEVs, the electricity consumption for the production of hydrogen and that of electric boilers. The power generation term comprises all generation sources. The power feed-in terms in AC or DC nodes are positive in case of net feed-in and negative for net consumption. Not supplied power is considered in case the demand cannot be met with the existing generation capacities.

$$
\begin{aligned}
&P_{TotalPowerGeneration}^{node,time} + P_{FeedInPEV}^{node,time} + P_{NotSuppliedPower}^{node,time} = p_{Demand}^{node,time} + P_{LoadPEV}^{node,time} \\
&+ \sum_{chp\_tech} P_{ElectricHeating}^{node,chp\_tech,time} + \sum_{h2\_tech} P_{ElectricityDemandH_2}^{node,h2\_tech,time} \\
&+ \sum_{stor\_tech} P_{StorageLoad}^{node,stor\_tech,time} + \sum_{hydro\_tech} P_{ReservoirLoad}^{node,hydro\_tech,time} \\
&+ \sum_{transDC\_tech} P_{TransmissionDC}^{node,dc\_tech,time} + P_{TransmissionAC}^{node,time}
\end{aligned}
$$

Equation 5-1

$$\forall node, time$$

Total power generation

The total electricity generating capacity in a region is made up of power generation by conventional thermal, photovoltaic, wind turbines, CSP, hydroelectric, biomass, geothermal, storage, and CHP plants. The "other" technology can be defined in case a new technology, such as tidal energy, needs to be modelled.

$$
\begin{aligned}
&P_{TotalPowerGeneration}^{node,time} = \\
&\sum_{\substack{year\_class \\ conv\_tech}} P_{Generation}^{node,conv\_tech,year\_class,time} + \sum_{pw\_tech} P_{Generation}^{node,pw\_tech,time} \\
&+ \sum_{csp\_tech} P_{Generation}^{node,csp\_tech,time} + \sum_{hydro\_tech} P_{Generation}^{node,hydro\_tech,time} \\
&+ \sum_{bio\_tech} P_{Generation}^{node,bio\_tech,time} + \sum_{geo\_tech} P_{Generation}^{node,geo\_tech,time} \\
&+ \sum_{stor\_tech} P_{Generation}^{node,stor\_tech,time} + \sum_{chp\_tech} P_{Generation}^{node,chp\_tech,time} \\
&+ \sum_{other\_tech} p_{Generation}^{node,other\_tech,time}
\end{aligned}
$$

Equation 5-2

$$\forall node, time$$

Pollutant emissions

The emissions in each node are calculated as the sum of those from conventional thermal plants, of those of CHP plants and of other technologies, the emission factors are shown in Table 10.

$$M_{TotalEmissions}^{node,tech,pollutant,time} =$$

Equation 5-3

$$\sum_{\substack{conv\_tech \\ \in tech}} E_{FuelConsumption}^{node,conv\_tech,year\_class,time} \cdot f_{emission}^{fuel,pollutant} \cdot (1 - f_{CCS}^{conv\_tech,year\_class})$$

$$+ \sum_{\substack{chp\_tech \\ \in tech}} E_{FuelConsumption}^{node,chp\_tech,time} \cdot f_{emission}^{fuel,pollutant}$$

$$+ \sum_{\substack{csp\_tech \\ \in tech}} P_{CoFiring}^{node,csp\_tech,time} \cdot f_{emission}^{'gas',pollutant} \cdot p_{Intlen}$$

$$+ p_{Generation}^{node,other\_tech,time} \cdot f_{emission}^{node,other\_tech,pollutant} \cdot p_{Intlen}$$

$$\forall node, tech, pollutant, time$$

Limit on imports

In order to ensure that a certain share of electricity demand is produced in each area a limitation of imports can be set; additionally the imported value can also be set to a constant value.

$$\sum_{\substack{node \\ \in area}} \sum_{time} (\sum_{dc\_tech} P_{TransmissionDC}^{node,dc\_tech,time} + \sum_{ac\_tech} P_{TransmissionAC}^{node,ac\_tech,time}) p_{Intlen} \leq -e_{AnnualImports}^{area,'obs\_year'}$$

Equation 5-4

$$\sum_{\substack{node \\ \in area}} \sum_{time} (\sum_{dc\_tech} P_{TransmissionDC}^{node,dc\_tech,time} + \sum_{ac\_tech} P_{TransmissionAC}^{node,ac\_tech,time}) p_{Intlen} = -e_{AnnualImports}^{area,'obs\_year'}$$

Equation 5-5

$$\forall area$$

Operation expenditures

The equations used to calculate the operation expenditures are different for each technology though present the same structure. The variable operation costs, depending on the technology, can be calculated as a factor of power generation. Additionally, for those technologies consuming fuels a term can be added to account for the costs related to fuel provision and pollutant emissions. For thermal units the non-fuel costs related to start-up procedures, mostly wear and tear, can be added. Finally, the fix operation costs can be calculated as a percentage of the capital costs.

$$C_{Operation}^{tech} = C_{OperationVar}^{tech} + C_{OperationFix}^{tech}$$ Equation 5-6

$$C_{OperationVar}^{tech} =$$ Equation 5-7

$$\sum_{node}\sum_{tech}\sum_{(year\_class)}\sum_{time} P_{Generation}^{node,tech,time} \cdot f_{O\&Mvar}^{tech,'obs\_year'} \cdot p_{Intlen} + C_{Fuel\&Emissions}^{node,tech,(year\_class),time} + C_{StartUp}^{node,tech(year\_class),time}$$

$$C_{OperationFix}^{tech} =$$

$$\sum_{node}\sum_{tech}\sum_{(year\_class)} c_{Investment}^{tech,'obs\_year'} \cdot (P_{CapacityInstallation}^{node,tech,'obs\_year'} + p_{InstalledCapacity}^{node,tech,'obs\_year'}) \cdot f_{O\&Mfix}^{tech,'obs\_year'}$$ Equation 5-8

The operation costs related to fuel consumption and to emissions are proportional to the amount of fuel consumed. Here specific costs for the procurement of fuel (see Figure 25 and Figure 26, a CO_2 allowance price (Figure 27), a sequestration share as well as specific costs for CCS are assumed.

$$C_{Fuel\&Emissions}^{node,tech(year\_class),time} =$$ Equation 5-9

$$\sum_{conv\_tech}\left[\begin{array}{l} E_{FuelConsumption}^{node,tech(year\_class),time} \cdot \\ \left(c_{fuel}^{'obs\_year',fuel} \\ + \sum_{pollutant} f_{SpecificEmissions}^{fuel,pollutant} \cdot (c_{Certificate}^{'obs\_year',pollutant} \cdot (1 - f_{CCS}^{tech,(year\_class)}) + c_{CCS}^{'obs\_year',pollutant} \cdot f_{CCS}^{tech,(year\_class)}) \right) \end{array} \right]$$

$$\forall node,tech,(year\_class),time$$

The start-up costs due to wear and tear are calculated by multiplying the specific costs, the number of start-up procedures and their average block size. This approach is derived from detailed analysis of power plant operation by (Genoese, 2010) using the PowerACE model[65], and was applied to both conventional thermal units and to CHP plants (see Table 14).

$$C_{StartUp}^{node,tech(year\_class),time} = c_{StartUp}^{tech,(year\_class)} \cdot N_{StartUps}^{node,tech(year\_class),time} \cdot p_{AverageBlockSize}^{tech,(year\_class)}$$ Equation 5-10

$$\forall node,tech,(year\_class),time$$

Capital expenditures

The investment costs are also calculated with a different equation for each technology; however the structure is the same. For each technology the capital expenditures are proportional to the installed capacity. To take into account that amortisation times of

---

[65] Development founded by the Volkswagen foundation by Fraunhofer ISI, Universität Karlsruhe, TU Cottbus, Universität Mannheim (www.powerace.de).

transmission lines, thermal units and wind parks are different an annuity factor is included which depends on the interest rate and on the amortisation time of the asset.

$$C_{Installation}^{tech} = \sum_{node}\sum_{tech} c_{Investment}^{tech,'obs\_year'} \cdot P_{CapacityInstallation}^{node,tech,'obs\_year'} \cdot f_{Annuity}^{tech,'obs\_year'} \qquad \text{Equation 5-11}$$

With the following equation the equivalent annual payments over the amortisation time of the asset (N) are calculated for a given interest rate (i). The equation also considers the interest payments during the construction period (C) for which evenly distributed payments have been assumed.

$$f_{Annuity}^{tech,year} = \frac{(1+i)^{C} - 1}{C\cdot(1-(1+i)^{-N})} \qquad \text{Equation 5-12}$$

Total system costs

The objective function of the model is the sum of all decision-relevant costs in a year. These costs consist of operating and capital costs of conventional power plants, storage technologies, geothermal power plants, cogeneration plants, HVDC lines, photovoltaic systems, wind turbines, hydropower plants and biomass plants together. Besides, the costs of electric vehicle battery aging and those incurred due to load shedding are also reflected in the objective function.

$$C_{System} = \sum_{tech} C_{Operation}^{'obs\_year',tech} + \sum_{tech} C_{Investment}^{'obs\_year',tech} + C_{BatteryWearPEV}^{'obs\_year'}$$
$$+ \sum_{node}\sum_{time} P_{NotSuppliedPower}^{node,time} \cdot p_{Intlen} \cdot c_{NotSuppliedEnergy} \qquad \text{Equation 5-13}$$

5.3 Conventional thermal power generation

The approach followed is shown in 4.2.6, the installed capacity scenario in Table 44.

Maximum power generation

The available power generation capacity of each power plant type is limited by the total installed capacity. Due to planned maintenance or unplanned stops, the total installed capacity is not always available; this is represented in the model by an availability factor. Additionally, the parasitic consumption of thermal plants causes an appreciable reduction on the net electricity output of the plant.

$$P_{Generation}^{node,conv\_type,year\_class,time} \leq p_{InstalledCapacity}^{node,conv\_type,year\_class} \cdot f_{availabilty}^{conv\_type,year\_class} \cdot \frac{\eta_{net}^{conv\_type,year\_class}}{\eta_{gross}^{conv\_type,year\_class}}$$ Equation 5-14

$$\forall node, conv\_type, year\_class, time$$

Fuel consumption

The fuel consumption in conventional power plants is determined by their net efficiency and net output.

$$E_{FuelConsumption}^{node,conv\_type,year\_class,time} =$$ Equation 5-15

$$\frac{P_{PowerGeneration}^{node,conv\_type,year\_class,time}}{\eta_{net}^{conv\_type,year\_class}} \cdot p_{Intlen} + N_{StartUps}^{node,conv\_type,year\_class,time} \cdot p_{AverageBlockSize}^{conv\_type,year\_class} \cdot f_{StartUpFuel}^{conv\_type,year\_class}$$

$$\forall node, conv\_type, year\_class, time$$

Start-ups

The number of thermal units which start up in a certain time step result from the difference in the number of units in operation in that time step and those in operation prior to that time.

$$N_{StartUps}^{node,conv\_type,year\_class,time} \geq N_{InOperation}^{node,conv\_type,year\_class,time} - N_{InOperation}^{node,conv\_type,year\_class,time-1}$$ Equation 5-16

$$\forall time > 0, node, conv\_type, year\_class$$

The number of thermal units in operation can be calculated as the total output of one technology divided by the average block size.

$$N_{InOperation}^{node,conv\_type,year\_class,time} = \frac{P_{PowerGeneration}^{node,conv\_type,year\_class}}{p_{AverageBlockSize}^{conv\_type,year\_class}}$$ Equation 5-17

$$\forall node, conv\_type, year\_class, time$$

5.4 Wind and photovoltaic power generation

The followed approach to represent intermittent renewable power generation is presented in section 4.2.2. Annex 8.2 shows the assumed scenarios of renewable power generation.

Potential power generation

In each node the potential power generation is calculated using the capacity factor profile calculated with the resources module.

$$P_{Potential}^{node,pw\_tech,time} = f_{PotentialProfile}^{node,pw\_teh,time} \cdot p_{InstalledCapacity}^{node,pw\_tech,'obs\_year'}$$

$$\forall node, pw\_tech, time$$

Equation 5-18

Power generation

The realised power generation to meet demand may not coincide with the available potential in case of surpluses.

$$P_{Generation}^{node,pw\_tech,time} = P_{Potential}^{node,pw\_tech,time} - P_{Surplus}^{node,pw\_tech,time}$$

$$\forall node, pw\_tech, time$$

Equation 5-19

5.5 Concentrated solar power generation

The methodology used to represent solar thermal power generation is presented in section 4.2.1. Annex 8.2 shows the assumed power generation scenarios.

Variable	Description	Unit
$P_{SolarFieldPotential}^{node,csp\_tech,year,time}$	Solar field generation potential	[MW]
$P_{Cofiring}^{node,csp\_tech,time}$	Heat generation through co-firing	[MW]
Parameter	**Description**	**Unit**
$p_{InstalledSolarCapacity}^{node,csp\_tech,year}$	Installed thermal capacity of the solar field[66]	[MW]
$e_{InstalledStorageCapacity}^{node,csp\_tech,year}$	Thermal storage capacity	[MWh]
$f_{SM}^{node,csp\_tech,year}$	The Solar Multiple, describes the relation between solar field and thermal intake of the steam turbine at nominal capacity	[#]
$f_{SolarShare}^{csp\_tech,year}$	Minimum share of annual output produced from the solar field	[p.u.]
$f_{AnnualStorageLoss}^{node,csp\_tech,year}$	Annual thermal storage losses	[p.u.]

Potential solar field output

To determine the potential thermal output profile of solar fields in each region the installed capacity is multiplied by the assumed capacity factor profile.

$$P_{SolarFieldPotential}^{node,csp\_tech,year,time} = f_{Profile}^{node,csp\_tech,time} \cdot P_{InstalledSolarCapacity}^{node,csp\_tech,year}$$

$$\forall node, time, csp\_tech$$

Equation 5-20

---

[66] Assuming a DNI of 800 W/m²

Power balance

The power generation is calculated as the thermal intake multiplied again by the net efficiency. The steam can be produced in the solar field or by burning natural gas; additionally depending on the plant´s configuration the solar field heat can be stored.

$$P_{Generation}^{node,csp\_tech,time} + P_{Surplus}^{node,csp\_tech,time} =$$

$$\eta_{Net}^{csp\_tech,year} \cdot (P_{SolarFieldPotential}^{node,csp\_tech,time} + P_{Cofiring}^{node,csp\_tech,time} - P_{StorageLoad}^{node,csp\_tech,time} + P_{StorageDischarge}^{node,csp\_tech,time} \cdot \eta_{RoundTrip}^{csp\_tech,year})$$

$$\forall time, csp\_tech, node$$

Equation 5-21

Maximum power generation

The generation capacity is limited by the installed capacity and its availability factor. The factor takes into account the total availability of the plants.

$$P_{Generation}^{node,csp\_tech,time} \leq P_{InstalledCapacity}^{node,csp\_tech,year} \cdot f_{Availability}^{csp\_tech,year}$$

$$\forall time, csp\_tech, node$$

Equation 5-22

Plant design

The model allows setting the relation of the solar field to the power block by introducing the solar multiple of the plant and dividing by the efficiency of the power block. The size of the solar field was increased slightly in order to take the losses of the thermal storage system into account.

$$P_{InstalledSolarCapacity}^{node,csp\_tech} = \frac{P_{InstalledCapacity}^{node,csp\_tech,'obs\_year'} \cdot f_{SM}^{node,csp\_tech,'obs\_year'}}{\eta_{Net}^{csp\_tech,'obs\_year'} \cdot (1 - f_{AnnualStorageLoss}^{node,csp\_tech,'obs\_year'})}$$

$$\forall csp\_tech, node$$

Equation 5-23

Besides, the model allows determining the thermal storage capacity by additionally providing the storage ratio (Table 11) using the following equation.

$$P_{InstalledStorageCapacity}^{node,csp\_tech} = P_{InstalledSolarCapacity}^{node,csp\_tech,'obs\_year'} \cdot f_{StorageRatio}^{tech,'obs\_year'} \cdot (1 - \frac{1}{f_{SM}^{node,csp\_tech,'obs\_year'}})$$

$$\forall csp\_tech, node$$

Equation 5-24

Storage level

To reflect the changes in the filling level of the thermal storage system due to loading or discharging, its variation between two time steps must be equal to the thermal energy stored or discharged.

$$(P_{StorageLoad}^{node,csp\_tech,time} - P_{StorageDischarge}^{node,csp\_tech,time}) \cdot p_{Intlen} = E_{StorageLevel}^{node,csp\_tech,time} - E_{StorageLevel}^{node,csp\_tech,time-1}$$

$$\forall time \neq 0, node, csp\_tech$$

Equation 5-25

Besides, the following constraint limits the storage level to its installed capacity.

$$E_{StorageLevel}^{node,csp\_tech,time} \leq e_{InstalledStorageCapacity}^{node,csp\_tech}$$

$$\forall time, csp\_tech, node$$

Equation 5-26

It was additionally established that the energy stored at the beginning of the considered period must be equal to the amount of energy stored at the end of the period.

Co-firing

The co-firing with natural gas within the CSP power plants in each region is limited to a fraction of the produced amount of energy in the solar field.

$$\sum_{time} P_{Cofiring}^{node,csp\_tech,time} \leq P_{SolarFieldPotential}^{node,csp\_tech,time} \cdot (1 - f_{SolarShare}^{csp\_tech})$$

$$\forall csp\_tech, time, node$$

Equation 5-27

5.6 Hydroelectricity

The approach used to represent hydroelectricity is shown in section 4.2.3. In annex 8.2 the assumed power generation scenarios are shown.

Parameter	Description	Unit
$e_{InstalledStorageCapacity}^{node,hydro\_tech,year}$	Reservoir capacity	[MWh]
$f_{MinimumFlow}^{node,hydro\_tech,year}$	Minimum ecological flow	[p.u.]

Power generation potential

Again, the potential electricity generation potentials are calculated using a capacity factor profile.

$$P_{Potential}^{node,hydro\_tech,time} \cdot \eta_{Net}^{hydro\_tech,'obs\_year'} = P_{InstalledCapacity}^{node,hydro\_tech,'obs\_year'} \cdot f_{Profile}^{node,hydro\_tech,time}$$

$$\forall time, hydro\_tech, node$$

Equation 5-28

Energy balance

The storage level variation between two periods can be increased due to water inflow or pumping. Because of water pumping or excess water the storage level is reduced.

$$E_{StorageLevel}^{node,hydro\_tech,time} - E_{StorageLevel}^{node,hydro\_tech,time-1}$$

$$= (P_{Potential}^{node,hydro\_tech,time} + P_{StorageLoad}^{node,hydro\_tech,time} \cdot \eta_{Storage}^{hydro\_tech,'obs\_year'} - \frac{P_{Generation}^{node,hydro\_tech,time} + P_{Surplus}^{node,hydro\_tech,time}}{\eta_{Net}^{hydro\_tech,'obs\_year'}}) \cdot p_{Intlen}$$

$$\forall time, hydro\_tech, node \qquad \text{Equation 5-29}$$

Maximum power generation and storage

The electric power generation can only be as large as the total installed capacity.

$$P_{Generation}^{node,hydro\_tech,time} \leq P_{InstalledCapacity}^{node,hydro\_tech,'obs\_year'} \cdot P_{Availability}^{node,hydro\_tech,'obs\_year'} \qquad \text{Equation 5-30}$$

$$\forall time, hydro\_tech, node$$

To consider that rivers located below the hydroelectric plant require a certain water supply a minimum amount can be set as a percentage of the average flow.

$$P_{Generation}^{node,hydro\_tech,time} \geq p_{InstalledCapacity}^{node,hydro\_tech,year} \cdot \frac{h_{Utilisation}^{node,hydro\_tech,year}}{8760} \cdot f_{MinimumFlow}^{node,hydro\_tech,year} \qquad \text{Equation 5-31}$$

$$\forall time, hydro\_tech, node$$

The storage power is limited by the total installed pumped storage capacity.

$$P_{StorageLoad}^{node,hydro\_tech,time} \leq p_{InstalledCapacity}^{node,hydro\_tech,year} \cdot f_{Availability}^{node,hydro\_tech,'obs\_year'} \qquad \text{Equation 5-32}$$

$$\forall time, hydro\_tech, node$$

Storage level

The storage level is limited by the available capacity.

$$E_{StorageLevel}^{node,hydro\_tech,time} \leq e_{InstalledStorageCapacity}^{node,hydro\_tech} \qquad \text{Equation 5-33}$$

$$\forall time, hydro\_tech, node$$

Again, it was also set here that the energy stored at the beginning must be equal to the amount of energy stored at the end of the considered period.

5.7 Power generation from biomass

Maximum power generation

Power generation is limited by the installed capacity as well as by the availability of the generation units.

$$P_{Generation}^{node,bio\_tech,time} \leq P_{InstalledCapacity}^{node,bio\_tech,year} \cdot f_{Availability}^{bio\_tech,year}$$

$$\forall time, bio\_tech, node$$

Equation 5-34

Fuel consumption

The bio fuel consumption is calculated from the power generation and from the efficiency of the generators.

$$E_{FuelConsumption}^{node,bio\_tech,time} = \frac{P_{Generation}^{node,bio\_tech,time}}{\eta_{Net}^{bio\_tech,year}} \cdot p_{Intlen}$$

$$\forall node, bio\_tech, time$$

Equation 5-35

Constant power generation

In the present work power generation from biomass is taken from a scenario and a constant power generation was assumed for the year.

$$P_{Generation}^{node,bio\_tech,time} = P_{InstalledCapacity}^{node,bio\_tech,'obs\_year'} \cdot h_{Utilisation}^{node,bio\_tech,'obs\_year'} / 8760$$

$$\forall time, node, bio\_tech$$

Equation 5-36

5.8 Storage

The parameters of storage plants are shown in 4.2.8, and the existing capacity in Table 46. The storage model doesn't consider any water inflows, i.e. all energy used for electricity production has been previously stored.

Variable	Description	Unit
$E_{StorageCapacityInstallation}^{node,stor\_tech,year}$	New installed storage capacity	[MWh]
$P_{CapacityInstallation}^{node,stor\_tech,year}$	New installed generation capacity	[MW]
Parameter	**Description**	**Unit**
$e_{InstalledStorageCapacity}^{node,stor\_tech,year}$	Installed storage capacity	[MWh]
$p_{InstalledCapacity}^{node,stor\_tech,year}$	Installed power generation and storage capacity	[MW]
$c_{InvestmentStorage}^{stor\_tech,year}$	Specific investment costs for storage capacity	[k€/MWh]
$c_{Investment}^{stor\_tech,year}$	Specific investment costs for power block capacity	[k€/MW]

Maximum storage power

The following equation limits the available power generation and storage only requiring the use of one equation, the optimisation algorithm decides if at a certain time step the

electric energy is stored or fed back to the grid so that the total system costs are minimised.

$$P_{Generation}^{node,stor\_tech,time} + P_{StorageLoad}^{node,stor\_tech,time} \leq$$

$$(P_{CapacityInstallation}^{node,stor\_tech,'obs\_year'} + p_{InstalledCapacity}^{node,stor\_tech,'obs\_year'}) \cdot f_{Availability}^{stor\_tech,'obs\_year'}$$

$$\forall time, stor\_tech, node$$

Equation 5-37

Storage balance

The variation in the storage level between time steps depends on storage and generation, considering the losses related to load ($\eta_{Load}^{stor\_tech,'obs\_year'}$) and discharge ($\eta_{Discharge}^{stor\_tech,'obs\_year'}$) as well as those depending on the time the energy is stored ($f_{LossRate}^{stor\_tech,'obs\_year'}$)[67].

$$E_{StorageLevel}^{node,stor\_tech,time} - E_{StorageLevel}^{node,stor\_tech,time-1} =$$

$$(P_{StorageLoad}^{node,stor\_tech,time} \cdot \eta_{Load}^{stor\_tech,'obs\_year'} - P_{Generation}^{node,stor\_tech,time} / \eta_{Discharge}^{stor\_tech,'obs\_year'}$$

$$- (P_{StorageLevel}^{node,stor\_tech,time} + P_{StorageLevel}^{node,stor\_tech,time-1}) \cdot f_{LossRate}^{stor\_tech,'obs\_year'} / 2) \cdot p_{Intlen}$$

$$\forall time, stor\_tech, node$$

Equation 5-38

The storage level is limited by the total installed capacity.

$$E_{StorageLevel}^{node,stor\_tech,time} \leq (e_{InstalledStorageCapacity}^{node,stor\_tech,'obs\_year'} + E_{StorageCapacityInstallation}^{node,stor\_tech,'obs\_year'})$$

$$\forall time, stor\_tech, node$$

Equation 5-39

Again, the energy level at the beginning and at the end of the period has to be equal.

Storage ratio

The ratio of the installed storage capacity and installed power can be set to a fix value.

$$p_{InstalledStorageCapacity}^{node,stor\_tech,'obs\_year'} + P_{StorageCapacityInstallation}^{node,stor\_tech,'obs\_year'} =$$

$$f_{StorageRatio}^{stor\_tech,'obs\_year'} \cdot \frac{(P_{CapacityInstallation}^{node,stor\_tech,'obs\_year'} + p_{InstalledCapacity}^{node,stor\_tech,'obs\_year'})}{\eta_{Discharge}^{stor\_tech,'obs\_year'}}$$

$$\forall stor\_tech, node, StorRatioFix = 1$$

Equation 5-40

---

[67] Note that the $\eta_{Discharge}^{stor\_tech,'obs\_year'}$ and the $\eta_{Load}^{stor\_tech,'obs\_year'}$ variables represent the power consumed for loading and discharging the reservoir, and, in order to calculate the impact on storage level, the efficiency during the loading and discharging process has to be taken into account.

5.9 Geothermal electricity

In this work the power generation profile is derived from the heat demand profiles calculated with the resources module. As in the case of wind power the profile used is scaled based on the capacity factor. In case of excessive must-run generation in the system the plant's output can be reduced using the surplus variable. The power generation scenarios are shown in annex 8.2.

$$P_{Generation}^{node,geo\_tech,time} + P_{Surplus}^{node,geo\_tech,time} = p_{InstalledCapacity}^{node,geo\_tech,year} \cdot f_{Profile}^{node,geo\_tech,time} \qquad \text{Equation 5-41}$$

$$\forall time, geo\_tech, node$$

5.10 Combined heat and power

The combined heat and power module allows modelling plants with one and two degrees of freedom, the approach is presented in 4.2.7. The scenario containing the installed capacity of CHP units is shown in Table 47.

Variable	Description	Unit
$P_{HeatGenerationBoiler}^{node,chp\_tech,time}$	Heat production from the boiler	[MW]
$P_{HeatCondensation}^{node,chp\_tech,time}$	Heat condensed from heat production assuming one degree of freedom	[MW]
$P_{HeatProduction}^{node,chp\_tech,time}$	Heat production in the CHP process	[MW]
$P_{HeatGenerationEBoiler}^{node,chp\_tech,time}$	Generation of the electric boiler	[MW]
Parameter	**Description**	**Unit**
$p_{InstalledCapacityThermal}^{node,chp\_tech,year}$	Installed thermal generation capacity	[MW]
$p_{DemandHeat}^{node,chp\_tech,time}$	Heat demand of each CHP technology	[MW]
$f_{CoefficientE2H}^{node,chp\_tech,year}$	Electricity to heat coefficient	[W$_{el}$/W$_{th}$]
$f_{ExtractionLosses}^{node,chp\_tech,year}$	Loss factor of power gen. due to heat extraction	[W$_{el}$/W$_{th}$]
$f_{ElectricBoilerCapacity}^{node,chp\_tech,time}$	Installed capacity of the electric boiler related to the power generation capacity of the CHP	[p.u.]
$\eta_{Boiler}^{node,chp\_tech,year}$	Efficiency of the boiler	[p.u.]
$\eta_{ElectricBoiler}^{chp\_tech,time}$	Efficiency of heat production with the electric boiler	[p.u.]
$\eta_{CondOperation}^{node,chp\_tech,year}$	Efficiency of the CHP plant in condensation mode	[p.u.]

Maximum power generation

The power generation of CHP plants is limited to its installed generator capacity.

$$P_{Generation}^{node,chp\_tech,time} + P_{HeatProduction}^{node,chp\_tech,time} \cdot f_{ExtractionLosses}^{node,chp\_tech,'obs\_year'} \le p_{InstalledCapacity}^{node,chp\_tech,time} \cdot f_{Availability}^{node,chp\_tech,'obs\_year'} \qquad \text{Equation 5-42}$$

$$\forall time, chp\_tech, node$$

Power balance

The following equation relates electricity and heat generation, which in plants with one degree of freedom is straightforward, as both are related by the CHP coefficient. In case of an extraction-condensing unit the possibility of extracting part of the steam stream to feed a heating network requires modelling the impact of heat extraction caused on electricity output.

$$P_{Generation}^{node,chp\_tech,time} = f_{CoefficientE2H}^{node,chp\_tech,year} \cdot (P_{HeatProduction}^{node,chp\_tech,time} + P_{HeatCondensation}^{node,chp\_tech,time})$$
$$+ P_{HeatCondensation}^{node,chp\_tech,time} \cdot f_{ExtractionLosses}^{node,chp\_tech,year}$$
$$\forall node, chp\_tech, time$$

Equation 5-43

In case the plant has two degrees of freedom (i.e. as for extraction-condensing steam turbines) the following variable is set to zero.

$$P_{HeatCondensation}^{node,chp\_tech,time} = 0$$
$$\forall node, chp\_tech, time$$

Equation 5-44

Heat balance

The demand for heat in CHP plants is covered at all times through the provision of heat from the cogeneration process, from boilers using electricity or fuel or from the heat storage system.

$$P_{HeatProduction}^{node,chp\_tech,time} + P_{HeatBoiler}^{node,chp\_tech,time} \cdot \eta_{Boiler}^{chp\_tech,time} + P_{HeatEBoiler}^{node,chp\_tech,time} \cdot \eta_{EBoiler}^{chp\_tech,time} =$$
$$p_{HeatDemand}^{node,chp\_tech,time} - (P_{StorageDischarge}^{node,chp\_tech,time} - P_{StorageLoad}^{node,chp\_tech,time})$$
$$\forall time, chp\_tech, node$$

Equation 5-45

Fuel consumption

The fuel requirements of cogeneration plants are modelled as the fuel consumption of the boiler and that of cogeneration. The fuel requirements of the boiler are related to its efficiency. The fuel requirements of the CHP plant can be calculated as the equivalent electricity production in condensing operation mode divided by its efficiency. As for thermal generation units the fuel consumption due to start-ups procedures is included.

$$E_{FuelConsumption}^{node,chp\_tech,time} = p_{Intlen} \cdot (P_{Boiler}^{node,chp\_tech,time} / \eta_{Boiler}^{node,chp\_tech,'obs\_year'}$$
$$+ (P_{Generation}^{node,chp\_tech,time} + P_{HeatCondensation}^{node,chp\_tech,time} \cdot f_{ExtractionLosses}^{node,chp\_tech,'obs\_year'}) / \eta_{Condensation}^{node,chp\_tech,'obs\_year'})$$
$$+ N_{StartUps}^{node,chp\_tech,time} \cdot p_{AverageBlockSize}^{chp\_tech,'obs\_year'} \cdot f_{StartUpFuel}^{chp\_tech,'obs\_year'}$$
$$\forall time, chp\_tech, node$$

Equation 5-46

Electric heating

The electric boiler capacity is given as a share of the installed capacity of CHP.

$$P_{HeatGenerationEBoiler}^{node,chp\_tech,time} \leq p_{InstalledCapacity}^{node,chp\_tech,'obs\_year'} \cdot f_{ElectricBoiler}^{node,chp\_tech,'obs\_year',time}$$
$$\forall time, chp\_tech, node$$

Equation 5-47

Storage balance

The variation of the storage level is determined by loading and discharging as well as by the temperature loss modelled through a loss factor.

$$E_{StorageLevel}^{node,chp\_tech,time} - E_{StorageLevel}^{node,chp\_tech,time-1} = (P_{StorageLoad}^{node,chp\_tech,time} - P_{StorageDischarge}^{node,chp\_tech,time}$$
$$- (E_{StorageLevel}^{node,chp\_tech,time} + E_{StorageLevel}^{node,chp\_tech,time-1}) \cdot f_{LossRate}^{node,chp\_tech,'obs\_year'}/2) \cdot p_{Intlen}$$
$$\forall time, chp\_tech, node$$

Equation 5-48

Heat storage capacity

The storage capacity of the thermal storage system is given in hours of operation of the cogeneration plant at its nominal thermal capacity. Again, at the beginning and end of the period the storage level has to be equal.

$$E_{StorageLevel}^{node,chp\_tech,time} \leq p_{InstalledCapacityThermal}^{node,chp\_tech,'obs\_year'} \cdot f_{StorageRatio}^{node,chp\_tech,'obs\_year'}$$
$$\forall node, chp\_tech, time$$

Equation 5-49

5.11 Plug-in electric vehicles

The modelling approach for PEVs is introduced in 3.2, the used input data can be found in annex 8.1.

Variable	Description	Unit
$P_{EMobLoad}^{node,time}$	Electricity demand of the electric vehicle fleet	[MW]
$P_{EMobFeed}^{node,time}$	Electricity feed-in of the electric vehicle fleet	[MW]
$P_{LoadCL}^{node,veh\_type,time}$	Charging rate of an average PEV with controlled loading	[kW]
$P_{LoadV2G}^{node,veh\_type,time}$	Charging rate of an average PEV with bidirectional. controlled loading	[kW]
$P_{FeedV2G}^{node,veh\_type,time}$	Feed-in power of an average PEV with bidirectional. controlled loading	[kW]
$E_{BatteryLevelCL}^{node,veh\_type,time}$	Fill level of the battery with controlled loading	[kWh]

$E_{BatteryLevelV2G}^{node,veh\_type,time}$	Fill level of the battery with bidir. controlled loading	[kWh]
$F_{DoD\_V2G}^{node,veh\_type,time}$	Depth-of-Discharge with bidir. controlled loading	[p.u.]
$C_{CostDoD\_V2G}^{node,veh\_type,day}$	Wearing costs of electric vehicles per day	[k€]
Parameter	**Description**	**Unit**
$\eta_{grid2vehicle}^{veh\_type,year}$	Grid to vehicle efficiency	[p.u.]
$\eta_{vehicle2grid}^{veh\_type,year}$	Vehicle to grid efficiency	[p.u.]
$f_{VehicleShareUL}^{node,veh\_type,year}$	Vehicle share with uncontrolled loading	[p.u.]
$f_{VehicleShareCL}^{node,veh\_type,year}$	Vehicle share with controlled loading	[p.u.]
$f_{VehicleShareV2G}^{node,veh\_type,year}$	Vehicle share with bidir. controlled loading	[p.u.]
$p_{LoadUL}^{node,veh\_type,year,time}$	Charging power with uncontrolled loading	[kWel]
$n_{VehicleAmount}^{node,veh\_type,year}$	Amount of vehicles of each type	[1000#]
$f_{SharePlugged}^{node,veh\_type,year,time}$	Share of vehicles with grid contact	[p.u.]
$p_{Connection}^{veh\_type,year}$	Grid connection capacity	[kWel]
$p_{Driving}^{node,veh\_type,year,time}$	Electricity demand for driving	[kWel]
$p_{BatteryCapacity}^{veh\_type,year}$	Battery capacity	[kWhel]
$p_{BatteryLevelMax}^{veh\_type,year,time}$	Maximum battery level	[kWhel]
$p_{BatteryLevel}^{veh\_type,year,time}$	Minimum battery level	[kWhel]
$f_{CapacityFadeMax}$	Capacity fade assumed in the life-time of a battery	[p.u.]
$a_{CapacityFade}^{segment,veh\_type}$	Parameter a to include the capacity fade related to V2G as piecewise linear segments	[p.u.]
$b_{CapacityFade}^{segment,veh\_type}$	Parameter b to include the capacity fade related to V2G as piecewise linear segments	[p.u.]
Indices:	**Description:**	
veh_type	BEV and EREV each in three sizes small, medium and large.	
segment	Linear segments describing battery ageing	

Power demand and feed-in of the PEV fleet

The power consumption of electric vehicles in the network is given by the sum of the power consumption of the three different vehicle types divided by the charging efficiency and multiplied by the total number of vehicles.

$$P_{EMobLoad}^{node,time} = \sum_{veh\_type} n_{VehicleAmount}^{node,'obs\_year',veh\_type} \cdot (f_{VehicleShareUL}^{node,veh\_type,'obs\_year'} \cdot p_{LoadUL}^{node,veh\_type,time} +$$

Equation 5-50

$$f_{VehicleShareCL}^{node,veh\_type,'obs\_year'} \cdot p_{LoadCL}^{node,veh\_type,time} + \frac{f_{VehicleShareV2G}^{node,veh\_type,'obs\_year'} \cdot p_{LoadV2G}^{node,veh\_type,time}}{\eta_{grid2vehicle}^{veh\_type}})$$

$$\forall node, time$$

A similar equation applies for electricity feed-in:

$$P_{EMobFeed}^{node,time} = \sum_{veh\_type} n_{VehicleAmount}^{node,'obs\_year',veh\_type} \cdot f_{VehicleShareV2G}^{node,veh\_type,'obs\_year'} \cdot P_{FeedV2G}^{node,veh\_type,time} \cdot \eta_{vehicle2grid}^{veh\_type,'obs\_year'}$$

Equation 5-51

$$\forall node, time$$

Maximum charging power and feed-in

The charging and discharging rates of electric vehicles are limited by the connection capacity and by the share of vehicles plugged-in.

$$P_{LoadCL}^{node,veh\_type,time} / \eta_{grid2vehicle}^{veh\_type} \leq f_{SharePlugged}^{node,veh\_type,time} \cdot p_{Connection}^{veh\_type,'obs\_year'}$$

Equation 5-52

$$P_{LoadV2G}^{node,veh\_type,time} / \eta_{grid2vehicle}^{veh\_type} \leq f_{SharePlugged}^{node,veh\_type,time} \cdot p_{Connection}^{veh\_type,'obs\_year'}$$

$$P_{LoadV2G}^{node,veh\_type,time} \cdot \eta_{vehicle2grid}^{veh\_type} \leq f_{SharePlugged}^{node,veh\_type,time} \cdot p_{Connection}^{veh\_type,'obs\_year'}$$

$$\forall node, veh\_type, time$$

Energy balance

The difference in the battery level between two time steps is due to loading or unloading and by the electricity requirements for driving.

$$P_{BatteryLevelCL}^{node,veh\_type,time} - P_{BatteryLevelCL}^{node,veh\_type,time-1} =$$

Equation 5-53

$$(P_{LoadCL}^{node,veh\_type,time} - P_{FeedCL}^{node,veh\_type,time} - p_{Driving}^{node,veh\_type,time}) \cdot p_{Intlen}$$

$$P_{BatteryLevelV2G}^{node,veh\_type,time} - P_{BatteryLevelV2G}^{node,veh\_type,time-1} =$$

$$(P_{LoadV2G}^{node,veh\_type,time} - P_{FeedV2G}^{node,veh\_type,time} - p_{Driving}^{node,veh\_type,time}) \cdot p_{Intlen}$$

$$\forall node, veh\_type, time$$

The battery level, in order to be able to perform all trips scheduled and due to the limited charging rate, has to be comprised between a minimum and a maximum level.

$$p_{BatteryLevelMin}^{veh\_type,time} \leq P_{BatteryLevelCL}^{node,veh\_type,time} \leq p_{BatteryLevelMax}^{veh\_type,time}$$

$$p_{BatteryLevelMin}^{veh\_type,time} \leq P_{BatteryLevelV2G}^{node,veh\_type,time} \leq p_{BatteryLevelMax}^{veh\_type,time}$$

$$\forall node, veh\_type, time$$

Equation 5-54

Again, the energy level at the beginning and at the end of the period has to be equal.

Cost related to V2G

In this work the wearing costs related to electric vehicle power feed-in are calculated in base of the daily DoD. The DoD of each day is calculated as the sum of the discharge due to driving and due to V2G.

$$F_{DoD\_V2G}^{node,veh\_type,day} = \sum_{time \subset day} \frac{p_{Driving}^{node,veh\_type,time} + P_{FeedV2G}^{node,veh\_type,time}}{p_{BatteryCapacity}^{veh\_type,'obs\_year'}}$$

$$\forall node, veh\_type, day$$

Equation 5-55

The costs per day are calculated in a simplified model using a set of piecewise functions to model the non-linear relation between capacity fade and DoD. In order to calculate the cost it has been assumed that when the battery reaches a given capacity-fade the residual value is cero and that wearing costs are proportional to capacity fade.

$$C_{CostDoD\_V2G}^{node,veh\_type,day} \geq$$
$$\frac{(a_{CapacityFade}^{segment,veh\_type} + b_{CapacityFade}^{segment,veh\_type} \cdot F_{DoD\_V2G}^{node,veh\_type,day})}{f_{BatteryFadeMax}} \cdot p_{BatteryCapacity}^{veh\_type,'obs\_year'} \cdot p_{BatteryPrice}^{'obs\_year'}$$

$$\forall node, veh\_type, day$$

Equation 5-56

The wearing costs of the electric vehicle fleet are calculated as:

$$C_{BatteryWearPEV} = \sum_{node} \sum_{veh\_type} \sum_{day} n_{VehicleAmount}^{node,year,veh\_type} \cdot f_{VehicleShareV2G}^{node,veh\_type,year} \cdot C_{CostDoD\_V2G}^{node,veh\_type,day}$$

Equation 5-57

5.12 Hydrogen fuelling stations

The approach followed to represent the demand of FCV is presented in 3.3, the hydrogen demand of the FCV fleet is shown in Table 37.

Variable	Description	Unit
$P_{H_2Production}^{node,h2\_tech,time}$	Hydrogen production	[MW$_{chem}$]
$P_{H_2ElectricityDemand}^{node,h2\_tech,time}$	Electricity demand for hydrogen production	[MW$_{el}$]
Parameter	**Description**	**Unit**
$p_{H_2Consumption}^{node,h2\_tech,year,time}$	Hydrogen demand	[MW$_{th}$]

$p_{ElectrolyserCapacity}^{node,h2\_tech,year}$ Installed electrolyser capacity   [MW$_{el}$]

$\eta_{H_2Production}^{node,h2\_teh,year}$ Hydrogen production efficiency   [p.u.]

Electricity demand for the production of hydrogen

The electricity demand for the production of hydrogen is calculated assuming a constant efficiency.

$$P_{H_2ElectricityConsumption}^{node,h2\_tech,year,time} \cdot \eta_{H_2Production}^{node,h2\_teh,year} = P_{H_2Production}^{node,h2\_teh,year,time}$$
$$\forall node,h2\_tech,time$$

Equation 5-58

Maximum hydrogen production capacity

The electricity consumption is limited by the installed capacity of the hydrogen production system.

$$P_{H_2ElectricityConsumption}^{node,h2\_tech,time} \leq p_{InstalledCapacity}^{node,h2\_tech,'obs\_year'}$$
$$\forall node,h2\_tech,time$$

Equation 5-59

Energy balance

The variation of the storage level of hydrogen fuelling stations is given by the production and consumption of hydrogen by the following equation.

$$P_{StorageLevel}^{node,h2\_teh,time} - P_{StorageLevel}^{node,h2\_teh,time-1} = (P_{H_2Production}^{node,h2\_teh,time} - p_{H_2Consumption}^{node,h2\_teh,'obs\_year',time}) \cdot p_{Intlen}$$
$$\forall node,h2\_tech,time$$

Equation 5-60

Storage capacity

The level of hydrogen storage is limited by the size of the storage system. Its capacity is given in hours of the average hydrogen consumption.

$$P_{StorageLevel}^{node,h2\_tech,time} \leq f_{StorageRatio}^{h2\_tech,'obs\_year'} \cdot \frac{p_{H_2AnnualConsumption}^{node,h2\_tech,'obs\_year',time}}{8760}$$
$$\forall node,h2\_tech,time$$

Equation 5-61

Again, the storage level at the beginning and at the end has to be equal.

5.13 HVDC transmission

The parameters used to model HVDC transmission lines are presented in Table 25, in Table 48 the different existing, planned and candidate lines are characterised.

Variable	Description	Unit
$P_{Transport}^{node1,node2,dc\_tech,time}$	Electricity transport over HVDC lines from 1 to 2	[MW]
$N_{Installation}^{node1,node2,dc\_tech,year}$	Number of installed HVDC lines between 1 and 2	[#]
Parameter	**Description**	**Unit**
$p_{Rating}^{dc\_tech,year}$	Rating of lines	[MW]
$c_{InvestmentStation}^{dc\_tech,year}$	Specific investment costs of the transformer station	[k€/MW]
$c_{InvestmentLine}^{dc\_tech,year}$	Specific capital expenditures of the line	[k€/km*MW]
$c_{InvestmentSeaCable}^{dc\_tech,year}$	Specific capital expenditures of the sea cable	[k€/km*MW]
$n_{Installed}^{node1,node2,dc\_tech,year}$	Existing HVDC lines between node 1 and node 2	[#]
$f_{Losses}^{node1,node2,dc\_tech,year,time}$	Transmission loss factor	[p.u.]
$d_{DistanceLand}^{node1,node2,dc\_tech,year}$	Distance of the considered line/cable on land	[km]
$d_{DistanceSeaCable}^{node1,node2,dc\_tech,year}$	Distance of the considered cable under water	[km]

Transmission capacity

The transmission power between two electric nodes is limited by the number of installed lines and the transmission capacity of each of them.

$$P_{Transport}^{node1,node2,dc\_tech,time} \leq (n_{Installed}^{node1,node2,dc\_tech,'obs\_year'} + N_{Installation}^{node1,node2,dc\_tech,'obs\_year'}) \cdot p_{Rating}^{dc\_tech,'obs\_year'}$$

$$\forall node1, node2, dc\_tech, time$$

Equation 5-62

Transport including losses

The electricity transport over each DC line has been modelled using two positive variables; one for each direction. This approach allows taking into account transmission losses using a loss factor. The losses are distributed evenly on each node.

$$P_{Transmission}^{node,dc\_tech,time} = \sum_{node2} P_{Transport}^{node,node2,dc\_tech,time} \cdot \frac{1}{1 - 0.5 \cdot f_{Losses}^{node,node2,dc\_tech,year,time}} -$$

$$\sum_{node1} P_{Transport}^{node1,node,dc\_tech,time} \cdot \frac{1}{1 - 0.5 \cdot f_{Losses}^{node1,node,dc\_tech,year,time}}$$

$$P_{Transport}^{node1,node2,dc\_tech,time} \geq 0$$

$$\forall node, dc\_tech, time$$

Equation 5-63

5.14 HVAC transmission

The modelling approach followed assumes a linear relation between power feed-in in the defined zones and the power flows between them and is introduced in 0.

Variable	Description	Unit
$P_{TransportAC}^{ffz1,ffz2,time}$	Power transmission between ffz 1 and 2	[MW]
Parameter	**Description**	**Unit**
$p_{NTC}^{ffz1,ffz2}$	Available transfer capacity between ffz 1 and 2	[MW$_{el}$]
$f_{PTDF}^{ffz1,ffz2,ffz}$	Power Transmission Distribution Factors	[p.u.]

Power flow calculation

The power flow between two zones is calculated using the Power Transmission and Distribution Factors (PTDF) which assumes a linear relation between feed-in and power flows (the used factors can be found in Table 50). The PTDF represents how much the active power flow between two free flow zones changes when the feed-in is modified in another zone. This approach does not consider the potential bottlenecks that may occur inside the free flow zones, but only in the boundaries between them for which the power flows are calculated.

$$P_{TransportAC}^{ffz1,ffz2,time} = \sum_{ffz} \sum_{node \subset ffz} P_{TransmissionAC}^{node,time} \cdot f_{PTDF}^{fz1,ffz2,ffz}$$

$$\forall flowgate(ffz1,ffz2),time$$

Equation 5-64

Available transfer capacities

The AC transport over each intersection between free flow zones, also called flowgate, is limited by the Net Transfer Capacity which represents the "*maximum exchange program between two areas compatible with security standards applicable in both areas and taking into account the technical uncertainties on future network conditions*"[68], (the NTCs are shown in Table 49).

$$P_{TransportAC}^{zone1,zone2,time} \leq p_{NTC}^{zone1,zone2} \forall flowgate(zone1,zone2),time$$

Equation 5-65

---

[68] ENTSOE, Principles for Determining the Transfer Capacities in the Nordic Power Market, 28/03/2012.

6 Impact of electric mobility on the power system

6.1 Definition of scenario variants

The present analysis focuses first on year 2030, to analyse the impact in the development phase, and second on 2050 to analyse the impact in the maturity phase. As seen previously in 3.4.1 it is not expected that PEVs reach a share of more than 10% of the passenger vehicle stock before 2030. For that year the fleet scenarios assume for Germany a PEV stock of 5.1 million vehicles with an annual demand of 14.7 TWh, representing less than 3% of the total electricity demand. During the development phase up to 2030 the hydrogen demand for the transport sector would be negligible. For renewable power generation the scenario assumes a penetration of 52% in Europe and of 66% in Germany.

In the period from 2030 to 2050 a high penetration of EVs as well as of renewable power generation is assumed in the energy scenarios (see Chapter 3 and 4), and thus the results in this period will be used to assess the long term impact of electric vehicles in a renewable generation based power system. For 2050 66% of passenger cars would be PEVs consuming annually 49.1 TWh. For the same year the freight transport sector would demand 84.9 TWh for hydrogen production via electrolysis. The demand of PEVs and for hydrogen production would thus reach in Germany 20% of the total annual power demand. The renewable power generation would exceed 85% in Germany and Europe.

In the author's opinion the future trends of the power system namely the connection of remote renewable-rich regions with consumption centres with electricity highways and the deployment of smart grids to adapt demand to weather conditions are not mutually exclusive but complementary. In this dissertation the following deterministic scenarios have been considered for the REMix simulations which suppose a combination of both trends, for all medium fuel and CO_2 allowance costs are assumed.

- **Base case (*Base*)**

This scenario will be considered as the reference scenario as most scenario variants considered are a modification of this scenario. It assumes no solar electricity imports from North Africa (see Figure 19 and Figure 20) as well as the development of

controlled loading shown in Figure 18. The least cost expansion of the transmission network is based on underground cables with a capacity of 2.2 GW.

- ## **Overhead lines (OH)**

This scenario variant assumes in contrast to *Base* a less expensive expansion of the transmission network based on overhead lines with a capacity of 3200 MW. According to (DLR/IFHT/ISE, 2012) overhead lines present costs per km around 3.5 times lower than underground cables. However, when the whole HVDC project is considered including the converter station, this factor is reduced. For a 1000 km line the costs per MW are around half of those resulting with underground cables, while for a 250 km line these are only around 25% lower as the station comprises most of the total cost.

- ## **Costly underground cables (x2)**

This scenario assumes a twice as expensive expansion of the transmission network as in *Base*. These costs are based on the resulting costs of the interconnection between Spain and France. The line will come into operation in 2014 with a transmission capacity of 1400 MW and a nominal voltage of 320 kV. Due to the lower capacity, voltage level and to the costs related to the construction of a tunnel through the Pyrenees the specific costs of this interconnection double those resulting with the model for underground cables[69].

- ## **Trans-European Power System (Trans)**

This scenario assumes solar electricity imports from North Africa using concentrated solar thermal power generation with thermal storage accounting for around 15% of the annual European electricity demand by 2050 as shown in Figure 21. For Germany, the annual solar electricity imports assumed for 2050 reach 130 TWh.

- ## **No Electric Vehicles (NEV)**

In this scenario neither PEVs for personal mobility nor FCEVs for freight transport become a viable alternative. In consequence, the renewable power generation facilities

---

[69] Total costs of 700 million Euros, 64.5 km total length. INterconnexion ELectrique France Espagne (www.inelfe.eu).

installed in *Base* to cover the electricity demand of EVs are not included in this scenario.

- **Combined scenarios**

In addition, combined scenarios of the presented variants are considered, e.g. the scenario *Trans* with solar electricity imports assuming 100% of PEVs with controlled loading (*Trans-CL*). These combined scenarios are used in order to assess the impact of EVs depending on the power system´s situation.

- **Uncontrolled loading (*UL*)**

This scenario is a modification of *Base,* assumes that all PEVs are charged just after the last trip at the maximum possible rate and does not consider the contribution of PEVs to demand side management.

- **Controlled loading (CL)**

This scenario assumes that all PEVs are charged in times in which electricity presents the lowest value. The available demand shifting potential is calculated based on the driving behaviour and on the resulting energy requirements and charge state of the vehicle batteries as shown in Figure 11.

- **Vehicle to grid (V2G)**

This scenario is a variant of the *CL* case. The PEVs are able to feed electricity from the battery back into the grid if the economic gains are higher than the costs related to the battery wear.

- **Hydrogen (H2)**

In this scenario the electrolysers for hydrogen production have a capacity that doubles that of those in the *Base* scenario. In the *Base* scenario an utilisation of electrolysers of 4000 hours is assumed whereas in this variant it is reduced to 2000 hours. The size of the hydrogen storage system is, as in *Base,* 12 hours of the average demand.

- **Hydrogen plus (H2+)**

In this scenario in addition to a larger electrolyser capacity than in the *H2* scenario it is assumed that the system has a storage capacity of one week of the average demand.

o **No Electric Vehicles (NEV)**

This scenario without EVs can also be used combined with the *x2* scenario for instance to assess the impact of EVs in the *x2* scenario.

6.2   Methodology

The approach followed to solve the mathematical problem of this dissertation is to a large extent conditioned by the large size of the problem. The use of chronological time steps instead of typical days or typical load situations[70], the detailed representation of PEVs and CHP as well as the consideration of both the actual AC transmission network and DC lines contributes to a large increase in size and of solving time of the problem.

So as to solve the mathematical problem a two-tier approach was followed. In a first step the least cost expansion of the transmission network with HVDC lines, storage and of gas turbines for peak demand coverage in Europe and North Africa was calculated. In order to be able to solve this large problem in reasonable times the temporal resolution was increased to 5 hours. This first step also provides the interchanges over the AC network and over individual DC lines, which are used as input along with the expansion of the power system in the second step. Finally, the least cost dispatch of the system is calculated in Germany with a resolution of one hour considering the transmission capacity between the seven defined zones as well as the start-up costs of thermal units.

The program creating the mathematical problem was written in the GAMS language version 23.8.2[71] and solved with the CPLEX solver version 12.4[72]. The Barrier algorithm of CPLEX was used as it proved to be the fastest of all methods included.

6.3   First tier results: System expansion

In this section the results of the first tier will be presented. These are mainly DC lines expansion scenarios calculated using different assumptions regarding the development of EVs, of the transmission system expansion costs and of solar

---

[70] Such as peak, medium and base load.

[71] GAMS Development Corporation.

[72] IBM ILOG CPLEX Optimizer.

electricity imports. First the results assuming the central development scenario for EVs (following the *Base* scenario) will be presented on a map, secondly the sensitivities of these scenarios will be shown to quantify the contribution of electric mobility to relevant power system metrics.

6.3.1 Transmission system expansion scenarios

This section will introduce the results of REMix regarding the expansion of the power system for the *Base* scenario in 2030 and 2050, as well as for the *x2* and *Trans* scenarios in 2050. As the expansion of power generation capacities is exogenously defined by the energy scenario, the results will focus on the transmission network and storage expansion. However, the model will also allow for an additional expansion of generation capacity as alternative to storage and other balancing options.

The present transmission network is represented using a simplified high voltage alternating current (HVAC) model and point-to-point high voltage direct current (HVDC) lines. The power transport over the AC network is calculated between defined free flow zones using linear factors called Power Transfer Distribution Factors (PTDF) and take as transmission limits between the neighbouring zones the Net Transfer Capacities (NTC). The transmission capacity expansion is based on HVDC lines. In order to calculate the costs of each line each interconnection is characterized by its distance on land and under water and thus neglects operational, political and social aspects. As a conservative assumption the base scenario only takes underground cables as present higher political and social acceptance in spite of the higher costs.

The results for the 2030 base scenario are shown in Figure 39. The interconnection capacity sum between Germany and its neighbours is - under the assumptions made - of about 12 GW for HVDC lines and of about 11 GW for the HVAC network[73]. Figure 40 shows the results for the base scenario in 2050. Under the assumptions made a significant expansion of the network capacity with neighbouring countries is realized between 2030 and 2050. The transmission capacity sum of Germany with its neighbours reaches 19.5 GW with HVDC lines. The results assuming doubled transmission expansion costs (*x2*) are depicted in Figure 41. The *x2* scenario represents a more conservative scenario concerning the expansion of the transmission system; in this scenario the HVDC transmission capacity sum of Germany with its

---

[73] Assumes the network development plan by (ENTSO-E, 2010).

neighbours reaches 14.7 GW. The results of the scenario with solar electricity imports are shown in Figure 42, the network expansion is therefore more ambitious than in the *Base* scenario mainly because its realization requires the construction of transmission lines from northern Africa over southern Europe to the consumption centres in central Europe. The HVDC interconnection capacity of Germany, in this scenario, increases up to 27.5 GW, mainly due to the coupling point to the Alpine region, which allows the transmission of solar electricity from the south to Germany. It should be noted that the power transmission lines installed for the transmission of renewable power generation over long distances also allow the exchange and thus the trade between the interconnected areas.

Figure 39: Calculated HVDC transmission capacity scenario - *Base* scenario 2030

Source: Results of the REMix Model.
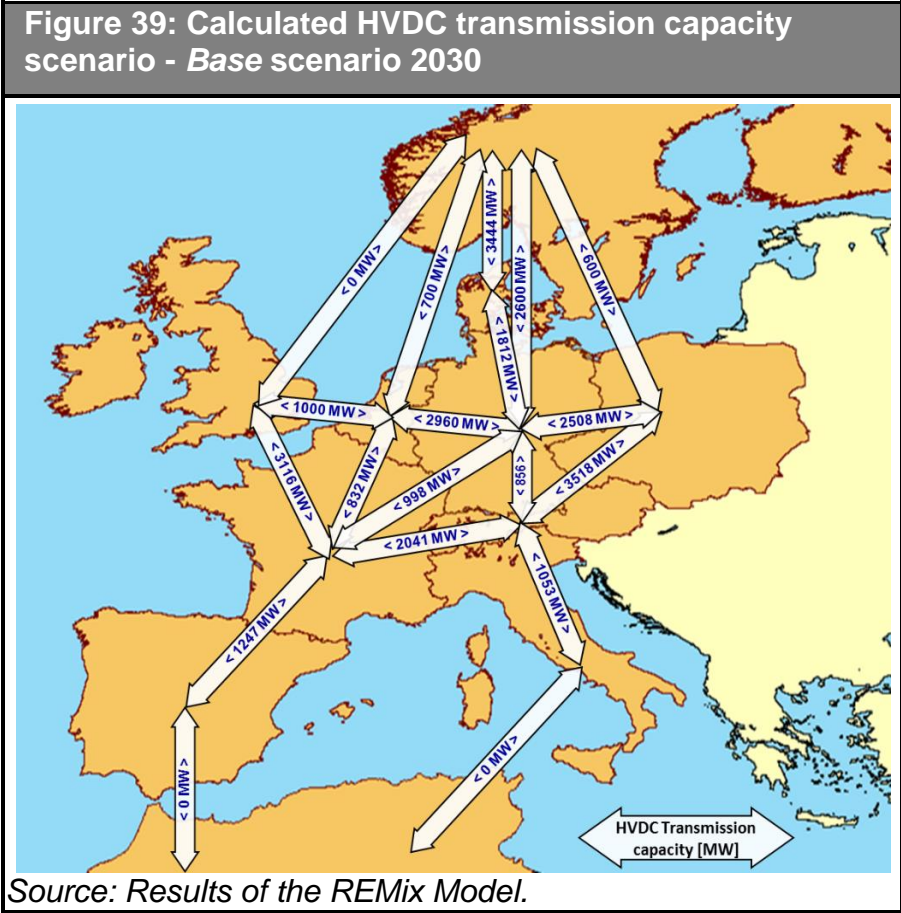
Both the power generation and storage capacity expansion were optimized simultaneously with the transmission system. The results pointed out that for the made assumptions installing transmission lines was in all cases more economic than installing generation and/or storage capacity. Therefore, the model did not return any additional capacities on top of those that were already assumed in the scenario.

Figure 40: Calculated HVDC transmission capacity scenario - *Base* scenario 2050
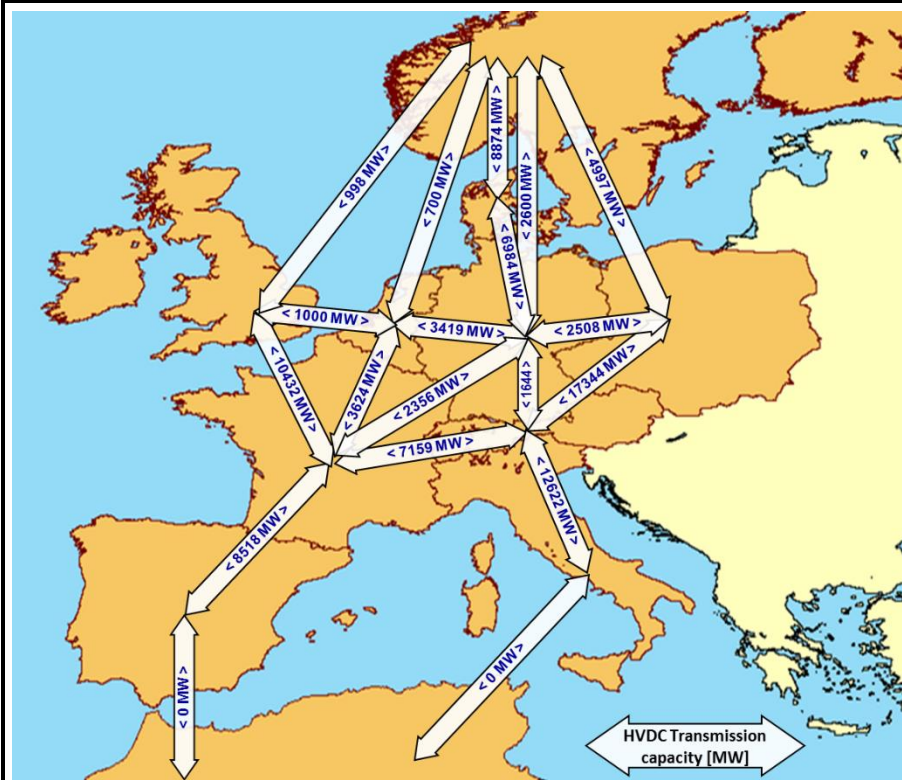
Source: Results of the REMix Model.

Figure 41: Calculated HVDC transmission capacity scenario – *x2* scenario 2050

Source: Results of the REMix Model.

Figure 42: Calculated HVDC transmission capacity scenario - *Trans* scenario 2050
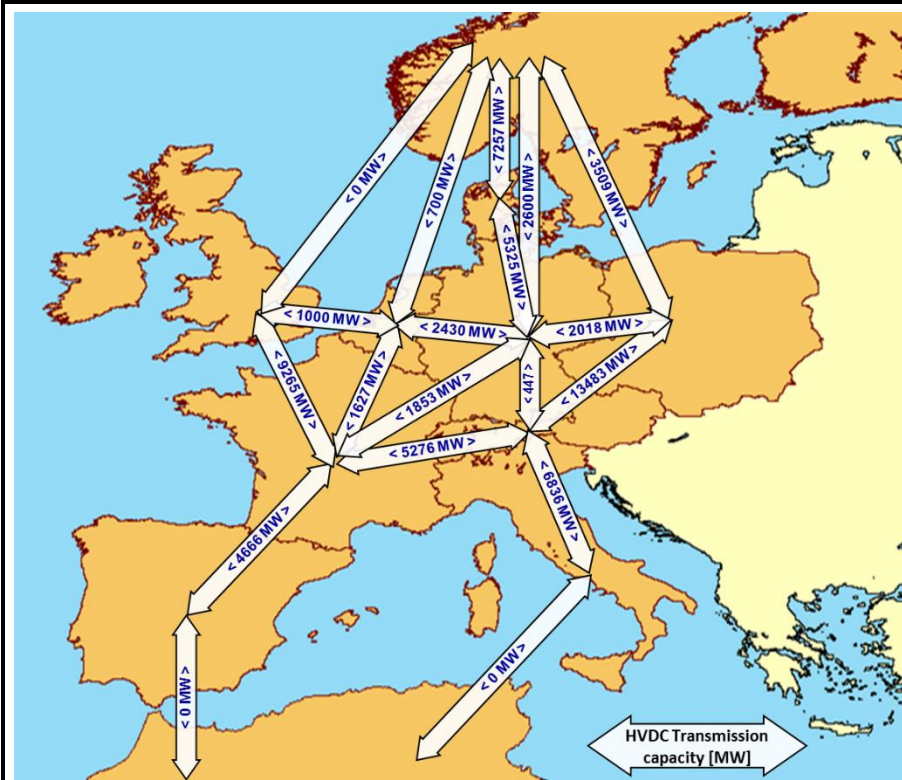
Source: Results of the REMix Model.
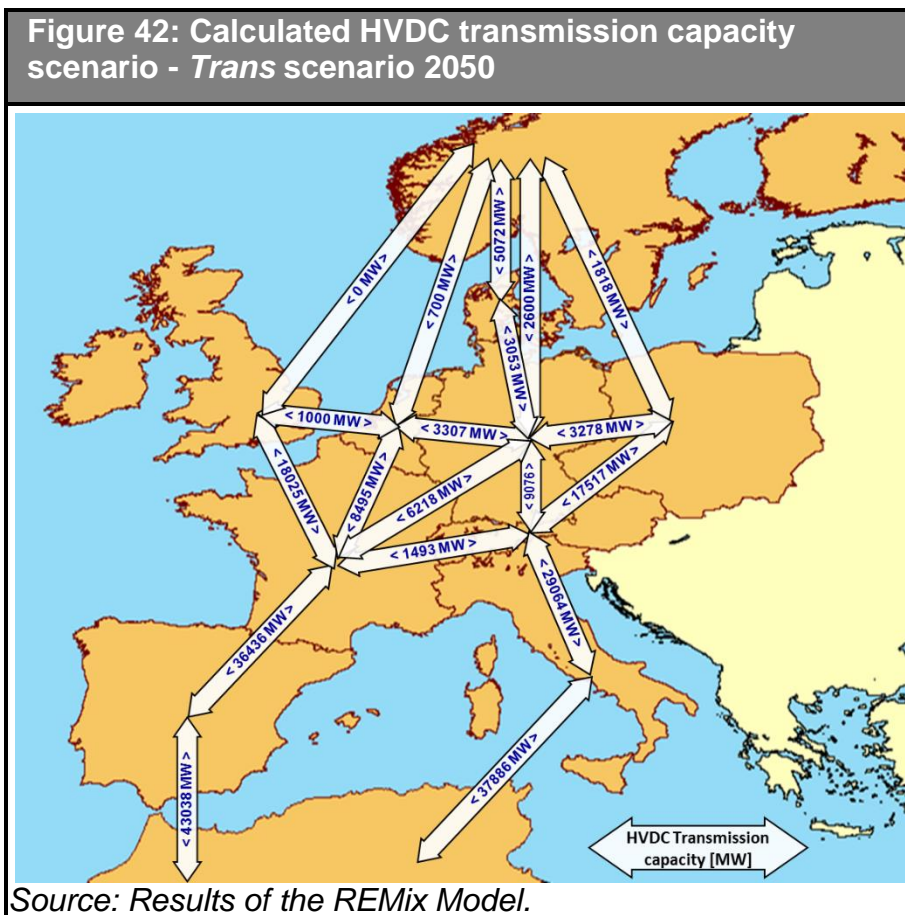
Figure 43 and Figure 44 show the least cost transmission system expansion between the seven defined regions in Germany for the same four selected scenarios presented above. The results for 2050 show a general increase in transmission capacity if compared to 2030. Both 2030 and 2050 results point out that the North-South transmission axis is much more relevant for load balancing and long-range power transfer than the East-West axis. Almost no additional East-West HVDC transfer capacity is required inside Germany under the assumptions made for this economic analysis. However it has to be noted that most of the power transport between Western and Eastern Europe is performed over the border between Austria and the Czech Republic with a transmission capacity of over 17 GW (see Figure 42). Among all transmission corridors in Germany the one connecting the North-West and the Western region with a capacity of around 15 GW in 2030 and of 26 GW in 2050 is the most relevant. These high requirements are due to the expansion of wind power generation in coastal regions and offshore.

Figure 43: Calculated HVDC transmission capacity scenario in Germany for 2030 scenario Base (left) and for 2050 scenario Base (right)

Source: Results of the REMix Model.

The results for 2050 assuming twice as high transmission expansion costs than in *Base* (*x2*) and with solar electricity imports (*Trans*) are shown in Figure 44. The results for the *x2* scenario show a similar but more moderate expansion than in *Base*. For the *Trans* scenario, the transmission capacity from the North of the country is reduced as in this case the volatile wind power generation is lower due to solar electricity imports. In order to allow for the transmission of solar electricity imports from the South the interconnection capacity to the regions Alps and France together increase in this scenario from around 4 GW to 15 GW.

Figure 44: Calculated HVDC transmission capacity scenario in Germany for 2050 scenario *x2* (left) and for 2050 scenario *Trans* (right)

Source: Results of the REMix Model.

6.3.2   Contribution of EVs to transmission system expansion

In this section the results of additional scenario variants regarding the electric vehicles fleet are presented to gain deeper insight on the impact of EVs on the power system and on the expansion of the transmission network.

First, the results of the *Base* scenario of installed HVDC lines from 2010 to 2050 and for four additional scenarios for 2050 are presented for all considered regions (Figure 45). Secondly, the same results are presented for Germany[74] (Figure 46), to analyse the implications of these scenarios for the transmission grid in the country. Finally, sensitivities of different EV variants for all considered regions will be calculated for the *Base* scenario in 2030 (Figure 47), in 2050 (Figure 48), with double transmission network expansion costs (*x2*) (Figure 49) and for the *Trans* scenario (Figure 50).

---

[74] Only 50% of the transmission lines length between Germany and neighboring countries is considered.

Figure 45: HVDC transmission expansion in all regions

Source: Results of the REMix Model.
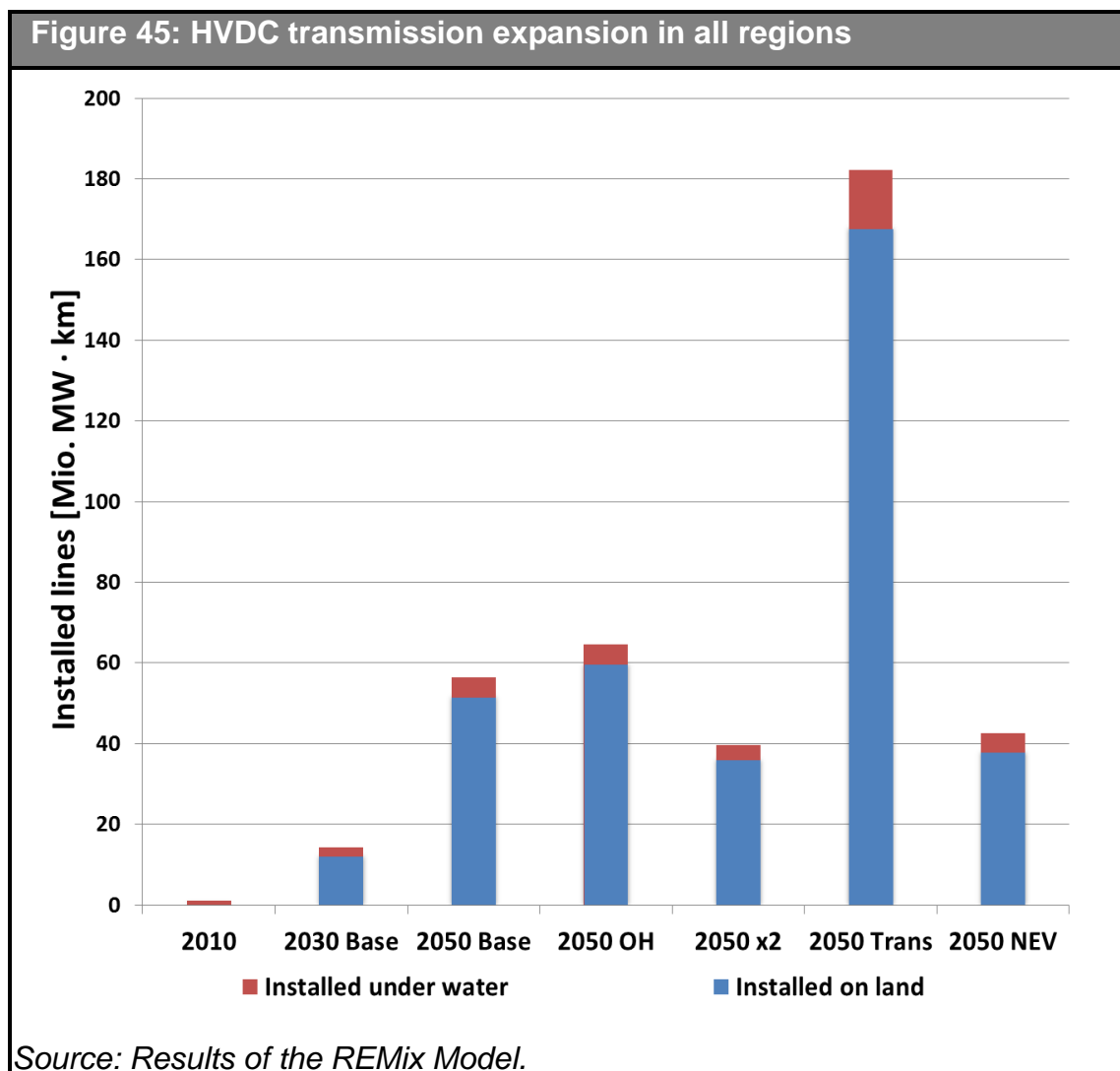
The results of the *Base* scenario in years 2010, 2030 and 2050 are shown of the left side of Figure 45. In this scenario the total length of HVDC lines grows from 1 Mio. km·MW in 2010, to 14 Mio. km·MW in 2030. Between 2030 and 2050 the installed capacity becomes four times as large from 14 to 56 Mio. km·MW. The additional variants selected for 2050 are *OH*, *x2*, *Trans* and finally *NEV*. The resulting expansion assuming overhead lines with lower investment costs increases of 14% compared to *Base*, decreases by 30% if double investment costs are assumed (*x2)*, increases by over 200% for the integration of solar electricity imports in the *Trans* scenario while it is reduced by 25% in case there are no EVs and therefore less power generation from renewable energy sources (*NEV*).

From the results for Germany (Figure 46) similar results can be drawn than the ones obtained for all regions in most cases. In Germany the length of HVDC lines is

increased from 0.1 in 2010 to 5.9 Mio. km·MW in 2030. Between 2030 and 2050 the installed capacity increases from 5.9 to 14.1 Mio. km·MW. The expansion assuming overhead lines is increased by around 6%, while it decreases by 17% in *x2*. The *Trans* scenario if compared to the *Base* scenario presents a more reduced expansion (-27%) as fluctuating wind power generation is substituted by controllable generation from solar thermal power plants located outside the country, and it is reduced by 32% in the *NEV* scenario.

Figure 46: HVDC transmission expansion in Germany

Source: Results of the REMix Model.
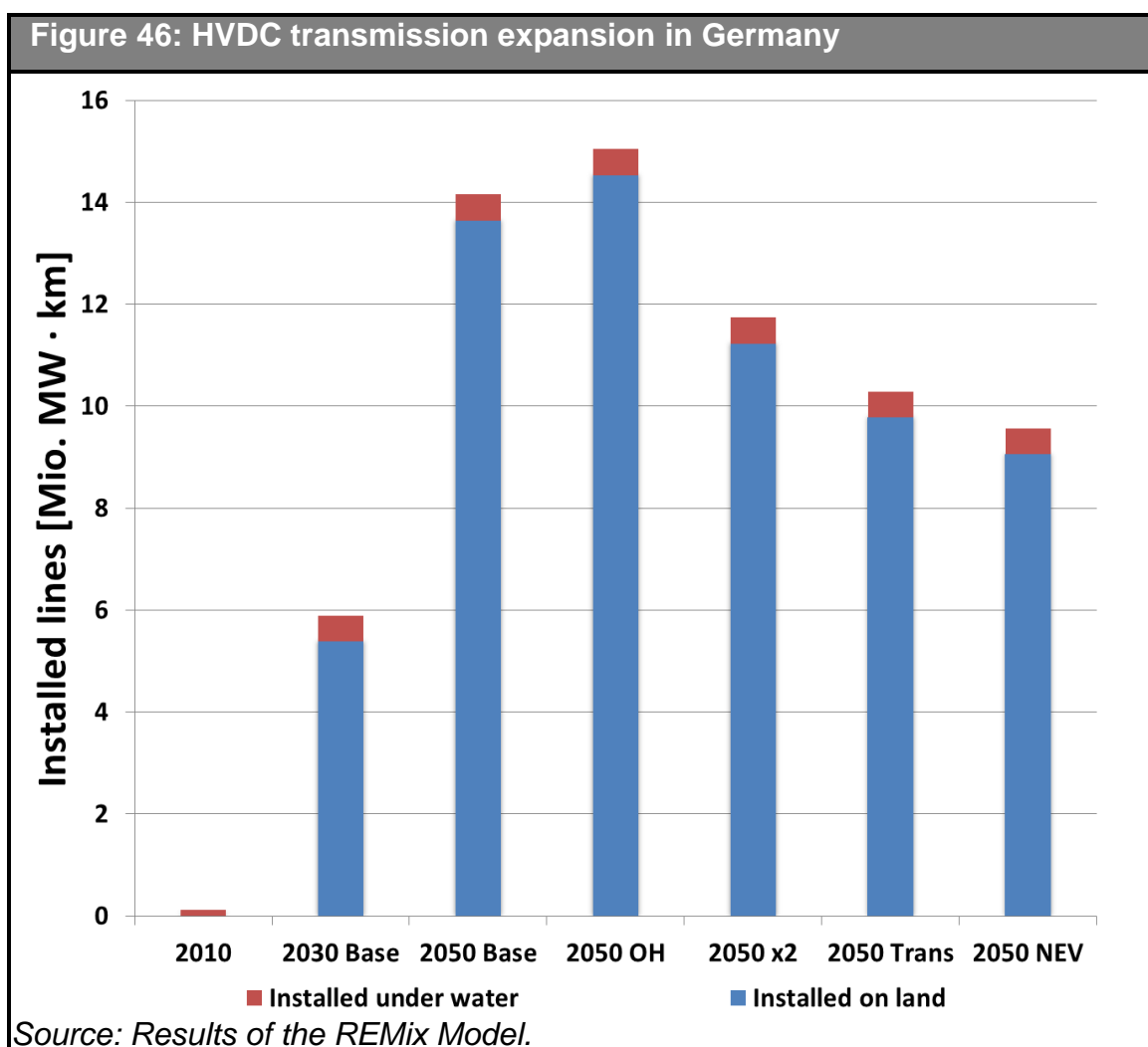
In 2030 electric vehicles are assumed to be responsible for less than 3% of the total demand and thus its impact on the supply system is only very small. 95% of the total electricity demand for EVs would come from PEVs by that year as the H_2 demand for FCVs is negligible. Implementing controlled loading strategies (*CL/V2G*) can reduce the required HVDC transmission expansion up to 2.9% if compared to *UL*, while the

total impact of EVs is a 7.4% increase. This is caused by the high share of vehicles presenting uncontrolled loading and due to the additional renewable power generation capacity required.

Figure 47: Sensitivity in 2030 (*Base*) of HVDC transmission expansion in all regions

Source: Results of the REMix Model.
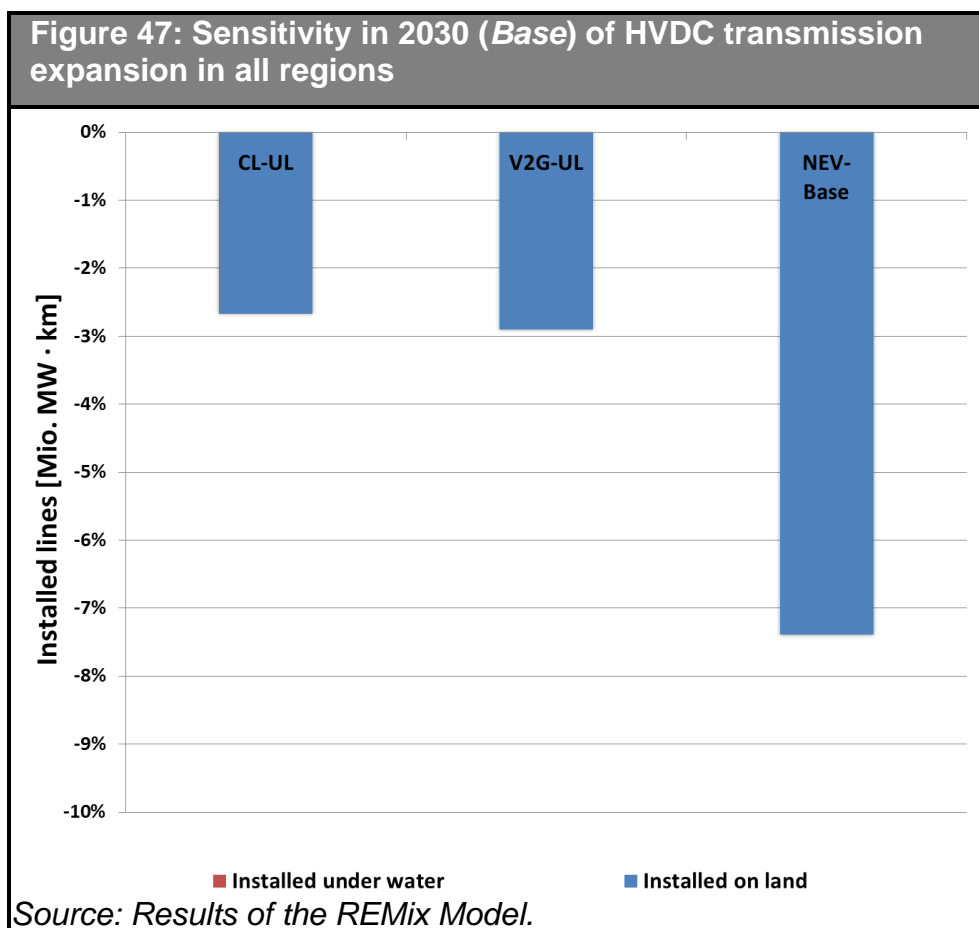
The results for 2050 for the *Base* scenario show a larger impact of EVs on the power system than in the previous case. By this year 21.4% of total demand in Germany and 18.2% in all considered regions is assumed to be caused by EVs. Shifting the demand of PEVs from an uncontrolled to a controlled strategy leads to a reduction in transmission network expansion of 9.2% for unidirectional (*CL-UL*) and of 9.4% for bidirectional loading (*V2G-UL*). Over-dimensioning electrolysers (*H2*) provides almost no savings, unless the hydrogen storage capacity is increased (*H2+).* The reduction of transmission capacity in the *H2+* scenario, 28.9%, and is larger than the reductions with *NEV*, 26.7%. Therefore, in case of weekly hydrogen storage the required transmission expansion for EVs can be completely offset.

Figure 48: Sensitivity in 2050 of HVDC transmission expansion in all regions

Source: Results of the REMix Model.

Figure 49: Sensitivity in 2050 (*x2*) of HVDC transmission expansion in all regions

Source: Results of the REMix Model.
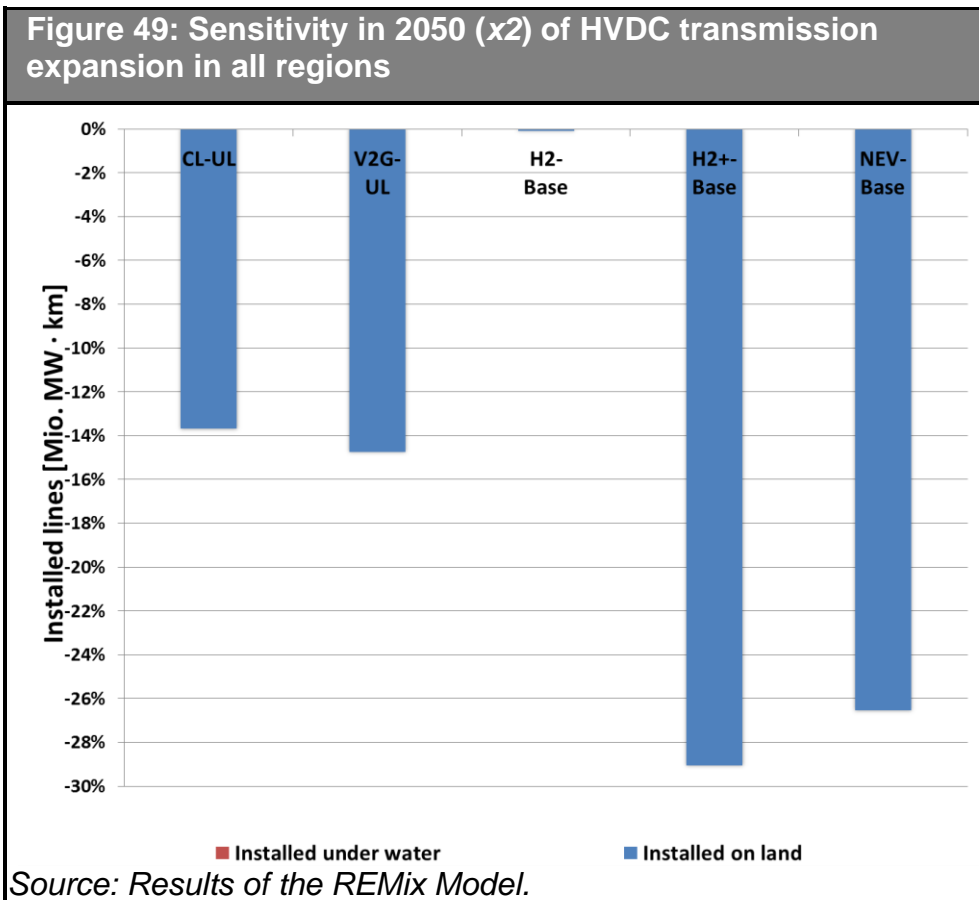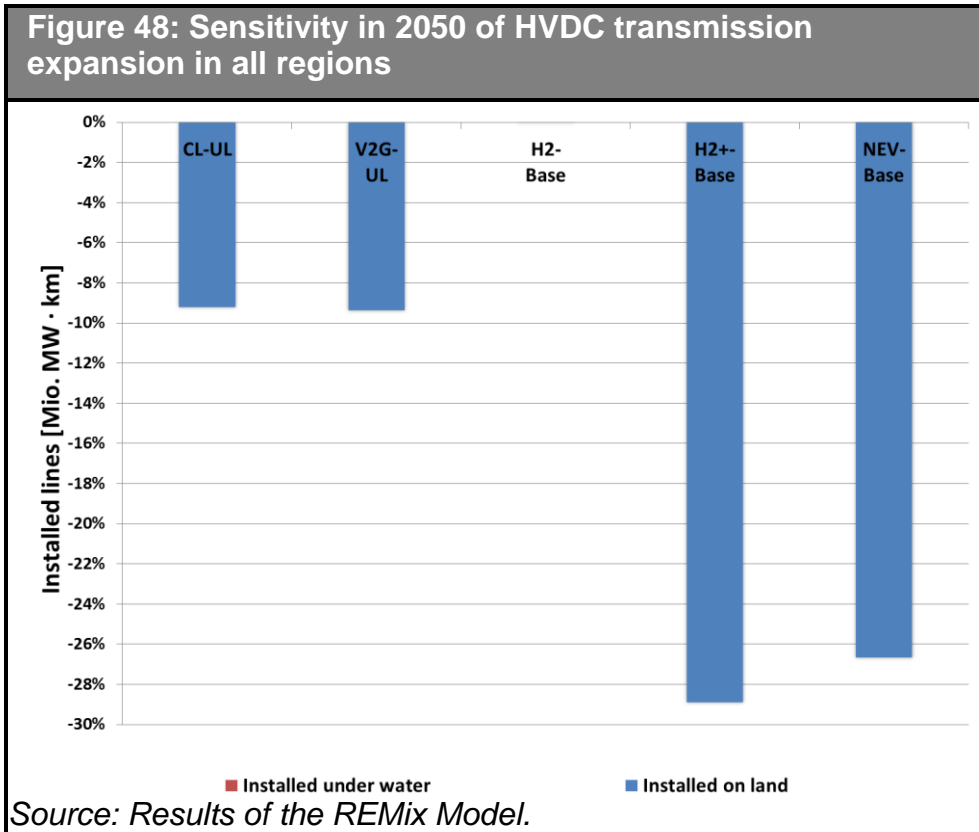
The relative transmission capacity savings achievable with intelligent loading strategies for PEVs are higher in the *x2* scenario for 2050 than in *Base*, 13.7% for unidirectional (*CL*) and 14.7% for bidirectional loading (*V2G*). The relative savings of a weekly H_2 storage and of EVs remains practically unchanged if compared to the previous case, 29.1% and 26.5% respectively; however the absolute savings are higher due to the higher HVDC expansion costs in *x2* (see Figure 45).

In the variants assuming solar thermal electricity imports the reductions are of 1.8% for *CL* and of 1.7% for *V2G*. The savings are of 4.1% in case of a weekly H_2 storage if compared to the *Base* scenario. The results show that in *Trans* the potential contribution of intelligent loading strategies is much lower than in *Base* or in *x2*. This occurs as there is on the one side less intermittent power generation requiring to be balanced and on the other higher interchange capacity to reduce the system's volatility.

Figure 50: Sensitivity in 2050 (*Trans*) of HVDC transmission expansion in all regions

Source: Results of the REMix Model.
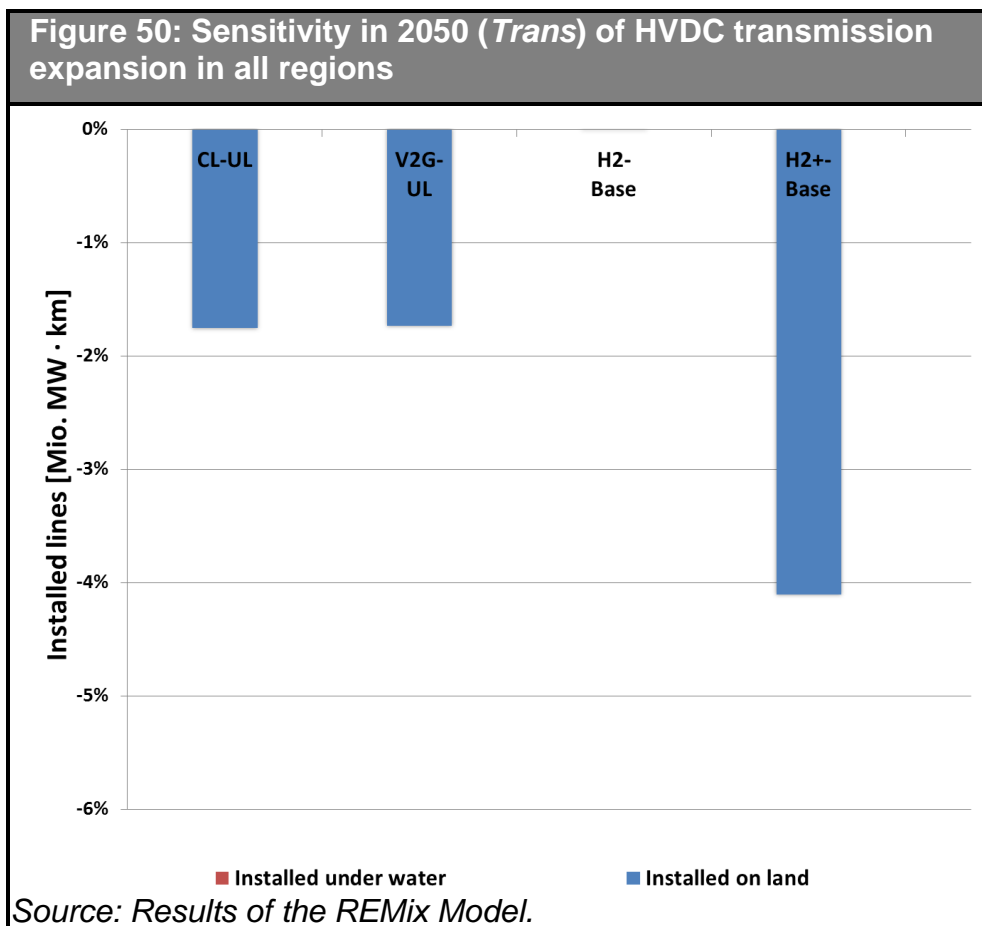
6.4   Second tier results: system dispatch

In this second step the results related to the dispatch of the German electricity system are presented. These comprise the system losses, the peak demand, the different costs and the prices. For the dispatch calculations the calculated transmission expansion as well as the interchanges with neighbouring countries are taken from the first tier results. The following three figures show as an example the load coverage during a week in autumn with important variations in power generation from RES. The power generation from wind turbines significantly increases from Monday to Wednesday; it is then reduced until Friday when it starts to increase again until Sunday. Figure 51, Figure 52 and Figure 53 show the results for years 2030, 2050 and for the same year assuming solar electricity imports (see DLR/IFHT/ISE, 2012).

Figure 51: Exemplary load coverage simulation in Germany with REMix, one autumn week in 2030

Source: Results of the REMix Model.
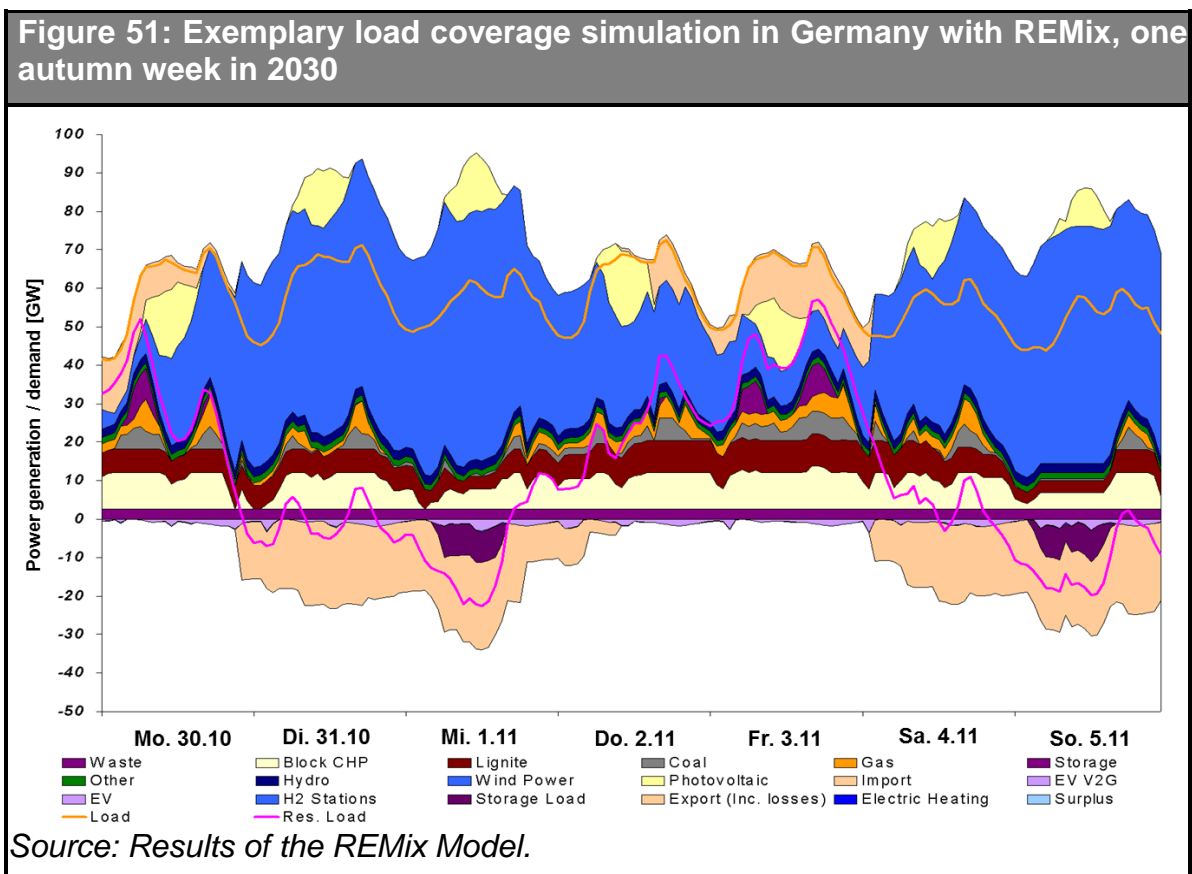
The coloured stacked areas above the x axis represent power generation from the sources given in the legend below, while those below the x axis represent the demand from controllable loads and storage plants. In this representation imports are displayed as generation while exports and renewable power surpluses are represented as demand. The orange line shows the demand from conventional loads and the pink line the residual demand which results by subtracting from the conventional load the power

generation from RES. The results for 2030 show that in times of negative residual load, when RES generation is larger than the conventional demand, exports and pumped storage increase while in times of low renewable generation the demand is partly covered by imports and storage plants.

Figure 52: Exemplary load coverage simulation in Germany with REMix, one autumn week in 2050

Source: Results of the REMix Model.
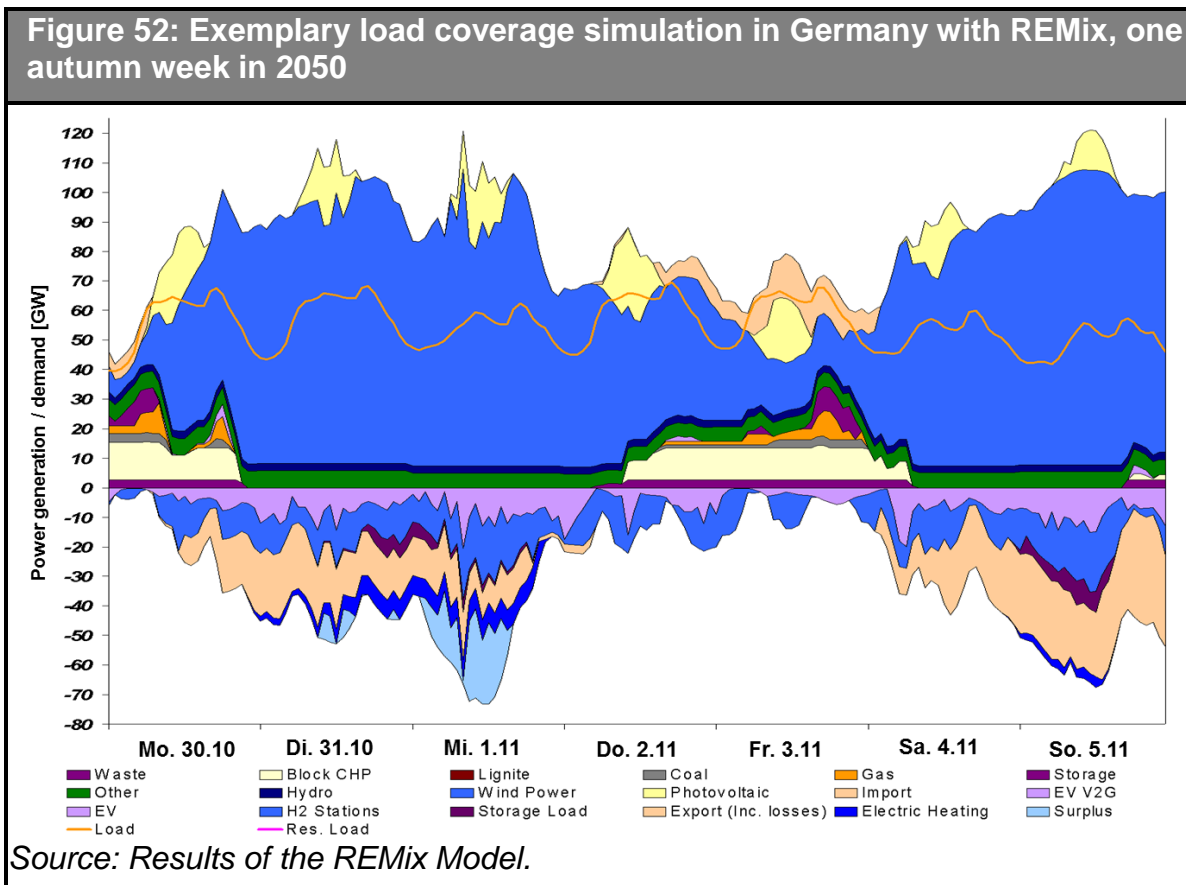
The results for the year 2050 show that excess renewable power generation is larger and cannot be completely exported, stored, or used in electric heaters with the assumed dimensioning.

Below, the situation for the same week in 2050 is shown assuming solar thermal electricity imports from North Africa. In this case, local generation from RES – mainly wind – is substituted by solar imports. It can be seen that for the presented week surpluses can be reduced to zero as there is less local intermittent power generation in the German system which is substituted by controllable solar thermal generation. Additionally it can be appreciated that exports are more reduced in this scenario, production from distributed CHP increases, gas units are not operated at all and the operation of pumped hydro storage is also significantly reduced. In this system the contribution of EV to stabilise renewable power generation is more reduced as there is less intermittent generation.

Figure 53: Exemplary load coverage simulation in Germany with REMix, one autumn week in 2050 assuming solar electricity imports

Source: Results of the REMix Model.
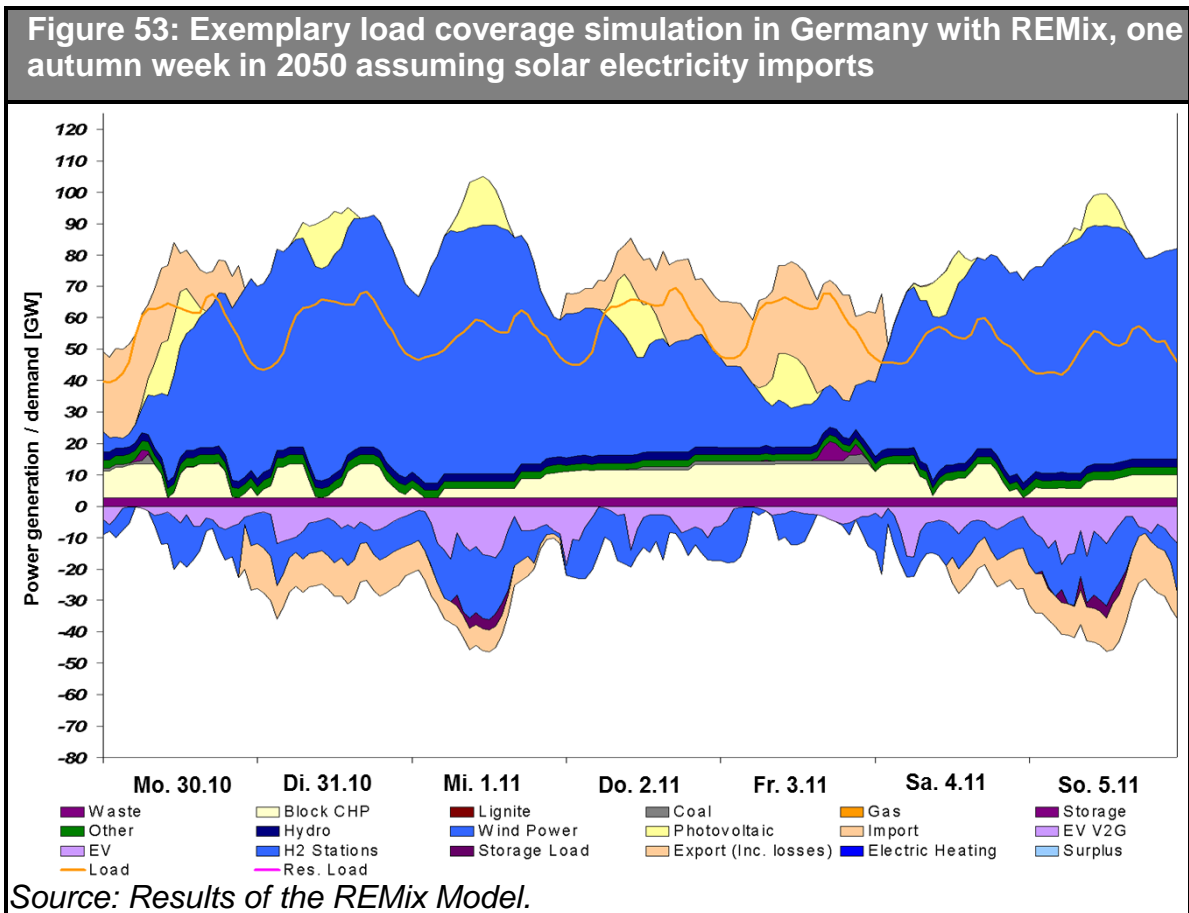
6.4.1   Impact of EVs on residual peak demand and on losses

The residual peak demand and system losses are shown in Figure 54. The residual peak demand is calculated as the average load to be covered by thermal generators including cogeneration during 5% of the hours with the highest load. The losses comprise pump losses, transmission losses and renewable surpluses. On the left side the evolution from 2010, 2030 and 2050 is shown. On the right side the same dispatch metrics are shown for four additional scenarios in 2050, these are: *OH*, *x2*, and *Trans*. It can be seen that from 2010 to 2050 along with the expansion of renewable power generation the volume of losses increases from 1.1 to 8.3 TWh and the level of the residual peak demand decreases from 69.7 to 37.7 GW as renewable generation displaces conventional power generation. In 2010 the losses consist mainly of those due to pumped storage, whereas in 2030 renewable generation surpluses are also relevant. In 2050 pumped storage plants are less utilized than in 2010 and also present lower losses as EVs with controlled loading reduce the arbitrage opportunities of storage plants. It has to be noted that the calculated pumped storage losses in 2010 are lower than in reality as some constraints to the operation of thermal units as well

as the provision of ancillary services by pumped storage have not been considered, which reduces the demand for flexible pumped storage generation.

Figure 54: Results of the sensitivities: system losses and residual peak demand

Source: Results of the REMix Model.
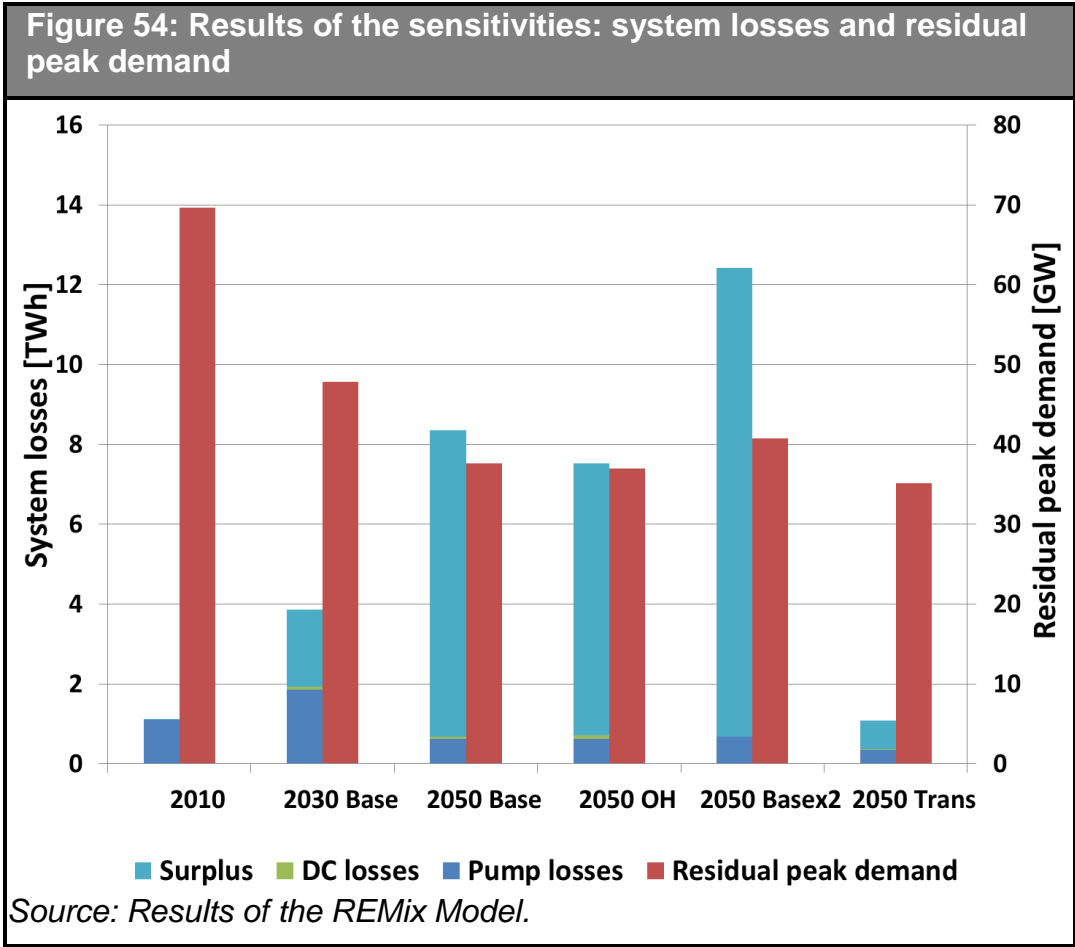
The use of overhead lines causes more lines to be economical and thus allows for higher export capacity in times of higher renewable generation and for higher imports in times of scarcity, thus reducing the residual peak demand to 37 GW and the annual losses to 7.5 TWh. The opposite effect is seen with a costlier transmission expansion (*x2*) which is more pronounced as the relative increase is of higher magnitude than the relative decrease assuming *OH.* In *x2* the residual peak demand and the losses increase to 40.7 GW and to 12.4 TWh respectively. The *Trans* scenario presents both a lower peak demand as well as lower system losses. The reason is that the output of solar thermal plants can be controlled while in the case of wind and solar power this not possible. Due to the controllable and thus more stable power supply in *Trans* both metrics decrease to 35.1 GW and 1.1 TWh.

Both the impact of EVs on the above presented metrics, as well as of controlled loading strategies of PEVs and of different hydrogen fuelling station configurations are presented in Figure 55. The impact of smart loading strategies of PEVs on the system

is calculated as the difference of the scenarios assuming controlled loading strategies with the scenario assuming uncontrolled loading (*CL-UL*, *V2G-UL*). The impact of larger electrolysers and that with a larger (weekly) storage is assessed by calculating the difference between the scenarios and the *Base* scenario (*H2-Base*, *H2+-Base*). Finally the impact of EVs is obtained by comparing the results of the *Base* scenario with those assuming no electric vehicles (*Base-NEV*). The results show that the impact of EVs in year 2030 is low as by that year the demand of EVs will only represent less than 3% of the total demand. Nevertheless, the savings resulting from controlled loading strategies reach 1.4 TWh, representing 9.5% of the total electricity demand of PEVs. In 2050 in the *Base* scenario the savings increase up to 4.7 TWh or 9.6% of the PEV demand, the savings in the *x2* scenario reach 12% while in the *Trans* scenario are of 3.5% of the PEV demand. Regarding the residual peak demand, the savings from *CL/V2G* are of around 1.2 GW in 2030 and of 4.5 GW in 2050 for the *Base* scenario, representing the installed capacity of 2 and 7.5 large combined cycle units. The reductions in the *x2* scenario are around 3.8 GW; in the *Trans* scenario they are reduced to 3.5 GW.

Throughout the analysed cases the impact of larger electrolysers is practically cero if the hydrogen storage does not increase in size as well. The results of the *H2* and *H2+* scenarios show that an over-dimensioned electrolyser would only make sense with a larger storage system. In the case of a storage capacity equivalent to one week of the average H_2 demand, the achievable reductions would be 6 TWh for *Base* and 8 TWh for the *x2* scenario. In *Trans* they would be significantly lower as in this scenario the total surpluses are low. The reduction in the residual peak load compared to *Base* for all scenarios for 2050 lies between 4 and 5 GW. The impact of EVs on surpluses is small but positive for all the three cases presented due to the additional renewable generation capacity required to ensure low carbon mobility; however the reduction provided by controlled loading compensates the increase in the *Base* scenario. The impact on the residual peak demand is positive in 2030 as most PEVs are expected to present uncontrolled loading and in 2050 it turns negative as most PEVs would be able to shift demand out from the peak hours.

Figure 55: Sensitivity analysis of the contribution of EVs to surplus reduction and to the residual peak demand in 2030 and 2050 for the Base, x2 and Trans scenarios in Germany
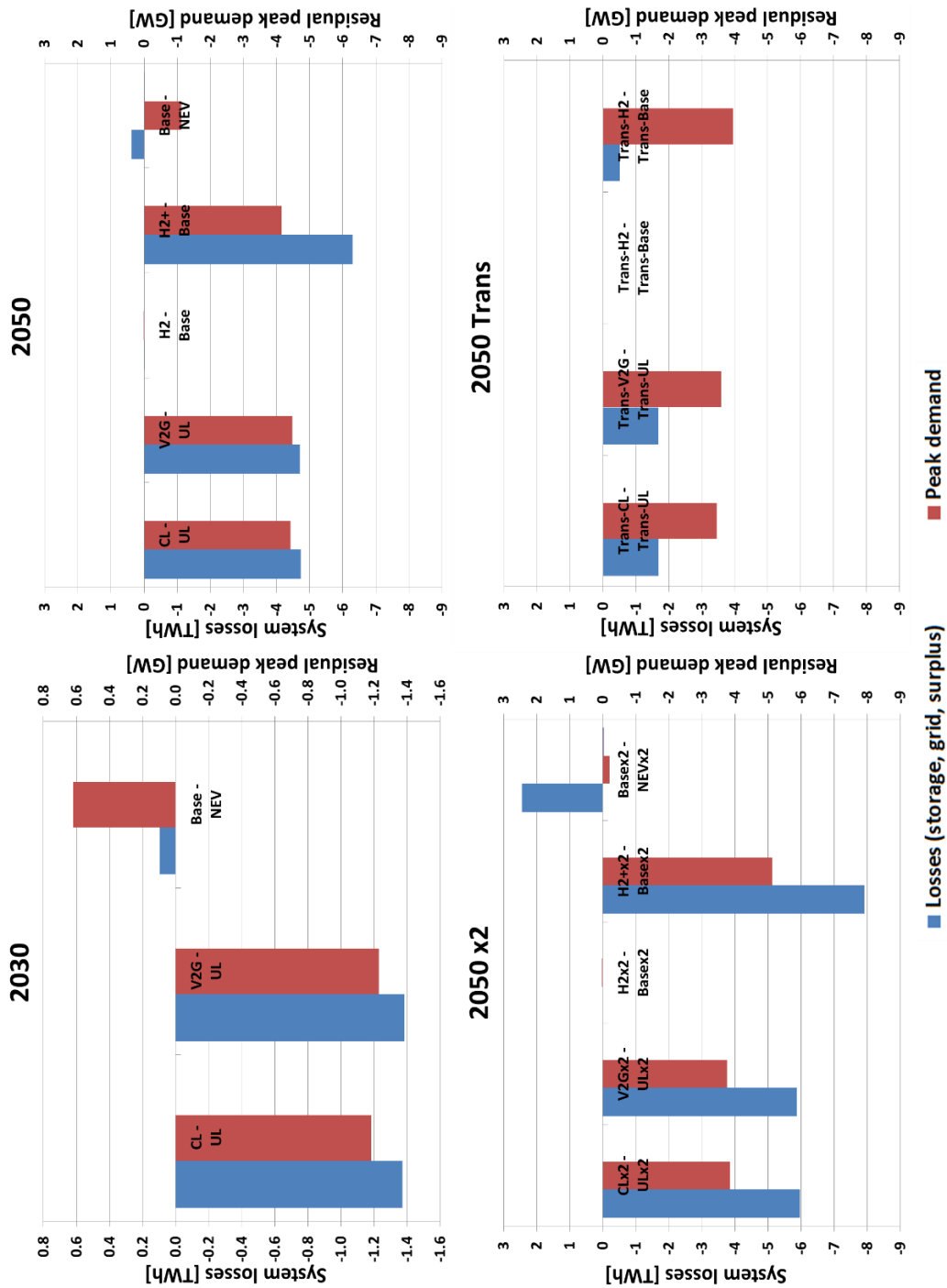
Source: Results of the REMix Model

6.4.2   Impact of intelligent loading strategies on system costs

In this section the impact on the operation and expansion costs of controlled loading both unidirectional (*CL*) and bidirectional (*V2G*) as well as of a more flexible hydrogen production (*H2* and *H2+*) is presented. The expansion costs consist first of the annuity due to investments in transmission expansion (section 6.3) and second of the impact on the generation side. The latter is estimated based on the residual peak load, assuming that additional investments in gas turbines are required in case of an increase of the peak load and are saved in case it decreases. The operation costs consist mainly of operation and maintenance costs of generators and lines, of fuel provision, of CO_2 certificates, of wearing costs of EV batteries providing V2G (see section 3.2.4), and of the costs related to not supplied energy, which is given by the value of lost load, in this work 2000 €/MWh have been assumed.

The results (see Figure 56) show that the potential savings for the power system are in the order of several hundreds of millions of Euros per year. However, these are not the only sources of savings as controlled loading could provide e.g. ancillary services and the related costs are not considered in the analysis. Nevertheless, the results for the four scenarios point out that the largest considered source of savings is operating costs followed by generation expansion. The savings in 2030 for *CL* reach 254 Mio. € and for *V2G* 288 Mio. €. In *Base* for 2050 these are of 858 Mio. € for *CL*, 867 Mio. € for *V2G* and 1021 Mio. € in case of a weekly storage for H2 (*H2+*). Higher network expansion costs (*x2*) increase the potential savings with controlled loading to 1012 Mio. € for *CL* and 1021 Mio. € for *V2G* and with a weekly H_2 storage (*H2+*) to 1255 Mio. € In the *Trans* scenario the savings are significantly reduced to 476 Mio. € for CL, to 481 Mio. € for V2G and to 426 Mio. € for *H2+*. It can be observed that after 2050 neither bidirectional loading nor larger electrolysers without increasing storage capacity presents relevant advantages regarding the considered system costs.

Figure 56: Sensitivity analysis of the contribution of EVs to annual operating costs, to the annuity of network and generation expansion in 2030 and 2050, for the Base, x2 and Trans scenarios in Germany
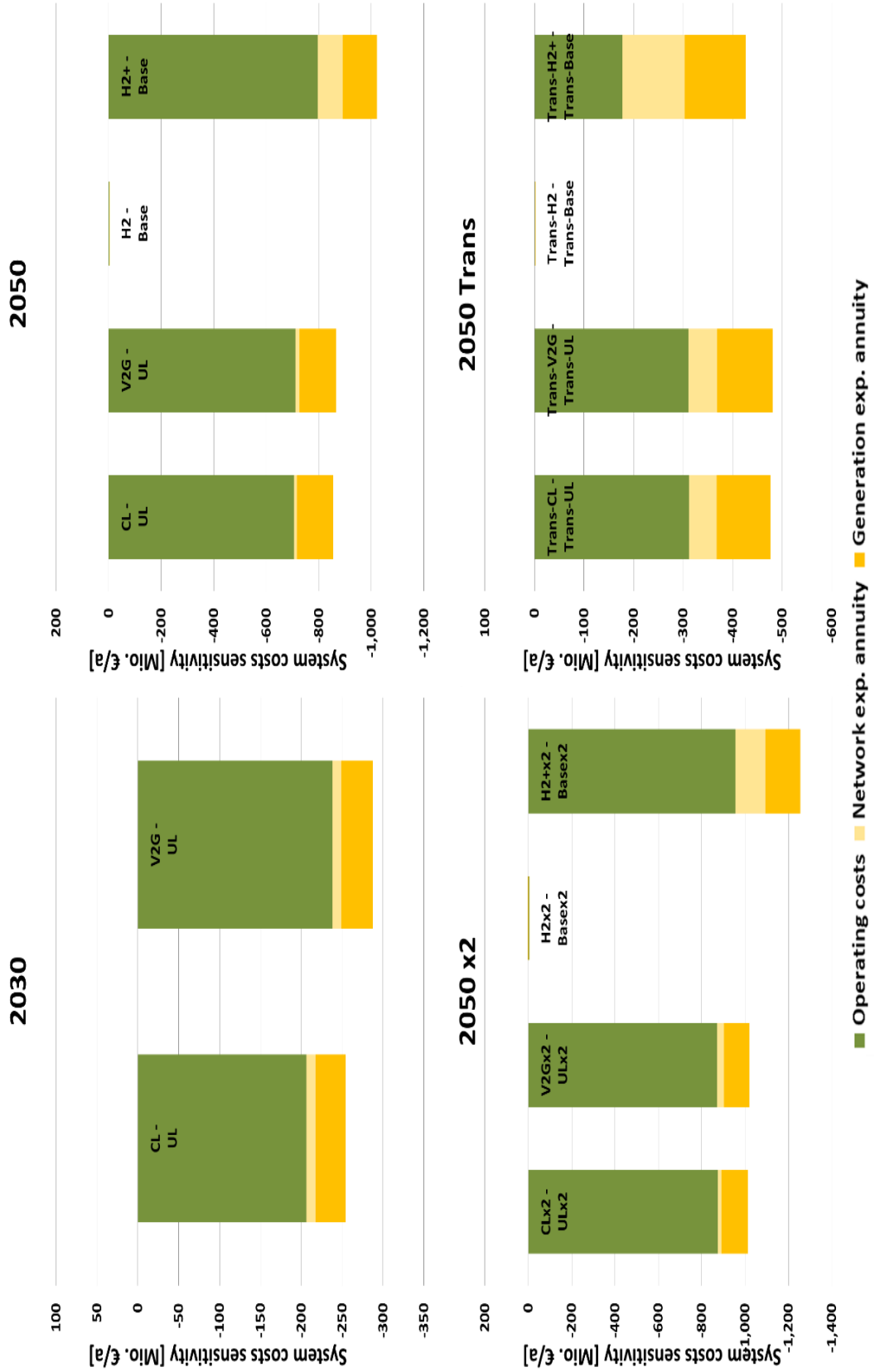
Source: Results of the REMix Model.

6.4.3   Impact of EV loading on the electricity price

The present section shows the impact of the different loading strategies and structural options of EVs in terms of the cost of the electricity bill. The wholesale electricity price is calculated in this work as the cost for the system of one additional unit of demand. This figure is calculated by the optimisation model as the shadow price of the demand constraint excluding subsidies, taxes, grid use etc. on each model node. Along the considered time horizon the average price of electricity increases from 48 €/MWh in 2010[75], to 63 €/MWh in 2030 up to 73 €/MWh in 2050 driven by the increase of fuel prices (mainly of natural gas). The volatility of prices, measured as the difference between the 90th and 10th percentile, increases from 2010 to 2050 together with the expansion of renewable power. In the different power system scenarios for 2050 the average price does not change much as it is mostly set by fuel prices. However, price volatility increases as it can be seen for the 2050 cases with transmission costs from 66 €/MWh in *Base* to 74 €/MWh in *x2*, decreases to 58 €/MWh for overhead lines (*OH*) and further to 38 €/MWh in *Trans*

Figure 57: Average price and variability for different scenarios of 2010, 2030 and 2050

Source: Results of the REMix Model.

---
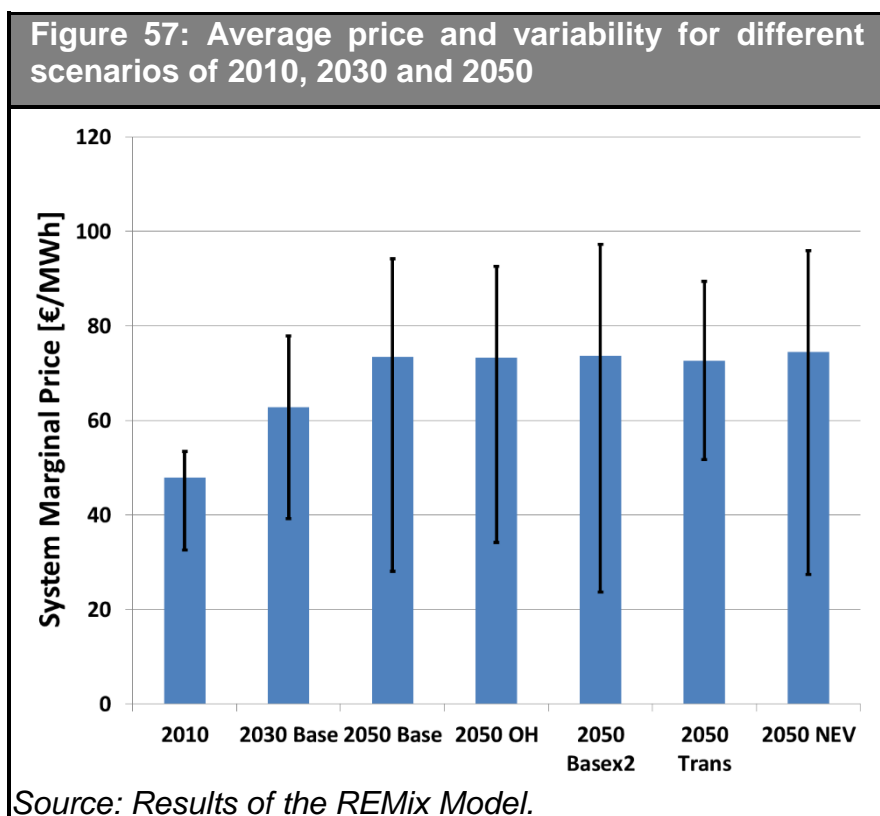
[75] The average EPEX Spot Market Price for Electricity in 2010 was 44 €/MWh. German Institute for Economic Research, 2011. The natural gas price assumed for the 2010 calculation was 18 €/MWh, obtained from Heren ESGM Report for the TTF Dutch Gas Market.

Figure 58: Sensitivity of the captured price[76] of PEVs, hydrogen fuelling stations and the conventional load in 2030 and 2050 for the *Base*, *x2* and *Trans* scenarios

Source: Results of the REMix Model.
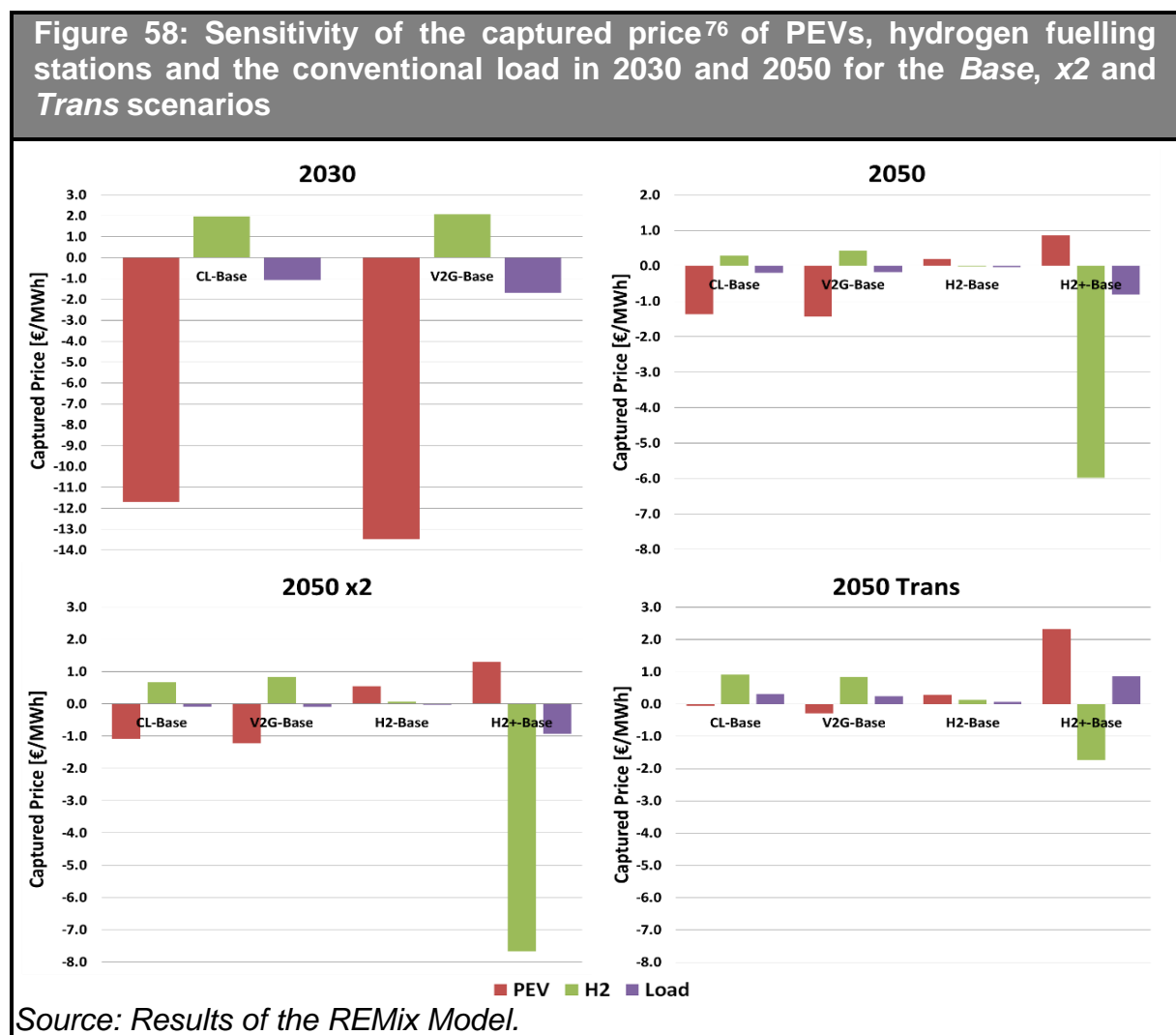
Figure 58 shows the impact on the average captured prices obtained by PEVs and for hydrogen generation assuming that the electricity tariff offered reflects the prices on the wholesale electricity market. The results show that for PEVs the potential savings from controlled loading strategies are largest in 2030 reaching 11.7 €/MWh for *CL* and 13.5 €/MWh for *V2G*, which assuming a consumption of 16 kWh/100 km leads to savings of 19 €cent/100 km and 22 €cent/100 km. In 2050, as the *Base* scenario already assumes a high penetration of intelligent loading strategies, the reduction will be significantly more modest. Again it is appreciated that a larger electrolyser capacity provides no relevant benefits if the storage capacity does not increase as well. However, with a weekly storage capacity the reductions in year 2050 reach in the *Base*

---

[76] As the average price to which the energy is demanded.

scenario 6, in the *x2* scenario 7.7 €/MWh and in *Trans* 1.7 €/MWh. This corresponds to savings of 23, 30 and 6.5 €cent/100 km[77].

Figure 59: Renewable power generation surplus in the seven defined regions in Germany – Base scenario 2050

Source: Results of the REMix Model.
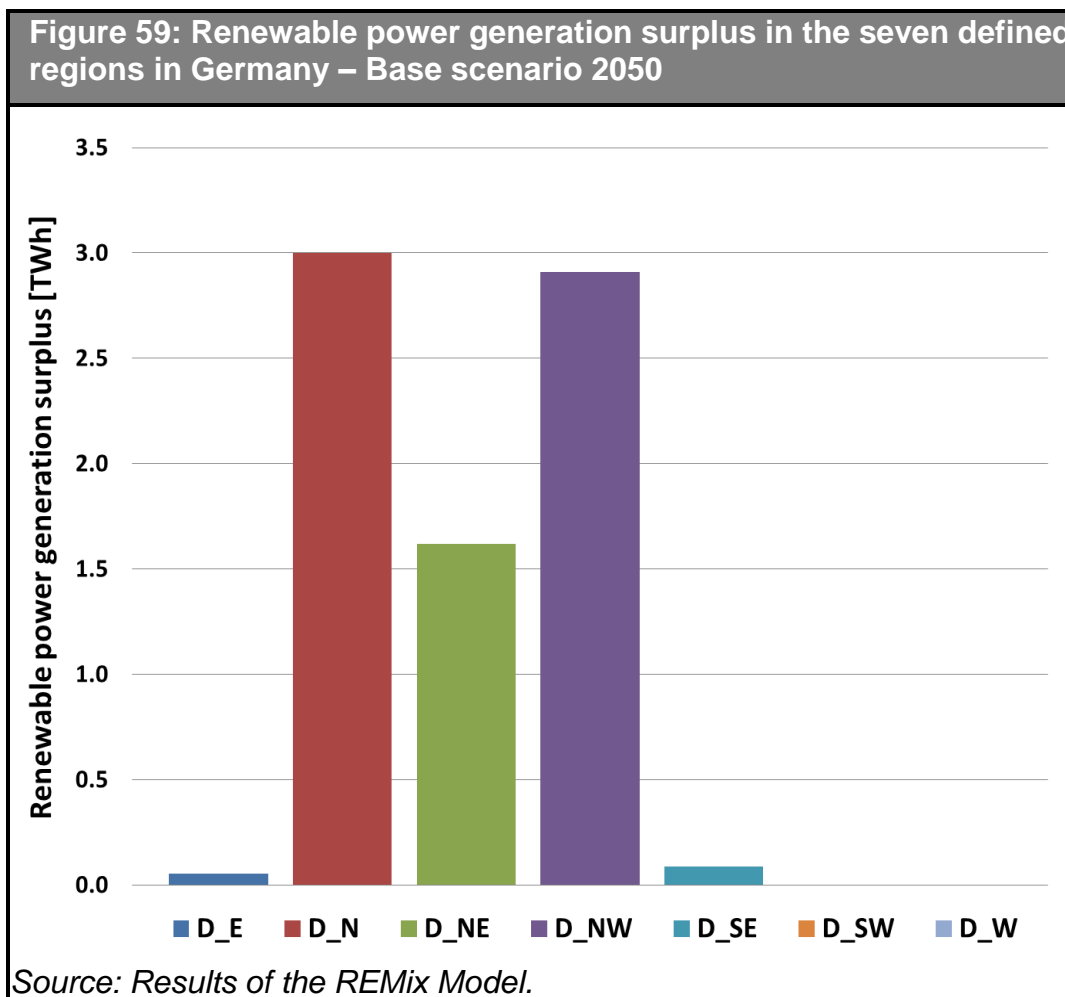
Another relevant result is how the captured price changes by region. In regions with higher installed wind power capacity, as in the north of Germany, the contribution of EVs to surplus reduction can be expected to be larger along with the economic incentives to do so. Figure 59 shows the annual surpluses from RES in *Base* for year 2050. It can be seen that these take place mostly in the northern wind-rich regions and account for 7.7 TWh per year.

The impact of controlled loading of PEVs on the captured price is depicted in Figure 60 for each defined region in Germany. It can be seen that the regions in which controlled loading strategies lead to higher savings are also the northern as well as the

---

[77] Assuming conversion efficiency from electricity to hydrogen of 67% and a consumption of 26 kWh/100 km.

eastern regions, in which the potential savings are between 1.6 and 2.1 €/MWh while in the southwest the achievable savings are around half of that value. Again in this case (see Figure 61) the *H2* scenario per se presents no advantage to *Base*, while if combined with a weekly H_2 storage the reduction is appreciable, ranging from 9-17 €/MWh in the northern regions to 2.3 €/MWh in the southwest. This represents savings of 35-66 €cent/100km and of 9 €cent/100km, respectively.

Figure 60: Sensitivity of the captured price of PEVs in 2050 Base scenario in the seven defined regions in Germany

Source: Results of the REMix Model.
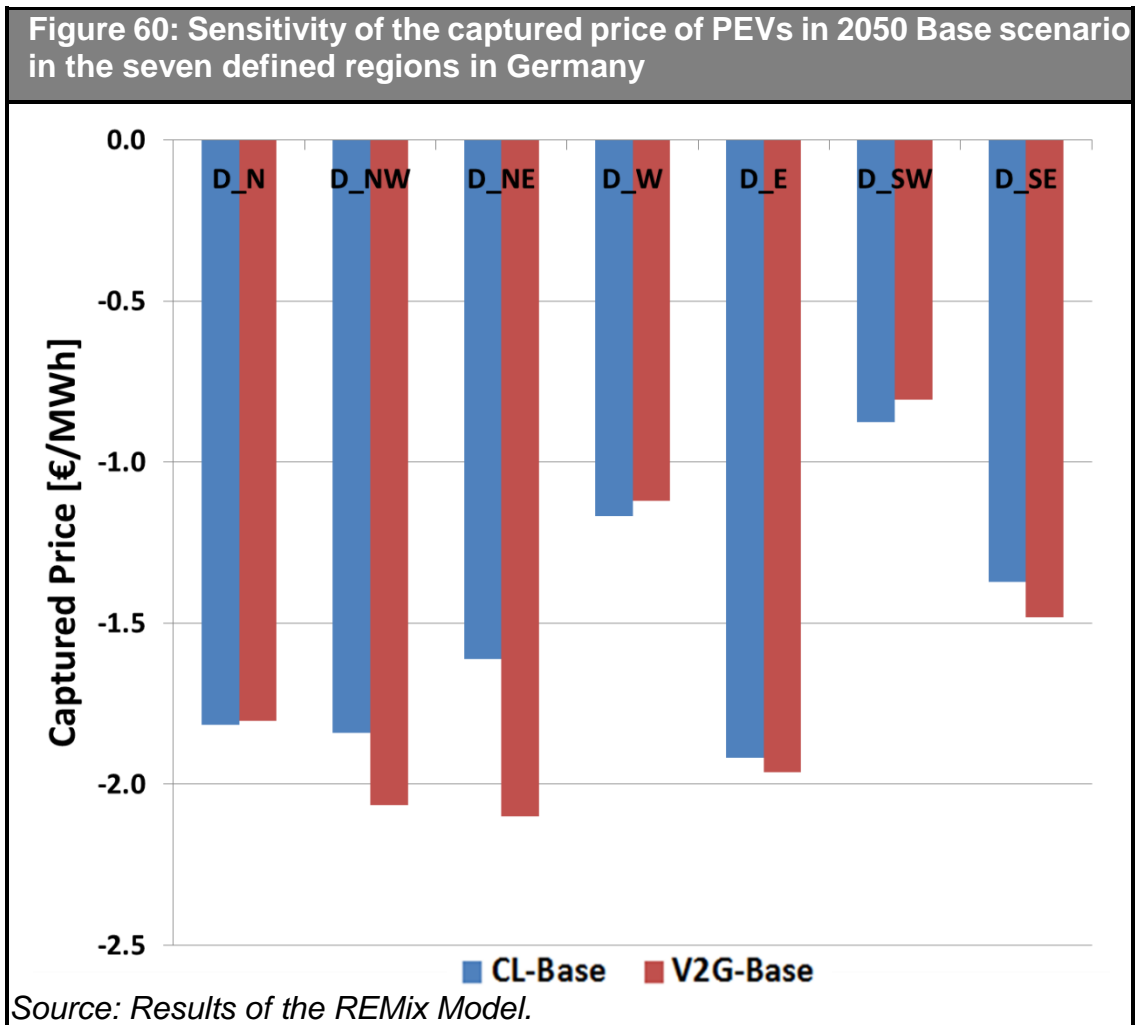
Figure 61: Sensitivity of the captured price of hydrogen loading stations for the 2050 Base scenario in the seven defined regions in Germany

Source: Results of the REMix Model.
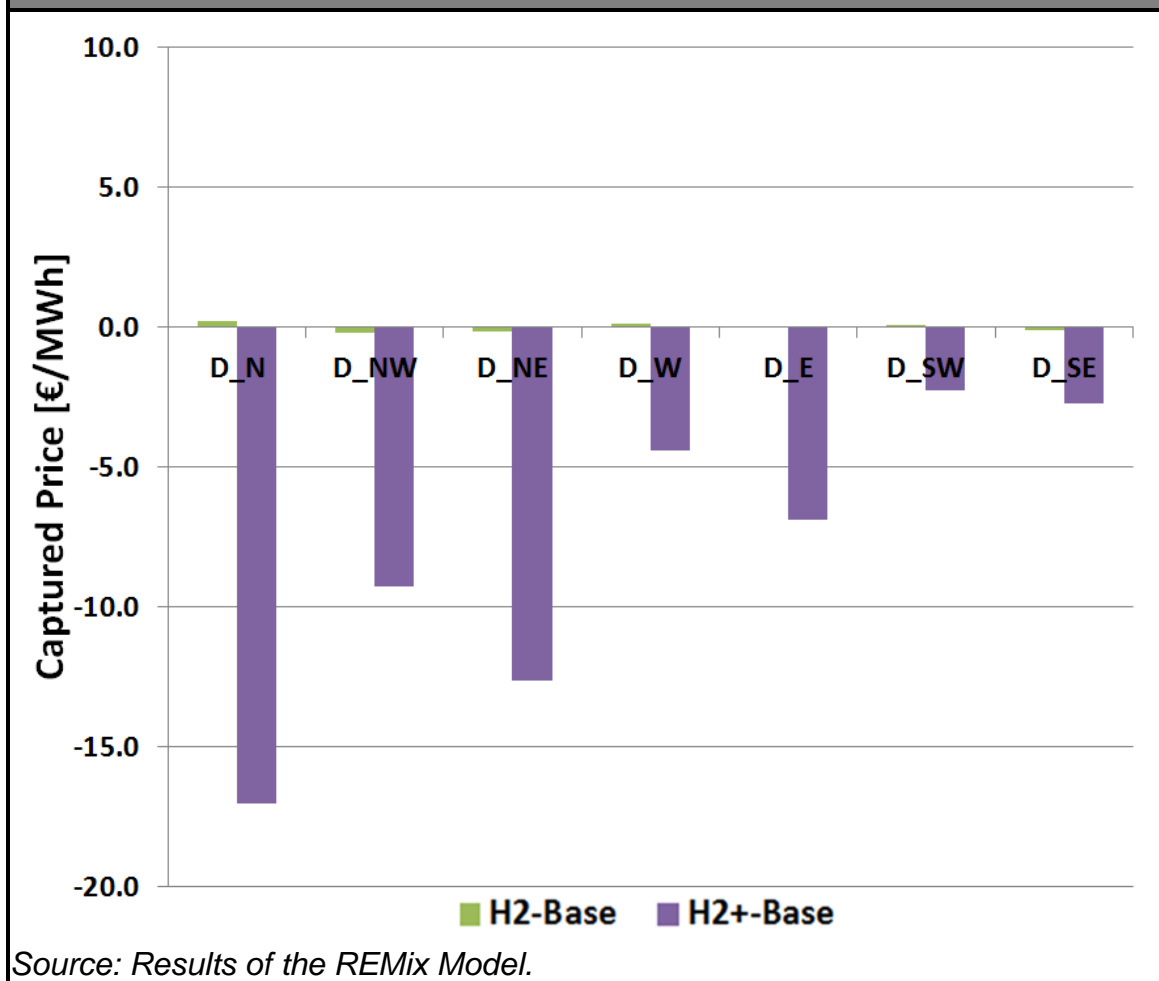
6.5   Summary of the main results

In this work an enhanced version of the simulation model REMix was developed in order to accurately model the effects of EV loading strategies. The model was applied to simulate the load coverage in the German electricity supply system consisting of seven regions with an hourly resolution for several scenarios of power generation, grid expansion, chemical storage and loading infrastructures for EVs. Due to the massive mathematical problem the analysis and calculation has been divided into two steps. In the first step the least cost system expansion and dispatch is calculated over a whole year with a resolution of 5 hours for all modelled regions in Europe and North Africa. In a second step the optimal load coverage is calculated with an hourly resolution, assuming the interchanges calculated in the first step and considering the start-up costs of thermal units.

The optimal HVDC transmission expansion was presented for a set of defined scenarios. The expansion in the *Base* scenario assumes underground cables which present a higher social and political acceptance. It is pointed out that:

- The most relevant transmission corridor in Germany is the one connecting the wind-rich region in the north-west to the population rich region in the west.

- The east-west transmission axis does not seem as relevant as the north-south axis. However, this depends on through which countries the interconnection between eastern and western Europe will be realised.

- The use of lower cost overhead lines only leads to a 6% higher transmission expansion if compared to underground cables in Germany. In case the transmission expansion costs double the reduction would be 17%.

- The scenario with solar electricity imports (*Trans*) requires in total three times as much network expansion, measured in MW·km, as in *Base*. However, in Germany this is reduced by 27% as solar thermal generation is less volatile than local generation from RES (mainly wind and PV).

- EVs increase the need for additional transmission lines as total electricity demand increases and due to the renewable power generation required to ensure emissions free driving.

- Intelligent loading strategies can compensate the transmission expansion increase due to EVs.

    - In 2030 EVs increase the expansion requirements by 7.4%, intelligent loading strategies can compensate part of the increase.

    - In 2050 EVs increase the transmission expansion requirements by 26%, which again can only be compensated in part with controlled loading. With a weekly H_2 storage capacity it can be more than compensated.

The second step of the analysis focuses on the system dispatch in Germany. The key conclusions are:

- From 2010 to 2050 with increasing RES generation, surpluses increase from 1.1 to 8.3 TWh while the residual peak load decreases from 69.7 to 37.7 GW.

- In 2030, the additional EVs will increase the residual peak load and system losses due to the expected high share of uncontrolled loading.

- In contrast, for the year 2050 additional EVs may lead to a small increase of surpluses and to a reduction of peak demand.

    o The residual peak load is reduced with controlled loading by 1.2 GW in 2030 and between 3.5 and 4.5 GW in 2050.

    o With controlled loading and especially with *H2+* the increases in system losses can be totally compensated.

    o Efficiency gains from controlled loading represent around 10% of the PEV demand for both 2030 and 2050.

Regarding the potential economic savings achievable with intelligent loading strategies and with a larger hydrogen storage capacity:

- The largest considered sources of savings are operating costs, followed by generation and transmission expansion.

- The considered savings achievable through controlled loading range from around 250 Mio. € (*CL*) and 300 Mio € (*V2G*) in 2030, and increase to around 850 Mio.(CL/V2G) in 2050.

Wholesale electricity prices are mostly determined by the variable costs of thermal units. The average electricity price increases from 2010 to 2050 driven by fossil fuel prices. However:

- Price variability is increased by fluctuating renewable generation and it can be reduced with additional transmission capacity or with a more stable supply of renewable electricity, e.g. with solar thermal generation with heat storage.

- The achievable reduction in electricity price obtained by EVs depends to a large extent on the deployment of intelligent loading strategies.

- The reductions for PEVs in 2030 are between 11.7 and 13.5 €/MWh or 19-22 €cent/100km. In 2050 the reduction is lower as there are more PEVs providing controlled loading.

- In 2050 with a weekly H_2 storage capacity, price reductions of 6 €/MWh are possible representing savings of 23 €cent/100 km.

- In the northern coastal regions of Germany the largest reductions are obtained. For PEVs with controlled loading the savings are twice as in the south while for H_2 fuelling stations with a weekly storage they are three times as high.

Consistently among all the scenarios it can be seen that:

- The additional benefits of bidirectional loading when compared to unidirectional controlled loading are reduced and for some cases practically non-existent. This is more evident in 2050, when the amount of PEVs providing controlled loading is higher.

- There is no point in increasing electrolyser capacity of hydrogen fuelling stations unless the storage capacity is increased as well. In other words, a larger electrolyser has no advantages in times of excess wind power generation if the additional hydrogen cannot be stored.

- In the scenarios with solar electricity imports the contribution of controlled loading strategies is significantly reduced.

- Consequently, in the case of a costlier transmission network expansion, the contribution of intelligent loading strategies is higher as there is less transmission capacity available to compensate the fluctuations of wind and solar power.

7   Conclusions and outlook

The results of this work prove that a power system based on renewable energy to power the passenger and freight transport sector is technically feasible to a large extent. With intelligent loading strategies electric vehicles can fully integrate the generation from renewable energy sources they need at transmission level and thus not only ensure a low carbon mobility but also that their impact on the power system is offset.

To address the long term CO_2 reduction goals for the transport sector, plug-in electric vehicles present better prospects than conventional vehicles using bio fuels due to the limited sustainable biomass resources. Plug-in passenger cars have in addition important cost advantages compared to fuel cell vehicles, due to the lower vehicle purchasing costs, the lower cost of the required infrastructure and also the higher energy efficiency.

The analysis considering the temporal and spatial characteristics of renewable power generation shows for the *Base* scenario that electric vehicles can integrate the additional renewable power generation they require and that with controlled loading relevant savings can be achieved.

- Electric vehicles lead to an increase of the transmission system requirements because of the additional demand and the additional renewable generation needed. With controlled loading part of the increase can be compensated, with weekly storage for hydrogen fuelling stations the required expansion can be completely offset.

- With uncontrolled loading the residual peak load of the system is increased. With controlled loading the residual peak load can even be reduced due to the required renewable power generation.

- The system losses, mainly renewable surpluses, are slightly increased by electric vehicles due to the additional renewable power generation needed. However, with controlled loading strategies the reduction in system losses represents around 10% of the PEV demand if compared to uncontrolled loading.

- The identified savings for the power system due to controlled loading strategies are mainly reductions in operation costs and in the required generation and network expansion. Controlled loading strategies of PEVs reduce the costs for

the power system by 250 Mio. € by 2030 (around 50 € per PEV and year) and by 850 Mio. € in 2050 (around 30 € per PEV and year). Assuming weekly hydrogen storages for fuelling stations these savings could account to 1,000 Mio. € in 2050. The estimation of these savings does not take into account effects of PEV and controlled loading on additional investments for the expansion of distribution grids.

- Controlled loading strategies as well as weekly hydrogen storage capacities for fuelling stations allow for relevant reductions in the average electricity price especially in the wind-rich northern regions of Germany. The savings through *CL* for PEVs in 2030 and in 2050 for passenger FCV with a weekly storage are around 20 €cent/100 km (around 40 € per vehicle and year[78]). In 2050, the increasing share of PEVs with controlled loading strongly reduce the relative savings for PEVs.

- In a situation with solar electricity imports controlling the load of electric vehicles becomes less beneficial. By increasing the costs of transmission expansion and thus reducing the number of transmission lines the potential contribution of EVs for renewable power integration increases.

The realisation of the scenario assumed in this work implies an ambitious infrastructure development. Large solar and wind farms will need to be installed as well as transmission lines connecting them with consumers located more than thousands of kilometres away. This work assumes that HVDC transmission will be based on underground cables in order to mitigate the impact on the landscape and to increase public acceptance.

The costs of the required IT infrastructure and for a larger hydrogen storage capacity have not been considered in this calculation. Nonetheless, though investments in IT would be needed to allow for controlled loading, the related costs would not exclusively be attributable to EVs. For large hydrogen storage capacities, its cost depends to a large extent on the availability of suitable geological formations. In times of high wind power generation and low electricity prices FCV owners will be able to fill-up for a lower

---

[78] Assuming 20.000 kilometers traveled per year (see Figure 17).

price. Depending on tank size and consumption of the vehicle this could also constitute a storage capacity of one week[79].

In this doctoral thesis, lower voltage grids have not been specifically analysed. The author expects that EVs and mainly distributed renewable power generation will lead to increased expansion of electricity distribution networks. And that controlled loading strategies result in a reduced need to expand these grids.

The provision of ancillary services could be an additional income source for electric vehicles. However, the author expects that the potential income per vehicle reduces along with the number of vehicles providing the service in a similar way as for the captured price (see Figure 58).

In this work a flexible operation of cogeneration units is assumed including heat storage as well as the possibility of using renewable power generation for heat production in times of low electricity prices. However, a flexible operation of heat pumps and of dual electric and fossil boilers are also conceivable in the future and can provide additional balancing capacity to the system.

In this work the assumed driving behaviour is based on survey data. Hence, it reflects past rather than future behaviour which may be different. Though the weight of individual mobility may be reduced as time passes the author does not expect relevant reductions in the use of passenger cars. Nevertheless, a shift from personal mobility using passenger cars towards collective transportation in busses, trains or even cars subject to a collective use structure, i.e. car sharing, could lead to a lower flexibility in charging times and thus to less capacity to integrate renewable power generation.

All in all a shift from a fossil fuelled mobility to one based on electricity from renewable sources allows for a large reduction of greenhouse gas emissions as it is required in the long run. Finally, an intelligent loading of plug-in electric vehicles and hydrogen production allows fully integrating the required renewable power generation to power a sustainable mobility.

---

[79] For an annual driving distance of 20.800 km and a range of 400 km.

8 Annex:

8.1 Vehicle fleet input data tables

Table 26: Vehicle stock scenario		2015	2020	2030	2040	2050
Vehicle		**2015**	**2020**	**2030**	**2040**	**2050**
BEV-S		0.066	0.336	1.140	2.568	4.967
BEV-M		0.107	0.247	0.639	2.155	4.597
BEV-L		0.013	0.009	0.037	0.701	1.275
D-S		1.772	2.484	1.462	0.331	0.169
D-M		9.694	9.480	4.950	1.062	0.212
D-L		4.753	4.763	2.953	0.778	0.108
D_Hyb-S		0.009	0.006	0.001	0.000	0.000
D_Hyb-M	Million	0.538	0.920	2.328	2.631	0.769
D_Hyb-L	vehicles	0.251	0.676	2.153	3.388	1.998
G-S		10.250	8.477	6.878	2.372	0.279
G-M		12.637	9.677	7.600	4.515	1.084
G-L		2.574	1.715	1.580	1.102	0.368
G_EREV-S		0.062	0.179	0.838	2.686	4.161
G_EREV-M		0.061	0.360	1.593	3.990	7.881
G_EREV-L		0.063	0.254	0.835	2.110	4.096
G_Hyb-S		0.010	0.116	1.871	5.938	4.669
G_Hyb-M		0.509	0.780	2.138	5.293	5.966
G_Hyb-L		0.000	0.002	0.214	0.342	0.126

Table 27: Annual distance driven		2015	2020	2030	2040	2050
Vehicle		**2015**	**2020**	**2030**	**2040**	**2050**
BEV-S		28.4	32.4	23.7	18.8	16.7
BEV-M		28.2	31.1	26.3	20.1	20.2
BEV-L		28.6	21.7	33.7	21.6	16.9
D-S		19.8	19.1	15.9	12.0	9.4
D-M		15.7	13.8	10.3	6.2	3.0
D-L		17.1	15.4	13.3	11.8	11.4
D_Hyb-S		53.9	49.1	35.5	27.2	0.0
D_Hyb-M	1000	24.5	20.4	15.4	11.6	7.0
D_Hyb-L	km / a	30.2	27.4	23.0	18.2	15.8
G-S		8.3	8.6	9.4	7.6	5.6
G-M		9.4	8.7	9.4	8.3	5.5
G-L		8.6	7.3	10.3	8.8	6.0
G_EREV-S		30.8	27.5	23.2	14.6	13.9
G_EREV-M		30.9	34.1	27.9	20.7	16.6
G_EREV-L		32.6	32.3	25.8	21.3	20.5
G_Hyb-S		52.4	30.8	20.2	15.0	12.4
G_Hyb-M		29.1	26.7	23.5	18.6	14.7
G_Hyb-L		0.0	3.2	9.7	7.8	5.5

Table 28: Uncontrolled loading profile of the average vehicle

In kWh

Vehicle	Year	00:00	01:00	02:00	03:00	04:00	05:00	06:00	07:00	08:00	09:00	10:00	11:00	12:00	13:00	14:00	15:00	16:00	17:00	18:00	19:00	20:00	21:00	22:00	23:00
BEV-S	2030	0.237	0.065	0.016	0.010	0.009	0.025	0.131	0.307	0.542	0.348	0.193	0.172	0.217	0.296	0.364	0.395	0.477	0.684	0.846	0.888	0.740	0.546	0.391	0.321
BEV-M	2030	0.356	0.136	0.044	0.023	0.014	0.032	0.166	0.402	0.706	0.487	0.279	0.233	0.303	0.406	0.483	0.517	0.637	0.901	1.130	1.220	1.101	0.830	0.602	0.479
BEV-L	2030	0.713	0.331	0.138	0.065	0.030	0.044	0.224	0.591	1.093	0.848	0.529	0.411	0.473	0.620	0.737	0.795	0.956	1.342	1.806	2.015	1.956	1.552	1.210	0.951
BEV-S	2050	0.123	0.022	0.009	0.007	0.004	0.015	0.075	0.179	0.305	0.181	0.116	0.115	0.164	0.210	0.236	0.241	0.307	0.424	0.497	0.507	0.411	0.283	0.204	0.166
BEV-M	2050	0.200	0.044	0.012	0.012	0.006	0.021	0.108	0.258	0.449	0.269	0.174	0.169	0.222	0.294	0.336	0.353	0.431	0.623	0.735	0.763	0.632	0.449	0.319	0.264
BEV-L	2050	0.211	0.053	0.015	0.013	0.007	0.022	0.112	0.269	0.470	0.289	0.192	0.189	0.260	0.335	0.373	0.387	0.483	0.674	0.792	0.822	0.687	0.495	0.353	0.285
EREV-S	2030	0.137	0.037	0.010	0.007	0.006	0.015	0.078	0.181	0.324	0.200	0.131	0.127	0.163	0.218	0.247	0.251	0.319	0.445	0.523	0.539	0.448	0.318	0.227	0.186
EREV-M	2030	0.209	0.069	0.016	0.010	0.008	0.019	0.101	0.247	0.441	0.287	0.186	0.172	0.207	0.276	0.324	0.332	0.429	0.595	0.704	0.759	0.661	0.474	0.337	0.275
EREV-L	2030	0.247	0.089	0.021	0.013	0.010	0.022	0.121	0.294	0.527	0.360	0.230	0.209	0.256	0.349	0.400	0.408	0.510	0.723	0.864	0.910	0.805	0.577	0.409	0.337
EREV-S	2050	0.076	0.013	0.005	0.004	0.003	0.009	0.048	0.113	0.195	0.116	0.080	0.081	0.112	0.140	0.160	0.158	0.200	0.277	0.321	0.324	0.259	0.178	0.128	0.108
EREV-M	2050	0.096	0.019	0.006	0.005	0.004	0.012	0.059	0.133	0.240	0.140	0.103	0.105	0.138	0.176	0.193	0.192	0.249	0.344	0.390	0.397	0.327	0.221	0.162	0.135
EREV-L	2050	0.155	0.033	0.010	0.008	0.006	0.018	0.093	0.211	0.382	0.223	0.156	0.156	0.204	0.267	0.298	0.300	0.387	0.540	0.617	0.630	0.520	0.358	0.259	0.215

Table 29: Power consumption profile of the average vehicle

In kWh

Vehicle	Year	00:00	01:00	02:00	03:00	04:00	05:00	06:00	07:00	08:00	09:00	10:00	11:00	12:00	13:00	14:00	15:00	16:00	17:00	18:00	19:00	20:00	21:00	22:00	23:00
BEV-S	2030	0.033	0.026	0.018	0.023	0.069	0.274	0.602	0.658	0.371	0.341	0.362	0.353	0.413	0.457	0.548	0.636	0.800	0.690	0.532	0.379	0.230	0.154	0.159	0.088
BEV-M	2030	0.050	0.039	0.032	0.030	0.110	0.400	0.831	0.878	0.539	0.485	0.523	0.497	0.577	0.635	0.762	0.876	1.122	0.967	0.747	0.515	0.326	0.219	0.204	0.123
BEV-L	2030	0.093	0.070	0.062	0.064	0.191	0.700	1.443	1.383	0.965	0.859	0.956	0.821	0.941	1.048	1.251	1.420	1.955	1.614	1.262	0.867	0.548	0.361	0.364	0.191
BEV-S	2050	0.018	0.015	0.012	0.010	0.040	0.146	0.325	0.365	0.229	0.217	0.237	0.232	0.263	0.270	0.319	0.368	0.453	0.400	0.312	0.210	0.131	0.090	0.087	0.050
BEV-M	2050	0.030	0.021	0.019	0.017	0.059	0.224	0.493	0.537	0.344	0.339	0.352	0.331	0.381	0.400	0.478	0.531	0.679	0.591	0.463	0.319	0.198	0.131	0.129	0.072
BEV-L	2050	0.030	0.022	0.022	0.020	0.067	0.231	0.510	0.575	0.384	0.383	0.400	0.371	0.441	0.447	0.523	0.589	0.728	0.632	0.507	0.337	0.211	0.145	0.137	0.074
EREV-S	2030	0.023	0.017	0.016	0.014	0.044	0.162	0.365	0.403	0.266	0.268	0.268	0.252	0.282	0.288	0.335	0.374	0.472	0.407	0.314	0.211	0.129	0.089	0.090	0.050
EREV-M	2030	0.033	0.025	0.022	0.021	0.066	0.236	0.520	0.555	0.376	0.371	0.375	0.338	0.376	0.391	0.462	0.518	0.668	0.564	0.437	0.293	0.176	0.121	0.124	0.073
EREV-L	2030	0.040	0.030	0.026	0.025	0.078	0.283	0.630	0.683	0.452	0.453	0.451	0.421	0.465	0.483	0.563	0.629	0.804	0.685	0.529	0.359	0.217	0.148	0.151	0.086
EREV-S	2050	0.013	0.009	0.009	0.007	0.024	0.092	0.211	0.236	0.155	0.157	0.164	0.155	0.173	0.179	0.205	0.232	0.290	0.250	0.194	0.132	0.082	0.057	0.055	0.030
EREV-M	2050	0.016	0.012	0.011	0.010	0.032	0.114	0.256	0.291	0.200	0.206	0.212	0.198	0.218	0.219	0.249	0.282	0.352	0.301	0.237	0.159	0.097	0.068	0.067	0.037
EREV-L	2050	0.026	0.020	0.018	0.015	0.051	0.183	0.412	0.462	0.313	0.317	0.323	0.303	0.339	0.342	0.393	0.444	0.557	0.476	0.373	0.251	0.153	0.106	0.106	0.059

Table 30: Fuel consumption

Vehicle	Year	00:00	01:00	02:00	03:00	04:00	05:00	06:00	07:00	08:00	09:00	10:00	11:00	12:00	13:00	14:00	15:00	16:00	17:00	18:00	19:00	20:00	21:00	22:00	23:00
BEV-S	2030	0.000	0.000	0.000	0.000	0.000	0.000	0.000	0.000	0.000	0.000	0.000	0.000	0.000	0.000	0.000	0.000	0.000	0.000	0.000	0.000	0.000	0.000	0.000	0.000
BEV-M	2030	0.000	0.000	0.000	0.000	0.000	0.000	0.000	0.000	0.000	0.000	0.000	0.000	0.000	0.000	0.000	0.000	0.000	0.000	0.000	0.000	0.000	0.000	0.000	0.000
BEV-L	2030	0.000	0.000	0.000	0.000	0.000	0.000	0.000	0.000	0.000	0.000	0.000	0.000	0.000	0.000	0.000	0.000	0.000	0.000	0.000	0.000	0.000	0.000	0.000	0.000
BEV-S	2050	0.000	0.000	0.000	0.000	0.000	0.000	0.000	0.000	0.000	0.000	0.000	0.000	0.000	0.000	0.000	0.000	0.000	0.000	0.000	0.000	0.000	0.000	0.000	0.000
BEV-M	2050	0.000	0.000	0.000	0.000	0.000	0.000	0.000	0.000	0.000	0.000	0.000	0.000	0.000	0.000	0.000	0.000	0.000	0.000	0.000	0.000	0.000	0.000	0.000	0.000
BEV-L	2050	0.000	0.000	0.000	0.000	0.000	0.000	0.000	0.000	0.000	0.000	0.000	0.000	0.000	0.000	0.000	0.000	0.000	0.000	0.000	0.000	0.000	0.000	0.000	0.000
EREV-S	2030	0.006	0.004	0.003	0.002	0.014	0.027	0.044	0.058	0.066	0.083	0.076	0.059	0.067	0.060	0.060	0.071	0.092	0.074	0.064	0.033	0.028	0.021	0.014	0.007
EREV-M	2030	0.009	0.007	0.005	0.003	0.022	0.042	0.064	0.087	0.102	0.128	0.115	0.089	0.102	0.089	0.089	0.106	0.137	0.111	0.095	0.049	0.042	0.033	0.020	0.009
EREV-L	2030	0.010	0.008	0.006	0.004	0.025	0.049	0.077	0.103	0.119	0.148	0.135	0.105	0.121	0.106	0.107	0.126	0.164	0.134	0.113	0.060	0.051	0.038	0.025	0.011
EREV-S	2050	0.001	0.001	0.000	0.000	0.002	0.005	0.012	0.013	0.013	0.015	0.017	0.015	0.015	0.016	0.017	0.019	0.025	0.021	0.017	0.011	0.008	0.005	0.003	0.002
EREV-M	2050	0.003	0.002	0.001	0.001	0.007	0.013	0.022	0.030	0.035	0.044	0.041	0.031	0.035	0.031	0.031	0.036	0.046	0.037	0.032	0.016	0.014	0.011	0.006	0.003
EREV-L	2050	0.005	0.004	0.003	0.002	0.013	0.024	0.040	0.054	0.062	0.079	0.072	0.055	0.062	0.055	0.055	0.064	0.082	0.067	0.057	0.029	0.026	0.019	0.012	0.006

Table 31: Share plugged

Vehicle	Year	00:00	01:00	02:00	03:00	04:00	05:00	06:00	07:00	08:00	09:00	10:00	11:00	12:00	13:00	14:00	15:00	16:00	17:00	18:00	19:00	20:00	21:00	22:00	23:00
BEV-S	2030	83%	83%	83%	83%	81%	76%	65%	53%	54%	52%	48%	46%	43%	42%	41%	39%	37%	40%	48%	58%	67%	72%	76%	80%
BEV-M	2030	84%	84%	83%	83%	82%	76%	65%	53%	54%	52%	48%	46%	44%	42%	41%	38%	37%	40%	48%	57%	67%	72%	76%	81%
BEV-L	2030	84%	84%	84%	83%	82%	76%	64%	53%	53%	52%	47%	45%	42%	41%	40%	38%	34%	37%	45%	55%	65%	71%	76%	81%
BEV-S	2050	84%	84%	84%	84%	83%	79%	70%	58%	57%	54%	50%	47%	46%	46%	46%	44%	44%	47%	54%	63%	71%	75%	78%	82%
BEV-M	2050	84%	84%	84%	84%	83%	78%	68%	57%	56%	53%	49%	46%	45%	45%	44%	43%	41%	45%	52%	61%	69%	74%	77%	81%
BEV-L	2050	85%	85%	85%	85%	84%	80%	71%	59%	58%	54%	50%	48%	46%	46%	46%	45%	45%	48%	55%	64%	71%	76%	79%	83%
EREV-S	2030	69%	69%	69%	68%	68%	64%	56%	47%	46%	43%	40%	38%	37%	37%	36%	35%	34%	37%	43%	51%	57%	61%	64%	67%
EREV-M	2030	69%	69%	69%	69%	68%	64%	55%	46%	46%	43%	40%	38%	36%	36%	35%	34%	33%	36%	41%	49%	56%	61%	63%	67%
EREV-L	2030	69%	69%	69%	68%	68%	64%	56%	46%	46%	43%	40%	38%	36%	36%	36%	35%	33%	36%	42%	50%	56%	61%	64%	67%
EREV-S	2050	69%	69%	69%	69%	68%	65%	58%	50%	49%	45%	42%	40%	40%	41%	40%	40%	39%	42%	47%	54%	59%	62%	65%	67%
EREV-M	2050	69%	69%	69%	69%	68%	65%	58%	50%	48%	45%	41%	40%	39%	40%	40%	39%	39%	42%	47%	53%	59%	62%	65%	67%
EREV-L	2050	69%	69%	69%	69%	68%	64%	57%	48%	47%	44%	40%	38%	37%	37%	37%	36%	36%	39%	44%	51%	57%	61%	64%	67%

Table 32: Maximum State-of-Charge

%. α=5%

Vehicle	Year	00:00	01:00	02:00	03:00	04:00	05:00	06:00	07:00	08:00	09:00	10:00	11:00	12:00	13:00	14:00	15:00	16:00	17:00	18:00	19:00	20:00	21:00	22:00	23:00
BEV-S	2030	0.731	0.738	0.738	0.738	0.725	0.683	0.640	0.616	0.640	0.646	0.640	0.616	0.598	0.580	0.555	0.531	0.495	0.479	0.501	0.537	0.580	0.616	0.646	0.683
BEV-M	2030	0.770	0.779	0.784	0.779	0.770	0.730	0.680	0.680	0.685	0.694	0.680	0.669	0.658	0.635	0.613	0.590	0.563	0.546	0.550	0.586	0.626	0.660	0.694	0.725
BEV-L	2030	0.752	0.770	0.776	0.774	0.770	0.720	0.684	0.670	0.682	0.680	0.663	0.645	0.637	0.616	0.591	0.569	0.540	0.526	0.535	0.555	0.598	0.647	0.675	0.711
BEV-S	2050	0.825	0.825	0.825	0.825	0.813	0.788	0.750	0.727	0.750	0.750	0.730	0.715	0.700	0.690	0.675	0.650	0.630	0.625	0.640	0.670	0.708	0.750	0.775	0.800
BEV-M	2050	0.841	0.841	0.841	0.841	0.834	0.805	0.768	0.761	0.768	0.768	0.761	0.750	0.732	0.721	0.710	0.695	0.668	0.659	0.671	0.703	0.732	0.768	0.794	0.814
BEV-L	2050	0.877	0.880	0.880	0.880	0.877	0.857	0.834	0.819	0.828	0.828	0.816	0.805	0.799	0.787	0.776	0.764	0.747	0.741	0.750	0.776	0.800	0.828	0.847	0.863
EREV-S	2030	0.789	0.789	0.789	0.789	0.782	0.756	0.723	0.704	0.717	0.717	0.704	0.697	0.678	0.671	0.665	0.652	0.625	0.625	0.638	0.658	0.691	0.717	0.737	0.763
EREV-M	2030	0.775	0.781	0.781	0.775	0.775	0.744	0.713	0.700	0.713	0.713	0.700	0.681	0.669	0.656	0.650	0.634	0.600	0.600	0.613	0.638	0.675	0.706	0.725	0.744
EREV-L	2030	0.782	0.788	0.788	0.782	0.772	0.749	0.716	0.703	0.703	0.709	0.703	0.690	0.670	0.663	0.657	0.644	0.611	0.611	0.624	0.640	0.673	0.703	0.729	0.751
EREV-S	2050	0.830	0.830	0.827	0.825	0.819	0.803	0.765	0.752	0.765	0.765	0.749	0.738	0.728	0.717	0.712	0.706	0.685	0.682	0.687	0.712	0.738	0.771	0.792	0.811
EREV-M	2050	0.830	0.830	0.830	0.830	0.825	0.805	0.775	0.754	0.770	0.770	0.755	0.750	0.730	0.725	0.720	0.710	0.690	0.690	0.700	0.720	0.750	0.775	0.795	0.815
EREV-L	2050	0.810	0.810	0.810	0.810	0.799	0.784	0.752	0.741	0.741	0.741	0.739	0.725	0.709	0.701	0.694	0.687	0.662	0.662	0.667	0.688	0.720	0.746	0.768	0.788

Table 33: Minimum State-of-Charge

%. α=5%

Vehicle	Year	00:00	01:00	02:00	03:00	04:00	05:00	06:00	07:00	08:00	09:00	10:00	11:00	12:00	13:00	14:00	15:00	16:00	17:00	18:00	19:00	20:00	21:00	22:00	23:00
BEV-S	2030	0.313	0.313	0.313	0.331	0.399	0.464	0.495	0.489	0.495	0.501	0.489	0.476	0.476	0.464	0.464	0.446	0.428	0.404	0.373	0.343	0.325	0.319	0.313	0.313
BEV-M	2030	0.262	0.266	0.271	0.298	0.365	0.415	0.442	0.442	0.446	0.455	0.433	0.419	0.424	0.415	0.415	0.392	0.370	0.347	0.325	0.298	0.280	0.275	0.262	0.262
BEV-L	2030	0.273	0.273	0.298	0.331	0.377	0.434	0.459	0.463	0.467	0.459	0.441	0.425	0.423	0.431	0.420	0.395	0.373	0.337	0.316	0.289	0.273	0.273	0.270	0.274
BEV-S	2050	0.225	0.225	0.227	0.240	0.275	0.330	0.360	0.365	0.375	0.390	0.375	0.375	0.368	0.360	0.360	0.350	0.330	0.300	0.275	0.250	0.245	0.240	0.230	0.225
BEV-M	2050	0.213	0.215	0.213	0.227	0.260	0.311	0.329	0.336	0.351	0.355	0.336	0.336	0.333	0.325	0.318	0.318	0.296	0.275	0.253	0.231	0.224	0.224	0.211	0.209
BEV-L	2050	0.173	0.173	0.173	0.181	0.202	0.239	0.261	0.265	0.274	0.275	0.274	0.268	0.265	0.260	0.260	0.251	0.239	0.216	0.202	0.187	0.181	0.175	0.173	0.171
EREV-S	2030	0.461	0.461	0.461	0.468	0.500	0.553	0.585	0.579	0.592	0.598	0.592	0.589	0.585	0.579	0.579	0.579	0.553	0.533	0.513	0.494	0.481	0.481	0.464	0.461
EREV-M	2030	0.469	0.469	0.469	0.475	0.513	0.569	0.600	0.600	0.600	0.606	0.600	0.600	0.600	0.600	0.600	0.588	0.569	0.538	0.519	0.506	0.488	0.488	0.475	0.463
EREV-L	2030	0.462	0.462	0.468	0.481	0.514	0.560	0.593	0.587	0.600	0.606	0.600	0.600	0.600	0.587	0.587	0.580	0.560	0.547	0.514	0.501	0.488	0.481	0.468	0.462
EREV-S	2050	0.425	0.428	0.425	0.431	0.452	0.495	0.528	0.528	0.538	0.538	0.538	0.538	0.538	0.538	0.536	0.528	0.512	0.485	0.468	0.452	0.440	0.436	0.431	0.425
EREV-M	2050	0.425	0.425	0.425	0.425	0.450	0.495	0.525	0.520	0.530	0.535	0.530	0.530	0.530	0.525	0.525	0.525	0.500	0.480	0.460	0.450	0.435	0.430	0.425	0.420
EREV-L	2050	0.371	0.374	0.376	0.382	0.408	0.451	0.482	0.482	0.493	0.498	0.498	0.498	0.498	0.498	0.488	0.482	0.466	0.451	0.429	0.414	0.403	0.392	0.376	0.371

8.2 Power system model input data tables

Table 34: Scenario of total electricity demand per region					
In TWh/a					
Region	**2010**	**2020**	**2030**	**2040**	**2050**
Alps	127.1	131.9	129.3	122.9	115.9
BeNeLux	220.0	236.8	244.2	244.1	239.3
DK-W	24.0	27.0	29.3	31.4	33.8
East	232.2	244.1	276.4	313.8	343.1
France	507.4	546.5	561.3	552.9	523.3
Germany	549.0	522.0	522.0	557.0	625.0
Iberia	304.8	355.6	403.5	444.8	473.0
Italy	344.5	376.8	393.4	395.3	386.2
North	387.3	400.6	406.6	407.4	406.2
UK-IE	460.4	515.9	556.1	576.7	574.0

Table 35:Scenario of conventional electricity demand per region					
In TWh/a					
Region	**2010**	**2020**	**2030**	**2040**	**2050**
Alps	127.1	130.8	126.5	112.1	88.4
BeNeLux	220.0	235.1	239.5	226.2	194.0
DK-W	24.0	26.8	28.8	29.3	28.1
East	232.2	241.7	270.2	287.1	272.1
France	507.4	542.4	550.2	513.1	426.0
Germany	549.0	516.2	506.6	502.7	491.0
Iberia	304.8	352.7	395.1	409.8	382.1
Italy	344.5	372.8	383.2	362.6	310.6
North	387.3	399.3	403.0	391.9	365.1
UK-IE	460.4	511.9	545.1	539.3	485.2

Table 36: Assumed power demand of H_2 fuelling stations per region					
In TWh/a					
Region	**2010**	**2020**	**2030**	**2040**	**2050**
Alps	0.0	0.1	0.1	5.3	19.0
BeNeLux	0.0	0.1	0.2	8.3	29.7
DK-W	0.0	0.0	0.0	1.1	4.1
East	0.0	0.2	0.4	14.6	52.3
France	0.0	0.2	0.5	16.6	59.5
Germany	0.0	0.3	0.7	23.7	84.9
Iberia	0.0	0.2	0.5	16.9	60.4

Italy	0.0	0.2	0.4	12.6	45.1
North	0.0	0.1	0.2	8.2	29.4
UK-IE	0.0	0.2	0.4	13.8	49.5

Table 37: Assumed H₂ demand of fuelling stations per region					
In TWh/a					
Region	**2010**	**2020**	**2030**	**2040**	**2050**
Alps	0.0	0.0	0.1	3.4	12.8
BeNeLux	0.0	0.1	0.1	5.3	19.9
DK-W	0.0	0.0	0.0	0.7	2.7
East	0.0	0.1	0.3	9.3	35.0
France	0.0	0.1	0.3	10.6	39.9
Germany	0.0	0.2	0.4	15.1	56.9
Iberia	0.0	0.1	0.3	10.7	40.5
Italy	0.0	0.1	0.2	8.0	30.2
North	0.0	0.1	0.1	5.2	19.7
UK-IE	0.0	0.1	0.2	8.8	33.1

Table 38: Assumed power demand of PEVs per region					
TWh/a					
Region	**2010**	**2020**	**2030**	**2040**	**2050**
Alps	0.0	1.0	2.6	5.4	8.5
BeNeLux	0.0	1.6	4.4	9.7	15.7
DK-W	0.0	0.2	0.5	1.0	1.6
East	0.0	2.2	5.8	12.1	18.7
France	0.0	3.9	10.6	23.2	37.8
Germany	0.0	5.5	14.7	30.5	49.1
Iberia	0.0	2.7	8.0	18.2	30.5
Italy	0.0	3.8	9.8	20.1	30.5
North	0.0	1.2	3.4	7.3	11.7
UK-IE	0.0	3.8	10.6	23.6	39.4

Table 39: Assumed maximum imports per region					
TWh/a					
Region	**2010**	**2020**	**2030**	**2040**	**2050**
Alps	38.1	38.1	38.1	29.3	24.3
BeNeLux	42.8	49.2	64.95	76	85.6
DK-W	8.4	8.4	10.4	11.4	13.4
East	18	18	40	91	149.5
France	3.7	13.7	38.7	73.7	113.7

Germany	0	1.808	37.35	89.45	130.65
Iberia	18.7	33.7	43.7	49.7	53.7
Italy	45	55	70	88.7	103.7
North	40.1	40.1	40.6	33.6	25.6
UK-IE	14.5	14.5	29.5	49.5	79.5

Table 40: Scenario of assumed solar electricity imports per region					
TWh/a					
Region	**2010**	**2020**	**2030**	**2040**	**2050**
Alps	0.00	0.00	0.00	0.00	0.00
BeNeLux	0.00	5.00	20.00	31.00	41.50
DK-W	0.00	0.00	1.10	1.65	2.75
East	0.00	0.00	22.00	73.00	132.50
France	0.00	10.00	35.00	70.00	110.00
Germany	0.00	1.81	37.35	89.45	130.65
Iberia	0.00	15.00	25.00	35.00	45.00
Italy	0.00	10.00	25.00	45.00	60.00
North	0.00	0.00	0.90	1.35	2.25
UK-IE	0.00	0.00	15.00	35.00	65.00

Table 41: Power generation from RES – *Base* scenario						
TWh/a						
Region	**Technology**	**2010**	**2020**	**2030**	**2040**	**2050**
Germany	Hydropower	20.4	22.2	23.5	24.4	25.1
Germany	Wind onshore	49.5	78.5	94.8	115.8	130.8
Germany	Wind offshore	0.7	37.8	107.9	174.9	206.2
Germany	Photovoltaic	12.5	44.8	62.1	72.9	82.8
Germany	Geothermal	0.0	1.7	7.1	17.7	31.6
Germany	Solid biomass	0.0	0.9	3.8	7.4	9.9
Alps	Solid biomass	4.4	7.2	9.9	16.3	16.3
Alps	CSP	0.0	0.0	0.0	0.0	0.0
Alps	Geothermal	0.1	0.4	1.3	3.0	4.4
Alps	Hydropower	80.9	81.8	82.6	83.5	84.3
Alps	Photovoltaic	0.2	1.3	4.1	10.1	29.6
Alps	Wave / Tidal	0.0	0.0	0.0	0.0	0.0
Alps	Wind power	0.2	0.5	0.7	1.2	2.9
BeNeLux	Solid biomass	6.5	10.2	10.2	10.2	10.2
BeNeLux	CSP	0.0	0.0	0.0	0.0	0.0
BeNeLux	Geothermal	0.0	0.1	0.6	1.5	3.2
BeNeLux	Hydropower	1.5	1.5	1.5	1.5	1.6
BeNeLux	Photovoltaic	0.2	1.5	6.5	13.2	23.3
BeNeLux	Wave / Tidal	0.0	0.1	0.4	0.9	1.9

BeNeLux	Wind power	7.3	25.8	50.0	75.6	107.8
DK-W	Solid biomass	1.7	2.2	3.0	4.5	6.5
DK-W	CSP	0.0	0.0	0.0	0.0	0.0
DK-W	Geothermal	0.0	0.0	0.0	0.0	0.0
DK-W	Hydropower	0.0	0.0	0.0	0.0	0.0
DK-W	Photovoltaic	0.0	0.1	0.5	0.8	1.2
DK-W	Wave / Tidal	0.0	0.1	0.2	0.4	0.8
DK-W	Wind power	6.1	11.8	15.9	18.8	22.7
East	Solid biomass	5.1	13.6	29.8	42.7	38.7
East	CSP	0.0	0.0	0.0	0.0	0.0
East	Geothermal	0.2	0.5	2.1	7.6	20.6
East	Hydropower	11.9	12.4	12.9	13.4	13.9
East	Photovoltaic	0.2	1.1	4.7	14.7	33.0
East	Wave / Tidal	0.0	0.1	0.3	1.0	2.7
East	Wind power	7.6	25.4	48.7	113.2	205.9
France	Solid biomass	9.0	23.4	41.0	86.1	135.5
France	CSP	0.0	0.0	0.0	0.0	0.0
France	Geothermal	0.5	1.5	5.3	11.2	21.6
France	Hydropower	71.8	71.9	71.9	71.9	71.9
France	Photovoltaic	0.6	4.6	15.7	28.2	45.3
France	Wave / Tidal	0.2	1.1	2.8	6.0	11.6
France	Wind power	23.0	82.8	129.5	172.7	224.9
Iberia	Solid biomass	7.1	17.1	26.1	27.9	25.1
Iberia	CSP	2.1	10.8	28.4	45.4	71.5
Iberia	Geothermal	0.8	3.3	10.0	21.7	42.0
Iberia	Hydropower	45.7	48.0	50.3	52.6	55.0
Iberia	Photovoltaic	0.6	4.8	14.8	27.3	44.0
Iberia	Wave / Tidal	0.4	1.9	4.4	9.7	18.8
Iberia	Wind power	21.4	68.4	93.2	127.0	165.6
Italy	Solid biomass	4.5	12.6	19.7	16.8	16.8
Italy	CSP	0.5	1.3	5.8	10.5	14.3
Italy	Geothermal	5.0	7.3	11.8	19.2	19.9
Italy	Hydropower	52.3	53.7	55.1	56.5	57.9
Italy	Photovoltaic	0.5	3.8	13.0	28.2	50.3
Italy	Wave / Tidal	0.1	0.3	0.8	2.0	4.3
Italy	Wind power	12.2	44.3	68.8	110.9	159.7
North	Solid biomass	18.0	26.4	34.9	56.5	63.3
North	CSP	0.0	0.0	0.0	0.0	0.0
North	Geothermal	0.0	0.1	0.4	0.7	1.0
North	Hydropower	239.4	243.6	247.7	251.9	256.0
North	Photovoltaic	0.2	1.2	3.6	5.9	10.8
North	Wave / Tidal	0.2	0.8	1.9	3.7	8.1

North	Wind power	12.7	38.6	53.6	65.2	95.8
UK-IE	Solid biomass	7.3	12.7	19.9	23.1	23.1
UK-IE	CSP	0.0	0.0	0.0	0.0	0.0
UK-IE	Geothermal	0.0	0.0	0.1	0.2	0.4
UK-IE	Hydropower	9.0	9.1	9.1	9.1	9.1
UK-IE	Photovoltaic	0.2	1.6	5.3	9.9	16.6
UK-IE	Wave / Tidal	1.3	5.3	13.4	29.7	59.8
UK-IE	Wind power	30.9	98.7	150.1	209.3	284.0

Table 42: Power generation from RES – *Trans* scenario						
TWh/a						
Region	**Technology**	**2010**	**2020**	**2030**	**2040**	**2050**
Germany	Hydropower	20.4	22.2	23.5	24.4	25.1
Germany	Wind onshore	49.5	77.8	83.1	90.9	95.8
Germany	Wind offshore	0.7	37.4	94.6	137.3	151.1
Germany	Photovoltaic	12.5	44.5	54.5	57.2	60.7
Germany	Geothermal	0.0	1.7	6.3	13.9	23.1
Germany	Solid biomass	0.0	0.5	0.0	0.0	0.0
Alps	Solid biomass	4.4	7.2	9.9	16.3	16.3
Alps	CSP	0.0	0.0	0.0	0.0	0.0
Alps	Geothermal	0.1	0.4	1.3	3.0	4.4
Alps	Hydropower	80.9	81.8	82.6	83.5	84.3
Alps	Photovoltaic	0.2	1.3	4.1	10.1	29.6
Alps	Wave / Tidal	0.0	0.0	0.0	0.0	0.0
Alps	Wind power	0.2	0.5	0.7	1.2	2.9
BeNeLux	Solid biomass	6.5	8.9	10.2	10.2	10.2
BeNeLux	CSP	0.0	0.0	0.0	0.0	0.0
BeNeLux	Geothermal	0.0	0.1	0.4	1.0	2.2
BeNeLux	Hydropower	1.5	1.5	1.5	1.5	1.6
BeNeLux	Photovoltaic	0.2	1.3	4.2	8.7	16.2
BeNeLux	Wave / Tidal	0.0	0.1	0.2	0.6	1.3
BeNeLux	Wind power	7.3	22.4	32.6	49.9	74.9
DK-W	Solid biomass	1.7	2.2	2.8	4.2	5.9
DK-W	CSP	0.0	0.0	0.0	0.0	0.0
DK-W	Geothermal	0.0	0.0	0.0	0.0	0.0
DK-W	Hydropower	0.0	0.0	0.0	0.0	0.0
DK-W	Photovoltaic	0.0	0.1	0.5	0.7	1.1
DK-W	Wave / Tidal	0.0	0.1	0.2	0.4	0.7
DK-W	Wind power	6.1	11.8	15.0	17.5	20.7
East	Solid biomass	5.1	13.6	22.1	42.7	38.7
East	CSP	0.0	0.0	0.0	0.0	0.0
East	Geothermal	0.2	0.5	1.5	3.6	10.2

East	Hydropower	11.9	12.4	12.9	13.4	13.9
East	Photovoltaic	0.2	1.1	3.5	6.8	16.3
East	Wave / Tidal	0.0	0.1	0.2	0.5	1.3
East	Wind power	7.6	25.4	36.2	52.6	101.8
France	Solid biomass	9.0	21.3	33.6	66.3	106.5
France	CSP	0.0	0.0	0.0	0.0	0.0
France	Geothermal	0.5	1.4	4.3	8.6	15.8
France	Hydropower	71.8	71.9	71.9	71.9	71.9
France	Photovoltaic	0.6	4.2	12.9	21.7	33.2
France	Wave / Tidal	0.2	1.0	2.3	4.6	8.5
France	Wind power	23.0	75.5	106.1	132.9	164.9
Iberia	Solid biomass	7.1	14.7	22.4	27.9	25.1
Iberia	CSP	2.1	9.3	24.4	38.5	62.1
Iberia	Geothermal	0.8	2.9	8.6	18.4	36.4
Iberia	Hydropower	45.7	48.0	50.3	52.6	55.0
Iberia	Photovoltaic	0.6	4.1	12.7	23.1	38.2
Iberia	Wave / Tidal	0.4	1.7	3.8	8.2	16.3
Iberia	Wind power	21.4	58.8	80.1	107.8	143.8
Italy	Solid biomass	4.5	10.8	17.0	16.8	16.8
Italy	CSP	0.5	1.1	4.5	7.7	10.6
Italy	Geothermal	5.0	6.3	9.3	14.6	19.9
Italy	Hydropower	52.3	53.7	55.1	56.5	57.9
Italy	Photovoltaic	0.5	3.2	10.1	20.7	37.1
Italy	Wave / Tidal	0.1	0.3	0.6	1.5	3.2
Italy	Wind power	12.2	37.9	53.4	81.3	117.8
North	Solid biomass	18.0	26.4	34.6	56.0	63.3
North	CSP	0.0	0.0	0.0	0.0	0.0
North	Geothermal	0.0	0.1	0.4	0.7	1.0
North	Hydropower	239.4	243.6	247.7	251.9	256.0
North	Photovoltaic	0.2	1.2	3.6	5.9	10.6
North	Wave / Tidal	0.2	0.8	1.9	3.7	7.9
North	Wind power	12.7	38.6	53.1	64.6	93.9
UK-IE	Solid biomass	7.3	12.7	18.3	23.1	23.1
UK-IE	CSP	0.0	0.0	0.0	0.0	0.0
UK-IE	Geothermal	0.0	0.0	0.1	0.2	0.3
UK-IE	Hydropower	9.0	9.1	9.1	9.1	9.1
UK-IE	Photovoltaic	0.2	1.6	4.9	8.5	13.6
UK-IE	Wave / Tidal	1.3	5.3	12.3	25.5	49.0
UK-IE	Wind power	30.9	98.7	138.2	179.9	232.8

Table 43: Power generation from RES – *NEV* scenario						
TWh/a						
Region	**Technology**	**2010**	**2020**	**2030**	**2040**	**2050**
Germany	Hydropower	20.4	22.2	23.5	24.4	25.1
Germany	Wind onshore	49.5	76.1	90.2	101.1	94.8
Germany	Wind offshore	0.7	36.6	102.7	152.8	149.5
Germany	Photovoltaic	12.5	43.5	59.1	63.7	60.1
Germany	Geothermal	0.0	1.6	6.8	15.4	22.9
Germany	Solid biomass	0.0	0.0	1.6	1.4	0.0
Alps	Solid biomass	4.4	6.4	8.2	12.2	15.5
Alps	CSP	0.0	0.0	0.0	0.0	0.0
Alps	Geothermal	0.1	0.4	1.1	1.9	3.0
Alps	Hydropower	80.9	81.8	82.6	83.5	84.3
Alps	Photovoltaic	0.2	1.1	3.4	5.1	6.6
Alps	Wave / Tidal	0.0	0.0	0.0	0.0	0.0
Alps	Wind power	0.2	0.4	0.6	0.6	0.7
BeNeLux	Solid biomass	6.5	9.8	10.2	10.2	10.2
BeNeLux	CSP	0.0	0.0	0.0	0.0	0.0
BeNeLux	Geothermal	0.0	0.1	0.6	1.2	2.1
BeNeLux	Hydropower	1.5	1.5	1.5	1.5	1.6
BeNeLux	Photovoltaic	0.2	1.4	5.9	10.6	15.5
BeNeLux	Wave / Tidal	0.0	0.1	0.3	0.7	1.3
BeNeLux	Wind power	7.3	24.6	45.9	60.7	71.9
DK-W	Solid biomass	1.7	2.2	2.9	4.1	5.3
DK-W	CSP	0.0	0.0	0.0	0.0	0.0
DK-W	Geothermal	0.0	0.0	0.0	0.0	0.0
DK-W	Hydropower	0.0	0.0	0.0	0.0	0.0
DK-W	Photovoltaic	0.0	0.1	0.5	0.7	1.0
DK-W	Wave / Tidal	0.0	0.1	0.2	0.4	0.6
DK-W	Wind power	6.1	11.7	15.5	17.1	18.5
East	Solid biomass	5.1	12.8	27.6	42.7	38.7
East	CSP	0.0	0.0	0.0	0.0	0.0
East	Geothermal	0.2	0.5	1.9	6.1	15.0
East	Hydropower	11.9	12.4	12.9	13.4	13.9
East	Photovoltaic	0.2	1.0	4.4	11.8	24.1
East	Wave / Tidal	0.0	0.1	0.2	0.8	2.0
East	Wind power	7.6	24.0	45.1	91.1	150.2
France	Solid biomass	9.0	22.5	38.7	74.8	110.6
France	CSP	0.0	0.0	0.0	0.0	0.0
France	Geothermal	0.5	1.5	5.0	9.7	16.5
France	Hydropower	71.8	71.9	71.9	71.9	71.9
France	Photovoltaic	0.6	4.4	14.8	24.5	34.5

France	Wave / Tidal	0.2	1.1	2.7	5.2	8.8
France	Wind power	23.0	79.9	122.1	150.1	171.2
Iberia	Solid biomass	7.1	16.7	24.8	27.9	25.1
Iberia	CSP	2.1	10.5	27.0	38.5	52.5
Iberia	Geothermal	0.8	3.2	9.5	18.4	30.8
Iberia	Hydropower	45.7	48.0	50.3	52.6	55.0
Iberia	Photovoltaic	0.6	4.7	14.1	23.1	32.3
Iberia	Wave / Tidal	0.4	1.9	4.2	8.2	13.8
Iberia	Wind power	21.4	66.5	88.8	107.8	121.6
Italy	Solid biomass	4.5	11.9	19.6	16.8	16.8
Italy	CSP	0.5	1.2	5.2	8.4	9.6
Italy	Geothermal	5.0	6.9	10.8	15.8	19.9
Italy	Hydropower	52.3	53.7	55.1	56.5	57.9
Italy	Photovoltaic	0.5	3.5	11.7	22.8	33.7
Italy	Wave / Tidal	0.1	0.3	0.7	1.6	2.9
Italy	Wind power	12.2	41.7	61.7	89.4	106.9
North	Solid biomass	18.0	25.9	33.6	49.9	63.3
North	CSP	0.0	0.0	0.0	0.0	0.0
North	Geothermal	0.0	0.1	0.4	0.6	1.0
North	Hydropower	239.4	243.6	247.7	251.9	256.0
North	Photovoltaic	0.2	1.2	3.5	5.2	6.9
North	Wave / Tidal	0.2	0.8	1.8	3.3	5.2
North	Wind power	12.7	37.8	51.6	57.6	61.5
UK-IE	Solid biomass	7.3	12.3	18.7	23.1	23.1
UK-IE	CSP	0.0	0.0	0.0	0.0	0.0
UK-IE	Geothermal	0.0	0.0	0.1	0.2	0.3
UK-IE	Hydropower	9.0	9.1	9.1	9.1	9.1
UK-IE	Photovoltaic	0.2	1.5	5.0	8.4	12.5
UK-IE	Wave / Tidal	1.3	5.1	12.6	25.2	45.1
UK-IE	Wind power	30.9	95.4	141.4	177.9	214.1

Table 44: Assumed thermal power generation capacity in European regions						
In MW **Region**	**Technology**	**2010**	**2020**	**2030**	**2040**	**2050**
Alps	CCGT	4289	5122	5301	3543	977
Alps	Gas Turbine	2399	2653	2696	1729	477
Alps	ST-Coal	1486	1133	0	0	0
Alps	ST-Lignite	0	0	0	0	0
Alps	ST-Nuclear	3000	2500	2000	1000	0
BeNeLux	CCGT	14029	14848	14363	13721	10693
BeNeLux	Gas Turbine	8716	9201	8894	8419	6562
BeNeLux	ST-Coal	5669	5859	5985	4370	2628

BeNeLux	ST-Lignite	0	0	0	0	0
BeNeLux	ST-Nuclear	5710	4498	2499	999	0
DK-W	CCGT	0	0	0	0	0
DK-W	Gas Turbine	2888	3885	4137	4572	4701
DK-W	ST-Coal	2907	2394	2155	1524	798
DK-W	ST-Lignite	0	0	0	0	0
DK-W	ST-Nuclear	0	0	0	0	0
East	CCGT	3844	4615	5346	6267	5099
East	Gas Turbine	4706	4002	4615	5390	4332
East	ST-Coal	19028	18320	17384	11859	3615
East	ST-Lignite	13705	13195	12521	8541	2604
East	ST-Nuclear	5050	4549	2525	0	0
France	CCGT	3872	8366	12609	14912	9337
France	Gas Turbine	19175	29873	40015	38540	24131
France	ST-Coal	8323	8323	10820	9836	6242
France	ST-Lignite	1677	1677	2180	1982	1258
France	ST-Nuclear	60016	45012	22006	5001	0
Germany	CCGT	16040	14920	11041	10198	11361
Germany	Gas Turbine	2686	2499	1849	1708	1902
Germany	ST-Coal	20299	15530	8520	4036	3625
Germany	ST-Lignite	19014	15286	7774	1316	3
Germany	ST-Nuclear	19600	3900	0	0	0
Iberia	CCGT	13886	17613	20768	19630	14397
Iberia	Gas Turbine	6398	5527	3445	3207	1637
Iberia	ST-Coal	13423	13711	13733	10454	2379
Iberia	ST-Lignite	1580	1614	1616	1230	280
Iberia	ST-Nuclear	6057	3533	2019	0	0
Italy	CCGT	25219	27706	29313	25707	15949
Italy	Gas Turbine	22950	22083	18656	12464	7732
Italy	ST-Coal	6299	5865	4000	2545	1167
Italy	ST-Lignite	0	0	0	0	0
Italy	ST-Nuclear	0	0	0	0	0
North	CCGT	2557	2898	2993	2954	2325
North	Gas Turbine	21438	23259	23525	20004	16548
North	ST-Coal	6517	5158	4642	3693	823
North	ST-Lignite	719	559	503	420	45
North	ST-Nuclear	7763	4387	994	0	0
UK-IE	CCGT	22066	33090	40774	44542	39531
UK-IE	Gas Turbine	11839	14267	15830	13121	11645
UK-IE	ST-Coal	39054	32869	23758	16773	7793
UK-IE	ST-Lignite	0	0	0	0	0
UK-IE	ST-Nuclear	8829	3924	2453	981	0

Table 45: Assumed capacity installation in European regions										
In MW Region	**Technology**	**1961-1970**	**1971-1980**	**1981-1990**	**1991-2000**	**2001-2010**	**2011-2020**	**2021-2030**	**2031-2040**	**2041-2050**
Germany	ST-Coal	5767	3937	8442	1588	566	4935	2435	0	0
Germany	ST-Lignite	4345	5305	3067	4868	1429	5921	0	0	0
Germany	CCGT	154	5113	176	2727	5569	6448	0	0	4913
Germany	Gas Turbine	15	159	69	75	67	2287	0	0	0
Germany	ST-Nuclear	0	6764	12836	0	0	0	0	0	0
Alps	CCGT	0	480	0	852	2957	1313	179	0	0
Alps	Gas Turbine	4	1057	560	601	176	1468	451	0	0
Alps	ST-Coal	91	24	1318	53	0	0	0	0	0
Alps	ST-Lignite	0	0	0	0	0	0	0	0	0
Alps	ST-Nuclear	328	1577	1095	0	0	1405	595	0	0
BeNeLux	CCGT	18	458	1300	6896	5357	1295	815	6457	2329
BeNeLux	Gas Turbine	627	4157	1486	1251	1195	5269	1202	948	0
BeNeLux	ST-Coal	740	2682	1019	1229	0	3611	1145	0	0
BeNeLux	ST-Lignite	0	0	0	0	0	0	0	0	0
BeNeLux	ST-Nuclear	0	2037	3673	0	0	825	1674	0	0
DK-W	CCGT	0	0	0	0	0	0	0	0	0
DK-W	Gas Turbine	91	447	786	1082	481	2079	528	1484	610
DK-W	ST-Coal	1021	607	903	377	0	1114	664	0	0
DK-W	ST-Lignite	0	0	0	0	0	0	0	0	0
DK-W	ST-Nuclear	0	0	0	0	0	0	0	0	0
East	CCGT	0	0	0	2366	1478	771	730	3287	310
East	Gas Turbine	0	2850	0	1298	557	2309	620	2082	0
East	ST-Coal	2700	10807	2013	2395	1114	12798	1077	0	0
East	ST-Lignite	3859	3861	4248	1186	552	7210	3574	0	0
East	ST-Nuclear	0	0	2488	819	1742	0	0	0	0
France	CCGT	0	112	0	581	3179	4611	4248	2874	0
France	Gas Turbine	741	2581	2471	6179	7202	14020	12613	9662	0
France	ST-Coal	3354	1067	3543	358	0	4422	6040	0	0
France	ST-Lignite	0	835	842	0	0	835	1345	0	0
France	ST-Nuclear	0	11115	38232	10670	0	0	11336	0	0
Iberia	CCGT	0	0	2	1310	12575	4857	5285	0	4255
Iberia	Gas Turbine	187	1020	2177	1644	1370	793	666	386	0
Iberia	ST-Coal	1241	4284	6226	1673	0	5813	6248	0	0
Iberia	ST-Lignite	173	770	356	281	0	977	359	0	0
Iberia	ST-Nuclear	0	365	5692	0	0	0	2019	0	0
Italy	CCGT	0	7	159	7337	17716	2809	2404	2778	7958
Italy	Gas Turbine	1255	6778	2084	9646	3187	7166	2584	3087	0
Italy	ST-Coal	1578	1898	157	2070	596	3042	0	0	0
Italy	ST-Lignite	0	0	0	0	0	0	0	0	0

Italy	ST-Nuclear	0	0	0	0	0	0	0	0	0
North	CCGT	0	0	0	290	2267	341	95	251	1639
North	Gas Turbine	1494	3563	3053	8535	4793	6878	3320	7874	1084
North	ST-Coal	4732	407	665	713	0	4256	0	0	0
North	ST-Lignite	0	157	277	145	140	0	218	62	0
North	ST-Nuclear	153	1587	4770	1253	0	0	0	0	0
UK-IE	CCGT	0	0	128	14393	7545	11024	7812	18160	2534
UK-IE	Gas Turbine	1154	4255	2333	2548	1548	7838	3896	3181	0
UK-IE	ST-Coal	20129	14477	4410	39	0	28421	0	0	0
UK-IE	ST-Lignite	0	0	0	0	0	0	0	0	0
UK-IE	ST-Nuclear	438	2787	4680	924	0	0	1528	0	0

Table 46: Assumed scenario of installed pumped storage capacity						
Region	**Unit**	**2010**	**2020**	**2030**	**2040**	**2050**
Alps		6012	6012	6012	6012	6012
BeNeLux		2404	2404	2404	2404	2404
East		2218	2218	2218	2218	2218
France		4922	4922	4922	4922	4922
Germany	MW	6700	8100	8100	8100	8100
Iberia		5754	5754	5754	5754	5754
Italy		8384	8384	8384	8384	8384
North		846	846	846	846	846
UK-IE		3086	3086	3086	3086	3086

Table 47: Assumed scenario of installed CHP power generation capacity in Germany					
In MW **Technology**	**2010**	**2020**	**2030**	**2040**	**2050**
CHP Distributed - Biomass	442	1604	1981	2308	2440
CHP Distributed - Natural gas	264	455	1182	1091	1055
CHP District heating - Coal	3400	3269	3320	2917	2708
CHP District heating - Natural gas	2031	3788	3909	4667	5500
CHP District heating - Lignite	3214	3214	2889	2000	0
CHP District heating - Waste	2310	2571	2571	2727	2727
CHP Small industrial - Biomass	2731	3774	4154	4423	4600
CHP Small industrial - Natural gas	1522	2622	3364	3907	4048
CHP Large industrial - Coal	2906	3000	2538	1231	417
CHP Large industrial - Natural gas	3704	3966	4483	4815	5417
CHP Local heating - Biomass	1808	2796	3352	3642	3731
CHP Local heating - Natural gas	692	1093	1463	1426	1434

Table 48: Existing, planned and candidate HVDC transmission lines									
Node1	**Node2**	**Capacity**	**Exist**	**Year**	**Dist. land**	**Dist. sea**	**Max lines**	**Min lines**	**Installed Lines**
BeNeLux	North	700	Existing	2010	0	580	1	1	1
D_N	North	600	Existing	2010	0	250	1	1	1
D_NE	North	600	Existing	2010	119	52	1	1	1
East	North	600	Existing	2010	0	245	1	1	1
UK-IE	BeNeLux	1000	Existing	2011	0	260	0	0	0
UK-IE	France	1000	Existing	2010	27	46	2	2	2
D_NW	North	1400	Planned	2015	0	600	0	0	0
DK-W	North	250	Existing	2010	0	130	2	2	2
DK-W	North	500	Existing	2010	0	130	1	1	1
DK-W	North	700	Planned	2014	0	130	0	0	0
DK-W	North	300	Existing	2010	0	87	1	1	1
DK-W	North	600	Existing	2010	0	56	1	1	1
Africa	Iberia		Candidate		1095	88	20	0	0
Iberia	France		Candidate		891	0	20	0	0
Africa	Italy		Candidate		1059	190	20	0	0
France	UK-IE		Candidate		426	46	20	0	0
France	BeNeLux		Candidate		551	0	20	0	0
France	D_SW		Candidate		375	0	20	0	0
Italy	Alps		Candidate		477	0	20	0	0
France	Alps		Candidate		554	0	20	0	0
BeNeLux	D_W		Candidate		154	0	20	0	0
Alps	D_SE		Candidate		209	0	20	0	0
D_E	East		Candidate		418	0	20	0	0
Alps	East		Candidate		398	0	20	0	0
North	D_NE		Candidate		700	600	20	0	0
D_N	DK-W		Candidate		240	0	20	0	0
DK-W	North		Candidate		170	130	20	0	0
UK-IE	BeNeLux		Candidate		340	260	20	0	0
UK-IE	North		Candidate		700	600	20	0	0
North	BeNeLux		Candidate		660	580	20	0	0
North	East		Candidate		820	245	20	0	0
D_N	D_NW		Candidate		94	0	20	0	0
D_N	D_NE		Candidate		255	0	20	0	0
D_NW	D_W		Candidate		199	0	20	0	0
D_NE	D_E		Candidate		148	0	20	0	0
D_W	D_E		Candidate		343	0	20	0	0
D_W	D_SW		Candidate		327	0	20	0	0
D_E	D_SE		Candidate		362	0	20	0	0
D_SW	D_SE		Candidate		189	0	20	0	0

Table 49: Net transfer capacities of the AC transmission grid between regions assumed for the REMix simulations			
In MW From	To	->	<-
BeNeLux	France	390	1574
D_E	D_SE	4752	4116
D_E	East	1318	977
D_N	D_NW	4718	1563
D_N	DK-W	597	2299
D_NE	D_E	2420	6188
D_NW	BeNeLux	867	171
D_NW	D_NE	1764	2538
D_NW	D_W	3402	3108
D_SE	Alps	1104	1380
D_SE	East	585	1143
D_SW	Alps	2428	788
D_SW	BeNeLux	330	424
D_SW	D_SE	2052	4582
D_SW	France	750	2283
D_W	BeNeLux	3862	1454
D_W	D_E	341	1272
D_W	D_SE	2047	915
D_W	D_SW	2254	1619
East	Alps	1399	200
France	Alps	2223	450
France	Italy	2455	841
Germany	Alps	2454	894
Germany	BeNeLux	3574	1786
Germany	DK-W	885	1997
Germany	East	1675	2818
Germany	France	790	1723
Iberia	France	717	712
Italy	Alps	3140	4019

Table 50: Power transmission distribution factors of the AC transmission grid between regions assumed for the REMix simulations

Flowgate		Transaction to Alps												
From	To	BeNeLux	D_E	D_N	D_NE	D_NW	D_SE	D_SW	D_W	DK-W	East	France	Iberia	Italy
BeNeLux	France	0.334	0.131	0.212	0.147	0.212	0.046	0.036	0.210	0.212	0.066	-0.209	-0.209	-0.035
D_E	D_SE	0.049	0.230	0.122	0.209	0.122	-0.043	0.006	0.061	0.122	0.074	0.018	0.018	0.003
D_E	East	0.090	0.354	0.198	0.324	0.198	0.005	0.025	0.111	0.198	-0.248	0.036	0.036	0.006
D_N	D_NW	0.000	0.000	1.000	0.000	0.000	0.000	0.000	0.000	1.000	0.000	0.000	0.000	0.000
D_N	DK-W	0.000	0.000	0.000	0.000	0.000	0.000	0.000	0.000	-1.000	0.000	0.000	0.000	0.000
D_NE	D_E	0.088	-0.222	0.344	0.695	0.344	-0.022	0.016	0.076	0.344	-0.093	0.033	0.033	0.006
D_NW	BeNeLux	-0.086	0.105	0.276	0.138	0.276	0.015	-0.006	0.015	0.276	0.046	-0.030	-0.030	-0.005
D_NW	D_NE	0.088	-0.222	0.344	-0.305	0.344	-0.022	0.016	0.076	0.344	-0.093	0.033	0.033	0.006
D_NW	D_W	-0.002	0.117	0.380	0.167	0.380	0.006	-0.010	-0.091	0.380	0.047	-0.003	-0.003	-0.001
D_SE	Alps	0.203	0.341	0.274	0.328	0.274	0.590	0.149	0.253	0.274	0.328	0.103	0.103	0.017
D_SE	East	-0.018	-0.140	-0.065	-0.125	-0.065	0.087	0.009	-0.022	-0.065	-0.357	-0.004	-0.004	-0.001
D_SW	Alps	0.455	0.320	0.407	0.337	0.407	0.256	0.704	0.465	0.407	0.209	0.322	0.322	0.054
D_SW	BeNeLux	-0.227	-0.076	-0.133	-0.087	-0.133	-0.014	0.036	-0.126	-0.133	-0.034	-0.065	-0.065	-0.011
D_SW	D_SE	0.030	-0.077	-0.018	-0.066	-0.018	-0.218	0.129	0.008	-0.018	-0.102	0.042	0.042	0.007
D_SW	France	-0.064	-0.007	-0.025	-0.010	-0.025	0.016	0.077	-0.017	-0.025	0.003	-0.248	-0.248	-0.042
D_W	BeNeLux	-0.353	0.103	0.069	0.096	0.069	0.045	0.005	0.321	0.069	0.055	-0.114	-0.114	-0.019
D_W	D_E	0.051	-0.194	-0.025	-0.162	-0.025	-0.016	0.015	0.096	-0.025	-0.080	0.021	0.021	0.003
D_W	D_SE	0.105	0.049	0.105	0.059	0.105	-0.062	0.022	0.162	0.105	-0.002	0.040	0.040	0.007
D_W	D_SW	0.194	0.160	0.231	0.174	0.231	0.040	-0.053	0.329	0.231	0.075	0.050	0.050	0.008
East	Alps	0.072	0.214	0.132	0.199	0.132	0.092	0.034	0.090	0.132	0.395	0.032	0.032	0.005
France	Alps	0.231	0.106	0.160	0.117	0.160	0.053	0.097	0.165	0.160	0.059	0.465	0.465	0.078
France	Italy	0.039	0.018	0.027	0.020	0.027	0.009	0.016	0.028	0.027	0.010	0.079	0.079	-0.155
Germany	Alps	0.657	0.661	0.681	0.665	0.681	0.845	0.853	0.717	0.681	0.536	0.424	0.424	0.071
Germany	BeNeLux	-0.666	0.131	0.212	0.147	0.212	0.046	0.036	0.210	0.212	0.066	-0.209	-0.209	-0.035
Germany	DK-W	0.000	0.000	0.000	0.000	0.000	0.000	0.000	0.000	-1.000	0.000	0.000	0.000	0.000
Germany	East	0.072	0.214	0.132	0.199	0.132	0.092	0.034	0.090	0.132	-0.605	0.032	0.032	0.005
Germany	France	-0.064	-0.007	-0.025	-0.010	-0.025	0.016	0.077	-0.017	-0.025	0.003	-0.248	-0.248	-0.042
Iberia	France	0.000	0.000	0.000	0.000	0.000	0.000	0.000	0.000	0.000	0.000	0.000	1.000	0.000
Italy	Alps	0.039	0.018	0.027	0.020	0.027	0.009	0.016	0.028	0.027	0.010	0.079	0.079	0.845

9   References

Asplund, G. (2008): High-Voltage Direct Current (HVDC) power transmission. Presentation at DESERTEC Hannover, Germany, 2008-04-23. ABB Power Systems HVDC, Ludvika, Sweden.

Axsen, J., et al. (2008): Batteries for Plug-in Hybrid Electric Vehicles (PHEVs): Goals and the State of Technology circa 2008. Institute of Transportation Studies, University of California, Davis. Research Report UCD-ITS-RR-08-14.

Ball, M. and Wietschel, M. (2009): The Hydrogen Economy: Oportunities and Challenges. Cambridge University Press.

Baños, et al. (2011): Optimization methods applied to renewable and sustainable energy: A review. *Renewable and Sustainable Energy Reviews*, 15 (4), p. 1753-1766.

Barsky, R. and Kilian, L. (2004): Oil and the Macroeconomy since the 1970s. *The Journal of Economic Perspectives*, vol. 18.

BCG, The Boston Consulting Group (2010): Batteries for Electric Cars. Challenges, Opportunities, and the Outlook to 2020. Online: http://www.bcg.de/expertise_impact/Industries/Automobil/PublicationDetails.aspx?id=tcm:89-36622.

BET, Büro für Energiewirtschaft und technische Planungen GmbH (2009): Kritische Würdigung der dena-Kurzanalyse zur Kraftwerks- und Netzplanung in Deutschland bis 2020 - Ergebnisse, Vorgehensweise, Annahmen und Schlussfolgerungen. Online: http://www.bet-aachen.de/fileadmin/redaktion/PDF/Veroeffentlichungen/2008/BET-Studie_Versorgungssicherheit_Strom.pdf.

BFE, Bundesamt für Energie (CH) (2009): Schweizerische Elektrizitätsstatistik 2008. Published: 04/06/2009. Bern.

Biberacher, M. (2004): Modelling and optimisation of future energy systems using spatial and temporal methods University of Augsburg, Institute for physics, Experimental Plasma Physics, Dissertation.

Biere, D., et al. (2009): Ökonomische Analyse der Erstnutzer von Elektrofahrzeugen. *Zeitschrift für Energiewirtschaft*, 33, pages 173-181

BMWi, Bundesministerium für Wirtschaft und Technologie (2010): Energiekonzept: für eine umweltschonende, zuverlässige und bezahlbare Energieversorgung. . Online: http://bmwi.de/BMWi/Navigation/Service/publikationen,did=360808.html.

Broussely, M., et al. (2005): Main aging mechanisms in Li ion batteries. *Journal of Power Sources*, 146 (1-2), p. 90-96.

Choi, S. S. and Lim, H. S. (2002): Factors that affect cycle-life and possible degradation mechanisms of a Li-ion cell based on LiCoO2 *Journal of Power Sources*, 111 (1), p. 130-136.

Czisch, G. (2005): Szenarien zur zukünftigen Stromversorgung: Kostenoptimierte Variationen zur Versorgung Europas und seiner Nachbarn mit Strom aus erneuerbaren Energien University Kassel, Institute for Electrical Engineering and Efficient Energy Conversion. Dissertation.

Dallinger, D., et al. (2010): Vehicle-to-grid regulation based on a dynamic simulation of mobility behavior. *Working Paper Sustainability and Innovation*, No. S 4/2010.

DENA, Deutsche Energie-Agentur GmbH (2005): Energiewirtschaftliche Planung für die Netzintegration von Windenergie in Deutschland an Land und Offshore bis zum Jahr 2020, project report, DEWI/E.ON Netz / EWI / RWE TN / VE Transmission for the DENA, Berlin.

DENA, Deutsche Energie-Agentur GmbH (2010): Integration erneuerbarer Energien in die deutsche Stromversorgung im Zeitraum 2015 – 2020 mit Ausblick auf 2025 (DENA-Netzstudie II), project report, 50Hertz Transmission / Amprion / DEWI / EnBW Transportnetze / EWI / Fraunhofer IWES / TenneT for the DENA.

DLR/IFHT/ISE (2012): Prospects for electric/ hybrid vehicles in a power supply system dominated by decentralized, renewable energy sources. Final report for the Federal Ministry for Economics and Technology; DLR Stuttgart, Fraunhofer-ISE Freiburg, IfHT RWTH Aachen, Juli 2012.

DOE, U.S. Department of Energy (2009): Annual Energy Outlook 2009. With Projections to 2030. Washington, DC 20585.

DWD, Deutscher Wetterdienst (2007): Windgeschwindigkeiten und Bodenrauhigkeit aus dem Lokalmodell Europa, Deutscher Wetterdienst, Offenbach.

EC, European Commission (2007): Limiting Global Climate Change to 2 degrees Celsius. The way ahead for 2020 and beyond. Communication from the Commission to the Council, the European Parliament, the European Economic and Social Committee and the Committee of the Regions.

EC, European Commission (2008): European Energy and Transport Trends to 2030 - Update 2007. European Commission - Directorate General for Energy and Transport.

ECF, European Climate Foundation (2010): Roadmap 2050: a practical guide to a prosperous, lowcarbon Europe - Volume I: Technical and Economic Analysis, by McKinsey & Company, KEMA, The Energy Futures Lab at Imperial College London, Oxford Economics and the ECF.

ENERCON (2010): ENERCON Wind energy converters. Product overview. Version: July 2010. Online: http://www.enercon.de/p/downloads/EN_Productoverview_0710.pdf.

Engel, T. (2010): Netzintegration von Smart Grid Vehicles, conference proceedings. 10. Mobilitätskonferenz für alternative und erneuerbare Mobilität, Berlin 17.02.2010.

ENTSO-E (2010): European Network of Transmission System Operators: „Ten-Year Network Development Plan 2010". Final report. https://www.entsoe.eu/system-development/tyndp/tyndp-2010/, 30. Juni 2010.

Espejo, C. and García, R. (2010): La energía solar termoeléctrica en España. *Anales de Geografía de la Universidad Complutense*, 30 (2).

ETSAP, Energy Technology Systems Analysis Programme (2010): Unconventional Oil & Gas Production - Technology Brief P02. Online: http://www.iea-etsap.org/web/E-TechDS/PDF/P02-Uncon%20oil&gas-GS-gct.pdf.

EUR, The European Parliament and the Council of the European Union (2009): Regulation (EC) No 443/2009 of the European Parliament and of the

Council, of 23 April 2009. Setting emission performance standards for new passenger cars as part of the Community's integrated approach to reduce CO2 emissions from light-duty vehicles.

Euractiv (2007): Euro 5 emissions standards for cars, 31 May 2007.

EURELECTRIC, Union of the Electricity Industry, (2011): European electricity industry views on charging Electric Vehicles - A EURELECTRIC position paper.

EUROSTAT (2008): Heating degree-days - Annual data.

EUROSTAT (2010): Electricity generated from renewable sources - % of gross electricity consumption. Online: http://epp.eurostat.ec.europa.eu/portal/page/portal/energy/data/main_tables.

EWIS, European Wind Integration Study (2008): Towards a Successful Integration of Wind Power into European Electricity Grids. Online: http://www.wind-integration.eu/downloads/library/EWIS-Interim-Report-Appendix.pdf.

Fischer, C. (2011): Wasserstoff als zukünftiger Energieträger. Kostenermittlung einer Tankstelle. Fachhochschule Nürtingen, Master Thesis.

Foley, A. M., et al. (2010): A strategic review of electricity systems models. *Energy*, 35 (12), p. 4522-4530.

Frontier/EWI (2010): Energiekosten in Deutschland - Entwicklungen, Ursachen und internationaler Vergleich. Final report for the German Ministry of Economics and Technology.

FVS, Forschungs Verbund Sonnenenergie (2004): Wasserstoff und Brennstoffzellen – Energieforschung im Verbund.

Gardiner, M. (2009): Energy requirements for hydrogen gas compression and liquefaction as related to vehicle storage needs. Online: http://www.hydrogen.energy.gov/pdfs/9013_energy_requirements_for_hydrogen_gas_compression.pdf.

Genoese, M. (2010): Energiewirtschaftliche Analysen des deutschen Strommarkts mit agentenbasierter Simulation. Universität Karlsruhe, Institute for Industrial Production, Karlsruhe.

GP/EREC, Greenpeace International, European Renewable Energy Council, (2007): Energy [r]evolution: A sustainable world energy outlook.

GRDC, Global Runoff River Data Center (2008): Discharge data. Koblenz.

Hacker, F., et al. (2009): Environmental impacts and impact on the electricity market of a large scale introduction of electric cars in Europe. The European Topic Centre on Air and Climate Change.

Hammer, A., et al. (2003): Solar energy assessment using remote sensing technologies. *Remote Sensing of Environment*, 86 (3), p. 423-432.

HBEFA (2010): Handbuch Emissionsfaktoren HBEFA 3.1. Download www.hbefa.net. Basel, Infras.

Helms, H. (2010): Electric vehicle and plug-in hybrid energy efficiency and life cycle emissions. In: Transport and air pollution 2010 conference proceedings, Zürich.

Hoogwijk, M., et al. (2003): Exploration of the ranges of the global potential of biomass for energy. Biomass and Bioenergy 25(2), 119–133.

Hundt, M., et al. (2009): Verträglichkeit von erneuerbaren Energien und Kernenergie im Erzeugungsportfolio, project report for E.On Energie AG.

ICCS-NTUA, Institute of Communication and Computer Systems of National Technical University of Athens (2007): Case Study Comparisons And Development of Energy Models for Integrated Technology Systems (Cascade Mints).

infas, DIW (2003): Mobilität in Deutschland. Bonn / Berlin.

IPCC, Intergovernmental Panel on Climate Change (2007): Climate Change 2007: Synthesis Report. Online: http://www.ipcc.ch/publications_and_data/publications_ipcc_fourth_assessment_report_synthesis_report.htm.

Johnke, B. (2001): Emissions from Waste Incineration. IPCC Report - Good Practice Guidance and Uncertainty Management in National Greenhouse Gas Inventories. Online: http://www.ipcc-nggip.iges.or.jp/public/gp/bgp/5_3_Waste_Incineration.pdf.

JRC, Joint Research Centre - European Commission (2008): Biofuels in the European Context: Facts and Uncertainties.

Kalhammer, F. R. and Kopf, B. M. (2007): Status and Prospects for Zero Emissions Vehicle Technology - Report of the ARB Independent Expert Panel 2007.

Kalhammer, F. R., et al. (2007): Status and Prospects for Zero Emissions Vehicle Technology. Report of the ARB Independent Expert Panel 2007. Prepared for State of California Air Resources Board, Sacramento, California. Online: www.arb.ca.gov/msprog/zevprog/zevreview/zev_panel_report.pdf.

Kempton, W. and Tomic, J. (2004): Vehicle-to-grid power fundamentals: Calculating capacity and net revenue. *Journal of Power Sources*, 144 (1), p. 268-279.

Kintner-Meyer, M., et al. (2010): Impact Assessment of Plug-in Hybrid Vehicles on the U.S. Power Grid. The 25th World Battery, Hybrid and Fuel Cell Electric Vehicle Symposium & Exhibition, EVS-25, Shenzhen, China, Nov. 5-9, 2010.

Link, J., et al. (2010): Optimisation Algorithms for the Charge Dispatch of Plug-in Vehicles based on Variable Tariffs. *Working Paper Sustainability and Innovation*, 3/2010.

Markel, T., et al. (2010): Transportation Electrification Load Development For a Renewable Future Analysis. The 25th World Battery, Hybrid and Fuel Cell Electric Vehicle Symposium & Exhibition, Shenzhen, China, Nov. 2010.

McCarthy, R. W. (2009): Assessing Vehicle Electricity Demand Impacts on California Electricity Supply, dissertation, Institute of Transportation Studies. University of California, Davis.

Mock, P. (2010): Entwicklung eines Szenariomodells zur Simulation der zukünftigen Marktanteile und CO2-Emissionen von Kraftfahrzeugen (VECTOR21). Dissertation, Universität Stuttgart, DLR Institute of Vehicle Concepts.

Mock, P. and Schmid, S. (2008): Brennstoffzellen- und Batteriefahrzeuge - Kurzfristiger Hype oder langfristiger Trend? *VDI-Berichte 2030: Innovative Fahrzeugantriebe 2008*.

Möser, K. (2002): Geschichte des Autos. Dampf Benzin oder Elektrizität: Die Konkurrenz der Systeme. Campus Verlag, Frankfurt/New York.

Naunin, D. (2007): Hybrid-, Batterie- und Brennstoffzellen-Elektrofahrzeuge: Technik, Strukturen und Entwicklungen. Expert Verlag.

NEP (2009): Nationaler Entwicklungsplan Elektromobilität der Bundesregierung. Online: http://www.bmbf.de/pubRD/nationaler_entwicklungsplan_elektromobilitaet.pdf

Nishi, Y. (2001): Lithium ion secondary batteries; past 10 years and the future. *Journal of Power Sources*, 100 (1-2), p. 101-106.

Nitsch, J., et al. (2011): Long term scenarios and strategies for the deployment of renewable energies in Germany under the consideration of European and global developments. „Lead study 2010". Project report for the Federal Ministry for the Environment, Nature Conservation and Nuclear Safety; DLR Stuttgart, Fraunhofer-IWES Kassel, IFNE Teltow, Februar 2011.

Nitsch, J., et al. (2012): Long term scenarios and strategies for the deployment of renewable energies in Germany under the consideration of European and global developments. Final report for the Federal Ministry for the Environment, Nature Conservation and Nuclear Safety; DLR Stuttgart, Fraunhofer-IWES Kassel, IFNE Teltow, March 2012.

Nordel (2008): Annual statistics 2008. Oslo.

NRC, National Research Council (2010): Transitions to alternative transportation technologies - Plug-in hybrid vehicles. Report online: http://www.nap.edu/openbook.php?record_id=12826. National Academy of Sciences.

OECD/IEA (2006): World Energy Outlook. International Energy Agency, Paris.

OECD/IEA (2008): Energy Technology Perspectives 2008: Scenarios and Strategies to 2050. International Energy Agency, Paris.

OECD/IEA (2009): World Energy Outlook - Global Energy Trends to 2030. International Energy Agency, Paris.

Ogden, J. (2004): Where will the hydrogen come from? System considerations and hydrogen supply. In: Sperling, D. and Cannon, J. S. (Hrsg.): The hydrogen energy transition: Moving toward the post petroleum age in transportation, p. Elsevier academic press.

Parks, K., et al. (2007): Costs and Emissions Associated with Plug-In Hybrid Electric Vehicle Charging in the Xcel Energy Colorado Service Territory. Technical report. *National Renewable Energy Laboratory*.

PDO, People's Daily Online. (2008): Shanghai plans China IV emissions standard in 2009. Online: http://english.people.com.cn/90001/90776/90882/6390256.html, April 10, 2008

Pehnt, M. (2010): Contribution to the volume „20 Jahre Recht der Erneuerbaren Energien". Würzburg

Pehnt, M., et al. (2011): Elektroautos in einer von erneuerbaren Energien geprägten Energiewirtschaft. *Zeitschrift für Energiewirtschaft*, 35, pages 221-234. May the 7th 2011.

Perujo, A. and Ciuffo, B. (2010): The introduction of electric vehicles in the private fleet: Potential impact on the electric supply system and on the environment. *Energy Policy*, 38 (8), p. 4549-4561.

Peterson, S. B., et al. (2010): Lithium-ion battery cell degradation resulting from realistic vehicle and vehicle-to-grid utilization *Journal of Power Sources*, 195 (8), p. 2385-2392

Pieltain, L., et al. (2011): Assessment of the Impact of Plug-in Electric Vehicles on Distribution Networks. *IEEE Transactions on Power Systems*, 26 (1), p. 206 - 213

Pimentel, D., et al. (2008): Biofuel Impacts on World Food Supply: Use of Fossil Fuel, Land and Water Resources. *Energies*, 1 (2), p. 41-78.

Platts (2008): UDI World Electric Power Plants Database (WEPP). Version 2008.

Pohl, S. E. (2008): Der Freikolbenlineargenerator - Theoretische Betrachtungen des Gesamtsystems und experimentelle Untersuchungen zum Teilsystem der Gasfeder. Dissertation. Deutsches Zentrum für Luft- und Raumfahrt.

Probst, A. and Tenbohlen, S. (2010): Challenges and opportunities for the power grid by electric-mobility.

Propfe, B. and Luca de Tena, D. (2010): Perspectives of electric vehicles: customer suitability and renewable energy integration. The 25th World Battery, Hybrid

and Fuel Cell Electric Vehicle Symposium & Exhibition, EVS-25, Shenzhen, China, Nov. 5-9, 2010.

Rehtanz, C. (2009): Netzdienstleistungen durch Elektrofahrzeuge –Technische und wirtschaftliche Herausforderungen. Conference: Energiespeicher in Stromversorgungsunternehmen mit hohem Anteil erneuerbarer Energieträger, Erfurt, 23/ 9/ 2009.

Ritchie, A. G. (2004): Recent developments and likely advances in lithium rechargeable batteries. *Journal of Power Sources*, 136 (2), p. 285-289.

Rosenkranz, C. (2003): The 20th World Battery, Hybrid and Fuel Cell Electric Vehicle Symposium & Exhibition, EVS-20, Long Beach, CA, November 15-19.

Roth, H. and Kuhn, P. (2008): Technik- und Kostenszenarien der Strombereitstellung in Deutschland bis 2040. IfE-Schriftenreihe Heft 55, Herrsching 2008.

SBA, Statistisches Bundesamt (2009): Haus- und Grundbesitz sowie Wohnverhältnisse privater Haushalte - Fachserie 15 Sonderheft 1 - 2008. Wiesbaden

Schillings, C., et al. (2004): Operational method for deriving high resolution direct normal irradiance from satellite data. *Solar Energy*, 76 (4).

Scholz, Y. (2012): Renewable energy based electricity supply at low costs: Setup and application of the REMix model for Europe (unpublished). Dissertation. DLR Institute of Technical Thermodynamics. University of Stuttgart.

Schuth, F. (2010): MINI E Berlin powered by Vattenfall – Erfahrungen mit Elektromobilität in Berlin. Personal communication, 11/ 5/ 2010.

Seidenberger, T., et al. (2008): Global biomass potentials. Report prepared for Greenpeace International. German Biomass Research Center, Leipzig.

Seifert, M. (2005): Feinstaub trägt zur Anreicherung von Schadstoffen im Boden bei, 04/12/2005.

SRU, Sachverständigenrat für Umweltfragen (2010): 100% erneuerbare Stromversorgung bis 2050: klimaverträglich, sicher, bezahlbar. Stellungnahme.

Trieb, F., et al. (2006): Trans-Mediterranean Interconnection for Concentrating Solar Power, project report, DLR / NERC / Abdelaziz Bennouna / NE / NREA / NEAL / IFEED / HWWA for the Bundesministerium für Umwelt, Naturschutz und Reaktorsicherheit (BMU).

Trieb, F., et al. (2009): Characterisation of Solar Electricity Import Corridors from MENA to Europe: Potential, Infrastructure and Cost. Report prepared in the frame of the EU project 'Risk of Energy Availability: Common Corridors for Europe Supply Security (REACCESS)' carried out under the 7th Framework Programme (FP7) of the European Commission (Theme - Energy-2007-9. 1-01: Knowledge tools for energy-related policy making, Grant agreement no.: 212011).

TSO, Transmission System Operators in Germany: Amprion GmbH, EnBW Transportnetze AG, transpower stromübertragungs GmbH, Vattenfall Europe Transmission GmbH (2009): Regionenmodell „Stromtransport 2013" - Übersicht über die voraussichtliche Entwicklung der installierten Kraftwerksleistung und der Leistungsflüsse in den Netzgebieten der deutschen Übertragungsnetzbetreiber. Online: http://www.50hertz.com/de/file/090901_Regionenmodell_Stromtransport_2013.pdf.

Turrentine, T. S., et al. (2011): The UC Davis MINI E Consumer Study. Institute of Transportation Studies, University of California, Davis, Research Report UCD-ITS-RR-11-05.

Tuttle, D. P. and Baldick, R. (2010): The Evolution of Plug-in Electric Vehicle-Grid Interactions. The University of Texas at Austin. Department of Electrical and Computer Engineering. Online: http://users.ece.utexas.edu/~baldick/papers/PEV-Grid.pdf.

UBA, Umweltbundesamt (2010): Datenbank „Kraftwerke in Deutschland"Liste der sich in Betrieb befindlichen Kraftwerke bzw. Kraftwerksblöcke ab einer elektrischen Bruttoleistung von 100 Megawatt.

UNPD, United Nations Population Division (2007): World Urbanization Prospects: The 2007 Revision Population Database. Online: http://esa.un.org/unup/.

VDE, Verband der Elektrotechnik Elektronik Informationstechnik e.V. (2010): Elektrofahrzeuge: Bedeutung, Stand der Technik, Handlungsbedarf. VDE Studie, Gesamttext. .

VDE, Verband der Elektrotechnik Elektronik Informationstechnik e.V. (2011): Stromübertragung für den Klimaschutz. VDE report, full text.

VGB, PowerTech (2009/2010): Zahlen und Fakten zu Stromerzeugung. Online: http://www.vgb.org/daten_stromerzeugung.html.

Wallentowitz, H. and Freialdenhoven, A. (2011): Strategien zur Elektrifizierung des Antriebsstranges. Technologien, Märkte und Implikationen. Vieweg+Teubner, Wiesbaden.

Wang, J., et al. (2011): Cycle-life model for graphite-LiFePo4 cells. *Journal of Power Sources*, 196 (8), p. 3942-3948.

Wittwer, C. (2010): Die Rolle des Speichers bei der Netzintegration von Elektrofahrzeugen. FVEE-Workshop Elektrochemische Energiespeicher und Elektromobilität, Ulm, 20/ 1/ 2010.

Wohlfahrt-Mehrens, M. (2010): Lithium ion batteries: battery materials and ageing processes. Advanced Battery Technologies for Automobiles and Their Electric Power Grid Integration Conference, 1-5/ 2 /2010, Mainz.

Xinhuanet (2011): Beijing to tighten vehicle emission standards, as automobile number hits 5 mln, 12/03/2011.

Zunft, S. (2005): Adiabate Druckluftspeicherkraftwerke: Ein Element zur netzkonformen Integration von Windenergie.

Résumé

PERSONAL DETAILS

Name   Diego Luca de Tena Costales
Birth   May the 31st 1985 in Madrid
Contact diego.lucadetena@gmail.com

EDUCATION

2008-2014   **University of Stuttgart**
Stuttgart, Germany
Doctoral student

2003-2008   **ICAI School of Engineering – Comillas Pontifical University**
Madrid, Spain
Industrial engineering with specialisation in electrical engineering
Full year exchange student at the University of Stuttgart
Thesis "*Analysis of the Iberian transmission network with increasing wind power feed-in*".

PROFESSIONAL POSITIONS

Since 2011   **ÅF Group**
International Division, Energy Markets Consulting
Madrid, Spain
Consultant
Power sector technical, economic and regulatory consulting to utilities, developers and regulatory agencies. Development of decision support tools.

2008-2011   **German Aerospace Center (DLR)**
Institute of Technical Thermodynamics
Stuttgart, Germany
Research assistant
Development of low carbon energy system scenarios and of decision support tools to demonstrate the feasibility and impact of a high penetration of renewable power generation and of electric mobility.

Summer '07 **Boston Consulting Group**
Madrid, Spain
Visiting Associate
Madrid, Spain
Branding strategy project for a telco and on natural gas supply contract.

2006-2007   **Institute for Research in Technology – ICAI School of Engineering**
Madrid, Spain
Research Scholar
Participated in a research project on a folding electrical scooter.

AWARDS

2008   **Endesa:** Second price for the best thesis of the year at the ICAI.

2006-2008   **Community of Madrid:** Academic excellence award in 2006, 2007 and 2008.